A Metabolic Analysis of Glucose and Glutamine Utilization in Hybridoma CC9C10

By

David Albert Petch

A thesis submitted in Partial Fulfillment of the Requirements of the University of Manitoba for the Degree of

MASTER OF SCIENCE

University of Manitoba
Department of Microbiology
Winnipeg, Manitoba
Canada

ISBN 0-612-13443-1

Name David Petch

Dissertation Abstracts International is arranged by broad, general subject categories. Please select the one subject which most nearly describes the content of your dissertation. Enter the corresponding four-digit code in the spaces provided.

Biological Sciences; Microbiology
SUBJECT TERM

0410
SUBJECT CODE

UMI

Subject Categories

THE HUMANITIES AND SOCIAL SCIENCES

COMMUNICATIONS AND THE ARTS
Architecture 0729
Art History 0377
Cinema 0900
Dance 0378
Fine Arts 0357
Information Science 0723
Journalism 0391
Library Science 0399
Mass Communications 0708
Music 0413
Speech Communication 0459
Theater 0465

EDUCATION
General 0515
Administration 0514
Adult and Continuing 0516
Agricultural 0517
Art 0273
Bilingual and Multicultural 0282
Business 0688
Community College 0275
Curriculum and Instruction 0727
Early Childhood 0518
Elementary 0524
Finance 0277
Guidance and Counseling 0519
Health 0680
Higher 0745
History of 0520
Home Economics 0278
Industrial 0521
Language and Literature 0279
Mathematics 0280
Music 0522
Philosophy of 0998
Physical 0523
Psychology 0525
Reading 0535
Religious 0527
Sciences 0714
Secondary 0533
Social Sciences 0534
Sociology of 0340
Special 0529
Teacher Training 0530
Technology 0710
Tests and Measurements 0288
Vocational 0747

LANGUAGE, LITERATURE AND LINGUISTICS
Language
- General 0679
- Ancient 0289
- Linguistics 0290
- Modern 0291

Literature
- General 0401
- Classical 0294
- Comparative 0295
- Medieval 0297
- Modern 0298
- African 0316
- American 0591
- Asian 0305
- Canadian (English) 0352
- Canadian (French) 0355
- English 0593
- Germanic 0311
- Latin American 0312
- Middle Eastern 0315
- Romance 0313
- Slavic and East European 0314

PHILOSOPHY, RELIGION AND THEOLOGY
Philosophy 0422
Religion
- General 0318
- Biblical Studies 0321
- Clergy 0319
- History of 0320
- Philosophy of 0322

Theology 0469

SOCIAL SCIENCES
American Studies 0323
Anthropology
- Archaeology 0324
- Cultural 0326
- Physical 0327

Business Administration
- General 0310
- Accounting 0272
- Banking 0770
- Management 0454
- Marketing 0338

Canadian Studies 0385
Economics
- General 0501
- Agricultural 0503
- Commerce-Business 0505
- Finance 0508
- History 0509
- Labor 0510
- Theory 0511

Folklore 0358
Geography 0366
Gerontology 0351
History
- General 0578
- Ancient 0579
- Medieval 0581
- Modern 0582
- Black 0328
- African 0331
- Asia, Australia and Oceania 0332
- Canadian 0334
- European 0335
- Latin American 0336
- Middle Eastern 0333
- United States 0337

History of Science 0585
Law 0398
Political Science
- General 0615
- International Law and Relations 0616
- Public Administration 0617

Recreation 0814
Social Work 0452
Sociology
- General 0626
- Criminology and Penology 0627
- Demography 0938
- Ethnic and Racial Studies 0631
- Individual and Family Studies 0628
- Industrial and Labor Relations 0629
- Public and Social Welfare 0630
- Social Structure and Development 0700
- Theory and Methods 0344

Transportation 0709
Urban and Regional Planning 0999
Women's Studies 0453

THE SCIENCES AND ENGINEERING

BIOLOGICAL SCIENCES
Agriculture
- General 0473
- Agronomy 0285
- Animal Culture and Nutrition 0475
- Animal Pathology 0476
- Food Science and Technology 0359
- Forestry and Wildlife 0478
- Plant Culture 0479
- Plant Pathology 0480
- Plant Physiology 0817
- Range Management 0777
- Wood Technology 0746

Biology
- General 0306
- Anatomy 0287
- Biostatistics 0308
- Botany 0309
- Cell 0379
- Ecology 0329
- Entomology 0353
- Genetics 0369
- Limnology 0793
- Microbiology 0410
- Molecular 0307
- Neuroscience 0317
- Oceanography 0416
- Physiology 0433
- Radiation 0821
- Veterinary Science 0778
- Zoology 0472

Biophysics
- General 0786
- Medical 0760

EARTH SCIENCES
Biogeochemistry 0425
Geochemistry 0996
Geodesy 0370
Geology 0372
Geophysics 0373
Hydrology 0388
Mineralogy 0411
Paleobotany 0345
Paleoecology 0426
Paleontology 0418
Paleozoology 0985
Palynology 0427
Physical Geography 0368
Physical Oceanography 0415

HEALTH AND ENVIRONMENTAL SCIENCES
Environmental Sciences 0768
Health Sciences
- General 0566
- Audiology 0300
- Chemotherapy 0992
- Dentistry 0567
- Education 0350
- Hospital Management 0769
- Human Development 0758
- Immunology 0982
- Medicine and Surgery 0564
- Mental Health 0347
- Nursing 0569
- Nutrition 0570
- Obstetrics and Gynecology 0380
- Occupational Health and Therapy 0354
- Ophthalmology 0381
- Pathology 0571
- Pharmacology 0419
- Pharmacy 0572
- Physical Therapy 0382
- Public Health 0573
- Radiology 0574
- Recreation 0575
- Speech Pathology 0460
- Toxicology 0383

Home Economics 0386

PHYSICAL SCIENCES
Pure Sciences
Chemistry
- General 0485
- Agricultural 0749
- Analytical 0486
- Biochemistry 0487
- Inorganic 0488
- Nuclear 0738
- Organic 0490
- Pharmaceutical 0491
- Physical 0494
- Polymer 0495
- Radiation 0754

Mathematics 0405
Physics
- General 0605
- Acoustics 0986
- Astronomy and Astrophysics 0606
- Atmospheric Science 0608
- Atomic 0748
- Electronics and Electricity 0607
- Elementary Particles and High Energy 0798
- Fluid and Plasma 0759
- Molecular 0609
- Nuclear 0610
- Optics 0752
- Radiation 0756
- Solid State 0611

Statistics 0463

Applied Sciences
Applied Mechanics 0346
Computer Science 0984
Engineering
- General 0537
- Aerospace 0538
- Agricultural 0539
- Automotive 0540
- Biomedical 0541
- Chemical 0542
- Civil 0543
- Electronics and Electrical 0544
- Heat and Thermodynamics 0348
- Hydraulic 0545
- Industrial 0546
- Marine 0547
- Materials Science 0794
- Mechanical 0548
- Metallurgy 0743
- Mining 0551
- Nuclear 0552
- Packaging 0549
- Petroleum 0765
- Sanitary and Municipal 0554
- System Science 0790

Geotechnology 0428
Operations Research 0796
Plastics Technology 0795
Textile Technology 0994

PSYCHOLOGY
General 0621
Behavioral 0384
Clinical 0622
Developmental 0620
Experimental 0623
Industrial 0624
Personality 0625
Physiological 0989
Psychobiology 0349
Psychometrics 0632
Social 0451

Nom _____

Dissertation Abstracts International est organisé en catégories de sujets. Veuillez s.v.p. choisir le sujet qui décrit le mieux votre thèse et inscrivez le code numérique approprié dans l'espace réservé ci-dessous.

_____ ☐☐☐ U·M·I

SUJET — CODE DE SUJET

Catégories par sujets

HUMANITÉS ET SCIENCES SOCIALES

COMMUNICATIONS ET LES ARTS
Architecture 0729
Beaux-arts 0357
Bibliothéconomie 0399
Cinéma 0900
Communication verbale 0459
Communications 0708
Danse 0378
Histoire de l'art 0377
Journalisme 0391
Musique 0413
Sciences de l'information 0723
Théâtre 0465

ÉDUCATION
Généralités 515
Administration 0514
Art 0273
Collèges communautaires 0275
Commerce 0688
Économie domestique 0278
Éducation permanente 0516
Éducation préscolaire 0518
Éducation sanitaire 0680
Enseignement agricole 0517
Enseignement bilingue et multiculturel 0282
Enseignement industriel 0521
Enseignement primaire. 0524
Enseignement professionnel 0747
Enseignement religieux 0527
Enseignement secondaire 0533
Enseignement spécial 0529
Enseignement supérieur 0745
Évaluation 0288
Finances 0277
Formation des enseignants 0530
Histoire de l'éducation 0520
Langues et littérature 0279
Lecture 0535
Mathématiques 0280
Musique 0522
Orientation et consultation 0519
Philosophie de l'éducation 0998
Physique 0523
Programmes d'études et enseignement 0727
Psychologie 0525
Sciences 0714
Sciences sociales 0534
Sociologie de l'éducation 0340
Technologie 0710

LANGUE, LITTÉRATURE ET LINGUISTIQUE
Langues
- Généralités 0679
- Anciennes 0289
- Linguistique 0290
- Modernes 0291

Littérature
- Généralités 0401
- Anciennes 0294
- Comparée 0295
- Médiévale 0297
- Moderne 0298
- Africaine 0316
- Américaine 0591
- Anglaise 0593
- Asiatique 0305
- Canadienne (Anglaise) 0352
- Canadienne (Française) 0355
- Germanique 0311
- Latino-américaine 0312
- Moyen-orientale 0315
- Romane 0313
- Slave et est-européenne 0314

PHILOSOPHIE, RELIGION ET THÉOLOGIE
Philosophie 0422
Religion
- Généralités 0318
- Clergé 0319
- Études bibliques 0321
- Histoire des religions 0320
- Philosophie de la religion 0322

Théologie 0469

SCIENCES SOCIALES
Anthropologie
- Archéologie 0324
- Culturelle 0326
- Physique 0327

Droit 0398
Économie
- Généralités 0501
- Commerce-Affaires 0505
- Économie agricole 0503
- Économie du travail 0510
- Finances 0508
- Histoire 0509
- Théorie 0511

Études américaines 0323
Études canadiennes 0385
Études féministes 0453
Folklore 0358
Géographie 0366
Gérontologie 0351
Gestion des affaires
- Généralités 0310
- Administration 0454
- Banques 0770
- Comptabilité 0272
- Marketing 0338

Histoire
- Histoire générale 0578
- Ancienne 0579
- Médiévale 0581
- Moderne 0582
- Histoire des noirs 0328
- Africaine 0331
- Canadienne 0334
- États-Unis 0337
- Européenne 0335
- Moyen-orientale 0333
- Latino-américaine 0336
- Asie, Australie et Océanie 0332

Histoire des sciences 0585
Loisirs 0814
Planification urbaine et régionale 0999
Science politique
- Généralités 0615
- Administration publique 0617
- Droit et relations internationales 0616

Sociologie
- Généralités 0626
- Aide et bien-être social 0630
- Criminologie et établissements pénitentiaires 0627
- Démographie 0938
- Études de l' individu et de la famille 0628
- Études des relations interethniques et des relations raciales 0631
- Structure et développement social 0700
- Théorie et méthodes. 0344
- Travail et relations industrielles 0629

Transports 0709
Travail social 0452

SCIENCES ET INGÉNIERIE

SCIENCES BIOLOGIQUES
Agriculture
- Généralités 0473
- Agronomie. 0285
- Alimentation et technologie alimentaire 0359
- Culture 0479
- Élevage et alimentation 0475
- Exploitation des pâturages 0777
- Pathologie animale 0476
- Pathologie végétale 0480
- Physiologie végétale 0817
- Sylviculture et faune 0478
- Technologie du bois 0746

Biologie
- Généralités 0306
- Anatomie 0287
- Biologie (Statistiques) 0308
- Biologie moléculaire 0307
- Botanique 0309
- Cellule 0379
- Écologie 0329
- Entomologie 0353
- Génétique 0369
- Limnologie 0793
- Microbiologie 0410
- Neurologie 0317
- Océanographie 0416
- Physiologie 0433
- Radiation 0821
- Science vétérinaire 0778
- Zoologie 0472

Biophysique
- Généralités 0786
- Medicale 0760

SCIENCES DE LA TERRE
Biogéochimie 0425
Géochimie 0996
Géodésie 0370
Géographie physique 0368
Géologie 0372
Géophysique 0373
Hydrologie 0388
Minéralogie 0411
Océanographie physique 0415
Paléobotanique 0345
Paléoécologie 0426
Paléontologie 0418
Paléozoologie 0985
Palynologie 0427

SCIENCES DE LA SANTÉ ET DE L'ENVIRONNEMENT
Économie domestique 0386
Sciences de l'environnement 0768
Sciences de la santé
- Généralités 0566
- Administration des hôpitaux 0769
- Alimentation et nutrition 0570
- Audiologie 0300
- Chimiothérapie 0992
- Dentisterie 0567
- Développement humain 0758
- Enseignement 0350
- Immunologie 0982
- Loisirs 0575
- Médecine du travail et thérapie 0354
- Médecine et chirurgie 0564
- Obstétrique et gynécologie 0380
- Ophtalmologie 0381
- Orthophonie 0460
- Pathologie 0571
- Pharmacie 0572
- Pharmacologie 0419
- Physiothérapie 0382
- Radiologie 0574
- Santé mentale 0347
- Santé publique 0573
- Soins infirmiers 0569
- Toxicologie 0383

SCIENCES PHYSIQUES
Sciences Pures
Chimie
- Généralités 0485
- Biochimie 487
- Chimie agricole 0749
- Chimie analytique 0486
- Chimie minérale 0488
- Chimie nucléaire 0738
- Chimie organique 0490
- Chimie pharmaceutique 0491
- Physique 0494
- PolymÈres 0495
- Radiation 0754

Mathématiques 0405
Physique
- Généralités 0605
- Acoustique 0986
- Astronomie et astrophysique 0606
- Électronique et électricité 0607
- Fluides et plasma 0759
- Météorologie 0608
- Optique 0752
- Particules (Physique nucléaire) 0798
- Physique atomique 0748
- Physique de l'état solide 0611
- Physique moléculaire 0609
- Physique nucléaire 0610
- Radiation 0756

Statistiques 0463

Sciences Appliqués Et Technologie
Informatique 0984
Ingénierie
- Généralités 0537
- Agricole 0539
- Automobile 0540
- Biomédicale 0541
- Chaleur et thermodynamique 0348
- Conditionnement (Emballage) 0549
- Génie aérospatial 0538
- Génie chimique 0542
- Génie civil 0543
- Génie électronique et électrique 0544
- Génie industriel 0546
- Génie mécanique 0548
- Génie nucléaire 0552
- Ingénierie des systèmes 0790
- Mécanique navale 0547
- Métallurgie 0743
- Science des matériaux 0794
- Technique du pétrole 0765
- Technique minière 0551
- Techniques sanitaires et municipales 0554
- Technologie hydraulique 0545

Mécanique appliquée 0346
Géotechnologie 0428
Matières plastiques (Technologie) 0795
Recherche opérationnelle 0796
Textiles et tissus (Technologie) 0794

PSYCHOLOGIE
Généralités 0621
Personnalité 0625
Psychobiologie 0349
Psychologie clinique 0622
Psychologie du comportement 0384
Psychologie du développement 0620
Psychologie expérimentale 0623
Psychologie industrielle 0624
Psychologie physiologique 0989
Psychologie sociale 0451
Psychométrie 0632

A METABOLIC ANALYSIS OF GLUCOSE AND GLUTAMINE UTILIZATION IN HYBRIDOMA CC9C10

by

DAVID ALBERT PETCH

A Thesis submitted to the Faculty of Graduate Studies of the University of Manitoba in partial fulfillment of the requirements for the degree of

MASTER OF SCIENCE

Declaration

I declare that this thesis is a report of the research carried out during the period of September, 1991 until March, 1994, in the Department of Microbiology, at the University of Manitoba under the supervision of Dr. M. Butler. The work completed has not been submitted for any other degree, and has not been reported by other persons in the literature.

June 25, 1994

Acknowledgments

I would like to thank very much my supervisor **Dr, Michael Butler** for his help and assistance during this project.

I am very grateful for **Mike Berry** who gave useful advice, encouragement, and teaching of some of the tricks of the trade. I would also like to express my gratitude to the following:

Andrew Christie for his help when I required assistance on use of the HPLC .

David Jan for running the fermentors which provided cells for experiments.

Norman Huzel for his help in learning certain computer programs.

Bill Ng for making conversations pleasant.

Norman Barnabe' for supplying a scheme on how to use the Glutamine Assay.

Prep room ladies for making life easier.

This work was supported by a jointly funded Industrial Research Grant from the Natural Sciences and Engineering Research Council of Canada and Apotex Fermentation Inc.

ABSTRACT

Glucose and Glutamine Metabolism of Hybridoma CC9C10

David Petch

Hybridoma cells play an important role in their ability to produce monoclonal antibodies (Mabs), which have uses in therapeutics, fermentation products, affinity separation, and antibody-antigen interactions. In order to attempt increasing the recovery of Mabs, an examination of metabolic analysis was attempted. This was performed in order to develop an understanding of substrate utilization, byproduct formation, and the amount of theoretical energy generated by cellular metabolism.

1) Hybridoma cell line CC9C10 cultures were shown to have a slight enhancement of metabolism on the first day in the presence of dichloroacetic acid (DCA) followed by a similar metabolism to the control for the remainder of the culture period.

Cell densities were similar for cultures with and without DCA supplementation when grown in serum, except upon cells entering the decline phase. CC9C10 cells supplemented with DCA had 100 to 200% higher viable cell numbers in the decline phase. There was no noted effect upon increased antibody production from this observation (CC9C10 cells grown in DMEM with 1.5 mM DCA had a net volumetric yield of 36.5 μg/ml, while cells without the 1.5 mM DCA addition had 33.2 μg/ml).

Glucose consumption rates among most cultures containing DCA on day one were higher than the controls (no DCA addition), some as high as 235%. Following day 1, all cultures had similar glucose consumption rates, although the DCA supplemented cultures were still slightly higher.

Lactate production rates in DCA supplemented cultures were typically higher than the control (no DCA addition), some as high as 59%. Following day 1 all cultures had similar production rates, although DCA supplemented cultures were still slightly higher.

2) Glucose metabolism of CC9C10 accounted for 59% of ATP generation, with glutamine metabolism contributing the remainder. A high proportion of glucose was metabolized via glycolysis (>95%), while the pentose phosphate pathway and TCA cycle accounted for a much lower level (3.6%, and 0.6%, respectively). Alanine and CO_2 production accounted for the major end products of glutamine and glucose metabolism (54.9%, and 22.4%, respectively). Glutaminolysis was the only source of glutamine catabolism, as end product analysis could be accounted for by incomplete oxidation to 3 or 4 carbon products and CO_2.

3) CC9C10 grown with maltose and galactose as alternative carbohydrates produced varying growth yields, compared to those grown with glucose.

Lactate levels generated from maltose were 137% higher than from that of glucose, while galactose had significantly lower levels (glucose based cultures had 361% more lactate produced) .

Antibody production from CC9C10 cells grown in glucose, maltose, galactose, fructose, sorbitol, and xylitol, resulted in similar antibody yields. However, the xylitol based culture had an antibody production rate 5.59x higher than the glucose based culture. Cells with lower growth rates and high antibody production rates were attributed to CC9C10 cells taking up the alternative carbohydrates at a lower level than glucose.

4) Glucose metabolism increased at higher levels of dissolved oxygen concentrations. Radioactive experiments show an increase in the glycolytic flux, and a decrease in the pentose phosphate pathway and the TCA cycle, most noticeably the

TCA cycle. Most of the glucose (>90%) was metabolized via glycolysis. Relatively low flux rates were observed throughout for the pentose phosphate and TCA cycle pathways.

Glutamine metabolism apparently was unaffected by further increases in the dissolved oxygen concentration.

5) When hybridoma CC9C10 was compared to its parent myeloma cell line SP2/0, the following observations were observed:

a) SP2/0 is less tolerant to shear created in a spinner flask or fermentor than CC9C10.

b) CC9C10 had a quicker doubling time than SP2/0 (14.8 hours, as opposed to 19.1 hours).

c) SP2/0 had a slightly higher glutamine utilization rate than CC9C10 (1.12x).

Overall, hybridoma CC9C10 cells metabolism was similar to its myeloma parent cell line SP2/0.

These factors are discussed with respect to glucose and glutamine metabolism.

TABLE OF ABBREVIATIONS

Abbreviations	Actual Name
ADP	Adenosine Di-Phosphate
BSA	Bovine Serum Albumin
DCA	Dichloroacetic acid
DMEM	Dubelccos Minimal Essential Medium
EDTA	(Ethylenedinitrilo)-tetraacetic acid disodium salt
ELISA	Enzyme Linked Immunosorbent Assay
F-12	Hams F-12 Medium
GDH	Glutamine Dehydrogenase
GOT	Glutamine - Oxaloacetate Transferase
HAT medium	Hypoxanthine Aminopterin Thymidine medium
HGPRT	Hypoxanthine Guanine Phosphoribosyl Transferase
HPLC	High Performance Liquid Chromatography
HSFM	Hybridoma Serum-Free Medium
IgG	Immunoglobulin G
KHBB	Krebs Henseleit Bicarbonate Buffer
Mab	Monoclonal Antibody
MDCK Cell	Madin Darby Canine Kidney (Cell Line)

PBS	Phosphate Buffer Saline
PDH	Pyruvate Dehydrogenase
PDHK	Pyruvate Dehydrogenase Kinase
PDHP	Pyruvate Dehydrogenase Phosphatase
PDHR	Pyruvate Dehydrogenase Reductase
PPP	Pentose Phosphate Pathway
q_{Amm}	Specific Ammonia Production Rate
q_{Gluc}	Specific Glucose Consumption Rate
q_{Gln}	Specific Glutamine Consumption Rate
q_{Lac}	Specific Lactate Production Rate
q_{Mab}	Specific Monoclonal Antibody Production Rate
RPMI	Royal Park Memorial Institute Medium
TCA	TriCarboxylic Acid Cycle
TK	Thymidine Kinase

TABLE OF CONTENTS

LIST OF FIGURES

LIST OF TABLES

CHAPTER 1

1.1 History

Hybridoma cells are important because of their ability to produce specific antibodies (monoclonal). The term monoclonal antibody refers to a homogenous antibody produced by a clone of antibody forming cells (Coleman, 1989).

Monoclonal antibodies have practical applications in therapeutic usage, fermentation products, affinity separation, diagnostic and chemical assays, and antibody-antigen interactions (Hubbard, 1983; Morrison and O, 1989). Antibodies are a class of proteins which are created in response to an antigen which specifically reacts with that antibody. They are responsible for immunity to infections and tumors (Coleman, 1989).

In the late 1800's when antibodies were unheard of, there was a debate as to whether immunity was cellular or humoural. Von Behring and Kitsato showed the transfer of antibodies by serum from one animal to another could confer resistance (Silverstein, 1989; Glacken *et al*, 1991). This brought forth questions as to how and where the antibodies formed within the immunized host (Bibel, 1988).

Buchner was the first to confront this problem. He suggested that an antitoxin was formed directly from the toxin itself (Silverstein, 1989).

Objections to Buchner's hypothesis were made that same year by Roux and Voillard. Together, they showed that the continuous bleeding of a horse immunized with tetanus toxin did not diminish the antibody titre, even after the equivalent removal of its entire original blood volume (Silverstein, 1989).

The major theory that would cause debate for several years was the side chain theory developed by Ehrlich. Ehrlich proposed that immunological specificity was due to a unique stereo chemical relationship between active sites on antigen and antibody,

and introduced the concepts of functional and affinity domains on the antibody molecule (Silverstein, 1989). His theory suggested that cells already knew how to make specific antibodies. Ehrlich suggested that specific side chains on cells would bind specific antigens, and be assimilated into the cell. Following this, the receptors are freed for renewed function, or regenerated by the cell. Overexposure to a receptor specific antigen would stimulate the cell to produce more of that receptor type, causing many to be released into the blood. This theory was not readily accepted, but no one would improve on his suggestion that antibody formation was a cellular response to the interaction of antigen with cell surface receptors for over sixty years.

In the following sixty years, several theories came forth. The most important one accepted today is the clonal selection theory, developed by Burnet, Talmage, and Lederberg.

Burnet suggested clones of cells were devoted to antibody synthesis towards a specific antigen, i.e. the antigen binds to a specific cell which then makes a clone of itself (Burnet, 1959).

Talmage devoted much of his research to the question of size and specificity of the antibody repertoire. He suggested "variable mixture of a limited number of different antibody specificities may be capable of distinguishing a far greater number of different antigenic determinants, because each combination of cross-reacting antibodies would appear as a distinct specificity" (Iverstein, 1989; Schneider and Lavoix, 1990). This meant the genetic coding of only 5000 types could be stored in the genome, rather than millions.

Lederberg stated that immunological specificity's were determined by a unique primary amino acid sequence, the information that becomes part of a unique sequence of nucleotides. He suggested precursor cells had a high random and spontaneous mutation rate within the immunoglobulin gene (Lederburg, 1959).

Antibodies obtained from serum were found to be heterogeneous (Coleman *et al,* 1989). A mixture of antibodies produced against an antigen contain a mixture of specific antibodies for different determinants of the antigen. Researchers were pursuing the antibody structure, and its relationship to antibody specificity, and other functional activities (Coleman *et al,* 1989), but only homogenous antibodies could give this information. In 1973, Cotton and Milstein fused rat and mouse myeloma cells that formed hybrids capable of secreting both immunoglobulins (Kohler and Milstein, 1975)

In 1975, Kohler and Milstein described a method for the production of antibodies of a pre-defined specificity (Kohler and Milstein, 1975). The cell lines were made by fusing mouse myeloma and mouse spleen cells from an immunized donor. The resultant was an immortal antibody secreting clone. The spleenocyte myeloma cell hybrid was selected for by Hypoxanthine-Aminopterin-Thymidine (HAT) medium. Aminopterin functioned in the medium by blocking purine synthesis, causing cells to use the alternative purine pathway for growth. Myeloma cells died, since they did not possess the enzyme (hypoxanthine phosphoribosyl transferase [HGPRT]) required for this pathway to function (Coleman *et al*, 1989). Spleenocytes died naturally within a few days. However, the hybridomas had a specific growth rate of 0.042 to 0.021 h^{-1}. Cultures of antibody producing cells were identified. Single cells from these cultures were isolated and allowed to undergo division in order to establish a cell line which produces a specific monoclonal antibody. Figure 1.1 shows a procedure for construction of hybridomas and selection of an antibody-secreting hybridoma (Coleman *et al*, 1989). Spleen cells are taken from an immunized animal and fused to a myeloma cell line that has been selected for its inability to secrete antibodies. A further characteristic from the myeloma is used as a genetic marker, which will distinguish them from the hybridomas which are derived from the fusion of the myeloma and a B cell lymphocyte. The hypoxanthine-guanine phosphoribosyl transferase (HGPRT) enzyme is a commonly used genetic marker for this task (Coleman *et al*, 1989).

Figure 1.2 shows how the antibody producing hybridomas are selected (modified from Butler, 1987). Cells can normally synthesize nucleotides from simple precursors. Addition of aminopterin blocks this pathway, forcing the cells to use the salvage pathways. The salvage pathways convert thymidine, hypoxanthine, and guanine to their corresponding nucleotides.

Cells that have a defective HGPRT gene will not grow in the presence of aminopterin will die, as they are unable to utilize the salvage pathways. This feature will cause myeloma cells that have not fused to spleen cells to die. Unfused spleen cells die, as they cannot survive *in vitro*. Only the fusion of a spleen cell with a myeloma cell ensures their survival. The medium in which hybridomas are selected for is called HAT medium (hypoxanthine, aminopterin,, and thymidine) (Butler, 1987).

The clones are then grown, and tested for their specificity by an immunoassay of supernatant medium with an appropriate antigen or target cells attached to microtitration plates (Freshney, 1987). Enzyme conjugated antimouse immunoglobulin may be used to detect the antigen, antibody complex.

The clones that test positive are recloned, retested, and frozen to ensure antibody production, and steady growth maintained (Butler, 1987).

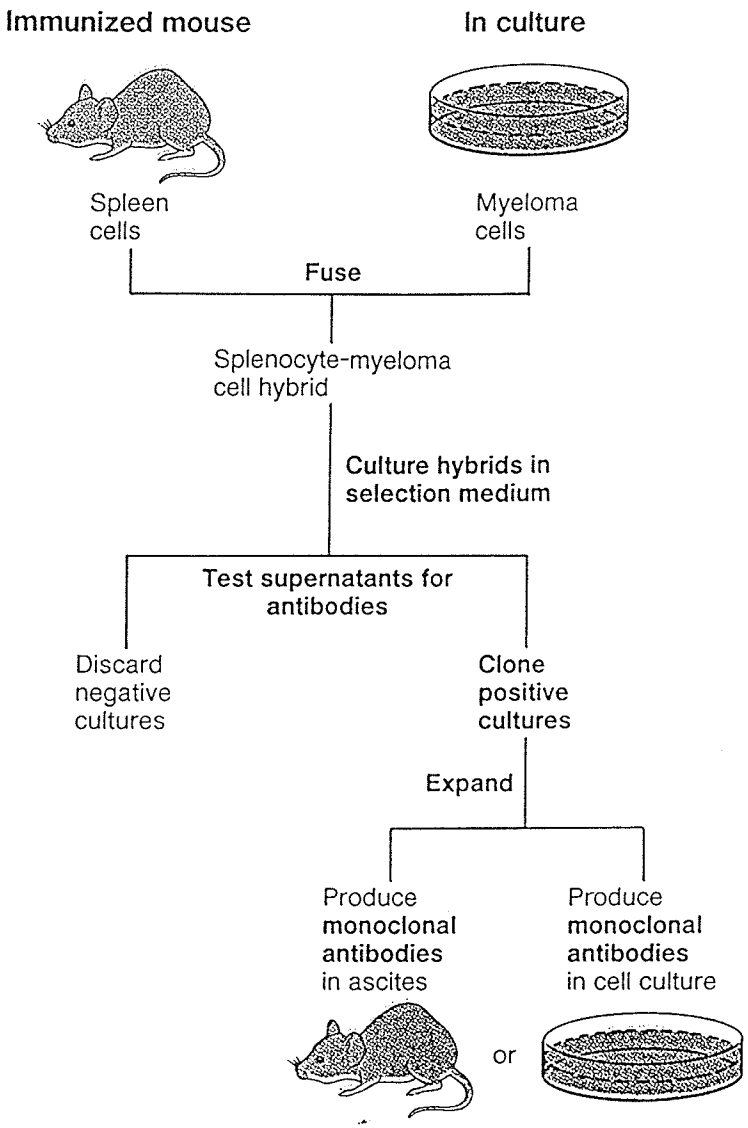

Figure 1.1. Production of monoclonal antibodies. Spleen cells or lymphocytes from an immunized mouse are fused with myeloma cells. The cells are suspended in selection medium, distributed into multiwell plates, and cultured. The selection medium supports growth of hybridomas (lymphocytes fused with myeloma cells) but not myeloma cells. Unfused spleen cells or lymphocytes die naturally within a few days. Culture supernatants are screened for antibody when cell growth is observed. Single hybridoma cells, from any well containing antibody, are cloned so that monoclonal antibodies can be produced in culture, or as ascites in mice (Fusing agents used are Sendai virus, or more commonly polyethylene glycol, selection medium used in HAT). Myeloma cells are killed in HAT since aminopterin blocks synthesis of purine and pyrimidines as myeloma cells do not possess an enzyme HGPRT, which would permit them to use an alternative metabolic pathway. Using hypoxanthine, spleenocytes and hybridomas possess HGPRT, it can therefore use hypoxanthine which allows for the selection of hybridomas (Coleman *et al*, 1989) .

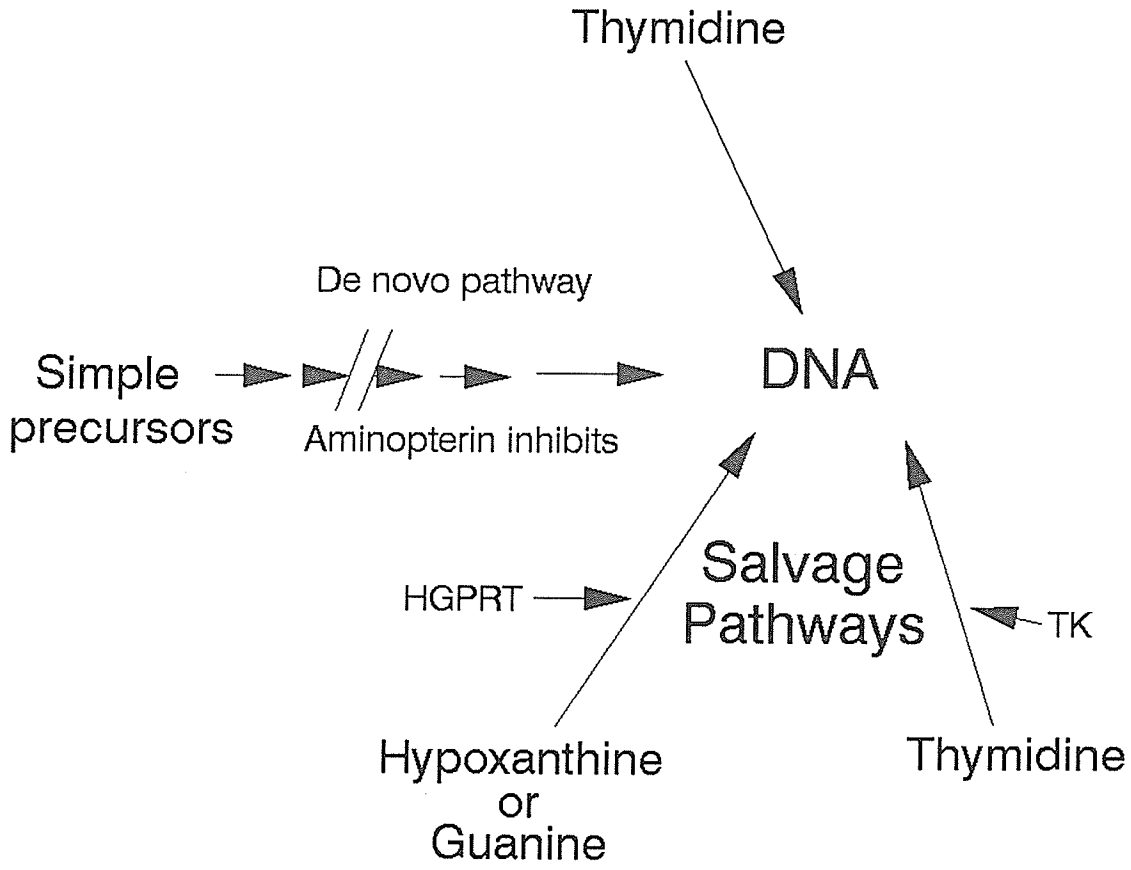

Figure 1.2. De novo and salvage pathways of nucleotide synthesis (adapted from Butler, 1987). Hypoxanthine Guanine Phosphoribosyl Transferase (HGPRT); TK (Thymidine Kinase).

1.2 The Use of Mammalian Cells in Producing Monoclonal Antibodies

Mammalian cells, although having some disadvantages, appear to be the best route at this point in time for obtaining therapeutic monoclonal antibodies. Attempts to increase product formation rates in mammalian cells has been progressing (Wilson, 1984). Microbial production of monoclonal antibodies has been considered, as mammalian cells grow more slowly, are more sensitive to shear, and require more expensive media than yeast (Colby *et al*, 1984). Microbial antibody production has been attempted in *E. coli* (Boss et *al*, 1984). Heavy and light chains of the antibody were expressed, and secreted, however there was little, if any glycosylation observed, as well as H-chain - L-chain association. Antibody production using *Saccharomyces cerevisiae* by Wood *et al* (1985) showed that a significant proportion of yeast heavy chain is N-glycosylated. Yeast and mammalian heavy chain will probably differ in carbohydrate composition, especially if the yeast heavy chain has outer chain oligosaccharides (Chapman and Kornfield, 1979; Ballou, 1982; and Colby *et al*, 1984).

Ozturk *et al* (1990) used two murine hybridoma cell lines (167.4G5.3 and S3H5γ 2bA2) which were adapted to grow in low serum and serum-free media by a weaning procedure. 167.4G5.3 produced less total IgG_1 after adaptation to low serum, while S3H5/γ2bA2 cells had higher antibody concentrations after adaptation due to higher growth rates and cell concentrations. Again, antibody productivity in low serum or serum-free media appeared to be cell line dependent.

Monoclonal antibody production has been observed to occur throughout the growth of a batch culture and stationary phase has been previously examined (Biblia and Flickinger, 1991). In batch culture, mammalian cells rapidly utilize glucose and glutamine (both are the major energy sources of mammalian cells) during the mid-exponential phase, causing the cells to enter the stationary phase due to a lack of nutrients (Schneider *et al*, 1990). Antibody production occurs throughout the mid-

exponential phase, into the stationary phase, where antibody production rates increase (Reuveny, S. *et al*, 1986). Several researchers (Tolbert et al, 1985, N. Emery, 1986), have noted that maintaining hybridomas under conditions of slow growth (perfused systems, immobilized cell reactors) caused specific antibody production to be higher as growth rates decreased, suggesting that antibody synthesis might be non-growth associated.

Although an antibody is not a primary metabolite (Stryer *et al* 1988), manufacturing such a large protein molecule would expend energy from the cell. The major carbon and energy sources of hybridomas are glucose and glutamine (McKeehan, 1986; Jenkins *et al*, 1992). Under such conditions of a continuous perfusion, providing hybridoma cells with fresh medium, non-growing hybridoma cells could maintain a sufficient pool of assembly mediating factors to sustain or even increase antibody assembly rates as growth rate decreases.

Eagle first demonstrated (Eagle, 1955) that mammalian cells could be grown in a medium consisting of a given amount of amino acids, vitamins, cofactors, carbohydrates, and salts supplied with a small amount of serum. Eagle developed this formulation to aid in the identification of the specific requirements for growth, since serum is chemically undefined.

In 1976, Hayashi, and Sato (1976) demonstrated that replacement of serum by hormones permited growth in a defined medium. They showed that medium supplemented with hormone substitutes for serum could allow growth of cells, without altering the characteristics of the individual cells, or the overall population

Replacement of serum to serum-free medium is beneficial, because of the high cost involved in purchasing serum (Ozturk *et al*, 1991), separation of serum proteins from products (Ozturk *et al*, 1991), contamination (Glassy *et al*, 1988), and factors present in the serum which could be inhibitory to antibody secretion (Glassy *et al*, 1988). Table 1.1 shows the advantages and disadvantages of serum-free media for

hybridomas (Glassy *et al*, 1988). Hybridoma cell lines must first be cloned in low serum conditions, and then gradually adapted to culture in a protein and serum-free defined medium (Ozturk *et al*, 1991; Schneider and Lavoix, 1990). Yen and Doigou (1983) culturing human lymphocytes found that doubling times between serum and serum-free media comparable. However, cells conditioned to grow in low serum, or serum-free media, by an adaptation procedure often have better growth. If the cells are maintained in low-serum, or serum-free for a long enough time span, they typically acheive higher growth rates than media containing higher serum levels (Maur, 1986).

Table 1.1. Advantages and disadvantages of serum-free media for hybridomas (Glassy et al, 1988).

Advantages:

1) Consistent and chemically defined composition.
2) Improves reproducibility of cell culture growth and product yield.
3) Decreases potential of contamination.
4) Reduces difficulty and savings with a low protein serum-free formulation.

Disadvantages:

1) Requires optimization for each hybridoma.
2) Applicable serum-free media have not been developed for all cell lines.
3) May require serum hormones and growth factors which are difficult to isolate and purify.
4) Frequently results in longer lag periods.
5) Cell growth rate maximum cell density and cell viability are often lower.
6) Protease inhibitors in serum may help protect cells from enzymes such as trypsin.

1.3 Glucose and Glutamine Metabolism

Glucose and glutamine are the major energy sources used by transformed mammalian cells in tissue culture (Miller *et al*, 1989). The major product of glucose metabolism, is lactate (Miller *et al*, 1989). CO_2 is another product which occurs upon oxidation through the TCA pathway (Lanks *et al*, 1988). The major end products of glutamine metabolism are lactate, CO_2, ammonium ion, aspartate, glutamate, and alanine (Lanks and Li, 1988; Haggstrom, 1991; Wu *et al*, 1991).

Glucose may be used by cultured cells as a substrate to form pyruvate, the pentose phosphate pathway (PPP) for producing NADPH + H^+ for the biosynthesis of lipids and other cellular compounds, and ribose-5-phosphate for nucleic acids (Coleman *et al,* 1989; Schroer *et al,* 1983). Figure 1.3 illustrates the routes of glucose metabolism (adapted from Stryer, 1988).

Changing the glucose concentration from 10 μM to 5 mM in batch culture dramatically increases the specific glucose consumption rate (Zielke *et al,* 1978). The specific glucose consumption rate is unaltered by further increases in glucose concentration (Low and Harbour, 1985). Rat hepatanoma cells cultured with glucose concentrations ≤ 5 mM only had half of the glucose incorporated into nucleotides. At 5 mM glucose, 90% was converted to lactate (Miller *et al*, 1989).

In most tissues, glycolysis is inhibited upon the availability of oxygen. Pasteur first noticed this in yeast, and was named the "Pasteur Effect" by Warburg (Warburg, 1956). Respiration is more efficient than fermentation from an energetic viewpoint. Thirty eight ATP can form from 1 glucose molecule passing through the TCA cycle, as opposed to 2 ATP produced from glucose forming lactate (Stryer, 1988). The Pasteur Effect does not occur in some tissues; even in the presence of oxygen there is a high glycolytic flux. This fact has been termed aerobic glycolysis, and it has different causes, depending upon the tissue under study (Krebs, 1972; Sols, 1975). The

addition of glucose has been shown to decrease the specific oxygen consumption rate (Glacken *et al,* 1988). and the extent of glutamine metabolism (Glacken *et al,* 1988)

Glutamine is considered a major carbon and energy source of rapidly dividing mammalian cells in culture (Ozturk ,and Palsson, 1991; Reitzer *et al,* 1979; Zielke *et al,* 1984). However, glutamine may also undergo complete oxidation to CO_2 via the TCA cycle, or partial oxidation to 3 or 4 carbon products such as lactate, alanine, or aspartate, as shown in Figure 1.3. The latter process, known as glutaminolysis, has been shown to provide a substantial proportion of the cellular energy requirement in transformed cells (Haggstrom, 1991; Lanks and Li, 1988; Wu *et al*, 1991). Glutamine is the most abundant amino acid in the plasma, and plays a crucial role in cellular physiology (Brosnan *et al,* 1987; Haussinger, 1990). Glucose has been assumed to be the primary energy source for cultured cells because of the rapid metabolism of glucose to lactate (Levintou, 1961; Morrel and Froesch, 1973; Paul, 1965). However, glutamine metabolism has been shown to provide 30-65% of the energy for mammalian cell growth (Reitzer *et al,* 1979; Zielke, *et al* ,1984).

Eagle stated that glutamine plays a critical metabolic role for the growth of cultured cells as well as serving as a protein precursor (Eagle, 1955). Glutamine is transported into the cell by system N^m. System N^m is a sodium dependent system which transports glutamine, histidine, and asparagine. This system is pH independent, but hormone sensitive, particularly to glucocorticoids and insulin (Hundal *et al,* 1987). Upon glutamine beingtransported into a cell, it can be catabolized via glutaminolysis, or incorporated into protein or nucleotide synthesis (Medina and DeCastro, 1990). Figure 1.3 represents the different routes which glutamine may go upon entry into a cell. Butler *et al* (1990b), measured the flux of glutamine through the membrane, and the activities of the enzymes of glutaminolysis and concluded that the rate limiting step of the metabolism of glutamine was membrane transport into the cell. The activity of the

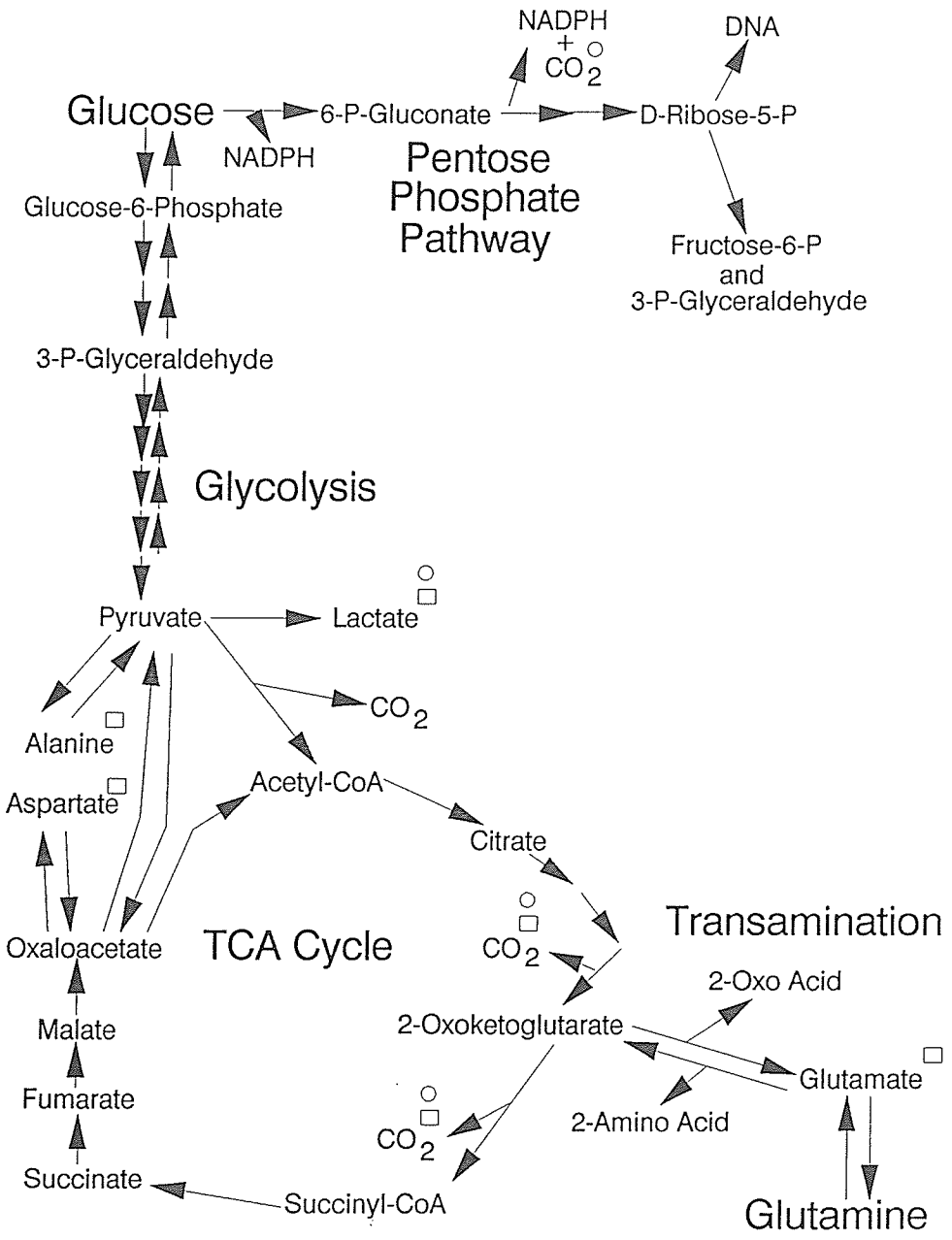

Figure 1.3 A representation of major end products of gluocose and glutamine metabolism in hybridomas. O represents the major end products of glucose metabolism. □ represents the major end products of glutamine metabolism. (Figure adapted from Stryer, 1988).

enzyme, glutamine dehydrogenase (GDH) increased to a low level, while glutamate-oxaloacetate transferase (GOT) increased to a level nearly two orders of magnitude greater than the activity of GDH (Butler, 1990b). This suggested that transamination was the more favored path for conversion of glutamate to α-ketoglutarate.

High ammonium ion concentrations, as a result of glutamine metabolism has been linked with cell growth inhibition (Butler and Spier, 1984; McQueen and Bailey, 1990a). Boron *et al* (1976), observed that measurements of NH_4^+ caused decreases in intracellular pH, involving the uptake of the weak acid NH_4^+ into the cytoplasm causing acidification. McQueen and Bailey (1990b) hypothesized a sequence of events after addition of NH_4Cl to a cell suspension:

"1) NH_4Cl dissociates into NH_4^+ and Cl^-, and NH_4^+ partially dissociates into NH_3 and H^+.

2) NH_3 rapidly permeates the cell membrane and reassociates into the cytoplasm, causing an intracellular alkalinization.

3) NH_4^+ slowly permeates the cell membrane, driven in by the membrane potential as well as the concentration gradient, and partially dissociates in the cytoplasm, causing intracellular acidification.

4) When pH falls below its original steady-state value, the H^+ pump is activated, and H^+ ions are pumped out of the cell to counteract the intracellular acidification caused by the NH_4^+ ion.

5) NH_4^+ creates a persistent acid load on the cells because it sets up a proton shuttle into the cell, in which NH_4^+ entry is balanced by NH_3 exit.

6) The additional acid load upsets the previous equilibrium between H^+ production and exit. The value of pH reaches a new, lower steady state value, at which the net rate of H^+ entry due to NH_4^+ leakage into the cell is actively balanced by the increased rate of H^+ exit due to active transport".

In vivo, mammalian cells remove NH_4^+ by converting it into urea, and excreting it into the urine (Pitts *et al* , 1947). *In vitro,* there is no such mechanism, so NH_4^+ just accumulates in the culture medium.

A large amount of glutamine is utilized in aerobic energy metabolism in HeLa cells (Reitzer *et al,* 1979). Schneider and Lavoix (1990) reported that the mean actual concentration of ammonia was proportional to glutamine concentration in the nutritive medium. The result of this proportionality would lead to a large accumulation of ammonia. Hassell and Butler (1990) have suggested replacing glutamine with glutamate, or 2-oxoglutarate in order to reduce the ammonia concentration of the medium .

1..4 The specific aims of the MSc. were to:

1) Adapt hybridoma CC9C10 cells to varying concentrations of dichloroacetic acid (DCA) in Royal Park Memorial Institute (RPMI) medium, Dubelccos's Minimal Essential Medium (DMEM), and Hybridoma Serum-Free Medium (HSFM), and study its effect on cell growth, glucose consumption, lactate production, oxygen consumption, and monoclonal antibody production. DCA has previously been shown to exert its effects on the pyruvate dehydrogenase enzyme (Whitehouse *et al*, 1973), which would lower lactate, pyruvate, and alanine levels.

2) Examine glucose metabolism (TCA cycle, PPP, and glycolysis), and glutamine metabolism (end product analysis) of hybridoma CC9C10 cells taken from mid-exponential phase to determine eacch percentage of cellular energy generated from glucose and glutamine metabolism.

3) Adapt CC9C10 hybridoma cells to alternative carbohydrate sources, examining their effects on cell growth, lactate production, and monoclonal antibody production.

4) To determine the effect of dissolved oxygen concentrations (10%, 50%, and 100% air saturation) upon a hybridoma culture grown in a fermentor setup in chemostat mode with respect to glucose and glutamine metabolism.

5) A metabolic comparison between hybridoma CC9C10 and its parent myeloma cell line SP2/0, to determine if there were any significant metabolic differences between the two. As hybridoma CC9C10 is the resultant of a fusion between a spleenocyte and myeloma cell, it theoretically has 50% of its myeloma parents genetics. Differences in

the levels of metabolism between the two cell lines may lend information as to what percentage of cellular energy is required for antibody production.

The objectives discussed above are important for optimizing hybridoma cell growth under different parameters with respect to glucose and glutamine metabolism.

CHAPTER 2

2.0 General Materials and Methods

2.1.0 Cell Line

a) The cell line chosen for experimentation was the mouse-mouse hybridoma cell line CC9C10. The hybrid cell line CC9C10 secretes a monoclonal antibody (IgG_{ik}) that binds insulin from human, beef, pork, rabbit, and sheep. The hybridoma was produced by fusing lymph node cells of a BALB/c mouse immunized with beef insulin with the SP2/O-Ag14 cell line (Schroer *et al,* 1983).

b) The SP2/0 myeloma cell line was chosen for a metabolic comparison with hybridoma CC9C10 (Shulman *et al*, 1978).

Both cell lines were shown to be mycoplasma-free by routine testing in an independent laboratory (Rh Pharmaceuticals).

2.1.1 Growth of Cells

a) The hybridomas were grown to stationary phase culture or a suspension culture. The hybridomas were grown in tissue flask (150 cm^2 T-flask) culture, where cells grew in suspension. Growth limitation was a problem for cells under these conditions, as spatial concentration gradients of metabolites can affect the mass transfer rates between the cells, liquid phase, and gas phase (Katinger and Schreirer,

1985). Due to the limitations of this system, it was used for maintaining cell lines, or experiments which required a large number of different cultures.

b) Suspension cell cultures were maintained by growing cells in Bellco spinner flasks of either 100 ml or 250 ml volume capacity. A magnetic stirrer was set at 80 rpm causing mixing of the cells, and media, ensuring that metabolites and cells were uniform throughout the culture, and that oxygen would not become limiting. Stirring of a culture promoted oxygen diffusion into the medium. The spinning of cultures were not be carried out at too fast rates, as mammalian cells are more sensitive to shear than bacteria or yeast (Miller *et al,* 1988). The cultures were incubated at 37^{o}C under a 5% or 10% CO_2 overlay depending upon whether the cells were grown in RPMI medium, or DMEM based media, respectively.

c) Hybridomas were grown in 1.2 liter cultures in a Celligen (New Brunswick) bioreactor at a stirring speed of 100 rpm at 37^{o}C under a 10% CO_2 overlay. Air saturation of the fermentor were set at 10% 50% and 100% to increase the oxygen concentration at each different level. A chemostat mode was maintained at a constant dilution rate of 1 volume per day.

d) Cells were cultured in 1.5 liter cultures in a LH (LH Series 210) bioreactor at a stirring speed of 100 rpm at 37^{o}C under a 10% CO_2 overlay. Air saturation levels were set at 50%. A chemostat mode was maintained at a constant dilution rate of 0.5 volumes per day.

2.1.2 Growth Medium Preparation

The growth medium consisted of either Royal Park Memorial Institute medium (RPMI) (Moore, 1967), Dubelccos Minimal Essential Medium (DMEM) (Dubelcco and Freeman, 1959), and DMEM - Hams F12 (Ham, 1965) (an equivalent amount of powdered DMEM and F-12) supplemented with serum, hybridoma serum-free medium ™ (HSFM™) purchased from GIBCO, or a serum-free medium (made in house):

a) RPMI and Fe-enriched calf serum were purchased from GIBCO. Glutamine and glucose were purchased from Sigma. Glucose, and glutamine were added to the media at concentrations of 10 mM or 20 mM, and 2 mM, respectively. Following this, the media were filter sterilized using Acrocap filters from Gelman Sciences, into sterile 500 ml bottles. Calf serum was added to the media such that the final concentration was 10% (v/v).

b) DMEM and Fe-enriched calf serum were purchased from GIBCO. Glucose and glutamine were added to the medium at concentrations of 17.5 mM, and 4 mM, respectively. The appropriate mixture of powdered DMEM was added, and suspended to the appropriate volume. The media was filter sterilized using a Gelman filter from Gelman Sciences, into sterile bottles. Fe-enriched calf serum was added to media, so the final concentration was 10% (v/v).

c) Hybridoma Serum- Free Medium ™.

d) The serum-free medium consisted of the following ingredients: Powdered F12 and DMEM (glutamine-free, glucose-free, and phenol red-free) were purchased from GIBCO, glucose, glutamine, phenol red, insulin, transferrin, Pluronic F-68 (Pluronic F-

68 is a powder added to medium aiding in increasing the viscosity of the medium), phosphoethanolamine, ethanolamine, and NaSe were purchased from Sigma. Table 2.1 illustrates the preparation of the serum-free medium.

2.1.3 CC9C10 Hybridoma Cell Line Maintenance and Routine SubCulturing

A sample of cells from a culture in the mid-log phase was added to growth medium such that the seeded cell density was 1×10^5 cells/ml. The caps were left loose to allow gas equilibrium and pH stabilization, as closing caps was observed to decrease cell health and density. The flasks were stored in a CO_2 incubator at 37°C with a 5%, or 10% CO_2 overlay. Cells used for experimentation were either grown in 100 ml or 250 ml Bellco spinner flasks as described above (2.1.1 b), except those cultures were stirred at 80 rpm.

2.1.4 Cell Counting

Samples of cell suspension (500 µl) were diluted 1:1 with 0.4% trypan blue in phosphate buffered saline (PBS) (Butler and Jenkins, 1989). Two grids of a haemocytometer were loaded with cell suspension and 10 squares counted. The cells which did not take up stain were counted as viable, and those which appeared blue were counted as non-viable. Cell counts were averaged from the 10 squares, and multiplied by 2×10^4 to give cells/ml. Total cell counts were determined by adding the total viable and non-viable cell counts.

Table 2.1 Preparation of Serum-Free Medium.

F-12 from Powder: $NaHCO_3$ to 3.7 g/l
Glutamine to 8 mM (0.513 g/l)

DMEM:

Glutamine free		Glutamine to 4 mM (0.293 g/l)
Glucose free	---------->	Glucose to 25 mM (2.25 g/l)
Phenol Red free		Phenol Red at 15 mg/l

Serum-free medium:

250 ml F12 + 250 ml DMEM:	6 mM glutamine 17.5 mM glucose 8.1 mg/l phenol red

Addition to 500 ml media:

Stock Solution	Concentration of Stock Solution	Volume Added to Media (ml)	Final Concentration
Bovine Insulin	5 mg/ml	1.0 ml	10 μg/ml
Bovine Transferrin	5 mg/ml	1.0 ml	10 μg/ml
Pluronic F-68	10% (w/v)	5.0 ml	0.1% (w/v)
Phosphoethanol-amine	50 mM	1.0 ml	100 μM
Ethanolamine	4 mM	1.25 ml	10 μM
Sodium Selenite	1×10^{-5} M	0.5 ml	10 nM

2.2 Cryopreservation of Hybridoma Cells

2.2.1 Freezing Procedure

Cells were frozen in liquid nitrogen for long term storage. A cell suspension was centrifuged at 1000 rpm for 5 minutes. The cell pellet was re-suspended in cell culture freezing medium (DMEM-F12 + 10% calf serum + 10% dimethylsulfoxide) such that the final cell density was 1×10^7 cells/ml. 1 ml aliquots of this cell suspension were added to freezing ampoules. The ampoules were sealed and placed into a foam box with ice at -80^{o}C overnight. The ampoules were fixed into freezing canes, and placed in a liquid nitrogen cylinder on the following day.

2.2.2 Recovery from Liquid Nitrogen

An ampoule of frozen cells was removed from liquid nitrogen, and rapidly thawed at 37^{o}C in a hot water bath. The cell suspension was transferred to a sterile plastic centrifuge tube (15 ml, Corning), and 10 ml of growth medium added. The cells were pelleted by centrifuging at 1500 rpm for 5 minutes. The cells were re-suspended in an appropriate volume of growth medium such that the cell density was 2×10^5 cells/ml.

2.3 Analysis of Culture Media

2.3.1 Glucose and Lactate Concentrations

Cell free samples (25 μl) of culture supernatant were injected into a YSI Model 27 Industrial Analyzer . The instrument was fitted with the appropriate membrane for determining glucose or lactate concentrations. The analyzer was calibrated by the injection of standard glucose solutions (25 μl; 200 mg/dl and 500 mg/dl). For lactate measurements, the analyzer was calibrated by the injection of standard lactate solutions (25 μl; 44.5 mg/dl and 133.6 mg/dl).

2.3.2 Monoclonal Antibody Determination

Monoclonal antibody levels were determined by two methods:

1) Enzyme Linked ImmunoSorbent Assay (ELISA) assay for cells cultured with serum.
2) ProAna ™Mabs column for cells cultured in serum-free medium.

2.3.2.1 ELISA Assay (Good for one plate)

2.3.2.1.1 ELISA Reagents

10x PBS

10.52 g/l Na_2HPO_4

3.09 g/l NaH_2PO_4

8.5 g/l NaCl pH adjusted to 7.2

0.1 M Carbonate Buffer

3.18 g/l Na_2CO_3

5.88 g/l $NaHCO_3$ pH adjusted to 9.5

Substrate Buffer

7.51 g/l glycine

0.203 g/l $MgCl_2 \cdot H_20$

0.136 g/l $ZnCl_2$ Added to 980 ml of water, pH adjusted to 10.4 with NaOH, and brought up to 1 l

2.3.2.1.2 ELISA Procedure

1) NUNC 96 well plates were coated (100 µl/well) with goat anti-mouse immunoglobulin G (IgG) 1/1000 dilution in 0.1 M carbonate buffer pH 9.5. The plate was covered with parafilm and incubated overnight at 4°C. For 1 ELISA plate: 12 µl antimouse IgG and 12 ml of carbonate buffer were mixed together, and 100 µl was placed into each plate well.

2) Phosphate buffered saline (PBS) - 0.1% Tween preparation:

40 ml PBS (10x concentrate)

360 ml H_2O

400 µl Tween 20

3) After overnight incubation, wells were washed 4 times with 200 µl/well PBS-0.1% Tween. PBS-0.1% Tween was left in wells 5 minutes each time, and the liquid was tapped out firmly. All subsequent washes were performed this way.

4) PBS-1% bovine serum albumin (BSA) preparation:

2.5 ml 10x PBS

22.5 ml H_20

0.25 g BSA

5) Wells were blocked with 200 µl/well PBS-0.1% BSA. The plate was Incubated for 1 hour at 37°C (Parafilm was put over the plate to avoid CO_2 exchange).

6) Wells were washed three times with 200 µl/well PBS-0.1% Tween.

7) PBS-0.1% BSA preparation: 5 ml 10x PBS

45 ml H_20

0.05 g BSA

8) Monoclonal antibody standards preparation: Dilutions were prepared in the range of 0.35 µg/ml to 0.00273 µg/ml using PBS-0.1% BSA as the diluent. i.e. If the monoclonal antibody (Mab) standard was 100 µg/ml, 10 µg Mab + 990 µl PBS-0.1% BSA was added → 1 µg/ml. Add 300 µl of PBS-0.1% BSA to 7 more tubes and 1 in 2 dilutions performed.

9) Unknown preparation: The dilutions were made in PBS-0.1% BSA. Dilution's were made from 1 in 200 to 1 in 1600.

10) Standards and unknowns were added to wells (100 µl/well) in duplicate.

11) The plate was incubated for 1 hour.

12) Wells were washed four times with 200 µl/well PBS-0.1% BSA.

13) Goat-antimouse IgG alkaline phosphatase preparation: 6 μl + 12 ml PBS-0.1% BSA. 100 μl/well was added, and incubated for 30 minutes at 37°C.

14) Wells were washed four times with 200 μl/well PBS-0.1% BSA..

15) Substrate preparation: A 15 mg tablet of p-nitrophenyl phosphate was thawed before hand. The tablet was added to 15 ml substrate buffer during the last wash with PBS-0.1% Tween (Step 14). 100 μl substrate/well added.

16) A kinetic run was performed over 30 minutes (measuring O. D. at 405 nm) or incubated at 37°C for 30 minutes in a Thermomax Plate Reader (Molecular Devices) and an end point reading was taken. A program called Softmax was linked to the Thermomax via computer. A standard template was prepared and used for all plates. The template contained Mab standards, and blanks, and diluted samples as previously mentioned. the Softmax offered two methods of determining antibody quantity: kinetic run, or an endpoint reading. During a kinetic run, the Thermomax was set to read the plates every 10 seconds. A plot of ΔO.D. vs. time was displayed for every well. Antibody concentration was determined on the basis of the slope of the kinetic run. The end point reading was determined by a final determination of O.D. to determine the antibody concentration (μg/ml).

2.3.2.2 ProAna ™Mabs Column

This column was purchased as a kit from Biolytica, a division of HyClone. The ProAna ™Mabs was used for the detection of monoclonal antibodies. It was delivered as a complete kit, ready to run in an HPLC system. Developed by Perstep Biolytica, ProAna ™Mabs was optimized for rapid quantitative analysis of monoclonal antibodies from crude samples i.e. fermentation broth.

The ProAna ™Mabs column was 50 x 5 mm, consisting of a 10 μM selectisphere HPLC silica support to which bacterial F_C receptor was attached. The ProAna ™Mabs binding, and elution buffer concentrates were diluted with de-ionized water, followed by filtration (0.45 μm). The pH of the Binding Buffer should be 5.0 ± 0.10. The pH of the Elution Buffer should be 1.6 ± 0.05. If required, the pH was adjusted by adding HCl or NaOH.

Monoclonal antibodies were detected by absorbance at 280 nm. To evaluate antibody quantity, a standard curve was made by plotting the peak height of the eluted peaks versus the concentration of IgG standard. One ml samples were injected and run in an analytical cycle.

This column was only used for analysis of serum-free medium, as medium containing serum contains a high background level of IgG antibodies.

Table 2.2 A typical analytical cycle for HPLC.

Time (min)	Event	Buffer	Flow Rate (ml/min)
0	Injection	-	-
0-2	Sample loading and washing	Binding Buffer	2
2-4	Elution	Elution Buffer	3
4-7	Equilibration	Binding Buffer	2

2.3.3 Glutamine Assay Procedure (adapted from Lund, 1986)

2.3.3.1 Glutamine Assay

Principle:

Reaction #1
(Endpoint)

$$\text{L-glutamine} + H_2O \xrightarrow[H^+]{\text{glutaminase}} \text{L-glutamate} + NH_4^+$$

Reaction #2

$$\text{L-glutamate} + NAD^+ + H_2O \xrightarrow[\text{glutamate dehydrogenase}]{\text{ADP}} \text{2-oxoglutarate} + NH_4^+ + NADH$$

The optimum pH for reaction #1 (glutamine hydrolysis) was 5.0 carried out in acetate buffer. The equilibrium of reaction #2 favored the formation of L-glutamate. To overcome the unfavorable kinetics a high concentration of NAD, a low proton concentration (pH 9.0) and a trapping agent for 2-oxoglutarate (hydrazine hydrate) were used in reaction #2 to activate glutamate dehydrogenase. Adenosine di-phosphate (ADP) aided in enhancement of the glutamate dehydrogenase enzyme activity.

The formation of NADH is proportional to L-glutamate in reaction #2. The formation of NADH was measured by the change in absorbance at 340 nm vs. time (O.D. / minute).

2.3.3.2 Stock Solutions

1) Acetate buffer (0.5 M, pH 5.0)

a) 6.8 grams of sodium acetate was dissolved in water, and made to 100 ml.

b) 2.9 ml glacial acetic acid was diluted up to 100 ml with water.

67.8 ml of 1a) and 32.2 ml of 1b) were mixed together. pH adjusted to 5.0.

2) Glutaminase (10 kU/l)

Glutaminase (Sigma G5382) was dissolved in 10 fold diluted acetate buffer to obtain 10 kU/l. Aliquot were made in 250 µl quantities.

3) Hydroxylamine (20 mM)

13.9 mg hydroxylamine was dissolved in 10 ml of water.

4) L-glutamine standard (100 mM)

146 mg L-glutamine was dissolved in 10 ml water.

5) Tris-EDTA (Tris 0.25 M, EDTA 5 mM)

3 g of Trizma base, and 185 mg EDTA were dissolved in 100 ml of water.

6) Hydrazine hydrate 62% (w/v).

7) β-NAD (30 mM)

200 mg β-NAD (free acid) was dissolved in 10 ml water. Aliquots were made in 1.5 ml quantities.

8) ADP (100 mM)

48.0 mg ADP-sodium salt was dissolved in 800 µl water, neutralized with 100 µl NaOH (2 M), and made up to 1 ml with water. Aliquots were made in 150 µl quantities.

9) Glutamate dehydrogenase (GDH)

Sigma G2626, 2500 kU/l

10) Tris/Hydrazine buffer

9 ml Tris EDTA (5) + 1.1 ml hydrazine hydrate (6) were mixed together. The pH of the solution was adjusted to 9.0 with 5 M HCl and made up to 15 ml. The solution was stable for 1 week in the refrigerator.

Solutions 1, 3, and 5 were stored in the refrigerator. Solutions 2, 4, 7, and 8 were stored at -20^{o}C.

2.3.3.3 Assay

The following solutions were made prior to use. Quantities were based on a 96 well plate analysis.

Solution A: 2.16 ml acetate buffer (1)

1.1 ml hydroxyl amine (3)

1.16 ml water

Kept in 37°C water bath, 108 µl glutaminase (2) added prior to use.

Solution B: 2.16 ml acetate buffer (1)

1.10 ml hydroxyl amine (3)

1.265 ml water

Solution C: 9.6 ml Tris/hydrazine (10)

3.1 ml water

Put at 37°C for 15 minutes.

1.44 ml NAD (7)

144 µl ADP (8)

90 µl GDH (9)

The above was added to solution C just prior to use.

Glutamine standard: Stock solution (4) diluted to give doubling dilutions ranging from 0.5 mM to 0.03215 mM.

2.3.3.4 Assay Procedure

A NUNC 96 well plate was divided into two sections. The first section (A) was treated with solution A (conversion of glutamine to glutamate). The second section (B) was treated with solution B (no conversion).

1) 70 µl samples were pipetted into wells. Each sample was present in both sections (A and B) of the 96 well plate. 70 µl standard glutamine solutions (in duplicate) were pipetted on the solution A section.

2) 50 µl solution A added to section A.
50 µl solution B added to section B.
Plates were covered with parafilm and incubated in a Thermomax microplate reader or CO_2 incubator for 75 minutes at 37°C (endpoint reaction).

3) After the incubation period, 120 µl of solution C was added to all of the wells, and mixed once in the Thermomax plate reader (37°C)
The absorbance was read at 340 nm for 3 minutes with the Softmax program (kinetic assay).

2.3.3.5 Preparation of Samples

Samples to be treated with solution A had glutamine concentrations in the range of 0.05 mM to 0.5 mM for analysis. Samples were diluted with water to fall within this range. If the expected glutamine concentration was between 2 to 6 mM, samples were diluted 1 in 15, and 1 in 10. If the expected glutamine concentration was between 0 to 1 mM, samples were diluted 1 in 5, or not diluted.

Samples which were treated with solution B should not have had glutamate concentrations in the range of 0.005 mM to 0.5 mM. Dilutions of 1 in 5 and no dilution of samples were found to be sufficient in batch culture samples.

2.3.4 Ammonia Concentrations

Ammonia concentrations were determined using an Orion 9512 ammonia probe connected to a Fisher Scientific accumet® pH meter 25. A series of standards consisting of 1×10^{-5}, 1×10^{-4}, 1×10^{-3}, 1×10^{-2}, and 1×10^{-1} M NH_4Cl were used for creating a standard curve before determination of samples. 1 ml of sample along with 10 µl of 10 M NaOH were added to a tube. A measurement from the probe was made upon the sample giving a constant mV reading.

2.3.5 Lactate Dehydrogenase Assay

Determination of lactate from this assay was used to determine the position of lactate from the fractions collected from running glutamine end-point standards through a Dowex-50W resin column Na form; mesh size 200-400 (55cm x 1 cm). Lactate concentrations were determined enzymatically by monitoring reduction of NAD during the conversion of lactate to pyruvate by lactate dehydrogenase:

$$\text{Lactate} + \text{NAD} \text{--------} > \text{Pyruvate} + \text{NADH} + H^+$$

The deproteinized samples were diluted with distilled water (4^{o}C) to give an appropriate concentration of lactate. For the assay, sample (20 μl) was added to 0.5 M glycine-hydrazine buffer, pH 9.0 (2.35 μl) together with 20 μl NAD (30mg/ml) in a Falcon 96 well plate which contained 50 μl lactate dehydrogenase (1000 U/ml, diluted 1 in 5). Two wells were used as the control for determining the initial absorbance at 340 nm (no addition of LDH). A standard template was prepared for all plates. The Thermomax plate reader was coupled to a program celled Softmax via a computer. The template contained blank wells, control wells, and lactate standards ranging from 0 to 2 mM. Samples were diluted accordingly such that they would fall within the standard range. After incubation at 37^{o}C for 30 minutes, the final absorbance of each sample was read. The lactate concentrations were determined by comparison with a lactate standard curve (0-10 mM) prepared by replacing sample with a range of standards diluted with perchloric acid (20% w/v), in the assay (Lloyd, 1978).

2.3.6 HPLC Analysis

245 μl standards and samples were added to 2 ml Eppendorf tubes and were treated with 5 μl of 0.025 M L-α-amino-n-butyric acid. 250 μl of 10% trichloroacetic acid was added. The samples were centrifuged at 13,000 rpm for 5 minutes at 4°C. The supernatant was removed and 500 μl of 0.2 M sodium borate buffer pH 10.4 was added. The tubes were again centrifuged at 13,000 rpm for 5 minutes at 4°C. 250 μl of sample was placed into a 500 μl microfuge tube, and analyzed following the incubation of the sample with 250 μl orthophthalaldehyde reagent for 1.7 minutes. The samples were injected into an Alltech C-18 reverse phase column using a Shimadzu SIL-9A auto injector. The column was controlled by an LKB 2100 series high performance liquid chromatography (HPLC) system. Results were analyzed using an LKB 2100 integrator unit and Wavescan v.1.02 software.

2.3.7 Determination of Oxygen Consumption

Hybridoma CC9C10 cells were grown in the presence or absence of 1 mM dichloroacetic acid in hybridoma serum-free medium (HSFM). Cells were adapted for 3 passages before the experiment. The cell suspension was placed in a Kontes flask such that there was no head space. A type P2 polarographic probe was connected to the Kontes flask to measure oxygen consumption. The oxygen probe was connected to a model 703 P oxygen meter for a visual display of oxygen consumption. The oxygen probe and meter were purchased from Uniprobe Instruments Limited. The Kontes flask was sealed such that only oxygen within the flask was accessible to the CC9C10 cells. The cells were shaken on a New Brunswick shaker base at 80 rpm, at 37°C. Cells in this experiment were grown to mid-exponential phase, before

experimentation. Once the cells reached mid-exponential growth, they were resuspended in Krebs Henseleit Bicarbonate Buffer at a density of 1.5×10^7 cells/ml.

Each measurement was performed in duplicate.

2.4.0 Glucose Separation by use of Amberlite or Dowex-1 Anion Exchange Resin

2.4.1 Resin Preparation

New resin (100 g) was washed with 2 liters of 0.5 M NaOH, followed by 2 liters of 0.5 M HCl to remove any impurities from the resin. The resin was washed with distilled water until the pH was neutral. A 0.5 M sodium tetraborate solution was added to the anion exchange resin. The mixture was swirled occasionally throughout the day, and allowed to sit overnight in order to convert the resin to the borate form. The resin was filtered using hardened filter paper (Whatman No. 50), and washed with distilled water until the pH was near neutral. The resin was stored as a slurry. The resin was filtered at least once a month, and resuspended in fresh distilled water.

2.4.2 Column Setup

D-[3-^{3}H]-glucose encountering the aldolase enzyme releases $^{3}H_2O$, which is an indicator of the glycolytic flux (Bontemps *et al*, 1978). To quantify the rate of the glycolytic flux, the ^{3}HOH required separation from the D-[3-^{3}H]-glucose. This was accomplished by Amberlite or Dowex-1 anion exchange resin in the borate form. 1 ml of resin (1 cm^{3}) was packed in Polyprep columns for the separation of ^{3}HOH and D-[3-^{3}H]-glucose. The ^{3}HOH eluted with distilled water while the glucose remained bound to the resin. Following elution of ^{3}HOH, the D-[3-^{3}H]-glucose was eluted using 3M acetic acid.

2.5.0 Use of Radiolabelled Glucose and Glutamine Molecules in Metabolic Flux Determination

2.5.1 Radiolabelled Molecules

2.5.1.1 Glucose

Butler *et al* (1990a) showed previously that the flux of glucose entering the TCA cycle, and PPP are minimal, as compared to the glycolytic flux to lactate.

D-[1-^{14}C]-glucose is used to determine the PPP flux. Upon glucose entering the PPP, it becomes 6-phosphogluconic acid, and then loses a carbon atom in the C1 position as CO_2 when being converted to ribose-5-phosphate (Butler, 1990a). Upon D-[6-^{14}C]-glucose entering the TCA cycle, it will undergo several rounds, before the carbon atom at the C6 position will be given off as CO_2 (Butler, 1990a). To determine the real value of the PPP, the D-[6-^{14}C]-glucose value must be subtracted from the D-

[1-^{14}C]-glucose, as D-[1-^{14}C]-glucose entering the TCA cycle will also have its carbon atom in the C1 position given off as CO_2 (Butler, 1990a).

D-[3-^{3}H-]-glucose releases ^{3}HOH when entering the glycolytic pathway. This is an indicator of the flux through the aldolase reaction which is a committed step of glycolysis (Bontemps, 1978).

Since the radiolabelled glucose molecules release labeled byproducts which are equivalent to one glucose molecule entering a designated pathway (1:1 ratio), the addition of the PPP flux value, and the glycolytic flux gives the specific glucose consumption rate.

2.5.1.2 Glutamine

The only form of radiolabelled glutamine currently available at the time of experimentation was uniformly labeled glutamine. This is unlike the glucose molecule which has various forms of specifically labelled molecules.

$^{14}CO_2$ release from glutamine illustrated the rate of glutamine oxidation i.e. the rate at which glutamine could form end products, or complete oxidation through the TCA cycle by CO_2 release.

The pattern of glutamine metabolism was analyzed by determination of the formation of the major metabolic end-products using a uniformly labelled substrate. The glutamine end products were separated by methods described in this Section 2.5.5. Figure 3.1 illustrates the routes of glutamine metabolism.

2.5.2 Efficiency of Filter Paper Absorbing CO_2

Filter paper (4.25 cm diameter) was saturated in 300 μl of phenylethylamine: methanol (1:1) for absorbing $^{14}CO_2$ produced from D-[1-^{14}C]-glucose and D-[6-^{14}C]-glucose, and L-[U-^{14}C]-glutamine. The filter paper quenched the counts to an extent, so the efficiency of $^{14}CO_2$ detection bound to filter paper was examined. Reaction flasks were filled with 1 ml growth medium (mentioned previously), and 0.45 μCi of $Na^{14}CO_3$. Filter paper (4.25 cm diameter) was folded and placed into the center well, followed by sealing the flask with subaseals. 300 μl of phenylethylamine : methanol (1:1) was injected using a needle through the subaseal on to the filter paper, followed by 300 μl of 10% TCA injected through the side arm subaseal slowly, touching the glass side, into the growth medium at appropriate time intervals. The flasks were shaken at 37°C for a further 2 hours. The filter paper was removed, placed into a scintillation vial with 5 ml of Ecolume, and placed in an LKB Rackbeta scintillation counter for radioactivity. Samples of six were used for determining both the average cpm of the control, and the filter paper samples. As a control, 0.45 μCi of $Na^{14}CO_3$ were placed into scintillation vials with 5 ml of Ecolume, and counted for radioactivity. The efficiency was determined to be 93.5% for the samples, as shown in Table 2.2.

2.5.3 Measurement of CO_2 Evolution

Cells at mid-exponential growth phase were harvested by centrifugation at 1500 rpm for 5 minutes, washed three times, and re-suspended in Krebs - Henseleit bicarbonate buffer (KHBB) pH 7.4 at 1 to 1.5 x 10^7 cells/ml. Growth medium and a radiolabelled substrate were placed into 10 ml Kontes side arm flasks. The radiolabelled substrate was one of the following: 0.25 μCi L-[U-^{14}C]-glutamine, 0.45 μ Ci of D-[1-^{14}C]-glucose, or 0.45 μCi of D-[6-^{14}C]-glucose. A cell suspension (200 μl) was added to each vial which was immediately stoppered with subaseal containing a Kontes center well with a filter paper wick (4.25 cm diameter). The flasks were shaken at 80 rpm in a New Brunswick G24 environmental incubator shaker at 37°C. The $^{14}CO_2$ was trapped in 300 μl of phenylethylamine : methanol (1:1) added to the wells by means of a syringe just prior to the injection of 300 μl of 10% (w/v) trichloroacetic acid into the cell suspension. The vials were shaken for 2 hours further. The filter paper in the center wells were removed to scintillation vials containing 5 ml of Ecolume, and counted for radioactivity.

Table 2.3. Determination of percentage of $NaH^{14}CO_3$ detected by filter paper.

Samples	$NaH^{14}CO_3$ Absorbed on to Filter Paper (cpm)	$NaH^{14}CO_3$ Standards (cpm)
1	84,800	79,800
2	87,500	79,600
3	83,800	79,000
4	84,500	79,300
5	82,500	79,400
6	84,800	78,600
7	83,400	78,600
8	87,800	78,600
Average	84,800	79,200
Percentage of Radioactivity Detected by Filter Paper	93.5%	

2.5.3.1 Krebs Henseleit Bicarbonate Buffer.

Added:	$MgSO_4$	0.141 g/l
	KCl	0.350 g/l
	KH_2PO_4	
	NaCl	6.90 g/l
	L-Glucose	2.00 g/l
	Sodium bicarbonate	2.10 g/l

The solution was allowed to stir for 5 minutes. pH was adjusted to 7.4 with 2 M NaOH or 2 M HCl, followed by filter sterilization with 0.2 μ Gelman Acrocap filters

2.5.4 Measurement of Glycolytic Flux

The glycolytic flux was determined by the release of tritium from D-[3-^{3}H]-glucose. This is an indicator of flux through the aldolase reaction which is a committed step of glycolysis (Bontemps, 1978).

Cells at mid-exponential phase were harvested as described in Section 2.5.3 for the measurement of CO_2 evolution. The cells were resuspended in KHBB pH 7.4 at 1 to 1.5 x 10^7 cells/ml. One ml of growth medium and 1 μCi/ml of D-[3-^{3}H]-glucose were placed into a 10 ml reaction flask. A cell suspension of 200 μl was added to the Kontes flask, which was immediately stoppered with a subaseal. The flasks were incubated at 37^{o}C, being shaken at 80 rpm. At appropriate time intervals, 200 μl samples were removed, and deproteinized using 50 μl of 20% perchloric acid (PCA). The protein pellet was removed by centrifugation, and the supernatant transferred to a new Eppendorf tube. The supernatant was neutralized with 150 μl of potassium hydroxide

(2 M) containing triethanolamine (0.5 M). The resultant PCA precipitate was removed by centrifugation and the 400 μl supernatant was frozen until ready for separation of ^{3}HOH from D-[3-^{3}H]-glucose. Upon thawing of samples, they were applied to 1 ml of Dowex-1-borate resin packed inside PolyPrep columns. Three ml of distilled water was added to the columns in 1 ml aliquots to elute the tritium. The entire fraction was collected in a small beaker. The fraction was taken in triplicate samples of 100 μl with 5 ml of Ecolume, and counted for radioactivity for 5 minutes. The D-[3-^{3}H]-glucose was eluted from the column by 10 ml of 3 M acetic acid.

2.5.5 Glutamine Assay for Measurement of End Products

2.5.5.1 Separation of Glutamine End Products

Cells were taken from mid-exponential growth phase, and centrifuged at 1500 rpm for 5 minutes and washed with KHBB three times. Cells were resuspended in KHBB at approximately 1 - 1.5 x 10^7 cells/ml, and kept on ice for no longer than one hour. One point two ml of growth medium was added to a 10 ml Kontes reaction flask with 4 μCi of L-[U-^{14}C]-glutamine. Two hundred and thirty five μl of the cell suspension was added to the flask, and immediately stoppered with subaseals. Two hundred μl of the cell suspension was removed at the appropriate time intervals, and centrifuged at 1500 rpm for 5 minutes. The supernatant was removed and the cell pellet was washed 3 times with 200 μl KHBB minus glucose, plus 10 mM glutamine (KHBB + glutamine).

All of the supernatants from the washings were combined with 850 μl of 10% TCA (with 0.1% Na azide and 10 mM glutamine) and centrifuged at 1.3 x 10^4 rpm for 5 minutes. The supernatant was removed, and the pellet was washed 2 times with

150 μl of 10% TCA (same as above), centrifuging at 1.3 x 10^4 rpm for 5 minutes. The supernatant from these two washings were combined with the other supernatant, frozen at -20°C, and stored until ready to be run on a Dowex-50W column. This gave the extracellular concentration of various glutamine metabolites.

The cell pellet was resuspended in 200 μl of 10% TCA (same as above) and centrifuged at 1.3 x 10^4 rpm for 5 minutes. This procedure was repeated twice more. All supernatant fractions were combined, and frozen at -20°C, and stored until they were ready to be run on a Dowex-50W column. This gave various intracellular glutamine metabolite concentrations.

The cell pellet was resuspended in 300 μl of KHBB, and frozen at -20°C. Upon sampling, 100 μl was taken and added to 5 ml of Ecolume, and counted for radioactivity. Samples were performed in triplicate. This indicated the amount of glutamine incorporated into total cellular protein.

For CO_2 production of L-[U-^{14}C]-glutamine, refer to Section 2.5.3.

2.5.5.2 Preparation of Dowex-50W Cation Exchange Resin and Column

The resin and column setup was performed by methods previously described (Blackburn, 1978; Boyer, 1986; Dus *et al,* 1966; Kerese, 1984; Moore. 1968; Spackman *et al*, 1958). Upon receiving 100 g of Dowex-50W (mesh size 200-400) resin, it was transferred to a Buchner funnel with hardened filter paper (Whatman No. 50). 2 liters of 0.5 M NaOH + 0.5 M NaCl were poured over the resin followed by distilled water until the pH was neutral. Following this 2 liters of 0.5 M HCl was poured over the resin. The washing of the resins with 0.5 M NaOH + 0.5 M NaCl, and 0.5 M HCl was performed in order to remove any contaminants present in the resin. The resin was washed with distilled water until the pH was neutral. The resin was added to an Erlenmeyer flask with excess 2 N NaOH and placed in a hot water bath at 50^{o}C for 15 minutes. This was repeated once more. The resin was filtered and washed with distilled water until the eluate was neutral pH. The resin was stored as a slurry in 0.2 M Na citrate pH 2.2.

The sodium citrate buffers were prepared by dissolving 0.2 M NaOH with 0.067 M citric acid (anhydrous), and 0.1% (w/v) Na azide in distilled water, and adjusting the pH accordingly to 2.2, or 3.25. After each column run, 0.7 M Na citrate pH 10.9 was passed through each column to ensure all amino acids were eluted from the resin. This buffer was prepared by dissolving 0.7M NaOH, 0.067 M citric acid, and 0.1% Na azide into distilled water, and adjusting the pH to 10.9.

Glass wool was added first to the bottom of a 50 cm^3 buret. The resin was poured to a dimension of 1.1 x 55 cm^3, such that the resin was continuous. Sodium citrate pH 2.2 was poured into a separatory funnel, and connected to the top of the column 20 cm above it. No buffer was added to top up the separatory funnel contents. The buffer was run overnight through the column to ensure that the pH was 2.2 throughout the resin. A sample with no protein and low pH was added to the top of the

column carefully to ensure the resin bed was not disturbed. The sample was allowed to completely drain into the resin. The column was washed with 10 ml Na citrate pH 2.2 to ensure all positively charged species bound to the resin. This buffer was allowed to drain completely into the resin, before changing the buffer to pH 3.25. The buffer was run through the resin until approximately 150 fractions were collected. All samples were collected using an LKB fraction collector set at 2 ml per fraction. Na citrate pH 3.25 was shown to elute all glutamine metabolic end products. 100 µl of each fraction was added to a scintillation vial with 5 ml Ecolume, and counted for 5 minutes. The quantity of each product was determined by the area under the peaks.

2.5.5.3 Amino Acid Detection

Initially, it was required to see what pH would elute and separate the glutamine end products in a cation exchange column: aspartate, glutamate, alanine, lactate, and glutamine (which may not yet have been utilized by the cells). Lactate being negatively charged, flowed through the column freely while all amino acids present bound to the resin. A 20 mM solution containing all of the molecules listed above was made and a 600µl aliquot of this was added to a Dowex 50 W column (55cm x 1.1 cm). After the fractions were collected, amino acid peaks were detected by the ninhydrin method. Peak identification was made by enzymatic methods or high performance liquid chromatography (HPLC). The position of lactate was determined using the LDH assay. Figure 2.1 shows a typical separation of standard which represented glutamine end products.

2.5.5.4 Ninhydrin Detection of Amino Acids

The ninhydrin assay method used was that described by Moore *et al* (1968). The buffer was made as follows:

Na Acetate Buffer 2 M pH 5.

4 M NaOH were added to distilled water, with a magnetic stirrer spinning. Upon the NaOH dissolving, 4 M acetic acid was added. The buffer was allowed to cool to room temperature. One part of the buffer was added to 3 parts dimethylsulfoxide. The pH was adjusted to 5.2 with acetic acid, or NaOH.

The solution was bubbled with N_2 for 15 minutes to remove any O_2 still in the solution, followed by the addition of ninhydrin (4 g/l). The stirrer speed was quick to ensure the ninhydrin crystals dissolved readily. This was followed by the subsequent addition of hydrindantin (0.625 g/l). These crystals took a while to dissolve, so there was no problem stirring for 60 minutes, as the mixture was stable under N_2 (g). The mixture was stored at 0 to 5^{o}C in an aluminum foil-wrapped bottle where it was stable for months.

Assay Conditions

400 µl of a fraction sample and 1.6 ml of the ninhydrin reagent were added to a glass test tube. Heating of the samples was performed at 100^{o}C for 5 minutes. The absorbance was read in a spectrophotometer at 570 nm. If looking for proline, the absorbance was measured at 440 nm. Since the color intensity of the ninhydrin was proportional to amino acid concentration, Figure 2.1 was made with absorbance (570 nm) vs. fraction number to reveal peaks.

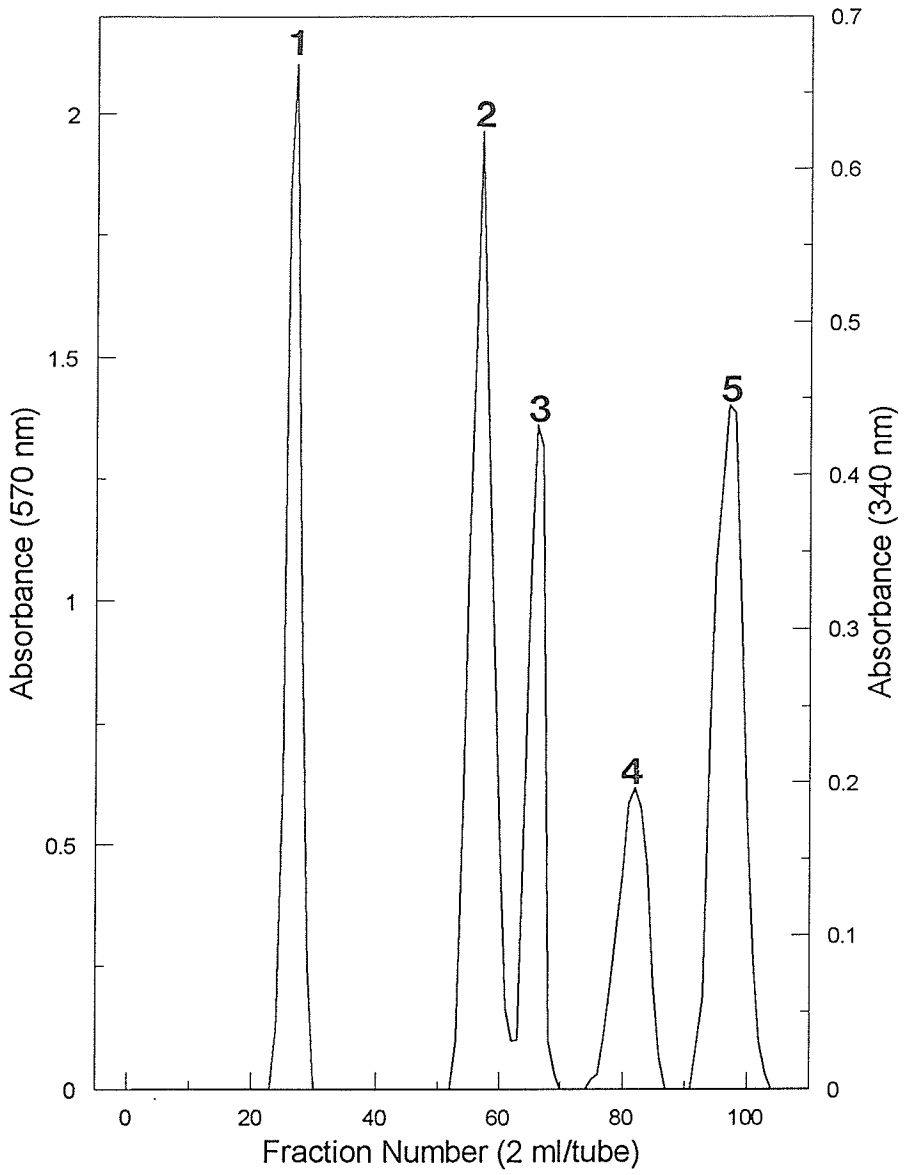

Figure 2.1. Separation of glutamine end products. A sample containing lactate (1), aspartate (2), glutamine (3), glutamate (4), and alanine (5) were separated using a Dowex-50W resin column Na form; mesh size 200-400 (55cm x 1.1 cm). A 20 mM solution containing all the compounds described above were suspended in an appropriate volume of 10% TCA. The pH was 1, almost identical to the pH of 10% TCA with no additives. A 600 µl sample was taken from this solution and applied to the column. Upon addition of sample, 10 ml of Na citrate pH 2.2 was allowed to flow through the column before the elution buffer (Na citrate pH 3.25) in order to ensure all positive species were bound. Ellution buffer was added to a 500 ml separatory funnel 20 cm above the column. The funnel was connected to the column and the buffer was allowed to flow. The column height was 55 cm by 1.1 cm. Two ml fractions were collected in an LKB fraction collector. The detection and absorbance of the amino acids was determined by the ninhydrin assay. The absorbance was read at 570 nm. The lactate was determined by using the LDH assay. The absorbance was read at 340 nm.

2.6.0 Measurement of Cellular Protein

Cellular protein was determined by the Bradford assay (Deutscher, 1990). Cells were taken from culture medium, centrifuged for 5 minutes at 1500 rpm, and washed 3 times with Krebs-Henseleit Bicarbonate Buffer (KHBB). The cells were resuspended in KHBB such that the cell density was 1 x 10^6 cells per 200 μl. The cell suspension was sonicated on ice in a plastic centrifuge tube for three 30 second intervals, which lysed the cells and prevented clumping of cell membranes. The samples were kept on ice until ready to use. Fifty microliters of sample was taken and combined with 50 μl of ddH_2O. Four ml of Bradford reagent was added, and the samples allowed to stand for 5 minutes. The absorbance was determined using a spectrophotometer set at 590 nm.

2.6.1 Bradford Protein Assay

A description of the Bradford assay (Deutscher, 1990) is shown below with modifications made on the volume of sample added, and the volume of Bradford reagent added. :

Range: 0.2-20 μg per ml of dye reagent.

Dye Reagent: 100 mg of Comassie Blue G was dissolved in a mixture of 100 ml 85% phosphoric acid and 50 ml of 95% ethanol. After the dye had completely dissolved, the volume was brought to one liter with cold water.

When using glass cuvettes, they were washed with acetone after every sampling, as the dye bound to the glass. If the dye remained bound after treatment with acetone, the cuvettes were treated with a small amount of dimethylsulfoxide, and rinsed thoroughly.

At high protein values, the level of free dye became significantly depleted. The linearity of the assay could be improved by using the formula A_{595} - A_{495} to take into account the depletion of free dye.

After several hours of incubation, the Comassie dye precipitated from the solution. A gentle mixing of the sample before measuring the absorbance resolved this problem.

A sample could only be read once, as dye bound to the cuvette would decrease further absorbance readings.

Mechanism: The absorbance maximum for the dye in an acidic solution shifts from 465 nm to 595 nm after adding protein due to stabilization of the anionic form of the dye by both hydrophobic and ionic interactions. The dye mainly reacts with arginine residues, and to a lesser extent histidine, lysine, tyrosine, tryptophan, and phenylalanine residues (Deutscher, 1990).

2.7 Chemicals and Supplies

2.7.1 Laboratory Chemicals

a) Glucose, galactose, sorbitol, maltose, xylitol, fructose, lactate, methanol, pluronic F-68, sodium chloride, sodium carbonate, sodium bicarbonate, dichloroacetic acid, insulin, transferrin, sodium selenite, dimethylsulfoxide, ninhydrin, phenol red, trypan blue, hydrindantin, hydrazine hydrate, brilliant blue G, sodium hydroxide, trichloroacetic acid, triethanolamine, potassium chloride, sodium phosphate, (ethylenedinitrilo)-tetraacetic acid disodium salt (EDTA), polyoxyethylene sorbitan monolaurate, sodium phosphate dibasic, potassium hydroxide, zinc chloride, magnesium sulfate, hydroxylamine, boric acid, sodium tetraborate, citric acid, ammonium chloride, trizma base, formic acid, formic acid sodium salt, phenylethylamine, lactate dehydrogenase, glutaminase, β-nicotinamide adenenine dinucleotide, adenine di-phosphate, glutamate dehydrogenase, goat antimouse IgG, bovine serum albumin powder, bovine serum albumin fraction 5 powder, p-nitrylphenyl phosphate, alanine, glutamate, aspartate, Dowex-1 resin, Dowex-50W resin, ethanolamine, and phosphoethanolamine were purchased from Sigma.

b) Hydrochloric acid, acetic acid, nitric acid, and phosphoric acid were purchased from Mallinckrodt.

c) Dubelcco's phosphate buffered saline, Dubelcco's modified essential medium, Ham's F-12, Royal Park Memorial Institute medium (RPMI), and Fe-enriched calf serum were purchased from Gibco.

2.7.2. Supplies

a) 25, 75, and 150 cm^2 T-flasks; 1, 10, and 25 ml serological pipettes; 15 and 50 ml centrifuge tubes were purchased from Corning.

b) 100, and 250 cm^3 spinner flasks were purchased from Bellco.

c) Polyprep columns, and microfuge tubes were purchased from CanLab.

2.7.3 Radioactive Chemicals

D-[1-^{14}C]-glucose, D-[6-^{14}C]-glucose, D-[3-^{3}H]-glucose, D-[U-^{14}C]-glucose, and L-[U-^{14}C]-glutamine were purchased from Amersham, U. K. Radioactive counts were determined using as scintillation counter (LKB Rackbeta), and Ecolume as the scintillant.

2.8 Mathematical Formulas

2.8.1 Determination of Specific Consumption / Production Rates of Media Components for Cells Grown in a Fermentor in Chemostat Mode:

Hybridoma CC9C10 cells were grown in a fermentor at various oxygen concentrations, in chemostat mode. In order to calculate the specific consumption / production rate of media components, the following equation was derived:

$$\frac{ds}{dt} = F_iS_i - F_oS_o - nvq_s$$

Where: $\frac{ds}{dt}$ represents the change in substrate concentration over time

F_iS_i represents the initial flow rate ($\mathbf{F_i}$) and the initial substrate/product concentration ($\mathbf{S_i}$)

F_oS_o represents the final flow rate ($\mathbf{F_o}$) and the final substrate/product concentration ($\mathbf{S_o}$)

nvq_s represents cell concentration at equilbrium (**n**), the volume of liquid the fermentor [**v** (liters)], and the specific consumption/production rate $\mathbf{q_s}$.

When the fermentor was run in chemostat mode, an equilibrium is established such that the substrate concentration, and viable cell number are constant over time. Upon this occurring,

$$\frac{ds}{dt} = 0$$

The formula became:

$$0 = F_iS_i - F_oS_o - nvq_s$$

Since the flow rates were equal **D** [dilution rate (liters/day)] replaced F_i and F_o. Rearranging the formula gave:

$$q_s = \frac{D(S_i - S_o)}{nv}$$

The volumetric change was 1.2 liters per day. The volume of the fermentor was 1.2 liters. Canceling units was performed as shown below:

$$q_S = \frac{\frac{\mu mol}{ml}}{\frac{10^6 cells}{ml} * days} x \frac{1x10^3 nmol}{\mu mol} x \frac{1day}{24hrs} x \frac{1hr}{60min}$$

qs = nmol/minute per 10^6 cells

2.8.2 Determination of Specific Consumption / Production Rates of Media Components for Cells Grown in a Batch Culture:

Hybridoma CC9C10 cells were grown in batch mode in T-flasks, or Bellco spinner flasks. In order to calculate specific consumption / production rates of media components, the following equation was derived:

$$q_s = \frac{d[S]_o^t}{\int_o^t dxdt}$$

Where: q_S represents specific consumption / production rate

$d[S]_o^t$ represents change in substrate / product concentration over time

$\int_o^t dxdt$ represents change in cell number (**dx**) with time (**dt**)

Substrate / product concentrations were determined by methods in Section 2.3. Units of substrate / product were expressed in mM. $\int_o^t dxdt$ represents the viability index of a culture over a specified time period. The viability index was determined by using the Trapezoid method in SigmaPlot. At each time point in a growth curve, a value for the viabilty index was attained. By plotting a graph of substrate or product utilized or consumed, respectively, against the viablity index (See Figure 2.2), the specific consumption / production rates were determined (nmol/minute per 10^6 cells). Cancelling units was perfomed as shown below:

$$x = q_S = \frac{\frac{\mu mol}{ml}}{\frac{10^6 cells}{ml} * days} x \frac{1x10^3 nmol}{\mu mol} x \frac{1day}{24hrs} x \frac{1hr}{60\text{min}}$$

qs = nmol/minute per 10^6 cells

2.8.3 Determination of Doubling Time for Cells in an Exponential Growing Phase

The following formulas below were used in conjunction in order to determine the doubling time of cells.

$$N=N_o 2^X$$

Wnere N represents the final cell number (10^6 cells/ml)

No represents the initial cell number (10^6 cells/ml)

2^X represents the number of generations of exponential growth

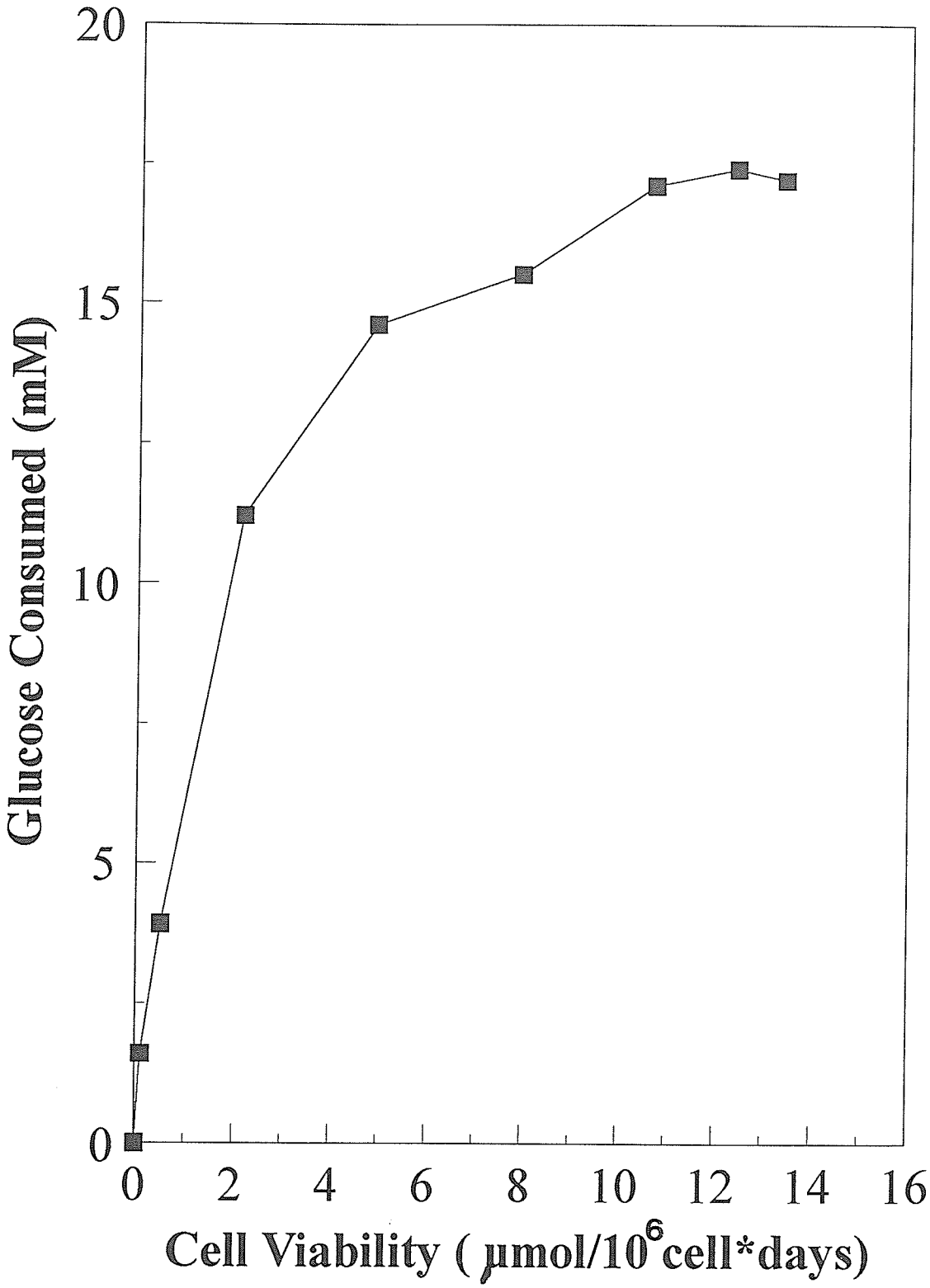

Figure 2.2. Representation of glucose consumption plotted against viability index from a typical batch culture fermentation. By taking a linear portion of the line and determining the slope gives the specific consumption rate (nmol/minute per 10^6 cells)

The log of the formula was taken in order to simplifiy the equation:

$$\log_{10}N = \log_{10}N_O + x\log_{10}2$$

$$x = \frac{\log_{10}(N - N_o)}{\log_{10}2}$$

A new equation was introduced to display doubling time (DT):

$$DT = \frac{t - t_o}{x}$$

Where	DT	represents doubling time (hours)
	t	represents the final time point (hours)
	t_o	represents the initial time point (hours)
	x	represents the number of generations of exponential growth

The procedure shown above was used in the determination of cell doubling time.

CHAPTER 3

3.0 Effects of Dichloroacetic Acid on Hybridoma CC9C10

3.1 Introduction

Dichloroacetate may exert many different effects, depending upon which tissue of an organism is examined *in vivo*. Dichloroacetic acid (DCA) has been previously reported to increase the respiratory quotient (rate of CO_2 formation/rate of O_2 consumption) and lower blood glucose concentration on injection into alloxan-diabetic rats (Lorini and Ciman, 1962). DCA has also been shown to increase glucose oxidation, inhibit fatty acid oxidation in skeletal muscle of diabetic rats (Stacpoole and Felts, 1970; Stacpoole and Felts, 1971; Stacpoole, 1989), and inhibit the oxidation of acetate and long chain fatty acids (McAllister *et al*, 1973). DCA lowers blood lactate, pyruvate, and alanine by increased substrate utilization of pyruvate, and lowers blood glucose by increased tissue consumption of the precursors of gluconeogenesis (Goodman *et al*, 1978). In starved rats, DCA has been shown to activate pyruvate dehydrogenase, have no influence on net glucose utilization, and stimulate fatty acid synthesis from isolated hepatocytes. However, in hepatocytes isolated in meal fed rats, DCA was found to activate LDH, increase utilization of lactate and pyruvate without affecting an increase in net utilization of glucose, and increase the rate of fatty acid synthesis (Crabb, 1976).

Experiments conducted by Crabb *et al* (Crabb et al, 1981; Stacpoole, 1989), observed *in vivo* that DCA had no effect on normal, non-diabetic control animals. This suggested that DCA had no effect on insulin-dependent tissues. However, on experiment *in vivo* involving a normal patient with insulinized tissue upon DCA therapy showed a decrease in blood sugar (Stacpoole *et al*, 1988).

Media used to grow hybridomas contains insulin, whether it is contained in calf serum, or supplemented in serum-free medium. Experimentation was performed to examine the possibility that DCA would have an effect on insulinized tissues.

Dichloroacetic acid (DCA) exerts its effects by activating the pyruvate dehydrogenase (PDHC) complex (EC 1.2.4.1). Other halogenated compounds have also been shown to activate PDHC, but to a lesser extent (Whitehouse *et al*, 1973).

PDHC catalyzes the aerobic oxidation of pyruvate to acetyl-CoA (Denton *et al*, 1975), placing the pyruvate into the citric acid cycle. PDHC is a multi-enzyme complex consisting of three different subunits: pyruvate dehydrogenase component, dihydrolipoyl transacetylase and dihydrolipoyl dehydrogenase. Thiamine pyrophosphate lipamide, and flavin adenine dinucleotide serve as catalytic cofactors. Coenzyme A, and NAD^+ are stoichiometric cofactors (Stryer, 1988).

Pyruvate dehydrogenase phosphatase (PDHR) converts the inactive phosphorylated form of PDH into the active, dephosphorylated form (Crab *et al*, 1976).

DCA appears to exert its effects by non competitively inhibiting the action of pyruvate dehydrogenase complex kinase (PDHCK) (Whitehouse, and Randle, 1973). This would allow pyruvate dehydrogenase phosphatase (PDHP) to convert the inactive phosphorylated form of PDH to the active dephosphorylated form. With PDH being in the active form, one would expect a decrease in lactate levels, with a greater flux of pyruvate entering the TCA cycle. Decreasing lactate levels in culture medium would prevent it from lowering the pH significantly, and allowing more energy to be produced (glucose produces a net of 38 ATP upon complete oxidation through the TCA cycle, as opposed to 2 ATP being produced when it forms lactate). Activation of PDH by DCA could allow glucose to provide more energy for the cells, shunting more of it through the TCA cycle. This may cause a higher cell density resulting in higher monoclonal antibody production, which would make worth examination of DCA supplementation to culture media. The purpose of this study was to examine cell viability, lactate

production, glucose consumption, and Mab production with respect to the addition of DCA under different growth vessels and media .

3.2 Materials and Methods

3.2.1 Cell line: Refer to Section 2.1.0a.

3.2.2 Culture: Refer to Section 2.1.1a and b, and 2.1.2a, b, and c.

3.2.3 Cell counting: Refer to Section 2.1.4.

3.2.4 Intracellular protein content: Refer to Section 2.7.

3.2.5 Analysis of culture media: Refer to Section 2.3.

3.2.7 Determination of oxygen consumption: Refer to Section 2.3.7.

3.3.0 Results

3.3.1 Effect of DCA Addition to Hybridoma CC9C10 Grown in RPMI in Spinner Flasks

Hybridoma CC9C10 was grown in RPMI + 10% calf serum + 20 mM glucose + 2 mM glutamine ± 1.5 mM Dichloroacetic acid (DCA). The experiment was performed in duplicate, with cells grown in the medium above with or without 1.5 mM DCA. Cells were grown in 250 ml Bellco spinner flasks at 37^{o}C under a 5% CO_2 overlay. The cells were rotated at 80 rpm using a magnetic stirrer base. J. Berry examined DCA concentrations: 0, 0.1, 0.5, 1, 1.5, 2, 3, 4, and 5 mM. It was observed that the cell density in 1.5 mM DCA had 11% more growth when compared to the control (0 mM DCA). From the results itt was concluded that 1.5 mM DCA was the most suitable concentration to use on CC9C10 when grown in culture (Berry J., 1992).

Figure 3.1 illustrates the total viable cell density of cells grown in medium with or without 1.5 mM DCA. Both cultures peaked on day 2 , with viable cell numbers of 1.12 x $10^{6,}$ and 9.34 x 10^{5} viable cells/ml, grown with or without 1.5 mM DCA, respectively. There was no stationary phase observed for either culture. The addition of DCA to medium, increased the final cell density by 20%.

Total glucose consumption and lactate production for cells grown in media with or without DCA are shown in Figure 3.2. Cells grown with 1.5 mM DCA had a lower level of glucose consumed (5.9 mM), as opposed to 6.7 mM obtained for cells grown without 1.5 mM DCA. Total lactate production was lower in cells cultured with 1.5 mM DCA, at 8.28 mM, as opposed to 9.95 mM for cells grown without 1.5 mM DCA. The lactate to glucose ratios were 1.40, and 1.49, for cells grown with or without 1.5 mM DCA, respectively.

Table 3.1 illustrates the specific glucose consumption rates for CC9C10 grown in medium with or without 1.5 mM DCA. As seen in Table 3.1, the overall specific glucose consumption rates were similar among both cultures.

Table 3.2 illustrates the specific lactate production rates for CC9C10 grown with or without 1.5 mM DCA. As seen, there is a trend for CC9C10 grown in the presence of 1.5 mM DCA had a slightly lower lactate production rate as opposed to cells grown in the absence of 1.5 mM DCA.

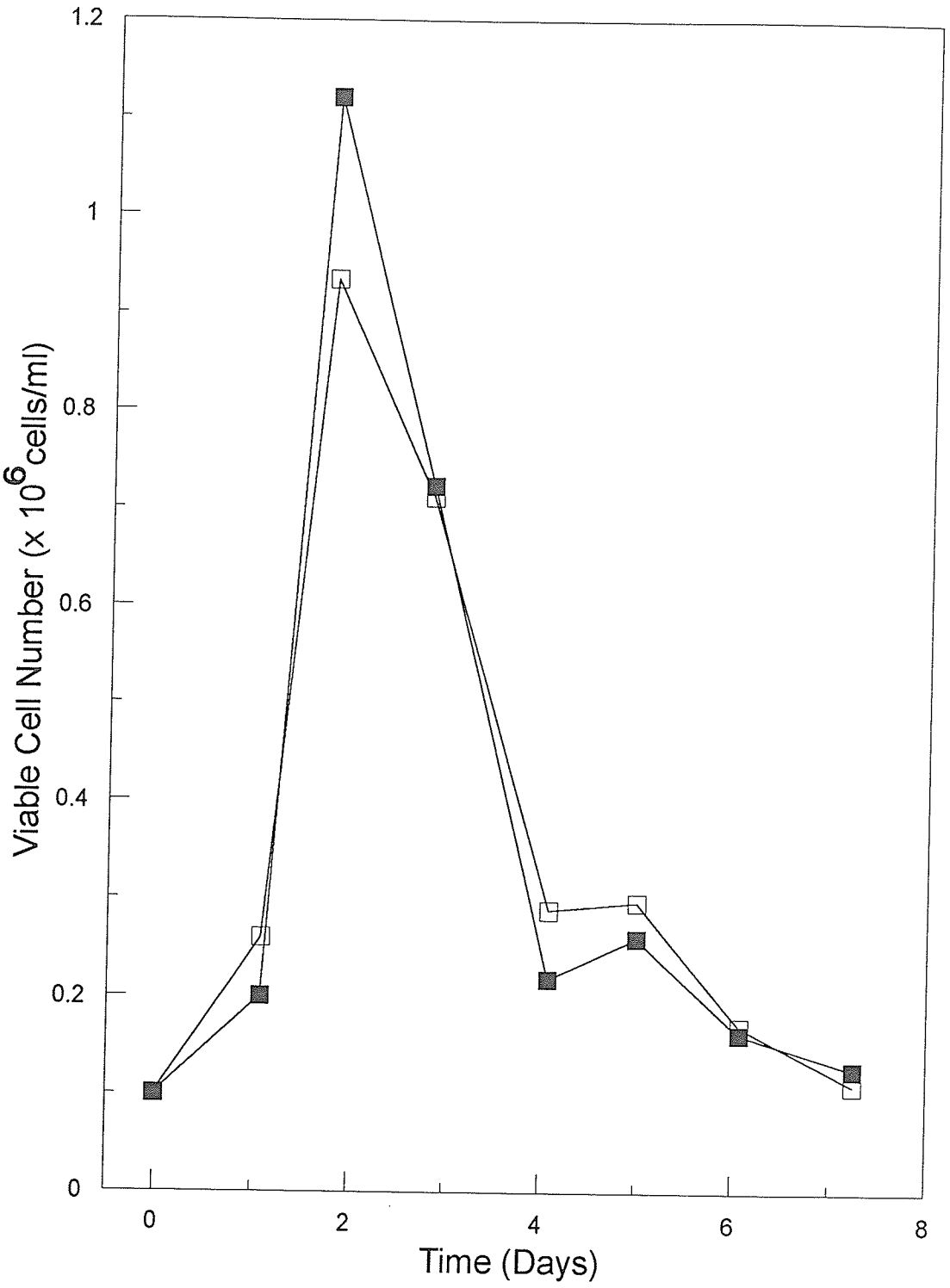

Figure 3.1. Viable cell number of CC9C10 grown ±1.5 mM DCA. CC9C10 cells were grown in RPMI containing 1.5 mM DCA (▫) or without 1.5 mM DCA (▪). (n=2).

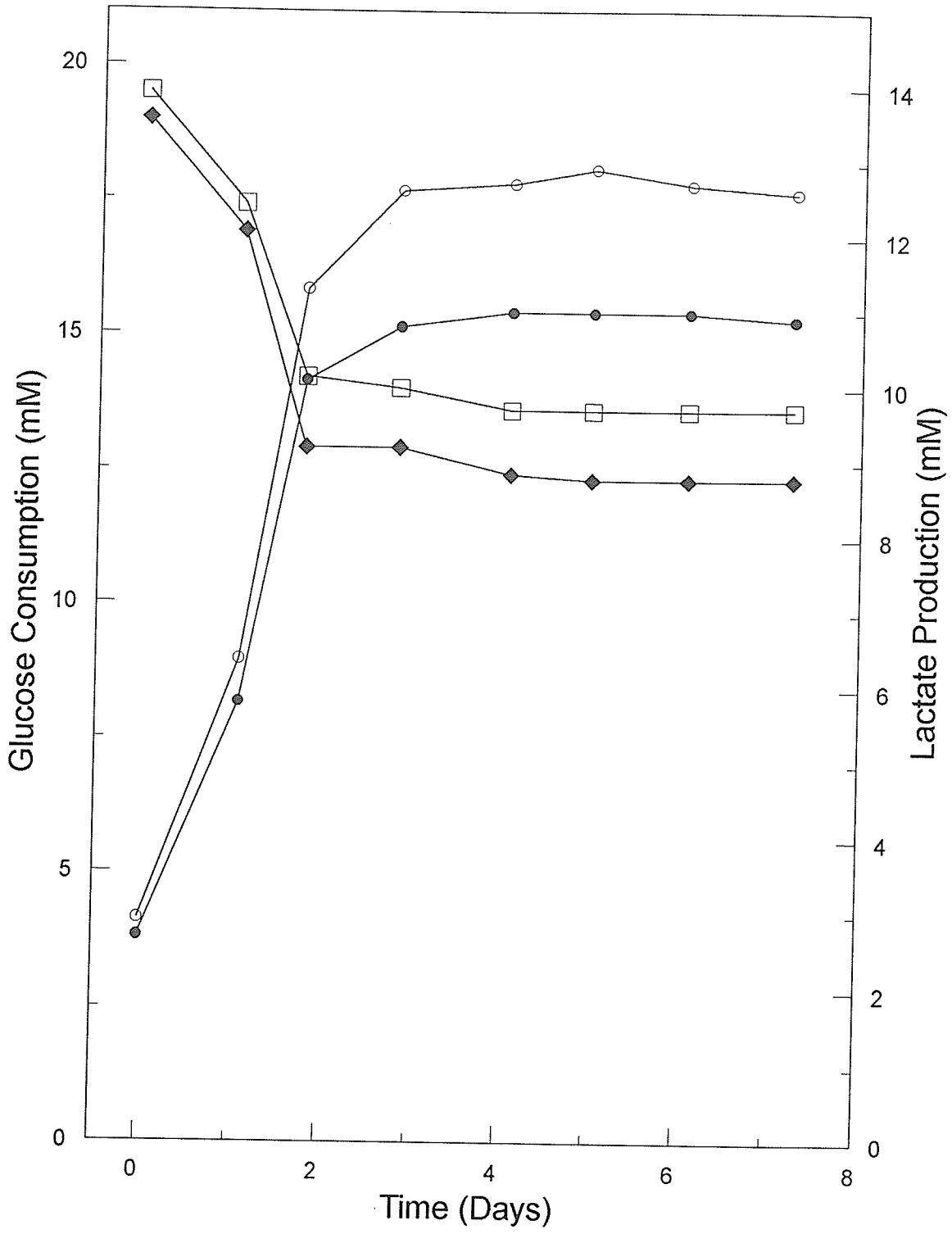

Figure 3.2. Glucose consumption and lactate production profiles for CC9C10 grown in RPMI + 10% calf serum + 20 mM glucose + 2 mM glutamine ±1.5 mM dichloroacetic acid. Glucose consumption is shown cells grown with (♦), or without 1.5 mM DCA (□). Lactate production is shown for cells grown with (●) or without (○) 1.5 mM DCA. (n=2).

Table 3.1. Specific Glucose Consumption Rates for CC9C10 Grown in RPMI + 10% Calf Serum + 20 mM Glucose + 2 mM Glutamine ± 1.5 mM Dichloroacetic Acid. (n=2).

	Specific Glucose Consumption Rates ($\mu mol/10^6 cell*days$)	
Time (Days)	**RPMI (± S. E. M.)**	**RPMI + 1.5 mM DCA (± S.E. M.)**
Day 1	19.4 (± 1.9)	19.4 (± 1.9)
Day 2	4.78 (± 0.26)	3.19 (± 0.06)
Day 3	0	0.196 (± 0.18)
Day 4	0.847 (± 0.08)	0.909 (± 0.08)

S. E. M. represents standard error of the mean.

Table 3.2. Specific Lactate Production Rates for CC9C10 grown in RPMI + 10% calf serum + 20 mM glucose + 2 mM glutamine ± 1.5 mM dichloracetic acid. (n=2).

	Specific Lactate Production Rates ($\mu mol/10^6$ cell*days)	
Time (Days)	RPMI (± S. E. M.)	RPMI + 1.5 mM DCA (± S. E. M.)
Day 1	31.9 (± 2.1)	28.7 (± 0.21)
Day 2	5.87 (± 0.26)	4.27 (± 0.06)
Day 3	5.51 (± 0.44	0.686 (± 0.05)
Day 4	0.82 (± 0.05)	0.455 (± 0.05)

S. E. M. represents standard error of the mean.

3.3.2 CC9C10 Grown in T-flasks with Serum Supplemented DMEM at Varying DCA Concentrations

CC9C10 cells were grown in DMEM, a medium richer than RPMI (higher amino acid, and salt concentrations). To establish what the optimal concentration for growth of dichloroacetic acid (DCA), concentrations were 0, 1, 1.5, 2, 2.5, 3, 5, and 10 mM in DMEM cultures. Cultures were grown in duplicate (two separate T-flasks for every different DCA concentration), in a CO_2 incubator in 150 cm^2 T-flasks, at 37°C, under a 10% CO_2 overlay. The cells were adapted to the various concentrations of DCA for a minimum of 4 passages.

Figure 3.3 illustrates the viable cell densities of CC9C10 grown at various DCA concentrations mentioned above. The cell density in DMEM without addition of DCA peaked on day 4 at 1.42 x 10^6 viable cells/ml. Cultures with DCA added to the medium also had maximal viable cell densities observed on day 4, with the exceptions being cultures with 2, and 10 mM DCA additions. Cells cultured with 1.5 mM DCA had the highest viable cell density for DCA addition to cultures, at 1.58 x 10^6 viable cells/ml. Cells grown in 1, 2, 2.5, and 3 mM DCA all had similar densities. DCA did not appear to be toxic to the cells. CC9C10 grown with 5 mM DCA reached a maximal viable cell density of 1.01 x 10^6 cells/ml. Cultures supplemented with 10 mM DCA achieved a maximal viable cell density of 8.94 x 10^5 cells/ml on day 5. It appeared the addition of DCA up to a concentration of 3 mM DCA in the medium did not alter the growth phase of CC9C10, with respect to the culture without DCA addition.

There were no apparent stationary phases observed for CC9C10 in any of the cultures. The cells grown in all of the cultures reached the decline phase more or less at the same time frame, suggesting that the cells were lacking some medium component, causing them to enter the decline phase. The maximum viable cell number vs. increasing DCA concentrations is shown in Figure 3.4. The maximum

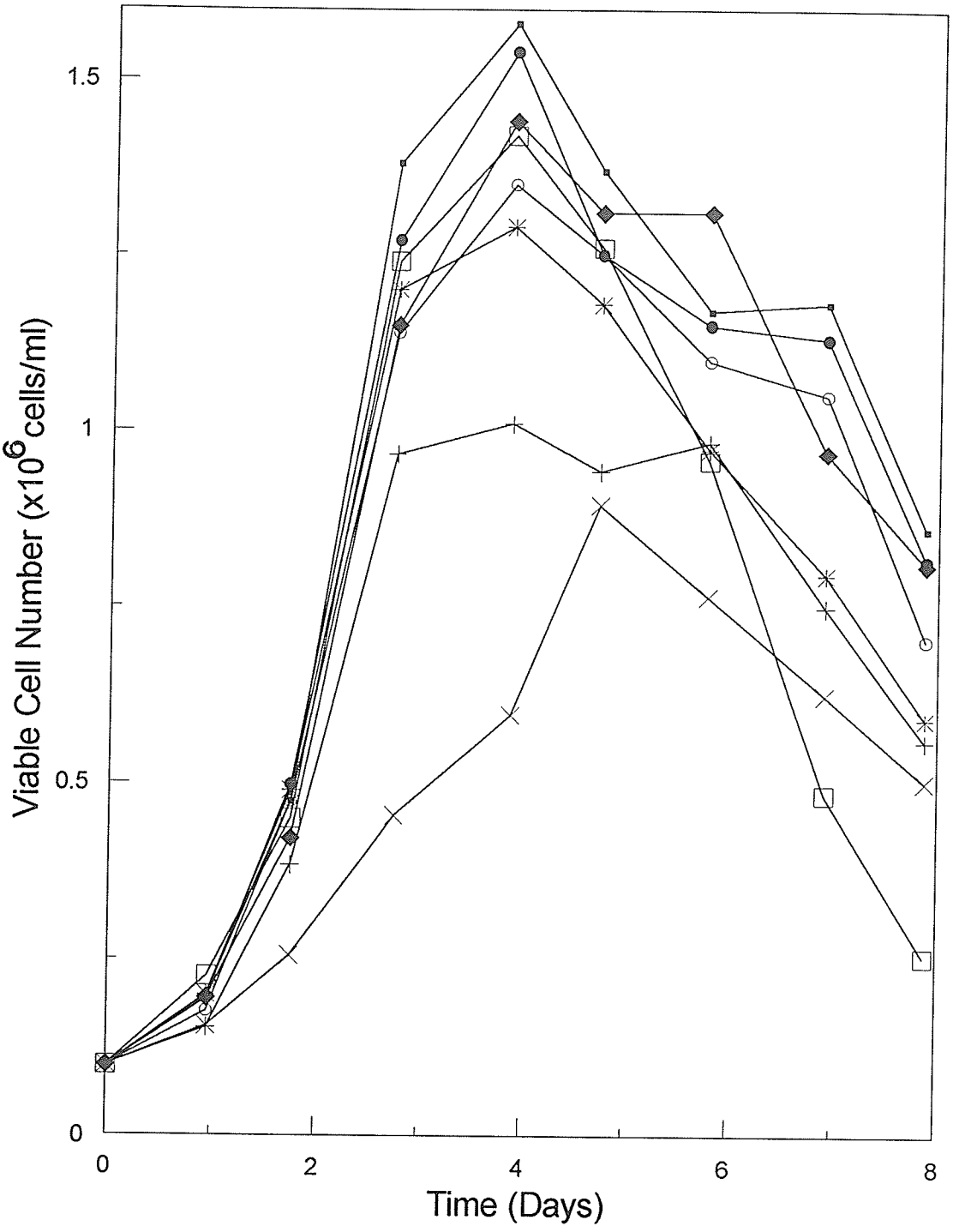

Figure 3.3. Viable Cell Number over time at various concentrations of dichloroacetic acid. CC9C10 cells were grown in DMEM + 10% calf serum + 25 mM glucose + 4 mM glutamine with dichloroacetic acid at concentrations of 0 mM (□), 1 mM (O), 1.5 mM (■), 2 mM (●), 2.5 mM (◆), 3 mM (*), 5 mM (+), and 10 mM (X). (n=2).

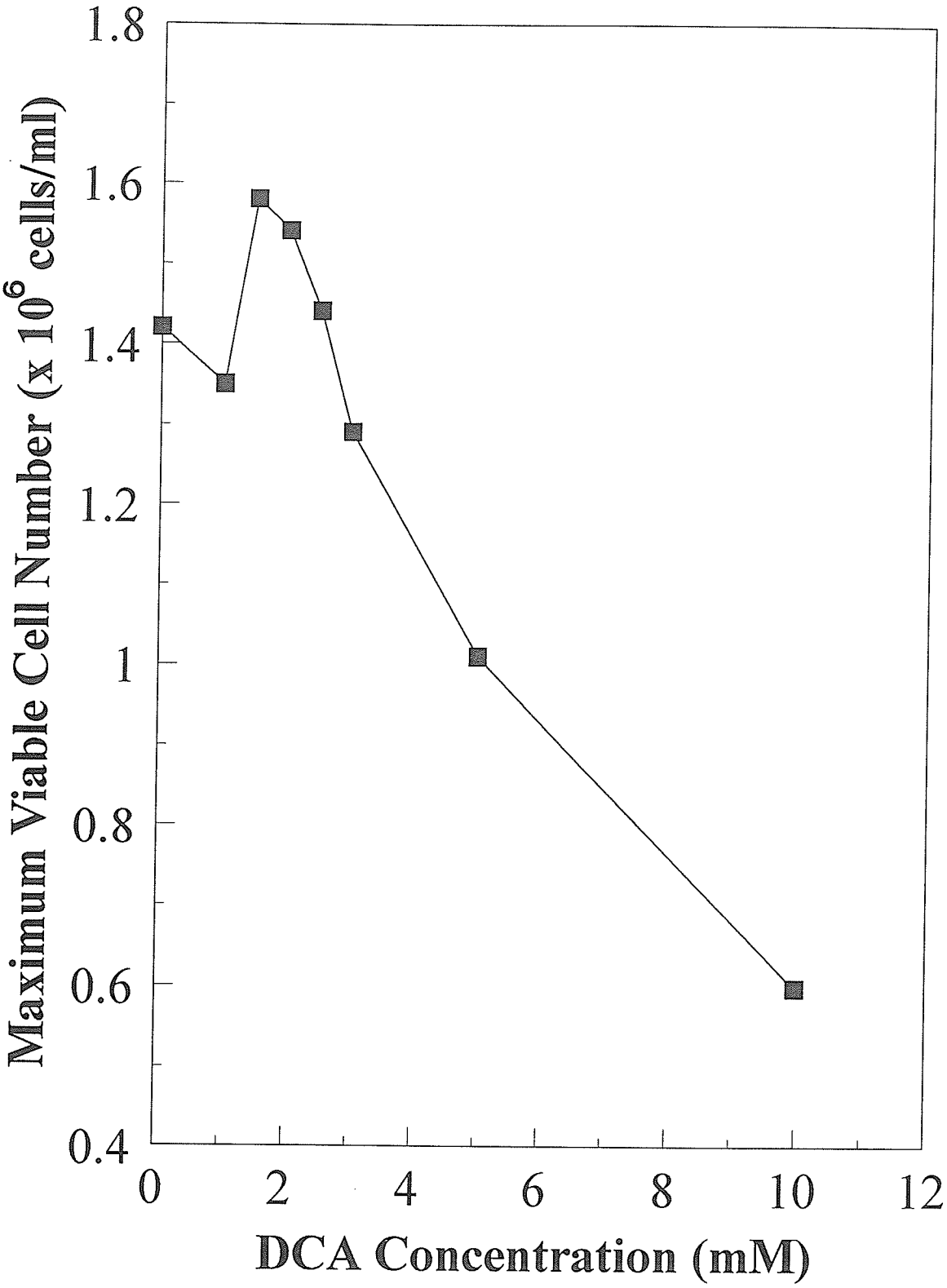

Figure 3.4. Maximum viable cell number with respect to varying concentrations of dichloroacetic acid. CC9C10 cells were grown in DMEM-F12 + 10% calf serum + 17.5 mM glucose + 4 mM glutamine with dichloroacetic acid at concentrations of 0, 1, 1.5, 2, 2.5, 3, 5, and 10 mM (n=2).

ffect of stimulation occurred at 1.5 mM DCA. DCA concentrations over 3 mM appeared to be growth inhibiting to hybridoma CC9C10.

The addition of DCA, regardless of concentration appeared to have some effect on maintaining higher viable cell numbers throughout the decline phase. Cell densities on the last measurement of the decline phase varied from 8.58 x 10^5 viable cells/ml (1.5 mM DCA culture gave the highest value) to 5.02 x 10^5 viable cells/ml (10 mM DCA culture), The culture with no DCA addition to medium has a final cell density of 2.54 x 10^5 viable cells/ml. The reason for cultures with DCA addition had final cell densities higher than the control was hypothesized to be due to DCA aiding in membrane stabilization when grown with 10% calf serum.

Glucose consumption for CC9C10 grown in medium with varying concentrations of DCA are shown in Figure 3.5. Glucose consumption is similar for CC9C10 grown with or without DCA. Cells grown without DCA addition have a total of 17.2 mM glucose consumed. Cells grown with DCA up to concentrations of 5 mM had similar levels of glucose consumed, and lactate produced for cultures without the addition of DCA. CC9C10 cell cultures with 10 mM DCA had low net glucose consumption when compared to the other cultures. This was attributed to a lower cell number than the other cultures.

Lactate production for CC9C10 grown in medium with various DCA concentrations is shown in Figure 3.6. Lactate production was similar for cells grown with or without the addition of DCA. The low lactate production value for cells grown with 10 mM DCA is attributed to a lower cell number.

Specific glucose consumption rates were determined for all cultures grown with or without the addition of DCA to culture medium, as shown in Table 3.3. Dichloroacetic acid at concentrations up to 5 mM raised the consumption rate, with the 5 mM culture having the greatest effect. The remaining glucose consumption rates

following day 2 were similar, with DCA cultures having lower specific consumption rates than the cultures without DCA addition.

Table 3.4 illustrates the various specific lactate production rates for CC9C10 grown with or without DCA between 3-5 mM had much higher specific lactate production rates than the controls (no DCA supplementation). CC9C10 cultured without DCA (control) had a specific lactate production rate of 23.6 μmol/10^6 cell*days, on day 1. Cells grown in the presence of DCA had similar specific lactate production rates to the controls. Following day 1, cells cultured with DCA had slightly lower production rates than the control. There was no observable trend other than the fact that specific lactate production decreased over time. Cultures containing 10 mM DCA appeared to be toxic to cell growth, as indicated by peak cell density.

From the results, 1.5 mM DCA was selected as the most appropriate concentration to add to the culture medium, as indicated by batch growth profile, and lactate production. These results were similar to experiments where 1.5 mM DCA was added to RPMI medium.

The antibody concentration determined over the growth of cells in medium containing 1.5 mM DCA is shown in Figure 3.7. The final antibody titre was 34.7 μg antibody/ml of culture medium. This value was required for comparison to CC9C10 cultures grown in 250 ml Bellco spinner flasks

The next area of study chosen was to grow CC9C10 in DMEM + 10% calf serum + 4 mM glutamine with or without the addition of 1.5 mM DCA, in Bellco spinner flasks, at 37^{o}C, under a 10% CO_2 overlay, with the magnetic stirrer being rotated at 80 rpm. The only difference between this and the previous experiment was that cells were grown in spinner flasks.

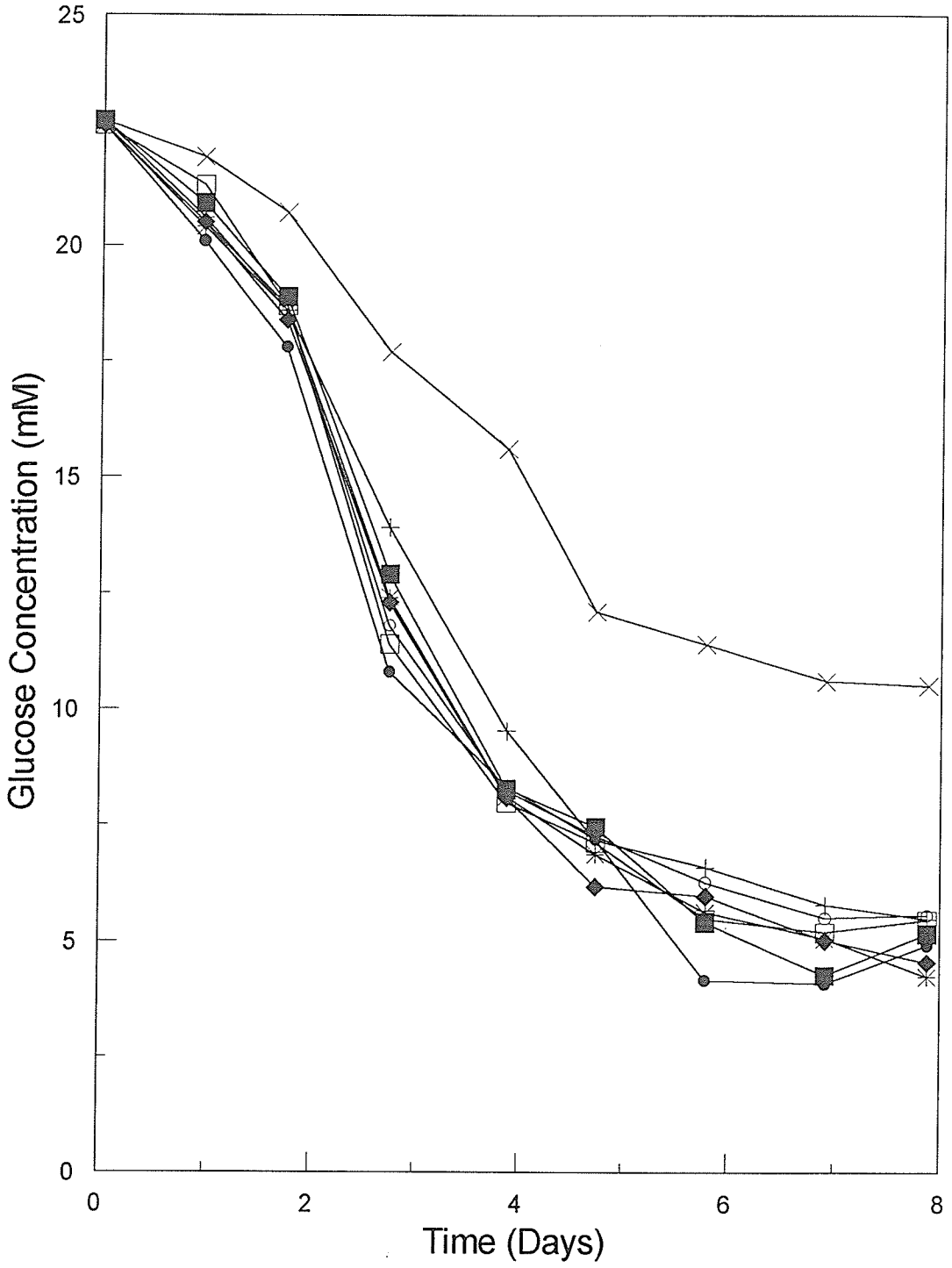

Figure 3.5. Glucose consumption over time at various concentrations of dichloroacetic acid. CC9C10 cells were grown in DMEM + 10% calf serum + 25 mM glucose + 4 mM glutamine with dichloroacetic acid at concentrations of 0 mM (□), 1 mM (○), 1.5 mM (■), 2 mM (●), 2.5 mM (◆), 3 mM (*), 5 mM (+), and 10 mM (X). (n=2).

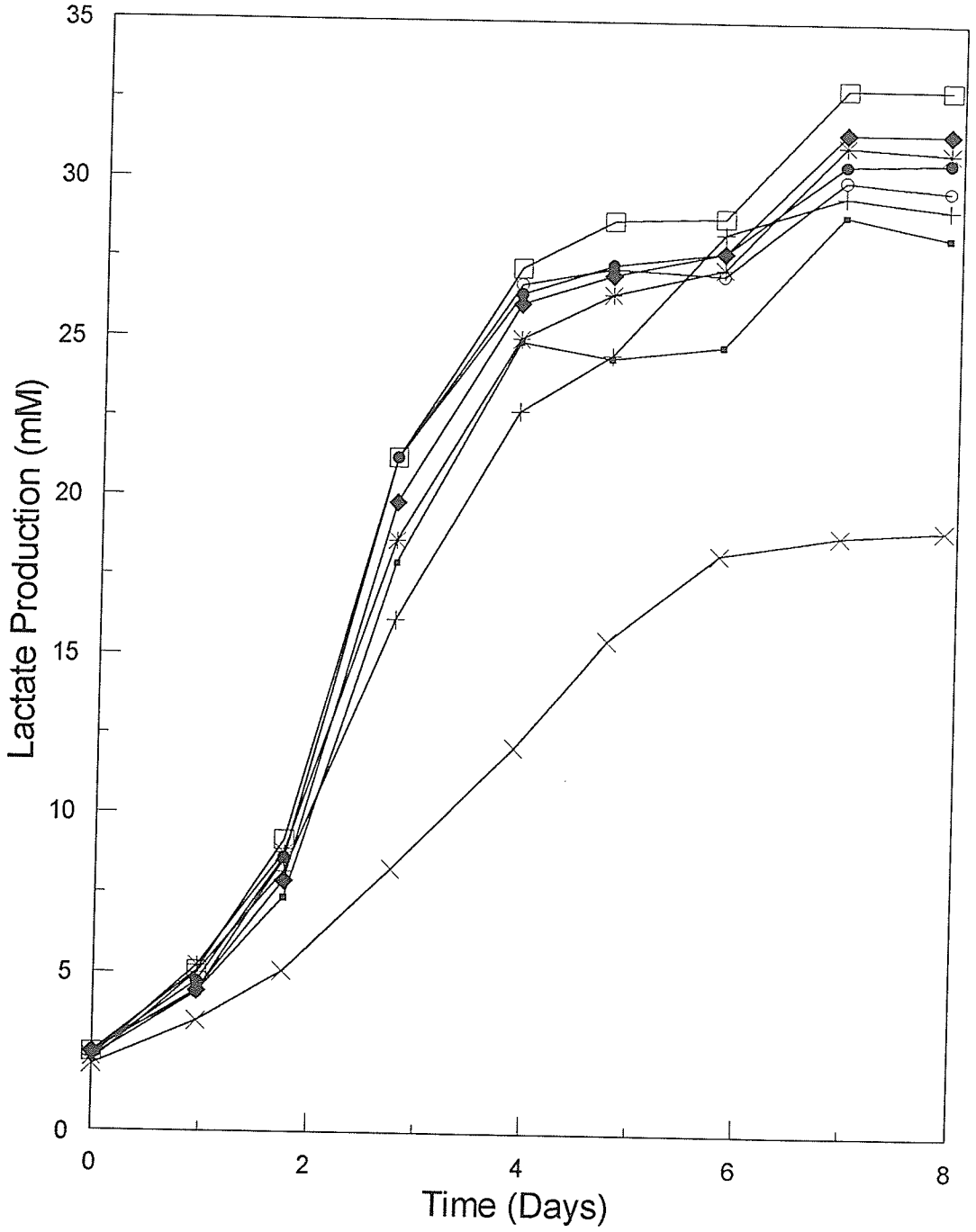

Figure 3.6. Lactate production over time at various concentrations of dichloroacetic acid. CC9C10 cells were grown in DMEM + 10% calf serum + 25 mM glucose + 4 mM glutamine with dichloroacetic acid at concentrations of 0 mM (□), 1 mM (○), 1.5 mM (■), 2 mM (●), 2.5 mM (◆), 3 mM (*), 5 mM (+), and 10 mM (X). (n=2).

Table 3.3. Specific glucose consumption rates for hybridoma CC9C10 grown at various concentrations of dichloroacetic acid in DMEM + 10% calf serum. + 4 mM glutamine + 25 mM glucose . (n=2).

Time (Days)	Specific Glucose Consumption Rates (μmol/10^6 cell*days)							
	DMEM + Added Dichloroacetic Acid (mM)							
	0 (± S,E.M.)	1 (± S,E.M.)	1.5 (± S,E.M.)	2 (± S,E.M.)	2.5 (± S,E.M.)	3 (± S,E.M.)	5 (± S,E.M.)	10 (± S,E.M.)
Day 1	12.1 (±0.4)	23.4 (±1.5)	18.8 (±0.05)	26.7 (±0.66)	22.3 (±1)	22.9 (±3)	28.4 (±1)	10.7 (±0.1)
Day 2	6.6 (±0.2)	4.59 (±0.6)	4.82 (±0.25)	5.27 (±0.09)	5.69 (±0.45)	4.2 (±0.15)	5.95 (±0.23)	5.48 (±.0.03)
Day 3	4.35 (±0.12)	4.4 (±0.03)	3.16 (±0.03)	3.3 (±0.08)	4.82 (±0.2)	3.72 (±0.05)	3.54 (±0.09)	4.81 (±0.39)
Day 4	1.24 (±0.03)	1.37 (±0.03)	1.5 (±0.05)	1.02 (±0.02)	0.968 (±0.04)	1.72 (±0.03)	2.24 (±0.09)	1.81 (±0.07)

S,E.M. represents standard error of the mean.

Table 3.4. Specific lactate production rates ± standard error of the mean for hybridoma CC9C10 grown at various concentrations of dichloroacetic acid in DMEM + 10% calf serum. + 4 mM glutamine + 25 mM glucose. (n=2).

Time (Days)	Specific Lactate Production Rates (μmol/10^6 cell*days)							
	DMEM + Dichloroacetic Acid (mM)							
	0 (± S,E.M.)	1 (± S,E.M.)	1.5 (± S,E.M.)	2 (± S,E.M.)	2.5 (± S,E.M.)	3 (± S,E.M.)	5 (± S,E.M.)	10 (± S,E.M.)
Day 1	23.6 (±0.8)	21.5 (±1.4)	21.5 (±1.2)	24.3 (±0.6)	20.6 (±0.9)	28.3 (±3.7)	37.5 (±1.3)	18.6 (±0.2)
Day 2	10.4 (±0.3)	10 (±1.2)	7.13 (±0.37)	8.89 (±0.15)	9.33 (±0.73)	8.28 (±0.3)	9.43 (±0.36)	7.07 (±.0.04)
Day 3	7.18 (±0.2)	8.09 (±0.06)	5.57 (±0.06)	5.96 (±0.14)	7.56 (±0.32)	5.9 (±0.08)	5.98 (±0.15)	5.16 (±0.42)
Day 4	2.18 (±0.05)	2.1 (±0.05)	2.28 (±0.07)	2.11 (±0.05)	2.26 (±0.1)	2.56 (±0.04)	3.3 (±0.13)	3.3 (±0.13)

S.E.M. represents standard error of the mean.

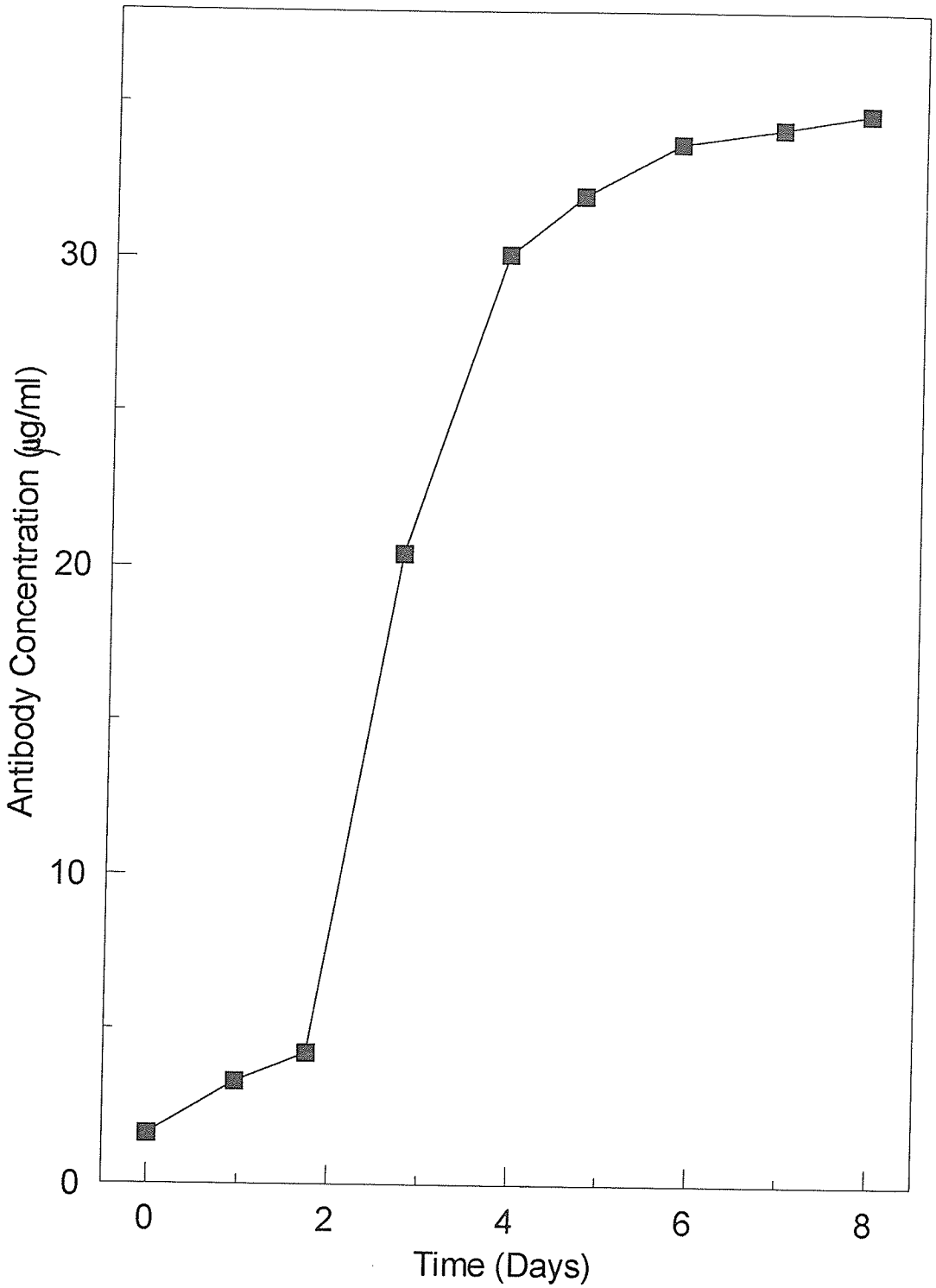

Figure 3.7. Antibody concentration over time for CC9C10 grown in DMEM + 1.5 mM dichloroacetic acid. (n=2).

3.3.3 CC9C10 Cells Grown in Spinner Flasks Containing DMEM + 10% Serum

Figure 3.8 illustrates the growth of CC9C10 over time, in DMEM + 10% calf serum + 25 mM glucose + 4 mM glutamine ± 1.5 mM dichloroacetic acid. The growth of cells was similar whether DCA was present, or absent. Cells grown with DCA supplementation reached a 6% higher peak density than the control at 2.1×10^6 viable cells/ml. Cells grown without DCA reached 1.97×10^6 viable cells/ml. Towards the end of the experiment it appeared that the addition of DCA helps improve cell viability, although small. The cellular protein levels increased initially during the growth of cells with or without DCA, but both rapidly declined after day one, similarly.

Glucose and lactate profiles of CC9C10 cells grown with or without DCA are shown in Figure 3.9. Total glucose consumption and lactate production for cells grown without DCA were similar. Examination of the glucose, lactate, and cell growth profiles of CC9C10 grown with DCA do not show any benefits upon comparison when grown without DCA

The antibody level of supernatant from C9C10 grown with or without 1.5 mM DCA was determined to see if DCA had an influence on antibody production. Figure 3.10 illustrates the antibody concentration over the course of the experiment. The antibody concentrations near the end of the experiment were similar (33.2 μg/ml) for cells grown without 1.5 mM DCA as opposed to 36.5 μg/ml for cells grown with 1.5 mM DCA. Using T-flasks and identical medium, the antibody concentration was near 34.7 μg/ml the end of the experiment for hybridoma CC9C10 cells grown in identical medium as above. There was no significant difference between the antibody levels in all instances.

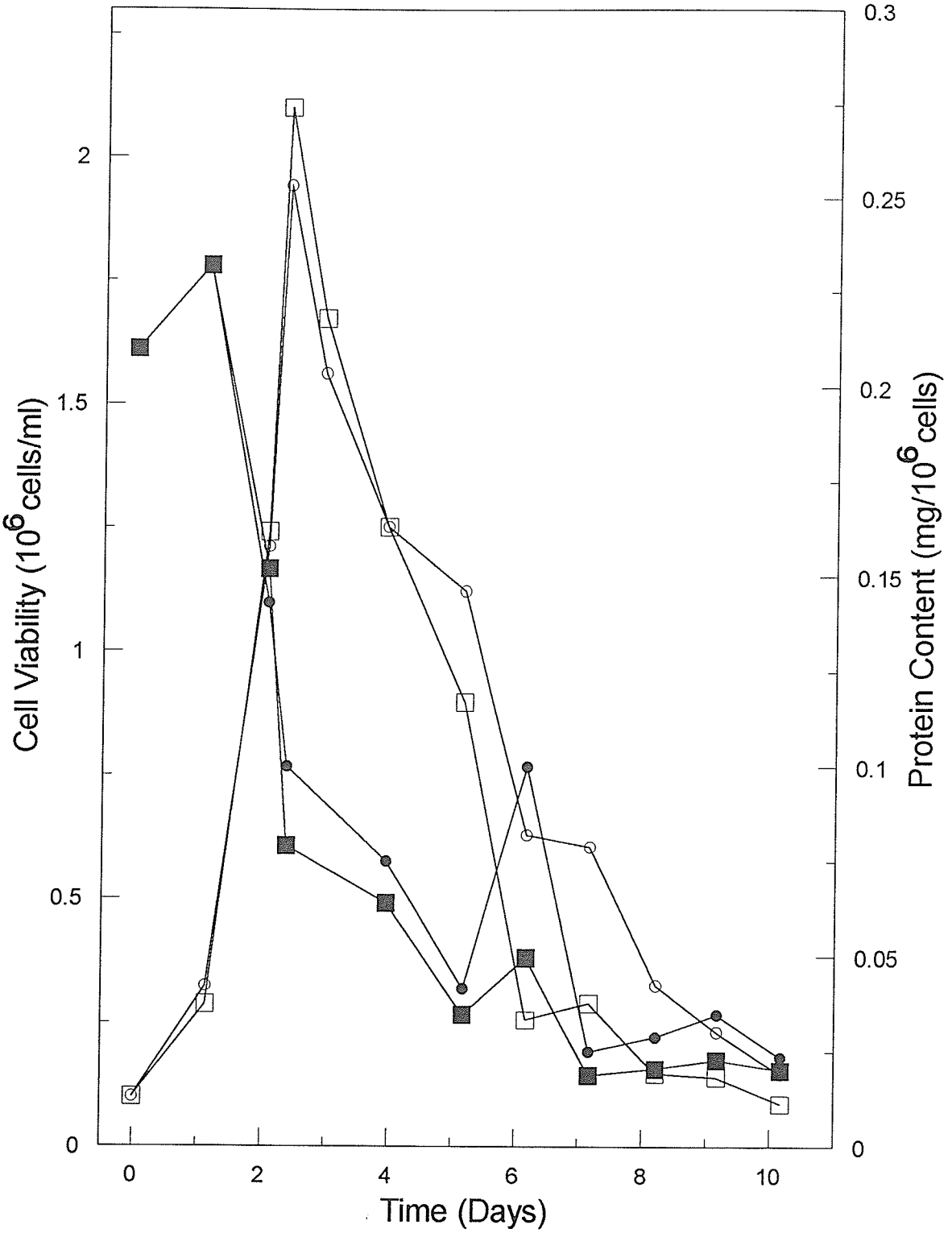

Figure 3.8. CC9C10 cells grown in DMEM ± 1.5 mM dichloroacetic Acid. Viable cell number is represented by cells grown with (□), or without 1.5 mM DCA (○). Cell protein content is represented by cells grown with (■), or without 1.5 mM DCA (●). (n=2).

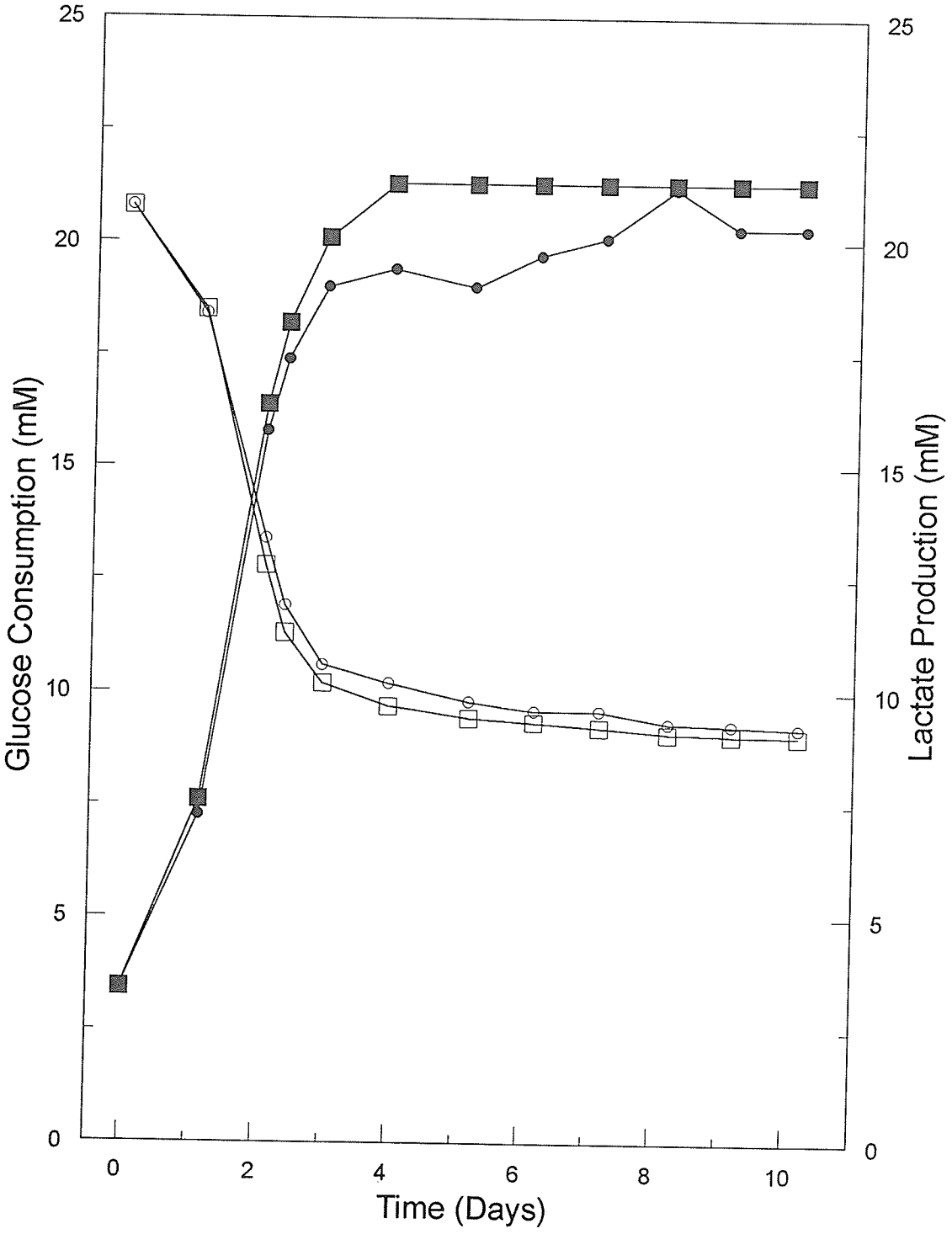

Figure 3.9. Glucose consumption and lactate production for CC9C10 cells grown in DMEM ±1.5 mM dichloroacetic acid. Glucose consumption is represented by cells grown with (□), or without 1.5 mM DCA (○). Lactate production is represented by cells grown with (■), or without 1.5 mM DCA (●). (n=2).

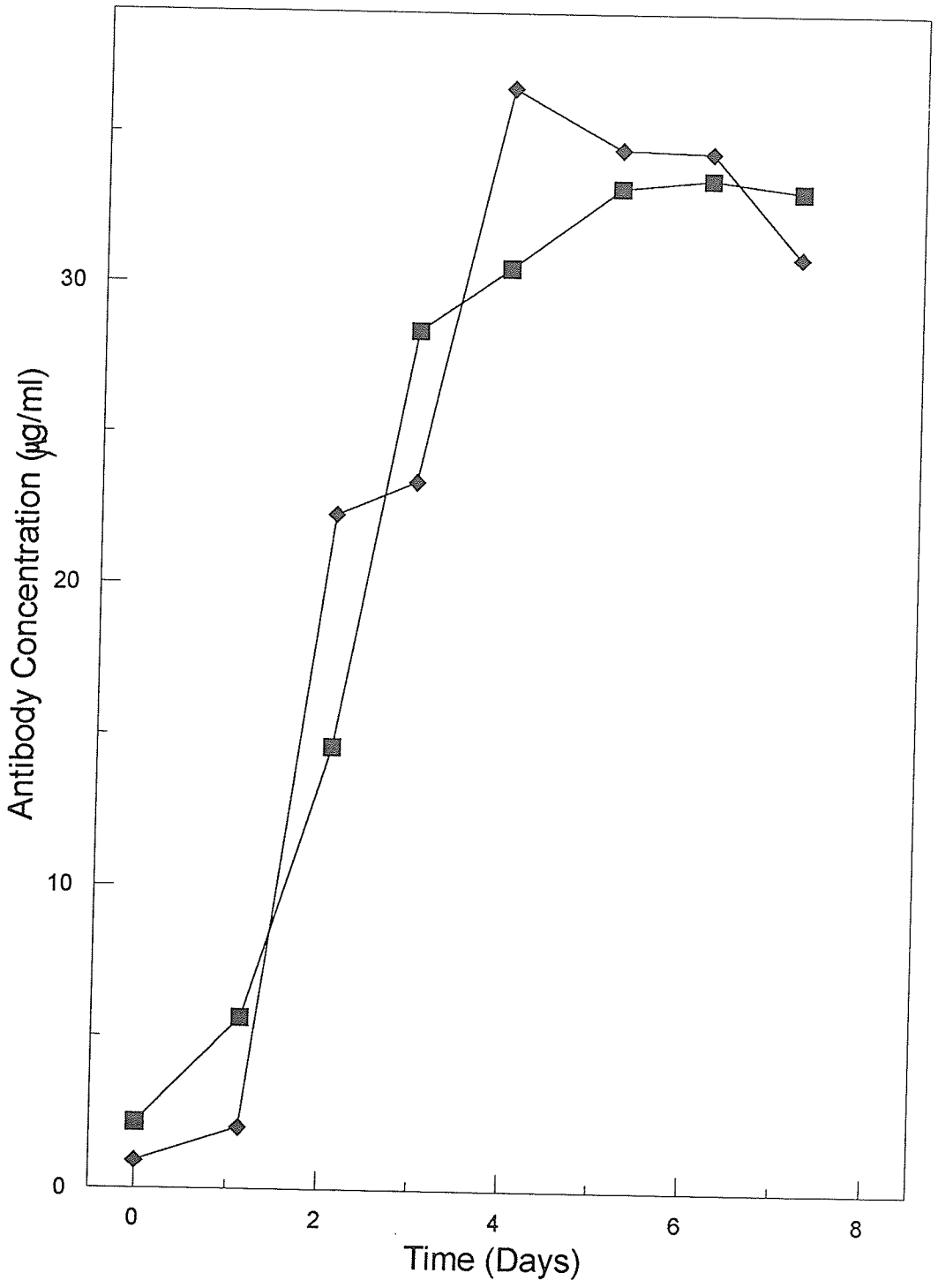

Figure 3.10. Antibody concentration for CC9C10 grown in DMEM ± 1.5 mM dichloroacetic acid. Antibody concentrations are shown for cells grown with (♦) or without 1.5 mM DCA (■). (n=2).

3.3.4 CC9C10 Grown in Hybridoma Serum-Free Medium with Dichloroacetic Acid at Varying Concentrations

Dichloroacetic acid added to cultures containing serum from Sections 3.2.1 to 3.2.3 had improved cell viability and increased the maximum cell yield in the decline phase. This was not accompanied by higher antibody concentrations. Since dichloroacetic acid (DCA) did not appear to have any other significant effect on CC9C10 cells grown in RPMI or DMEM with serum supplementation, attempts were made to see if DCA added to hybridoma serum-free medium (HSFM) would effectively have a positive effect on CC9C10 cell growth, viability, lactate production, and glucose consumption. CC9C10 were grown in 150 cm^2 T-flasks with HSFM at 37°C under a 10% CO_2 overlay. Cells were grown in duplicate (two separate T-flasks for each DCA concentration) with or without DCA at various concentrations, being fed with the addition of 4.2 ml, and 3.25 ml of a 2 M glucose and 200 mM glutamine stock solution on days 2 and 3, respectively. DCA concentrations used in this experiment were at 0, 1, 1.5, 2, and 2.5 mM. Cells were inoculated at 1 x 10^5 viable cells/ml, and adapted for a minumum of 4 passages. Adaptation for 4 passages was employed to ensure that cell metabolism would not be affected by the exposure of the new medium component (DCA).

CC9C10 cultures which were not fed any glucose and glutamine had a growth curve shown in Figure 3.11. CC9C10 cultures were fed glucose and glutamine produced a growth curve shown in Figure 3.12. CC9C10 which were not supplemented with additional glucose and glutamine reached a higher peak cell density than those which were fed. However, all cells in the experiment reached peak viable cell density on day 3. Cells which were not fed, and with no addition of DCA reached a maximal cell level of 2.14 x 10^6 viable cells/ml. Cells not fed, with the addition of DCA up to 2.5 mM reached maximal cell densities below 2 x 10^6 viable cells/ml. Upon cells entering the decline phase, they experienced a decrease in viable cell number. Maximum viable

cell number of hybridoma CC9C10 grown in HSFM containing various DCA concentrations is shown in Figure 3.13. The maximum effect of growth stimulation occurred at 1 mM DCA. DCA concentrations over 1 mM appeared to be toxic to hybridoma CC9C10 cells in the medium.

Cells with 1 mM DCA grew to a similar level of the control, but cells grown with higher DCA concentrations had a reduction of cell number, with 2.5 mM DCA appearing to be the most toxic level as shown in Figure 3.11. Cultures were fed on days two and three. DCA cultures which were fed with the glucose/glutamine supplement had lower maximal cell numbers than those cells which were not fed. Again, DCA concentrations above 1 mM were observed to give lower maximal cells numbers. Levels of DCA exceeding 1 mM with or without feeding was toxic to CC9C10, which decreased cell viability.

CC9C10 were supplemented with 2 M glucose and 200 mM glutamine stock solution, 4.5 ml on day 1, and 3.25 ml on day 2. Feeding resulted in an increase of the glucose supernatant concentration by a value of 35 mM on day one, and 25 mM on day two. Glutamine concentration increased by a value of 3.10 mM on day 1, and 2.14 mM on day 2

Supplemented CC9C10 cultures shared similar rates of glucose consumption when compared to the control. Consumption rates appeared linear until day three, which was associated with the cells reaching the stationary phase. This is illustrated in Figure 3.14.

CC9C10 supplemented with glucose displayed similar amounts of glucose consumed even though 35 mM, and 25 mM glucose and glutamine were added on days one and two, respectively. This is illustrated in Figure 3.15.

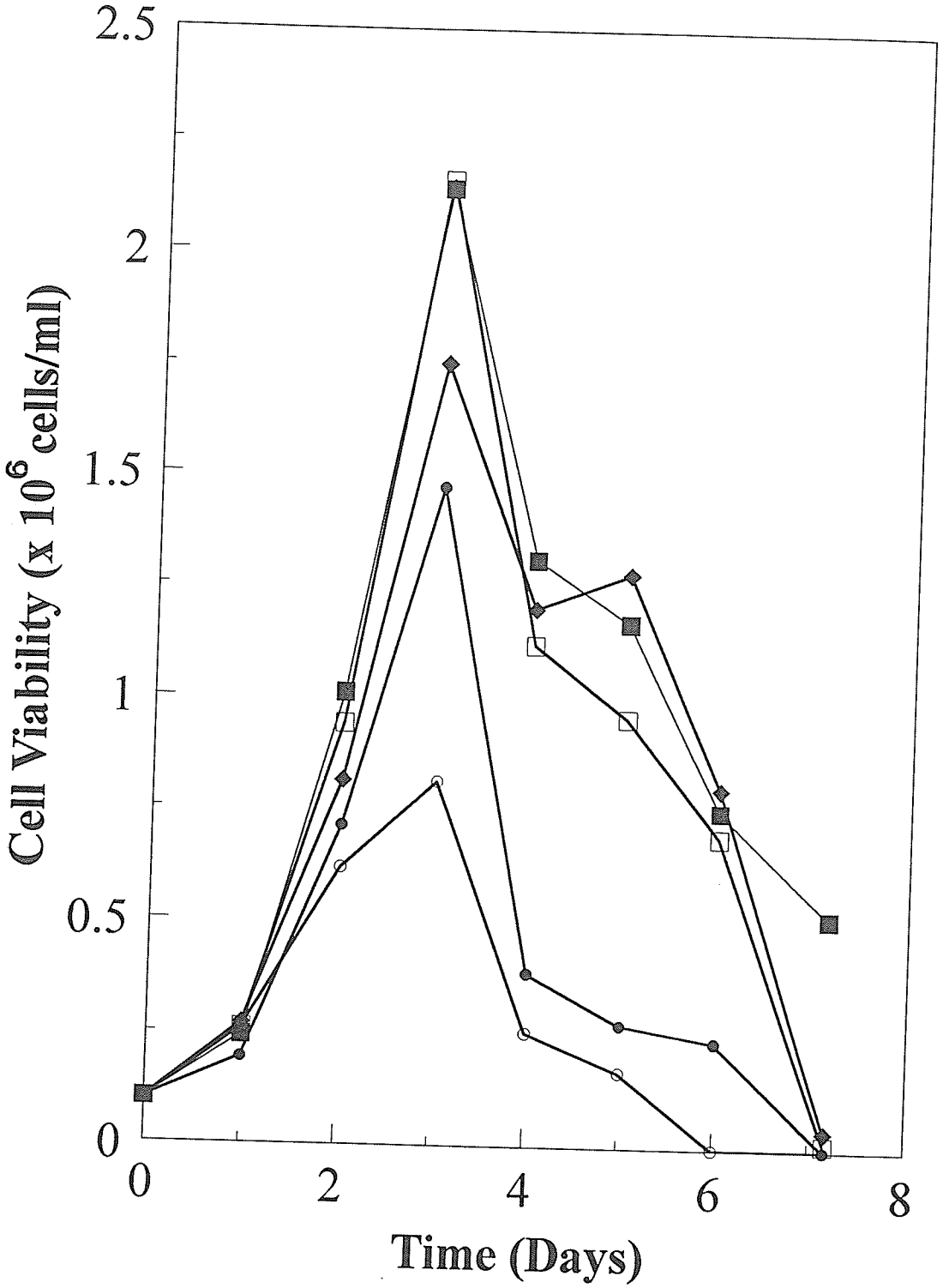

Figure 3.11. Viable cell numbers for cultures not fed with supplement. CC9C10 were grown in HSFM, and supplemented with various concentrations of dichloroacetic acid. Cultures were unfed. Viable cell number is indicated by cells grown in HSFM with dichloroactic acid at concentrations of 0 mM (■) 1 mM DCA (□), 1.5 mM DCA (◆), 2 mM DCA (●), and 2.5 mM DCA (O). (n=2).

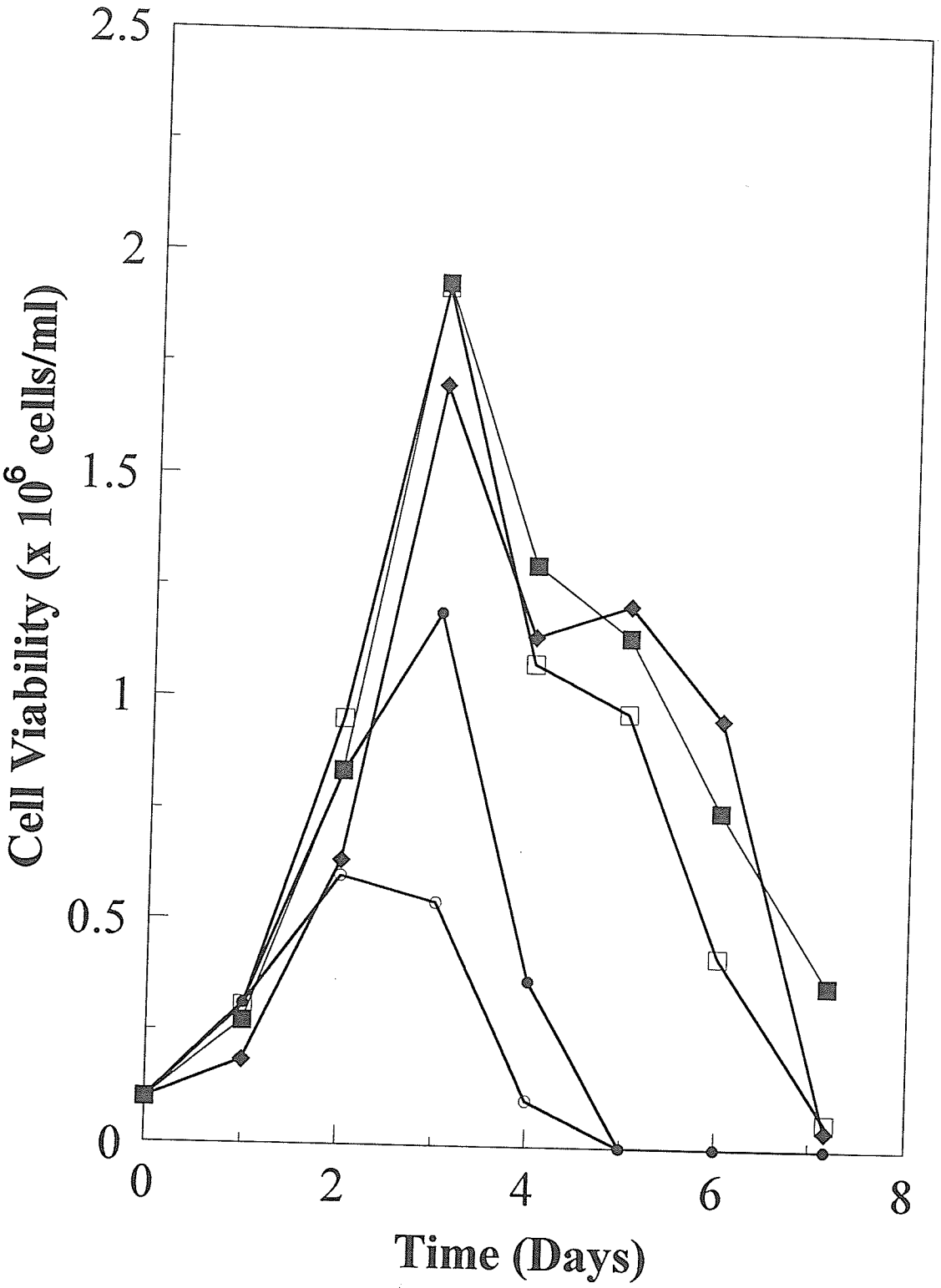

Figure 3.12. Viable cell number for cultures fed with supplement. CC9C10 were grown in HSFM, and supplemented with various concentrations of dichloroacetic acid. Cultures were fed with the addition of 2 M glucose, or 200 mM glutamine on days two and three. Viable cell number is indicated by cells grown in HSFM with dichloroactic acid at concentrations of 0 mM (■) 1 mM DCA (□), 1.5 mM DCA (◆), 2 mM DCA (●), and 2.5 mM DCA (O). (n=2).

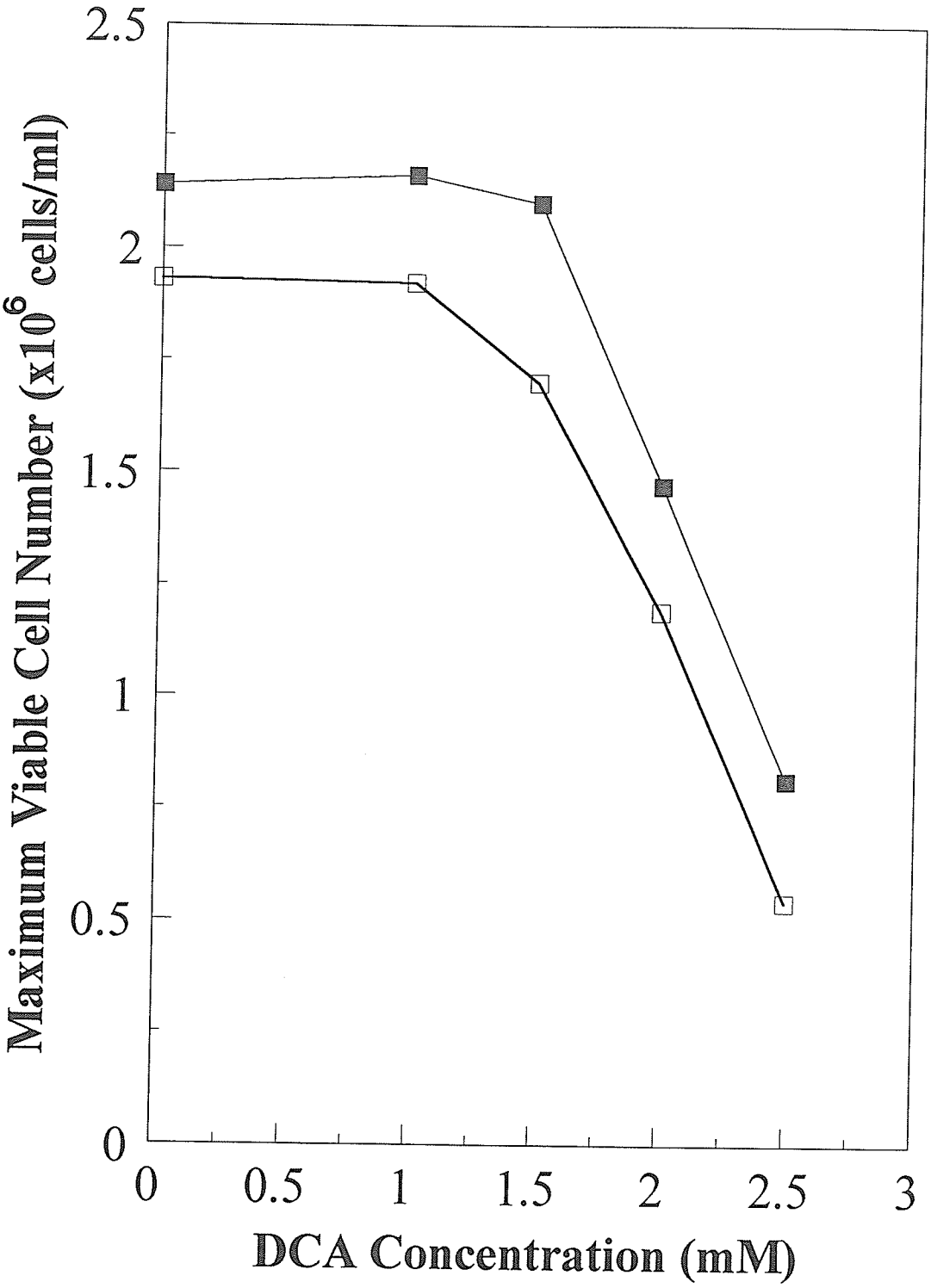

Figure 3.13. Maximum viable cell number vs. dichloracetic acid concentration. Maximum viable cell number of hybridoma CC9C10 cultures which were supplemented with additional glucose/glutamine on days two and three (□), or not fed (■), with respect to varying concentrations of dichloroacetic acid.

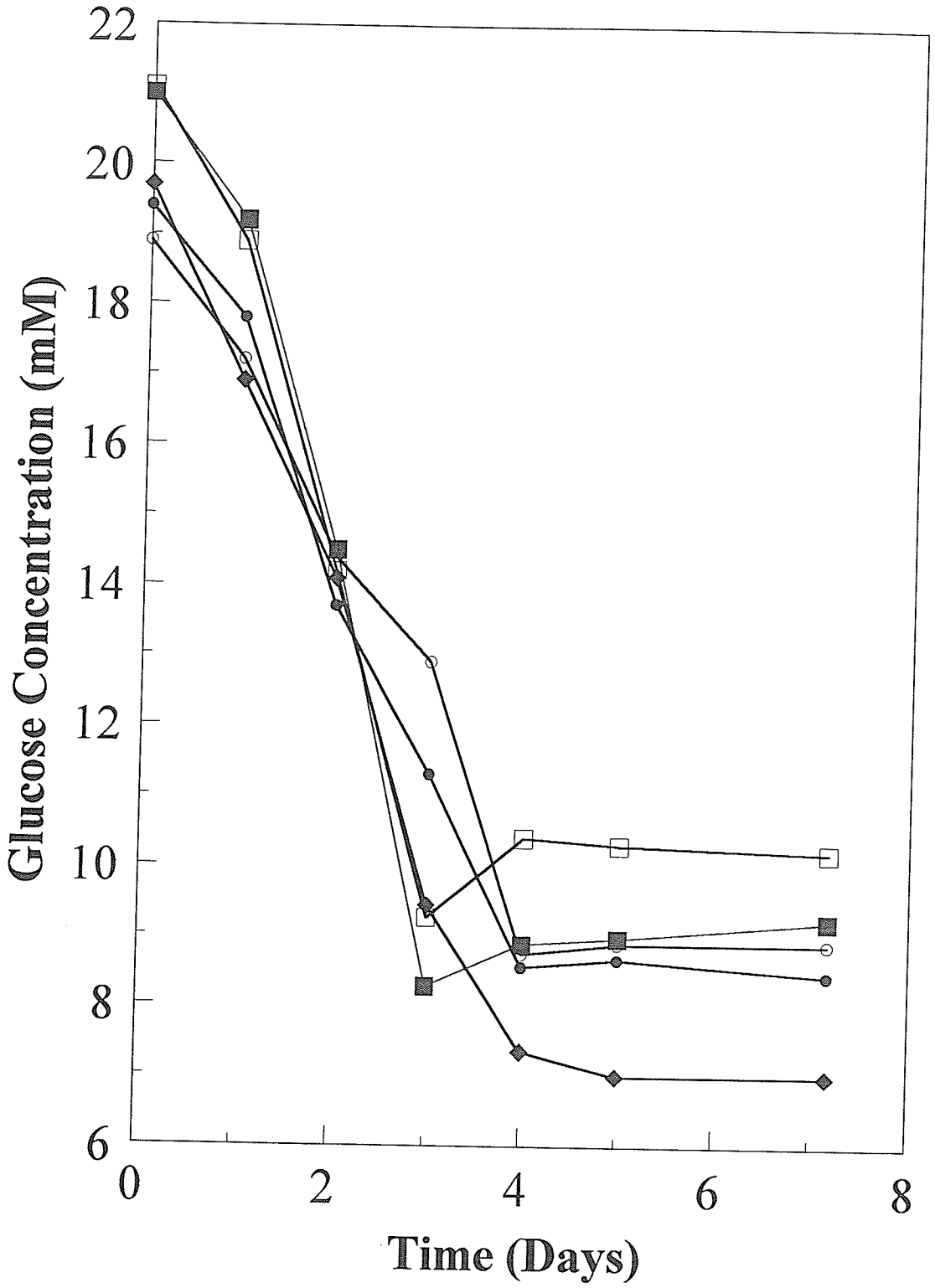

Figure 3.14. Glucose concentration for CC9C10 grown in HSFM without feeding. Glucose concentration is indicated by cells grown in HSFM at dichloroacetic acid concentrations of 0 mM (■), 1 mM DCA (□), 1.5 mM DCA (◆), 1.5 mM DCA plus the addition of 0.5 mM DCA on day 2 (◊), 2 mM DCA (●), and 2.5 mM DCA (O). (n=2).

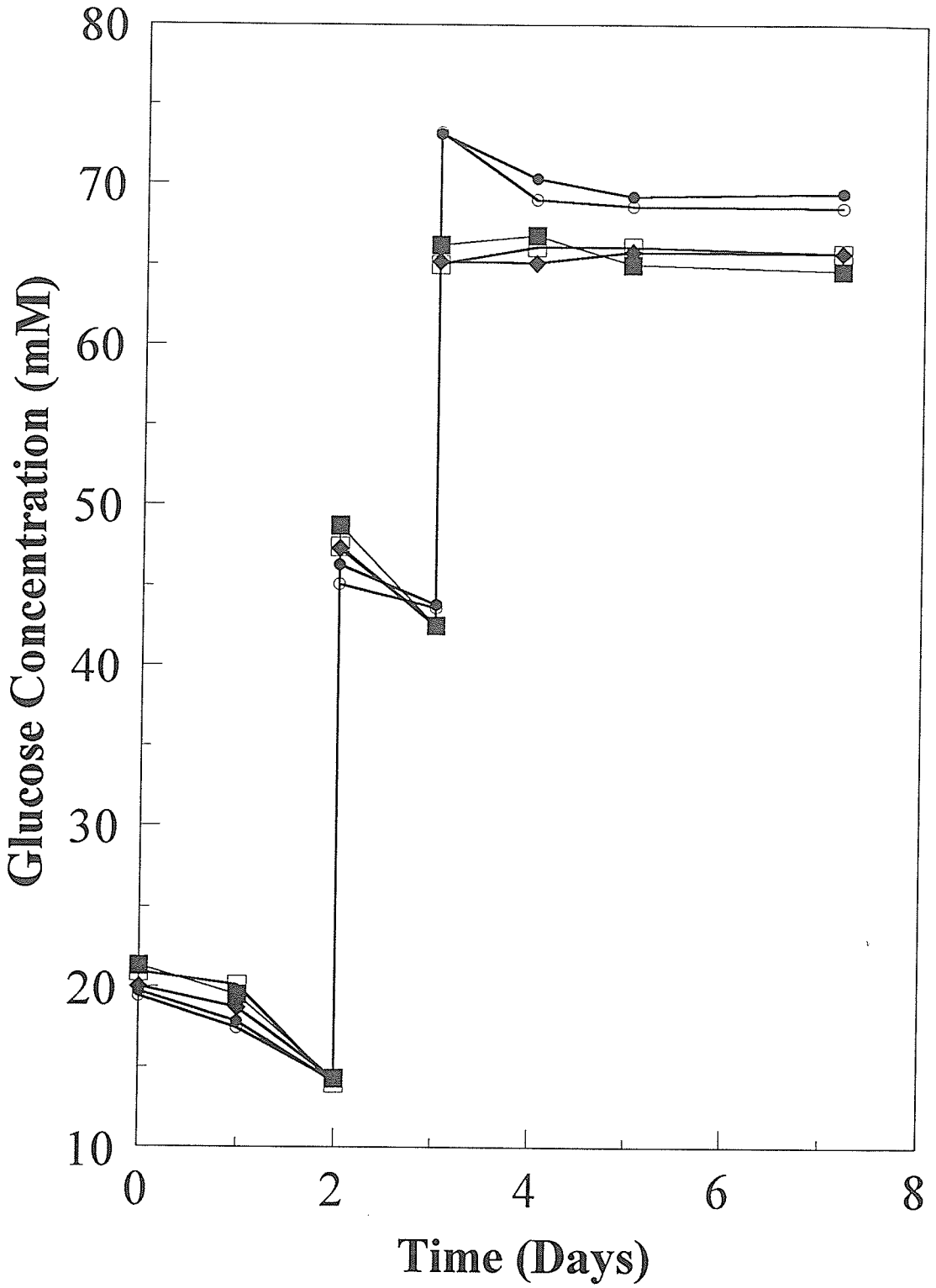

Figure 3.15. Glucose consumption for CC9C10 grown in hybridoma serum-free medium (HSFM) with feeding. Glucose consumption is indicated by cells grown in HSFM at dichloroacetic acid concentrations of 0 mM (■), 1 mM DCA (□), 1.5 mM DCA (◆), 2 mM DCA (●), and 2.5 mM DCA (O). (n=2).

Lactate production is shown for all CC9C10 cultures with or without glucose/glutamine supplementation. Cells supplemented with glucose and glutamine had slightly higher levels of lactate, although not significant. These differences may be viewed on Figures 3.16 and 3.17. Lactate production was linear until day 3, which was associated with CC9C10 cells reaching the stationary phase.

Specific glucose consumption rates of hybridoma CC9C10 grown in HSFM with DCA at various concentrations, with or without feeding of a glucose/glutamine mixture are determined as illustrated in Table 3.5.

The HSFM culture on day 1 had a specific glucose consumption rate of 14.7 $\mu mol/10^6$ cell*days. Cultures with 1.5 mM DCA specific glucose consumption rates on day 1 41% higher than the control culture on day 1. Following day 1, all cultures had similar consumption rates. The addition of DCA caused an increase in the specific glucose consumption, although not significant.

Specific lactate production rates of CC9C10 grown in HSFM at various DCA concentrations without feeding are determined as shown in Table 3.6. The specific lactate production rate of CC9C10 grown in HSFM was 26.4 $\mu mol/10^6$ per cell*days. Cultures with DCA had slightly higher production rates than the control.

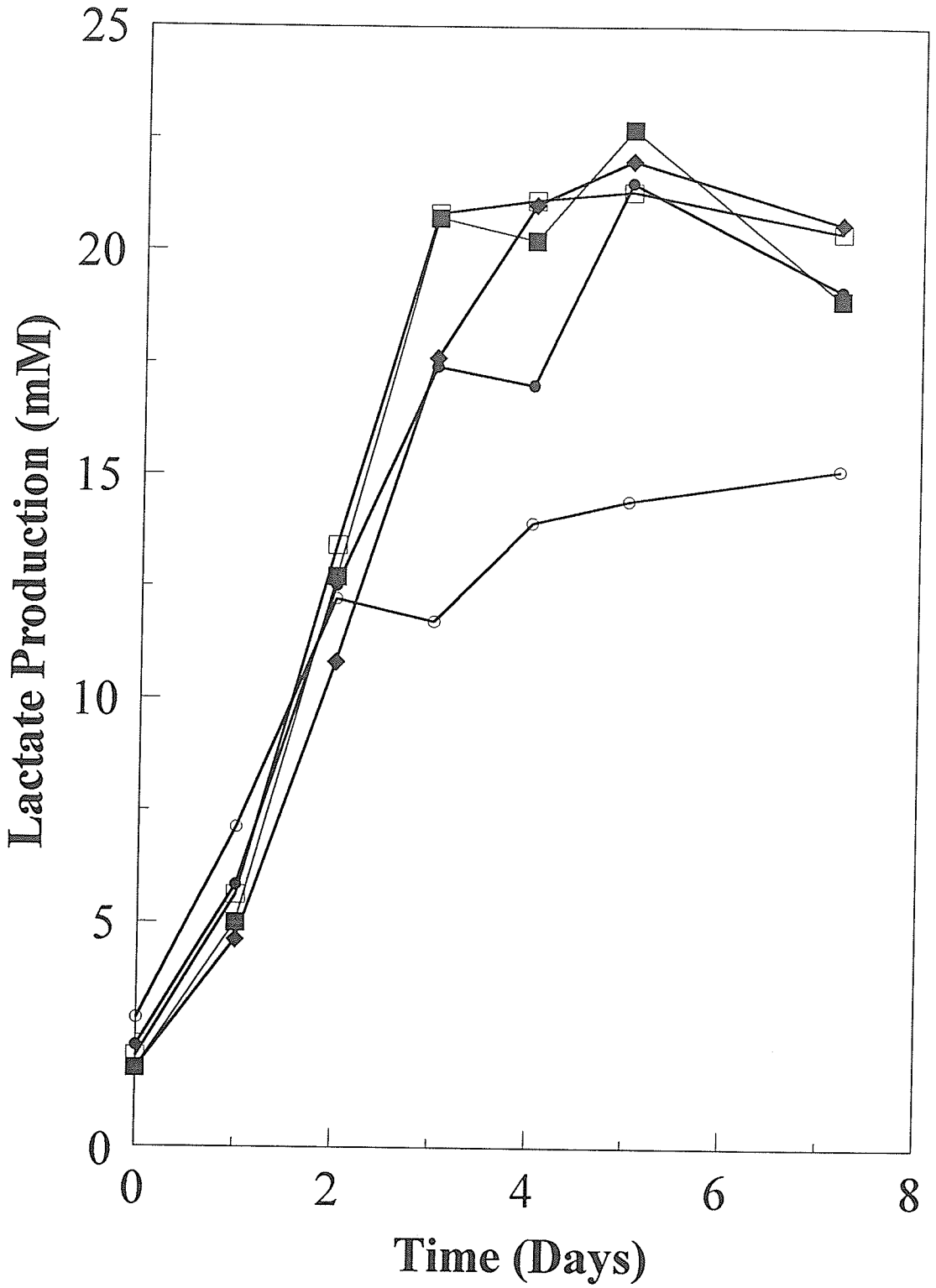

Figure 3.16. Lactate Production for CC9C10 grown in HSFM without feeding. Lactate production is indicated by cells grown in HSFM at dichloroacetic acid conentrations of 0 mM(■), 1 mM DCA (□), 1.5 mM DCA (◆), 2 mM DCA (●), and 2.5 mM DCA (O). (n=2).

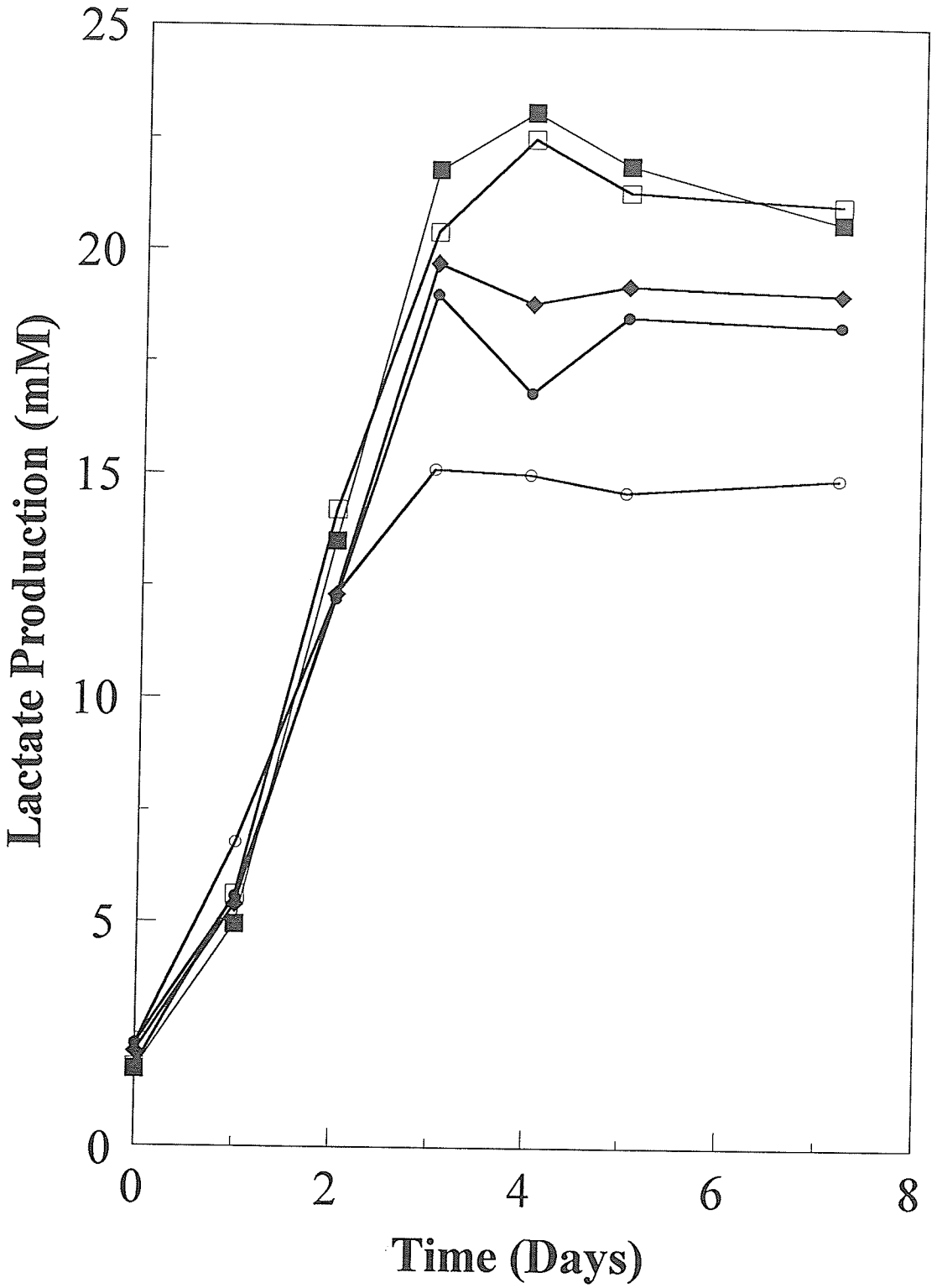

Figure 3.17. Lactate Production for CC9C10 grown in HSFM with feeding. Lactate production is indicated by cells grown in HSFM at dichloroacetic acid concentations of 0 mM(■), 1 mM DCA (□), 1.5 mM DCA (◆), 2 mM DCA (●), and 2.5 mM DCA (O). (n=2).

Table 3.5. Specific glucose consumption rates for CC9C10 grown in HSFM at various dichloroacetic acid concentrations without feeding of a glucose/glutamine supplement. (n=2).

Time (Days)	Specific Glucose Consumption Rates (μmol/10^6 cell*days)				
	HSFM + Dichloroacetic Acid (mM)				
	0 (± S. E. M.)	1 (± S. E. M.)	1.5 (± S. E. M.)	2 (± S. E. M.)	2.5 (± S. E. M.)
Day 1	14.7 (±0.4)	16.9 (±0.3)	20.7 (±0.41)	16.5 (±0.2)	12.7 (±1.6)
Day 2	4.66 (±0.07)	5 (±0.16)	3.44 (±0.24)	5.76 (±0)	4.55 (±0.41)
Day 3	1.93 (±0.21)	1.51 (±0.19)	1.78 (±0.12)	1.08 (±0)	1.24 (±0.14)
Day 4	-	-	0.83 (±0)	3.97 (±0)	8.94 (±0.95)

S.E.M. represents standard error of the mean.

Table 3.6. Specific lactate production rates for CC9C10 grown in HSFM at various dichloroacetic acid concentrations without feeding of a glucose/glutamine supplement.
(n=2)

Time (Days)	Specific Lactate Production Rates ($\mu mol/10^6$ cell*days)				
	HSFM + Dichloroacetic Acid (mM)				
	0 (± S. E. M.)	**1** (± S. E. M.)	**1.5** (± S. E. M.)	**2** (± S. E. M.)	**2.5** (± S. E. M.)
Day 1	26.4 (±0.7)	27.5 (±0.6)	24.2 (±1.3)	36.6 (±0.6)	31.5 (±4.1)
Day 2	7.62 (±0.11)	8.32 (±0.27)	8.51 (±0.67)	9.34 (±0)	8.24 (±0.91)
Day 3	2.49 (±0.27)	2.28 (±0.25)	2.81 (±0.1)	2.22 (±0)	2.12 (±0.16)

S.E.M. represents standard error of the mean.

3.3.5 Oxygen Consumption of CC9C10 Grown in HSFM With or Without the Addition of 1 mM Dichloroacetic Acid

Oxygen consumption was compared between CC9C10 grown with or without 1 mM DCA in HSFM. Figure 3.16 illustrates the measure of oxygen consumption over time. Each oxygen measurement was performed in duplicate. Cells grown in the absence of DCA had an oxygen consumption value of 4±0.42 nmol/minute per 10^6 cells. Cells grown in the presence of 1 mM DCA had an oxygen consumption value of 3.10±0.28 nmol/minute per 10^6 cells. There was a slight enhancement in the oxygen consumption rate with the addition of 1 mM DCA to the culture.

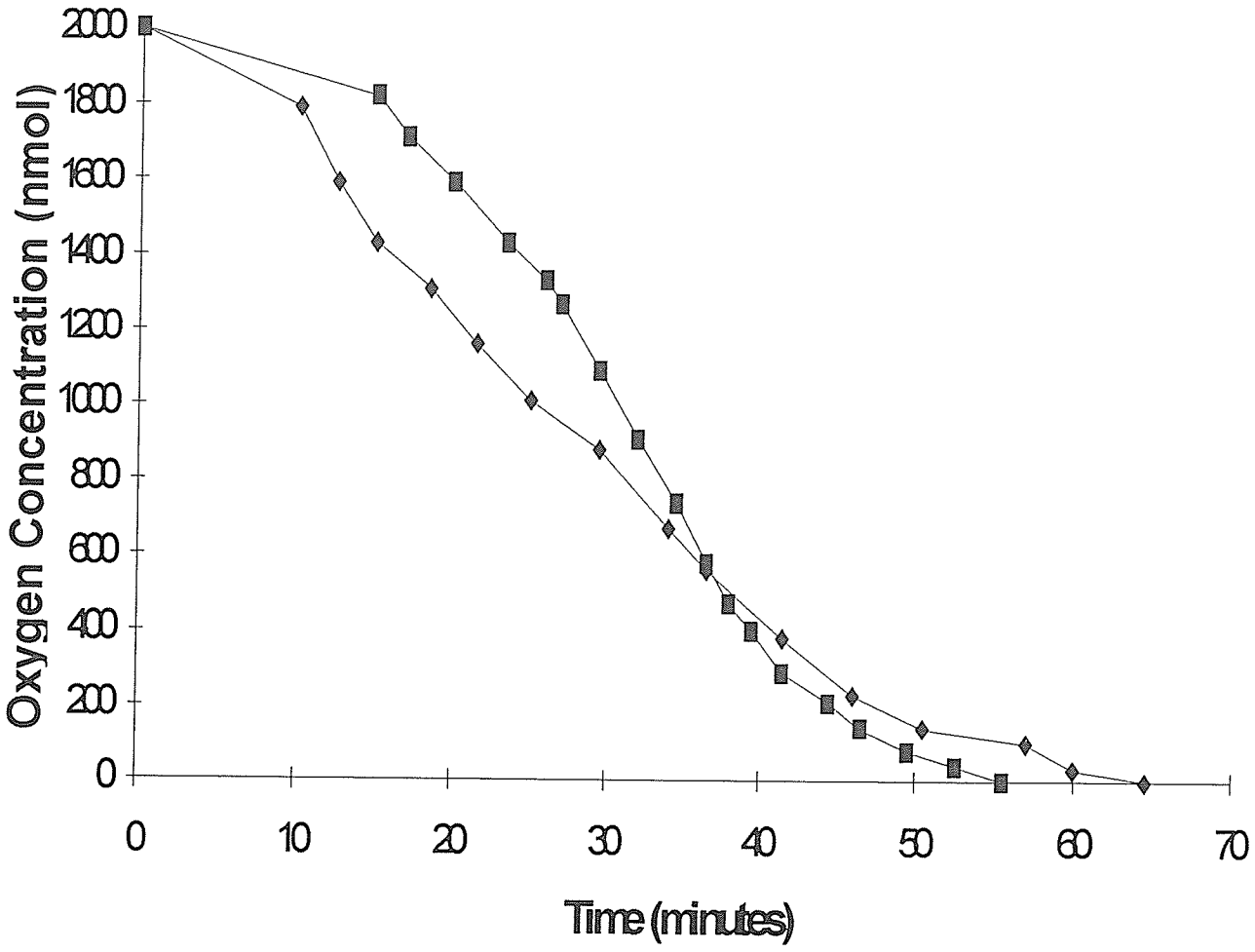

Figure 3.18. Oxygen consumption for hybridoma CC9C10 grown in serum-free medium with the addition of 1 mM dichloroacetic acid (■), and without the addition of dichloroacetic acid (◆). (n=2).

3.4 Discussion

Hybridoma CC9C10 cells were grown in RPMI and DMEM (which were serum supplemented), and hybridoma serum-free media in order to evaluate the effects of DCA. Cells grown in the spinner flasks reached a slightly higher density, being attributed to better aeration, and mixing of cells with nutrients. Cells grown in the T-flasks exhibited higher densities in the decline phase as opposed to the spinner flasks, which was attributed to less shear force on the culture medium. Cells cultured in RPMI grown in 250 ml Bellco spinners gave the poorest growth. The cells grew to a lower cell density as opposed to the other media, as RPMI was a less rich medium than DMEM-F12, or HSFM with respect to nutrient concentrations. Upon culturing CC9C10 in DMEM, they were grown in 150 cm^2 T-flasks, or 250 ml Bellco spinners. Cultures in T-flasks peaked near 1.5 x 10^6 viable cells/ml, while cells cultured in spinner flasks reached 2 x 10^6 viable cells/ml. Cells grown in HSFM were placed in 150 cm^2 T-flasks and reached a density near 2 x 10^6 viable cells/ml. CC9C10 cells cultured with DCA and serum in DMEM or RPMI were observed to have better cell viability than cells which did not have DCA addition upon the cells entering the decline phase (100 to 200%). Cells cultured with HSFM however did not show this trend. Reasons for this occurrence were unknown. The cultures of DMEM containing DCA did not display an increase in antibody production, although having a higher viable cell number than the control. CC9C10 cells cultured with DCA in serum containing media showed higher levels of growth than cells cultured in HSFM (no serum). DCA appeared to be toxic in serum containing medium beyond 3 mM supplementation. HSFM cultures experienced DCA toxicity beyond 1 mM supplementation. It appeared that the serums large bulk proteins had some sort of protective effect upon CC9C10 cells exposed to DCA, probably by coating the cell membrane, slowing the diffusion of DCA into the cell. As HSFM had no

serum, there was no protective mechanism for the cells, which resulted in a lower viable cell number over the growth of the culture.

In RPMI medium, cultures containing 1.5 mM DCA had a specific lactate production rate on day 1 which was 11% lower than cultures supplemented with DCA. Specific lactate production rates in DCA supplemented cultures remained lower than cultures without DCA addition for the remainder of the experiment. In DMEM medium, specific lactate production rates on day 1 were lower in all cultures supplemented with varying concentrations of DCA than the control, except cultures containing 3 and 5 mM DCA, which were 20% and 59% higher. Following day 1, all cells cultured with DCA had lower specific lactate production rates than the control (no DCA addition). In HSFM, specific lactate production rates were higher in DMEM supplemented at various concentrations, with 2 mM DCA having the greatest difference (39% higher than the control). Following day 1, specific lactate production rates were higher in DCA supplemented than the control.

The cells cultured in HSFM were either fed, or not fed with 4.4 ml and 3.25 ml of a glucose/glutamine (2 M and 200 mM, respectively) supplementation on days 2 and 3, respectively. Cultures which were fed reached slightly lower levels of growth than nonfed cultures. This suggested that the cells were overfed, due to the glucose and glutamine concentrations in the medium being toxic.

Specific glucose consumption rates in RPMI with or without DCA addition on day 1 were identical (19.4 μmol/minute per 10^6 cells). Following day 1, the rates remained similar In DMEM supplemented at various concentrations with DCA specific glucose consumption rates were higher than the control with the greatest difference occurring at 5 mM (235% higher). Following day 1, all specific consumption rates in DCA supplemented cultures were lower than the control. HSFM cultures supplemented with DCA up to concentrations of 2 mM on day 1 had higher specific glucose

consumption rates than the control, with the largest difference at 1.5 mM DCA (41% higher).

Monoclonal antibody levels were measured to see if DCA addition had an effect upon increasing their levels. CC9C10 cells grown with 1.5 mM DCA had a total volumetric yield of 36.5 μg/ml, compared to 33.2 μg/ml from the control cultures. This suggested that DCA did not alter glucose metabolism significantly, or increase the energy level of CC9C10 cells enough to stimulate further antibody production.

Oxygen consumption measurements were performed on hybridoma CC9C10 cells grown in HSFM. The initial oxygen consumption rate in the cultures containing 1 mM DCA was 3.10 nmol/minute per 10^6 cells while the culture without DCA addition was 4 nmol/minute per 10^6 cells. While the initial oxygen consumption rate was quickest for the culture lacking DCA, the DCA containing culture consumed the entirity of the oxygen first.

As HSFM with DCA was toxic, the addition of bovine serum albumin (BSA) may have prevented the detrimental effects that DCA caused by having large bulk proteins sticking to the outer surface of the cell membranes. BSA addition to medium containing a similar amount of protein as a 10% serum supplemented medium should be tested. As bulk protein factors in the serum protected the hybridoma CC9C10 cells from the toxic effects of DCA, a similar level of protein supplemented from the BSA may provide a similar protective mechanism.

The addition of dichloroacetic acid did not have any noted benefits when added to culture. Specific glucose consumption and lactate production rates remained similar, antibody levels were similar, and cell yields were similar except when DCA reached a near toxic level. It was concluded that the addition of DCA to effect the growth of hybridoma cells was not a worthwhile procedure, for the above noted reasons, especially since the FDA is pushing for Industrial processes involving the growth of mammalian cells to be serum- or protein- free.

3.5 Summary

1) Specific glucose consumption rates were examined for cells grown in RPMI, DMEM, and HSFM. In RPMI, the rates were similar between the control, and the 1.5 mM DCA culture.

In DMEM + 10% calf serum + 4 mM glutamine, glucose consumption of the control was 12.1 μmol/10^6 cell*days on day 1. Cultures supplemented with DCA up to 5 mM had and average consumption of 22 μmol/10^6 cell*days. Following day 1, cultures containing DCA displayed consumption rates slightly lower than the control.

In HSFM, on day 1, the specific glucose consumption rates in DCA supplemented cultures were slightly higher than the control, although not significantly. Following day 1, all cultures had similar glucose consumption rates.

Overall, the addition of DCA seemed to have an effect on CC9C10 grown in medium richer than RPMI on day 1. After day 1 however, all cultures showed similar specific glucose consumption rates, suggesting that DCA increasing the specific glucose consumption rate was negligible.

2) Specific lactate production rates were examined for CC9C10 cells grown in RPMI + 10% calf serum + 20 mM glucose, DMEM-F12 + 10% calf serum + 4 mM glutamine, + HSFM. In RPMI, specific lactate production rates in DMEM supplemented cultures were 10% lower than the control. As the batch culture progressed, the DCA supplemented cultures specific lactate production rates continued to decrease in relation to the control.

CC9C10 grown in DMEM + 10% calf serum had specific lactate production rates on day 1 in cultures supplemented with DCA whose rate fluctuated around the control. The control has a specific lactate production rate of 23.6 μmol/10^6 cell*days. Following day 1, the rates are similar among all the cultures.

In CC9C10 cultured with HSFM, the specific lactate consumption rates on day 1 for cultures supplemented with DCA at concentrations of 1, 1.5, 2, and 2.5 mM, had rates of 27.5, 24.2, 36.6, and 31.5 μmol/10^6 cell*days, as opposed to the controls value of 26.4 μmol/10^6 cell*days.

3) Oxygen consumption was determined for cells grown in HSFM with or without 1 mM DCA. Cells grown with 1 mM DCA had an initial consumption rate of 3.10 nmol/minute per 10^6 cells, whereas the control has a consumption rate of 4 nmol/minute per 10^6 cells.

4) Antibody titers were determined for CC9C10 grown in DMEM cultures with or without 1.5 mM DCA in Bellco spinner flasks. Final antibody titers were 36.5 and 33.2 μ g/ml for cells cultured with and without 1.5 mM DCA, respectively. DCA was concluded not to enhance antibody production in the hybridoma CC9C10.

[1]CHAPTER 4

4.0 A Profile of Energy Metabolism in a Murine Hybridoma: Glucose and Glutamine Utilization

4.1 Introduction

The energy demands of mammalian cells in culture are provided by the catabolism of the major carbon substrates contained in the growth medium, which are usually glucose and glutamine (Butler and Jenkins, 1989). The relative importance of individual pathways of glucose and glutamine metabolism in providing the intracellular energy requirements has been a subject of considerable interest (Zielke *et al*, 1978; Reitzer *et al*, 1979; Lanks and Li, 1988, O'Rourke and Rider, 1989, Hassell and Butler, 1990).

Glucose metabolism can provide energy via glycolysis, the tricarboxylic acid cycle or the pentose phosphate pathway. Glucose also provides precursors for ribose formation by the pentose phosphate pathway, which is particularly important for nucleic acid synthesis during cell growth (Zielke *et al*, 1976; Wice *et al*, 1981). Glutamine is important in the provision of carbon and nitrogen for nucleic acid synthesis (Zetterberg and Engstrom, 1981). However, glutamine may also undergo complete oxidation to carbon dioxide or partial oxidation to 3 or 4 carbon products such as lactate, alanine or aspartate. The latter process is known as glutaminolysis and has been shown to provide a substantial proportion of the cellular energy requirement in transformed cells (Lanks and Li, 1988).

In this section we report an analysis of glucose and glutamine metabolism in an antibody-producing B-lymphocyte murine hybridoma. Rates of flux through the individual pathways of glucose and glutamine metabolism were determined during the

[1]The content of this chapter were included in a paper: Petch, D., Butler, M. A profile of energy metabolism in a murine hybridoma: glucose and glutamine utilization. J. Cell. Physiol. (in press).

exponential phase of growth of a batch culture. This flux data allowed a calculation of the energy released by each pathway and the relative importance of each pathway in meeting the energy requirement of the cell.

4.2 Materials and Methods

4.2.1 Cell line: Refer to Section 2.1.0a.

4.2.2 Culture conditions and growth medium: Refer to Section 2.1.1b, and 2.1.2a.

4.2.3 Cell counting: Refer to Section 2.1.4.

4.2.4 Intracellular protein content: Refer to Section 2.6.

4.2.5 Analysis of culture media: Refer to Section 2.3.

4.2.6 Radiolabelled compounds: Refer to Section 2.5.1

4.2.7 Measurement of CO_2 Evolution: Refer to Section 2.5.3.

4.2.8 Release of tritiated water: Refer to Section 2.5.4.

4.2.9 Analysis of metabolic end products: Refer to Section 2.5.5

4.3 Results

4.3.1 Cell Growth and productivity

The CC9C10 cells were grown in batch culture for 5 days (Figure 4.1). The specific growth rate was 0.041±0.004 h^{-1} (doubling time : 17.4±0.6 h) and the culture reached a maximum viable cell density of 1.05 x 10^6 cells/ml. The antibody concentration of the medium increased during culture to a maximum of 11 μg/ml. The specific antibody productivity which extended through the growth and decline phase was 2.8±0.2 μg protein/minute per 10^6 cells. The cell protein concentration was maximal during the growth phase at 0.4 mg protein/10^6 cells. Cell samples were taken during the mid-exponential phase (after 36 hours of culture) for measurements of metabolic flux.

4.3.2 Substrate utilization and by-product formation

The concentrations of glucose, glutamine, lactate and ammonia were measured in the culture medium at daily intervals (Figures 4.2 and 4.3). Glutamine was completely depleted from the medium in less than 3 days. However, glucose was only partially consumed with 60% of the original concentration remaining after 3 days. It is probably significant that the cessation of consumption of glucose by the cells was coincident with the peak cell density and the depletion of glutamine.

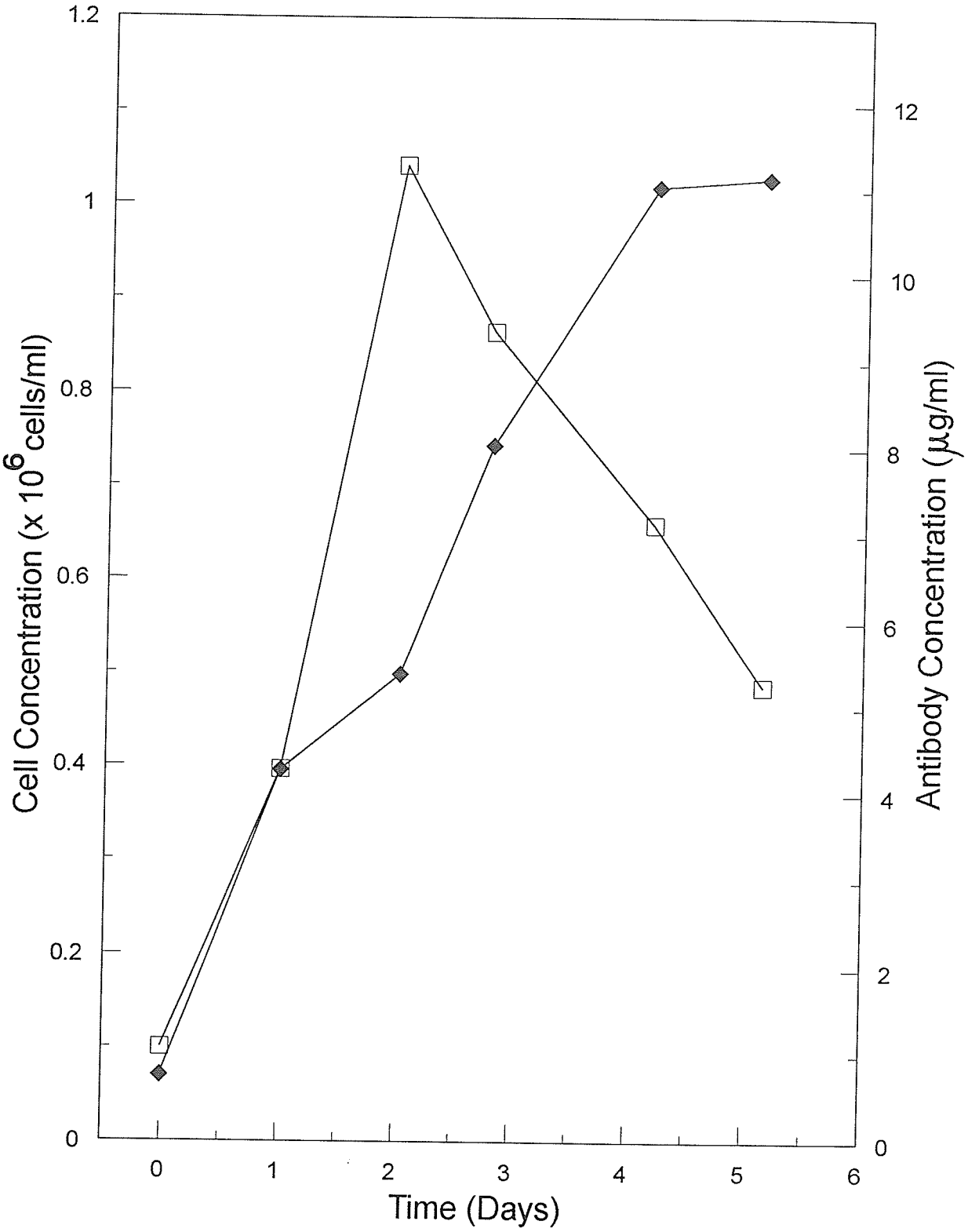

Figure. 4.1. Monoclonal antibody production during the growth of CC9C10 hybridomas. At daily intervals, samples (5 ml) were taken for determining the concentration of viable cells (□), and antibody production (♦).

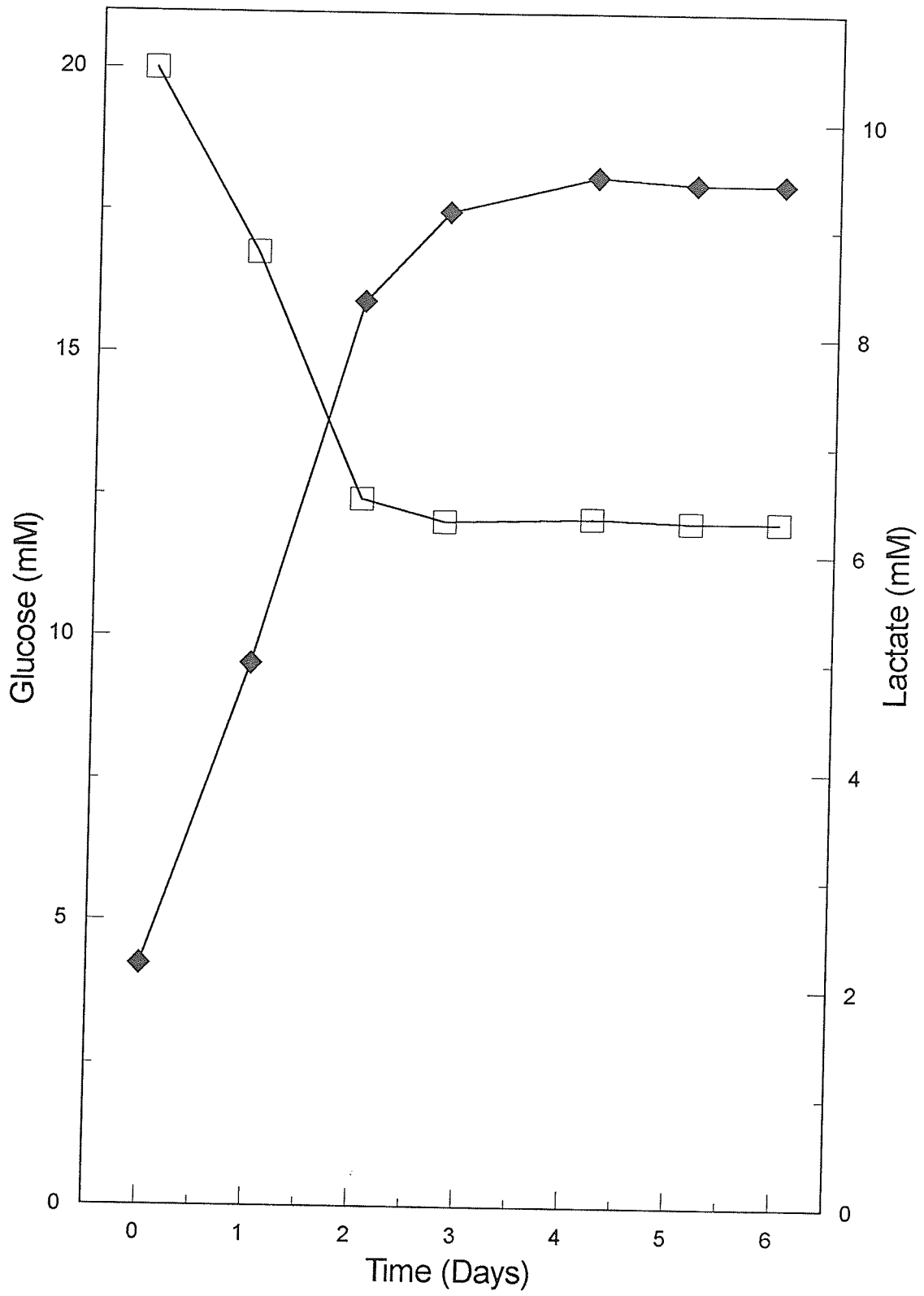

Figure 4.2. Glucose utilization and lactate production during the growth of CC9C10 cells. Glucose (□), and lactate (♦) concentrations were determined of a daily basis from the culture samples.

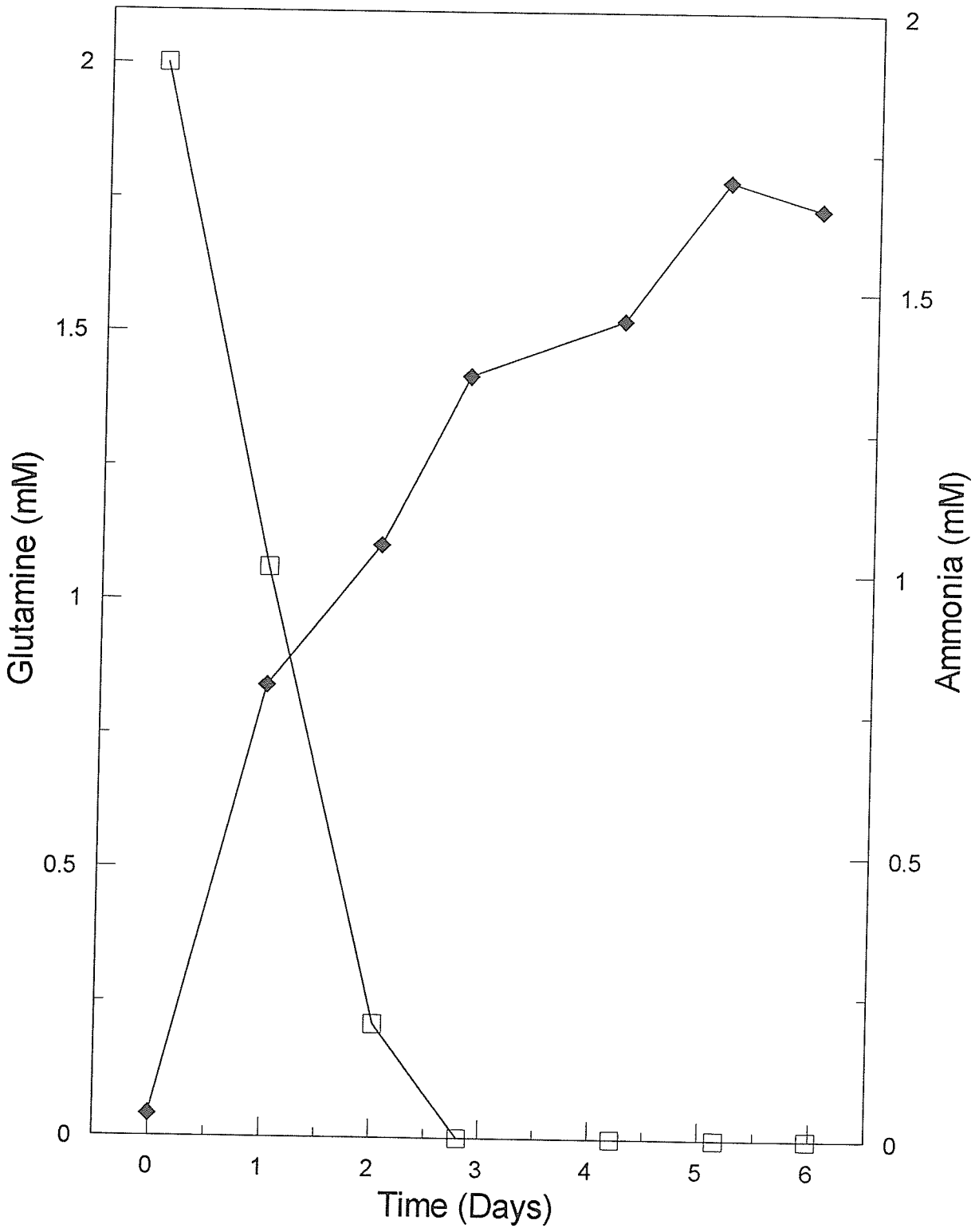

Figure 4.3. Glutamine utilization and ammonia production during the growth of CC9C10 cells. Glutamine (□), and ammonia (♦) concentrations were determined of a daily basis from the culture samples.

The initial specific consumption rates for glucose and glutamine were determined as 8.3±0.1 and 2.4±0.1 nmol/minute per 10^6 cells, respectively. The corresponding specific production rates of lactate and ammonia were 9.7±0.1 and 0.76±0.07 nmol/minute per 10^6 cells. These determinations corresponded to metabolic coefficients of 1.17 for lactate / glucose and 0.32 for ammonia /glutamine.

4.3.3 Glucose metabolism.

a) Pentose phosphate and TCA cycle.

In the pentose phosphate pathway, CO_2 is derived form the C-1 carbon of glucose during the oxidative decarboxylation of glucose 6-phosphate. However, in the TCA cycle, CO_2 can be derived equally from the C-1 or C-6 carbons (Katz and Wood, 1963).

In our experiments a steady state of metabolism was assumed from the constant rate of release of $^{14}CO_2$ from D-[1-^{14}C]-glucose (0.225 nmol/minute per 10^6 cells), or D-[6-^{14}C]-glucose (0.045 nmol/minute per 10^6 cells) over a 6 hour experimental period, which was determined by 6 independent time point measurements performed in duplicate.

The difference in the rates of $^{14}CO_2$ release from D-[1-^{14}C]-glucose and D-[6-^{14}C]-glucose has often been used as an indication of flux through the pentose phosphate pathway. A recent evaluation of this technique suggests that this should be interpreted as a measure of the minimum flux activity, the upper limit being the rate of $^{14}CO_2$ release from D-[1-^{14}C]-glucose alone (Larrabee, 1989). In our experiments a significantly higher (x7.5) $^{14}CO_2$ release was measured from D-[1-^{14}C]-glucose compared to D-[6-^{14}C]-glucose. Thus, the minimum rate of flux through the pentose

phosphate pathway was determined as 0.29 nmol/minute per 10^6 cells and the upper limit as 0.33 nmol/minute per 10^6 cells (Figure 4.4).

The TCA cycle flux was measured by the cell specific rate of $^{14}CO_2$ release from D-[6-^{14}C]-glucose. This rate was constant over 6 hours and determined as 0.045 nmol/minute per 10^6 cells (Figure 4.4).

b) Glycolysis.

The glycolytic flux was determined by the release of tritiated water from the metabolism of D-[3-^{3}H]-glucose (Bontemps *et al*, 1978). This is a measure of the flux of metabolites through the aldolase and triose phosphate isomerase reactions which are committed steps of the glycolytic pathway. The rate of formation of tritiated water was linear for 6 hours as measured by radioactive analysis of fractionated samples from an anion exchange column (Figure 4.5). The rate was determined as 7.6 nmol glucose/minute per 10^6 cells.

The relative flux of glucose through the 3 pathways were determined from the radioactive uptake experiments (Table 4.10). Glycolysis is clearly the major route for glucose catabolism with the TCA cycle and pentose phosphate pathway serving a minor role. This is consistent with data previously reported for transformed cells (Warburg, 1986).

The sum of the flux rates determined in the radioactive experiments (7.9 nmol/minute per 10^6 cells) was close to the initial uptake of glucose determined from culture (8.3 nmol/minute per 10^6 cells from Figure 4.2). The slight difference in values can be explained by the possibility of differences in the state of the cells at initial and mid-exponential phase and the higher error involved in the determination of the culture uptake rate which was based on samples taken at 24 hour intervals.

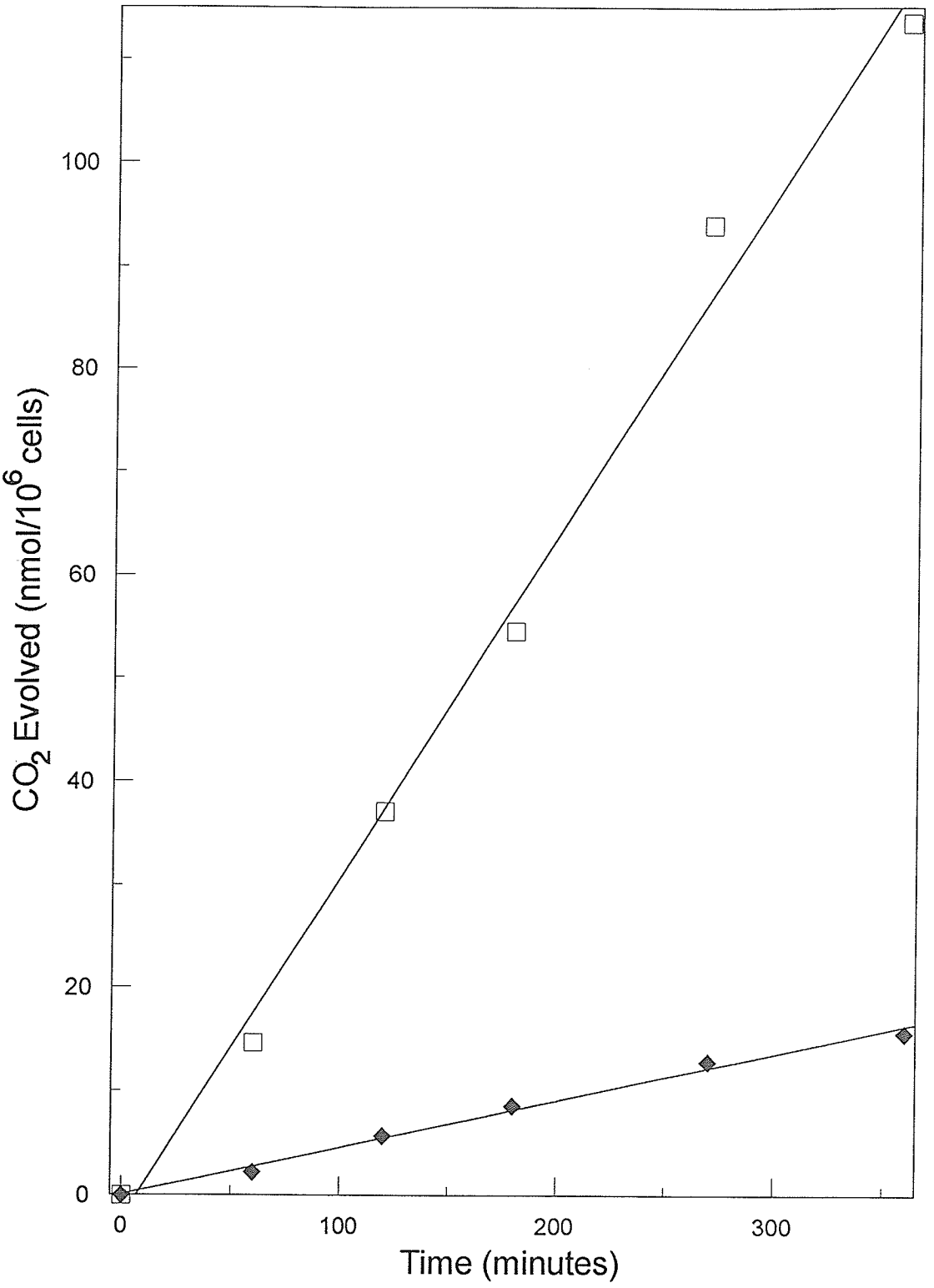

Figure. 4.4. The rate of $^{14}CO_2$ release from the metabolism of D-[1-^{14}C]- and D-[6-^{14}C]-glucose. The rate of $^{14}CO_2$ release was measured from CC9C10 hybridomas (2-3 x 10^6 viable cells/ml) incubated in normal growth medium (1 ml) containing 0.45 Ci of D-[1-^{14}C]-glucose (□), or D-[6-^{14}C]-glucose (♦) as described in Section 2.5.3. The cells were derived from batch culture after 36 hours of growth.

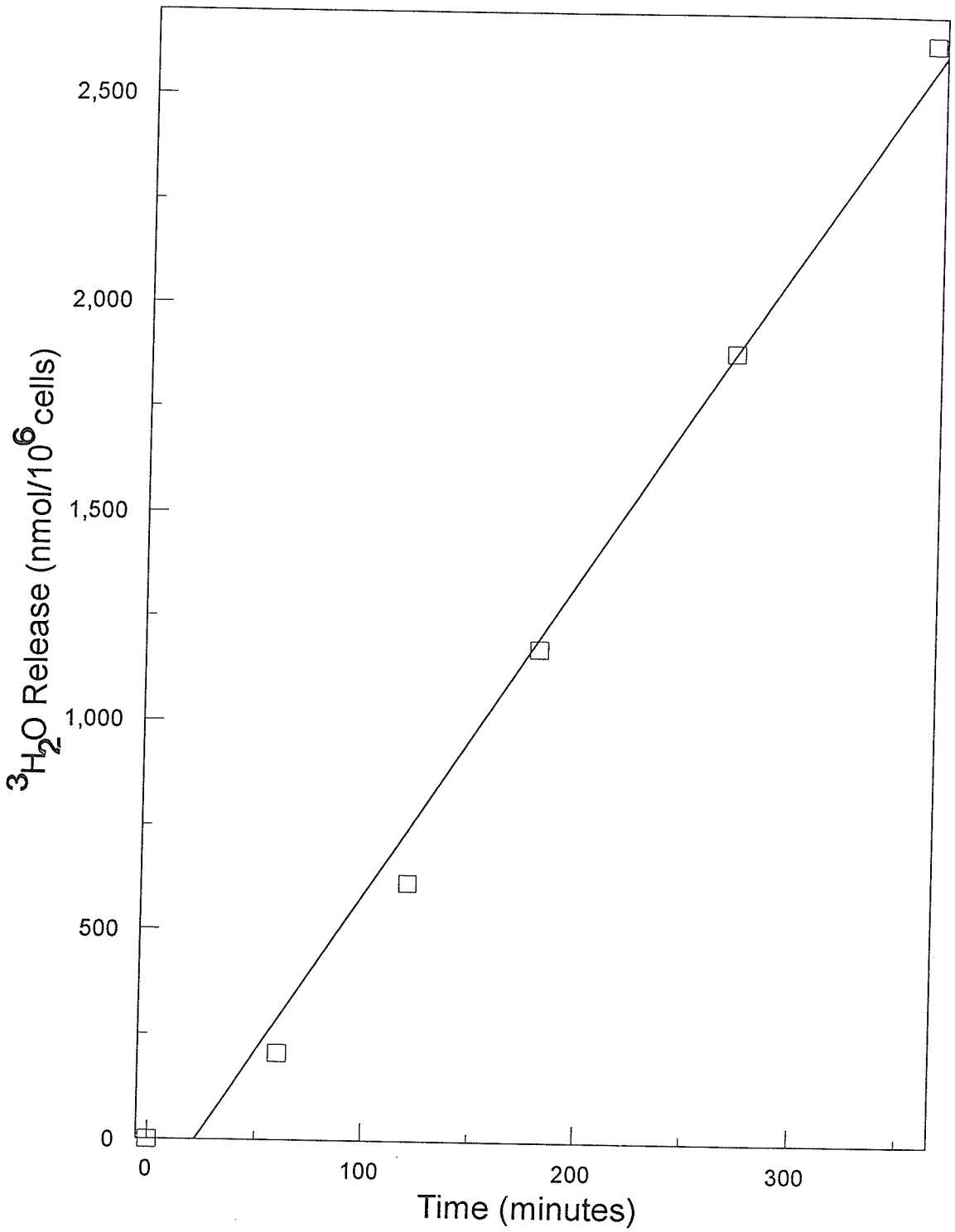

Figure 4.5. The rate of release of ^3H_2O from the metabolism of D-[3-^{3}H]-glucose. The rate of glycolytic flux in the CC9C10 hybridomas was measured by the rate of release of ^3H_2O from cells (2-3 x 10^6 viable cells/ml) incubated in normal growth medium (1 ml) containing D-[3-^{3}H]-glucose as described in Section 2.5.4. The cells were derived from batch culture after 36 hour growth.

4.3.4 Glutamine metabolism

a) End product analysis.

The metabolic pathways of glutamine metabolism were analyzed by the rates of appearance of selected end products in the culture medium during incubation with L-[U-^{14}C]-glutamine (Figure 4.6). The following were separated by a cation exchange column - lactate, glutamate, aspartate, and alanine. The peaks were identified from standard using ninhydrin to detect the amino acids and an enzymatic assay to detect lactate. The rates of appearance of each product was determined by radioactive counting of peaks obtained from culture samples at selected time intervals over a 6 hour period. The measured rate of increase in concentration of each end-product was linear over this period as calculated from 6 time point determinations. Alanine was the major end product of glutaminolysis and its formation accounted for >55% of the glutamine utilized.

The end products were determined from the extracellular content of the culture. An attempt was made to determine the intracellular content of these metabolic end-products, but the levels were too low for detection in our experiments (<1% of the extracellular concentrations).

Table 4.1. Flux analysis ± standard error of the meanof glucose metabolism. All pathways were linear for 6 hours
(n=12)

Pathway	Flux (nmol/min per 10^6 cells) (± S.E.M.)	Flux as % of glucose utilized (± S.E.M.)
Pentose phosphate	0.29 (±0.01)	3.60 (±0.13)
TCA cycle	0.045 (±0.002)	0.57 (±0.03)
Glycolysis	7.60 (±0.33)	95.8 (±4.2)
Total	7.89 (±0.35)	100 (±4)

S.E.M. represents standard error of the mean.

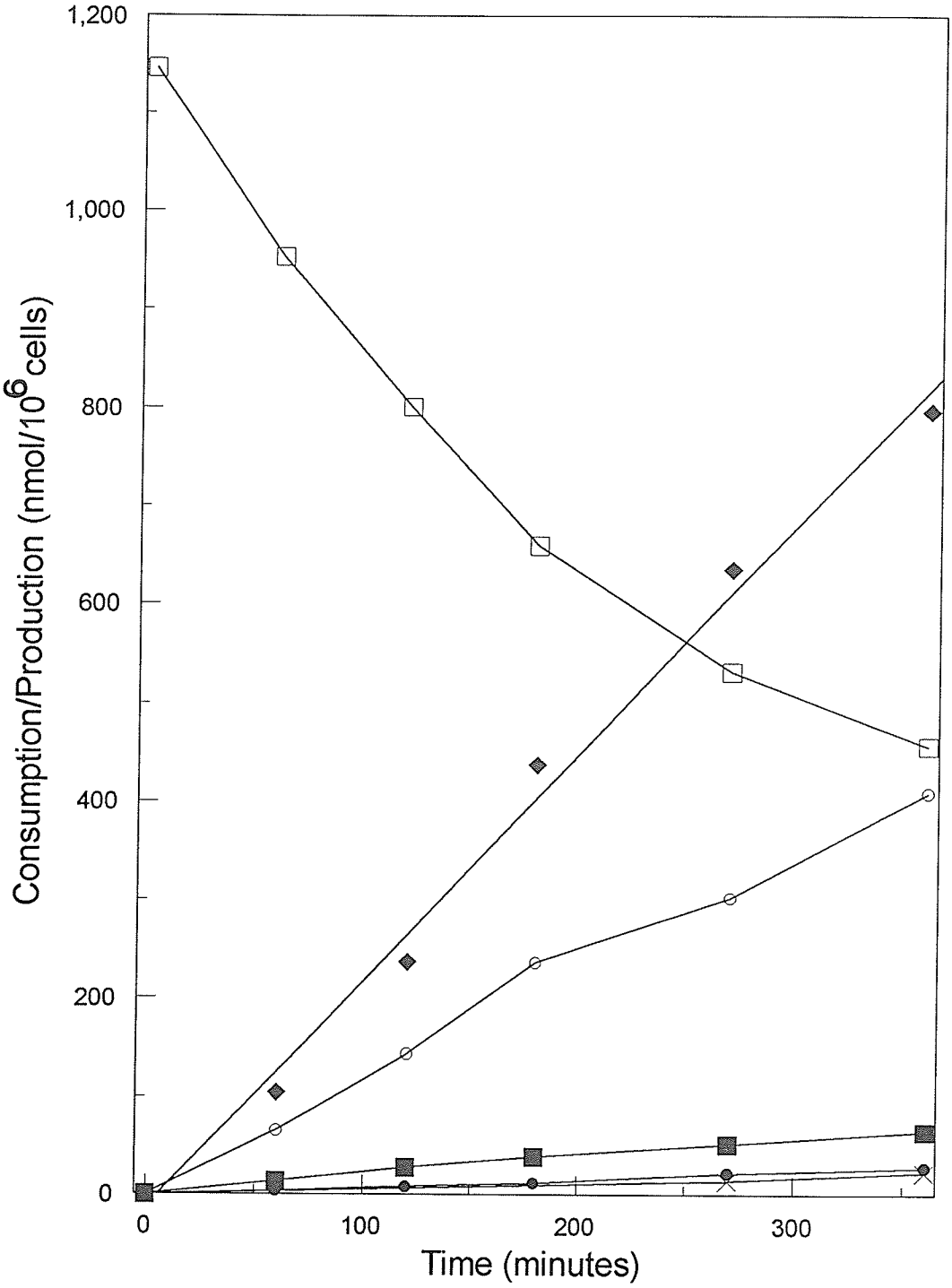

Figure 4.6. Glutamine consumption and its product release during the growth of CC9C10 cells. Glutamine (□), alanine (○), lactate (■), glutamate (●), aspartate (X), and CO_2 (◆) were measured from CC9C10 hybridomas (2-3 x 10^6 viable cells/ml) incubated in normal growth medium (1 ml) containing L-[U-^{14}C]-glutamine, as described in Section 2.5.3 and 2.5.5. The cells were derived from batch culture after 36 hour growth.

b) Oxidative metabolism.

The rate of release of $^{14}CO_2$ from L-[U-^{14}C]-glutamine was monitored in experiments over a 6 hour period (Figure 4.7). A constant rate of CO_2 production of 2.3 nmol/minute per 10^6 cells was measured over this period by 6 independent time point determinations. This corresponds to an equivalent conversion to CO_2 of 0.46 nmol of glutamine/minute per 10^6 cells (Table 4.2).

c) Protein incorporation.

The incorporation of glutamine into both intracellular and extracellular protein was measured by radioactivity over 6 hours (Figure 4.7). Incorporation into intracellular protein was at a constant rate for 4.5 hours and measured as 0.15 nmol/minute per 10^6 cells. The rate of incorporation of glutamine into extracellular protein was considerably lower at 0.005 nmol/minute per 10^6 cells.

Table 4.2 shows a summary of the pattern of metabolism of glutamine as analyzed by the experiments with L-[U-^{14}C]-glutamine. A small proportion of the glutamine (7.5%) incorporated into the cells was utilized for protein synthesis. A large proportion of the glutamine (67%) was converted into the 3 or 4 carbon products of glutaminolysis, alanine being the major end products. The rate of CO_2 release can be accounted for by the pathways of partial oxidation of glutamine to the 3 or 4 carbon end-products. The sum of the measured flux values was 2.1 nmol/minute per 10^6 cells which compared with a value of 2.7 nmol/minute per 10^6 cells for L-[U-^{14}C]-glutamine uptake which was determined independently. Both these values were close to the initial rate of glutamine utilization (2.4 nmol/minute per 10^6 cells) determined from assays of the culture (Figure 4.3).

Table 4.2. End product analysis of glutamine metabolism

Product	Flux (nmol product/min per 10^6 cells) (± S.E.M.)	Product formation as % of glutamine utilized (± S.E.M.)
Alanine	1.13 (±0.04)	54.6 (±1.9)
Aspartate	0.066 (±0.0068)	3.19 (±0.33)
Glutamate	0.079 (±0.003)	3.82 (±0.14)
Lactate	0.18 (±0.01)	8.70 (±0.48)
CO_2	0.46 (±0.02)	22.2 (±1)
Intracellular protein	0.15 (±0.01)	7.25 (±0.48)
Extracellular protein	0.005 (±0.0004)	0.24 (±0.02)
Total	2.07 (±0.08)	100 (±4)

S.E.M. represents standard error of the mean.

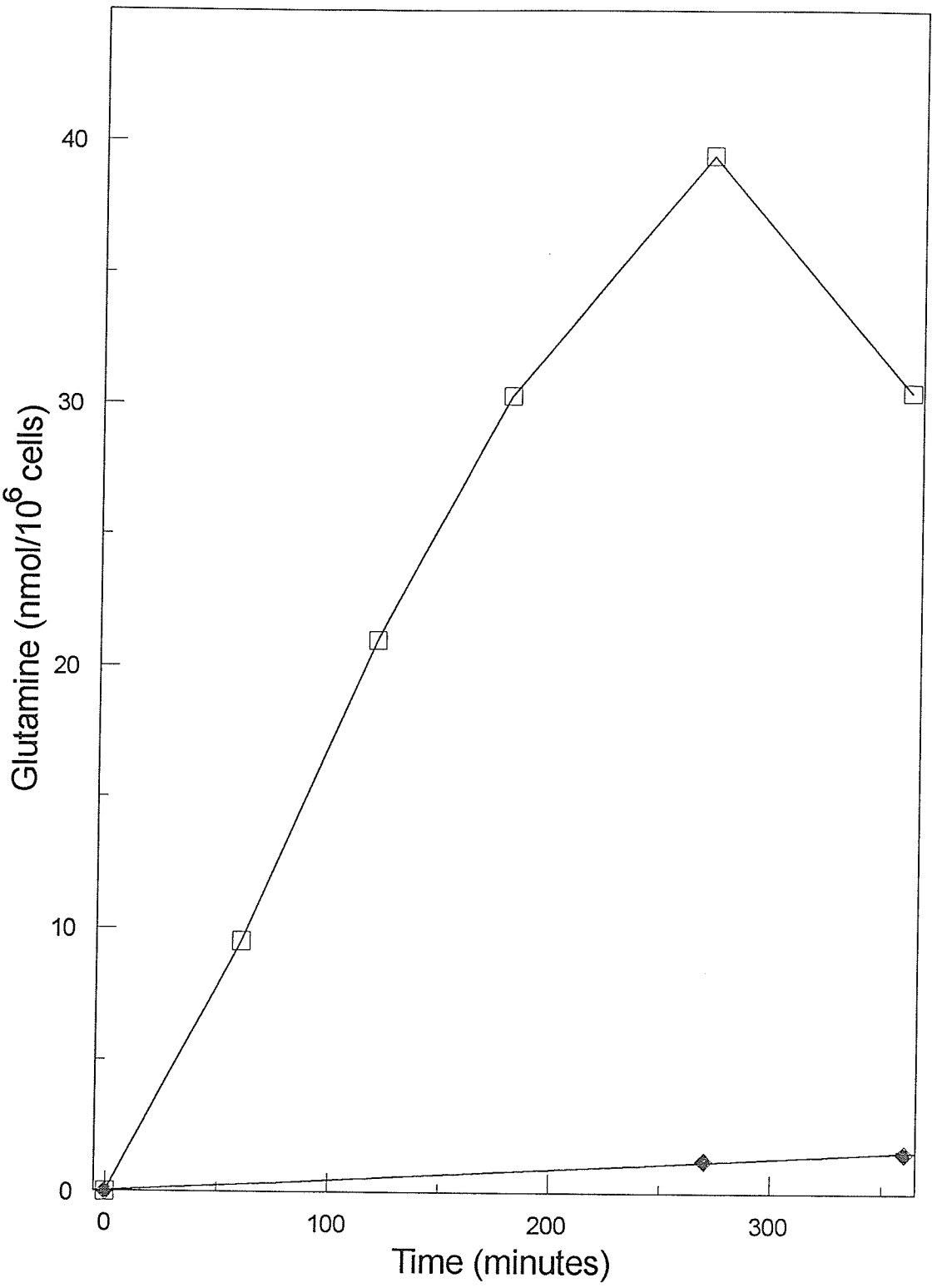

Figure 4.7. Glutamine incorporation into protein. The incorporation of L-[U-^{14}C]-glutamine into intracellular protein (□) and extracellular (♦) protein was determined for CC9C10 hybridomas over 6 hours as described in Materials and Methods. The cells were derived from batch culture after 36 hour growth.

4.3.5 Potential ATP production

The maximum potential ATP production was calculated from the experimental data of glucose and glutamine utilization and the metabolic flux rates (Table 4.3). Some stoichiometric assumptions were made in these calculations. The ATP yields for glucose utilization were based on 36 ATP mol/mol for the TCA cycle, 3 ATP mol/mol for the pentose phosphate pathway, and 2 ATP mol/mol for glycolysis. The lower limit of pentose phosphate flux (0.29 nmol/minute per 10^6 cells) was used in the calculation of ATP yield from this pathway.

Glutaminolysis was regarded as the incomplete oxidation of glutamine and could include the formation of aspartate, alanine, or lactate. The theoretical ATP yield for glutaminolysis was assumed to be 9 ATP mol/mol glutamine (Haggstrom, 1991). The CO_2 release from glutamine could be entirely accounted by glutaminolysis. Thus it could be assumed that complete oxidation of glutamine by the TCA cycle did not occur.

The calculated data (Table 4.3) showed that glycolysis provided 59% of the energy requirement of the cell. However, the energy provided by glutaminolysis was significant at 41% of the total.

Table 4.3. Potential ATP production from each pathway.

Substrate	Pathway	ATP formed (nmol/min per 10^6 cells) (± S.E.M.)	ATP as % of total production (± S.E.M.)
Glucose	Pentose phosphate	0.87 (±0.03)	2.89 (±0.15)
	TCA cycle	1.62 (±0.06)	5.38 (±0.20)
	Glycolysis	15.2 (±1)	50.5 (±3.3)
	Total from glucose	17.7 (±1.1)	58.8 (±3.6)
Glutamine	Ala formation	10.2 (±0.36)	33.9 (±1.2)
	Asp formation	0.59 (±0.061)	1.96 (±.020)
	Lac formation	1.62 (±0.09)	5.38 (±0.030)
	Total from glutamine	12.4 (±0.5)	41.2 (±1.3)
Glucose and glutamine	Overall total	30.1 (±1.6)	100 (±4)

S. E.M. represents standard error of the mean.

4.4 Discussion

The objective of the work described in this section was to analyze the metabolic pathways of glucose and glutamine utilized by a murine B-lymphocyte hybridoma capable of antibody secretion. The use of specifically radiolabelled glucose molecules enabled the precise determination of rates of flux through the major catabolic routes of glucose metabolism, using previously developed protocols. Similar protocols have not been developed for glutamine metabolism, and specifically labeled molecules are generally unavailable. So, the pattern of glutamine metabolism was analyzed by end-product analysis using a uniformly labeled substrate. The experimental data were analyzed to determine the theoretical ATP yield from each individual pathway. This enabled an assessment of the relative importance of each pathway in providing the energy requirements of the cell.

The importance of glutamine as a provider of energy in cultured cells has been widely recognized (Wice *et al*, 1981). The pattern of glutamine catabolism has been described as eight individual pathways comprising the metabolic network termed glutaminolysis (Haggstrom, 1991). These pathways originate from glutamine and produce combinations of CO_2, NH_4^+, alanine, aspartate, and lactate as end-products. These compounds have been shown to increase in cell concentration in culture in culture medium during growth of a number of cell lines in culture (Lanks and Li, 1988).

Glutamine probably enters the TCA cycle as 2-oxoglutarate and exits the mitochondria as malate, which can be converted in the cytoplasm to alanine, lactate or aspartate (McKeehan, 1982). This process would increase the cytoplasmic $NADH/NAD^+$ ratio and serve to drive lactate production via glycolysis (Lanks, 1986). This hypothesis is consistent with our data for the CC9C10 cells which shows that glucose utilization ceases when glutamine is completely depleted from the culture media. Also, the end-product analysis indicates that all glutamine catabolism can be

accounted for by incomplete oxidation to 3 or 4 carbon products and CO_2. The data suggest that alanine is a major end-product of glutamine metabolism in CC9C10 cells. This is secreted into the culture medium as is aspartate, glutamate and lactate.

The pattern of glucose metabolism in the CC9C10 cells was determined by flux analysis of three possible metabolic pathways. This analysis shows that a high proportion (>95%) of glucose is metabolized by glycolysis leading to the formation of lactate or possibly alanine. On the other hand, the proportion of glucose metabolized via the TCA cycle is extremely small (0.6%). This is consistent with previous analysis for a murine hybridoma and the explanation that this may be related to the low activity of pyruvate dehydrogenase in these cells (Fitzpatrick *et al*, 1993). The pentose phosphate pathway accounts for 3.6% of metabolized glucose and is essential as a provider of ribose which is necessary for nucleic acid synthesis (Reitzer *et al*, 1980).

The relative contribution of glucose and glutamine metabolism to the provision of intracellular energy has shown considerable variations in previous reports and must depend upon the cell line and substrate concentrations used in the culture (Brand, 1985; Wu *et al*, 1992; O'Rourke and Rider, 1989). Our data show that 59% of ATP production is contributed by glucose metabolism in the CC9C10 cells. This figure is higher than that of a similar study with a murine hybridoma (Fitzpatrick *et al*, 1993) where glucose was shown to contribute a maximum of 45%. However, the difference may be accounted for by the higher concentration of glucose (20 mM) used in our experiments with the CC9C10 cells - twice that of the earlier work.

The increased importance of glutamine as a provider of cellular energy following mitogenic stimulation of lymphocytes has been recognized (Ardawi and Newsholme, 1983). Wu *et al* (1992) concluded that glucose and glutamine could contribute equally to intracellular ATP in rat spleenocytes and mesenteric lymphocytes following mitogenic stimulation. This is consistent with our data for the CC9C10 cells which are antibody-secreting B-lymphocyte hybridomas.

The analysis reported in this section is important for the understanding of the roles of the major carbon substrates and associated by-product formation during cell growth in culture. This can form the basis for the development of control strategies such as specific nutrient feeding in order to ensure an efficient flux through the pathways of energy metabolism that would be necessary to support high antibody production during the large-scale culture of hybridomas (Glacken, 1988; Seaver, 1986).

4.5 Summary

The antibody-secreting murine hybridoma, CC9C10 was grown in batch culture in a medium containing 20 mM glucose and 2 mM glutamine. After 2 days of exponential growth, the glutamine content of the medium was completely depleted, whereas the glucose content was reduced to 60% of the original concentration. The glucose and glutamine metabolism was analyzed at mid-exponential phase by use of radioactively labelled substrates. Glycolysis accounted for the metabolism of most of the glucose utilized (>96%) with flux through the pentose phosphate pathway (3.6%) and the TCA cycle (0.6%) accounting for the remainder. Glutamine was partially oxidized via glutaminolysis to alanine (55%), aspartate (3%), glutamate (4%), lactate (9%), and CO_2 (22%). Calculation of the theoretical ATP production from these pathways indicated that glucose could provide 59% and glutamine 41% of the energy requirement of the cells.

CHAPTER 5

5.0 The Effect of Carbohydrate Source on The Growth and Antibody Production of a Murine Hybridoma

5.1 Introduction

There have been many reports that mammalian cell lines can grow in media supplemented with carbohydrates other than glucose (Eagle, 1958; Burns *et al*, 1976; Cristafalo & Kritchevsky, 1965; Imamura *et al*, 1982). In particular the monosaccharides, mannose, fructose and galactose and the disaccharides, maltose, trehalose and turanose have been shown to support the growth of a variety of cell lines. The polyols (sugar alcohols), xylitol and sorbitol can replace glucose and support the growth of a number of cell lines including human diploid fibroblasts (Demetrakopoulos & Amos, 1976) although this was not substantiated in all mammalian cells (Burns *et al*, 1976).

The type of carbohydrate present in the growth medium can affect the metabolism of cultured cells. Fructose or maltose caused a decrease in production of lactate and a decreased drift in pH in Madin Darby Canine Kidney (MDCK) cell cultures (Imamura *et al*, 1982). This can be an advantage in the process control of large-scale mammalian cell cultures. Substantial increases of intracellular ribose have been reported following the presence of fructose, xylitol, D-xylulose or tegatose in the cultures of rat hepatocytes (Vincent *et al*, 1989).

Monoclonal antibodies form part of a long list of products which are now produced routinely from mammalian cell cultures and which require process control during large-scale operation. In such operations the role of media components in culture stability and cell productivity is important. With this in mind, we report a study of

the use of alternative carbohydrates in the culture of an antibody-secreting murine hybridoma

5.2 Materials and Methods

5.2.1 Cell line: Refer to Section 2.1.0a.

5.2.2 Growth of cells: Refer to Section 2.1.1a.

5.2.3 Growth medium: Refer to Section 2.1.2a.

5.2.4 Cell counting: Refer to Section 2.1.4

5.2.5 Cell adaptation: The cells were adapted for growth in each medium over 12 passages. Cultures at passage one contained 20 mM glucose and 20 mM of the substitute carbohydrate. The glucose concentration was reduced to zero by incremental changes of 5 mM over 10 passages. Cells were grown for 2 passages without glucose but in the presence of a substitute carbohydrate before conducting the experiments.

5.2.5 Analysis of culture media: Refer to Section 2.3.1

5.3 Results

5.3.1 Cell Growth

Cells were adapted to media containing alternative carbohydrate sources over 12 passages. Each adapted cell line was then monitored for 6 days in culture (Figure 5.1). The viable cell concentration reached a maximum at day 2 or 3 of culture in all cases before a rapid decline phase. The maximum cell density in the glucose-based culture was 1.04×10^6 cells/ml after 2 days growth (Table 5.1). The maximum cell densities in the other cultures decreased in the order maltose > galactose >fructose >sorbitol >xylitol >control (no glucose). However, significant growth was observed in all cultures, the lowest cell yield being in the xylitol culture at 51% with respect to the culture containing glucose. The specific growth rates varied from a high value of 0.0483 h^{-1} in the glucose-based culture to a low value of 0.0344 h^{-1} in the xylitol culture.

5.3.2 Lactate Production

The concentration of lactate was measured in all cultures on a daily basis (Figure 5.2). This showed that the production of lactate was greatest in the maltose-based culture and reached a level of 12 mM during the growth phase of the cells. A substantial increase in lactate was also observed in the glucose-based culture. However, minimal levels of production (<4 mM) were observed in all other cultures, including the control.

5.3.3 Glutamine Metabolism

The concentration of glutamine was determined in all cultures on a daily basisas shown in Figure 5.4. Glutamine consumption was determined for all cultures on day 1, as shown if Table 5.2. The highest specific glutamine consumption rate was measured in the control (no carbohydrate), at 11.3 nmol/minute per 10^6 cells, which was 354% higher than the glucose culture. All other cultures had a significantly higher glutamine consumption rate than glucose in the following order: control > fructose > xylitol > sorbitol > maltose > galactose with respect to the carbohydrate source.

5.3.4 Monoclonal Antibody Production

The Mab concentrations were analyzed in all cultures on a daily basis by ELISA (Figure 5.3). The highest concentration was measured in the xylitol-based culture at 16.2 μg/ml which was 39% higher final volumetric yield (total monoclonal antibody concentration) than the concentration found in the glucose based culture. The culture with no carbohydrate source reached an antibody level of 11.7 μg/ml The specific antibody productivity (q_{Mab}) was determined by plotting the Mab concentration against the integral of viable cell density vs. time (Renard *et al*, 1988). In all cultures this resulted in a straight line indicating a correlation between Mab concentration and the concentration of viable cells. The q_{Mab} was determined from the gradient (the gradient represents the linear portion of antibody production over time) of each plot. The value varied from 18.4 μg/10^6 cell*days for the xylitol culture and decreased in the other cultures in the following order: control (no carbohydrate source) > fructose > sorbitol > maltose > galactose > glucose with respect to the carbohydrate source (Table 5.1). The Mab productivity in the xylitol culture was a factor of x5.6 higher than in the glucose culture.

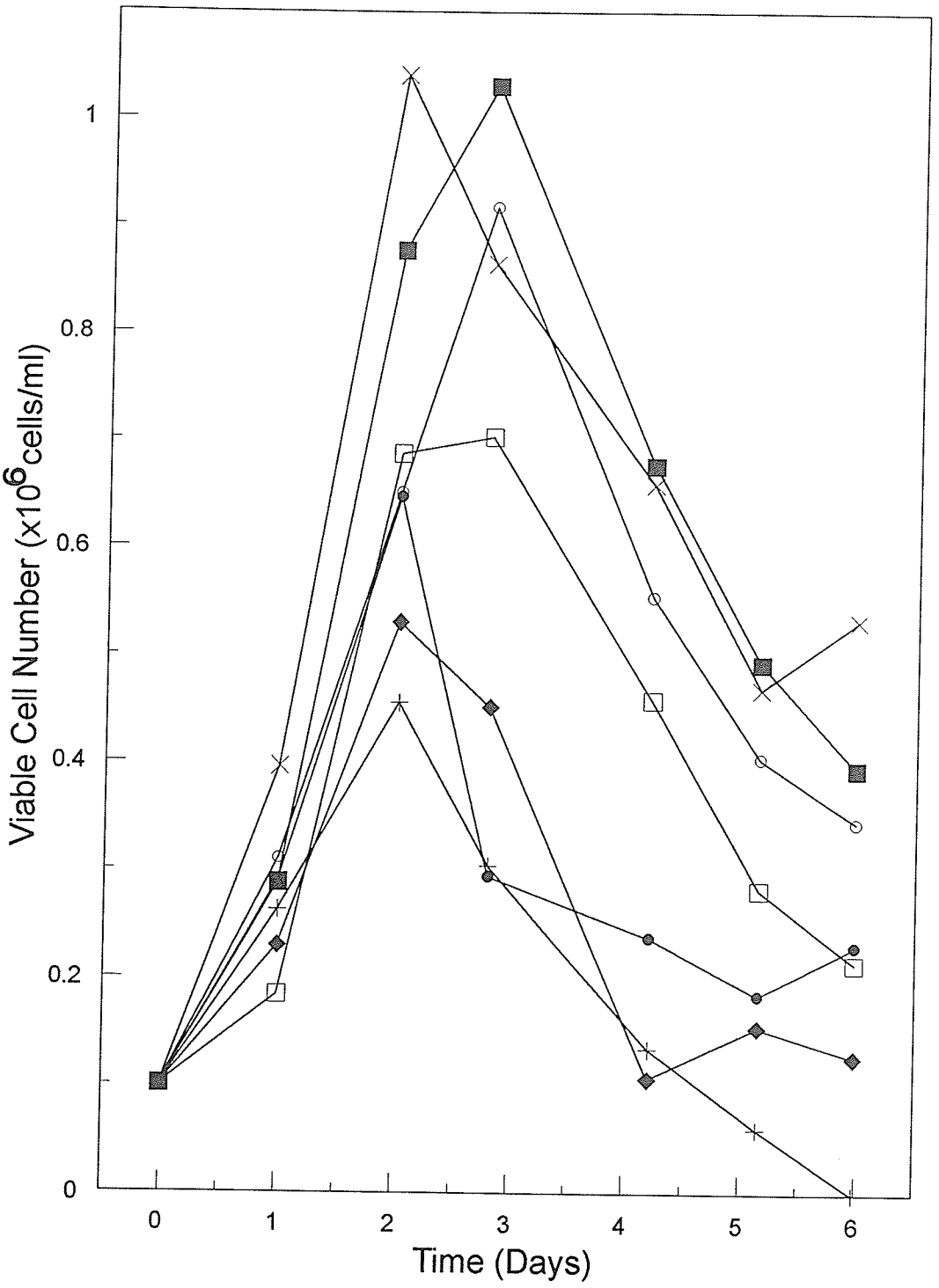

Figure 5.1. Growth of hybridomas in various carbohydrates. The CC9C10 hybridomas were adapted to each media over 12 passages. The adapted cells were inoculated into 50 ml of the appropriate medium containing 20 mM of glucose (X), galactose (O), maltose (■), fructose (□), sorbitol (●), or xylitol (◆), as the sole carbohydrate source, and control cultures (+) containing no added carbohydrate source. The viable cell concentration was monitored over 6 days in culture. (n=2).

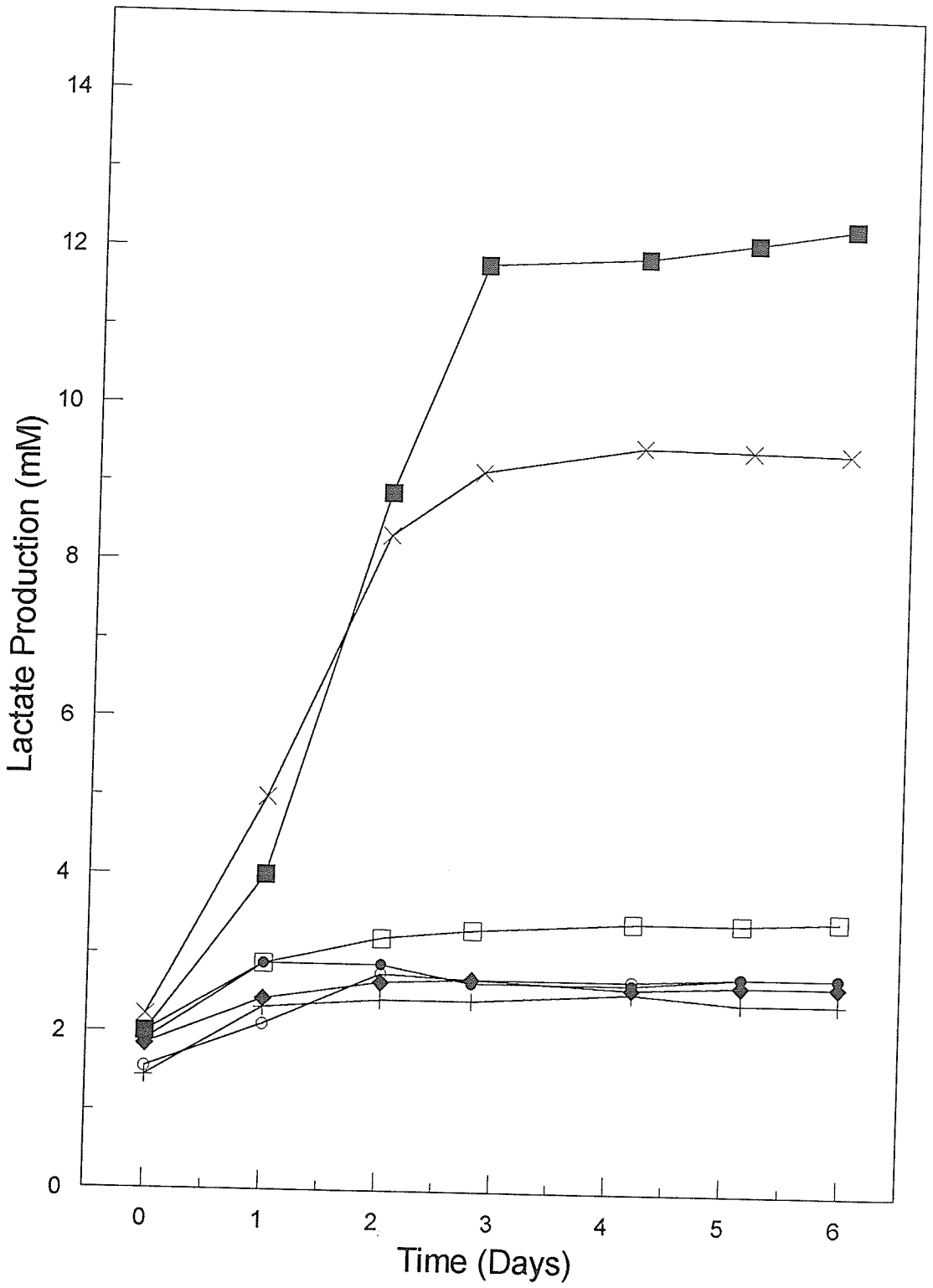

Figure 5.2 Lactate concentration in cultures of CC9C10 hybridomas grown in various carbohydrates. The lactate concentration was measured in the media of cultures of the CC9C10 hybridomas grown in medium containing 20 mM of glucose (X), galactose (O), maltose (■), fructose (□), sorbitol (●) or xylitol (◆) as the sole carbohydrate source, and control cultures (+) containing no added carbohydrate source. The viable cell concentration was monitored over 6 days in culture. (n=2).

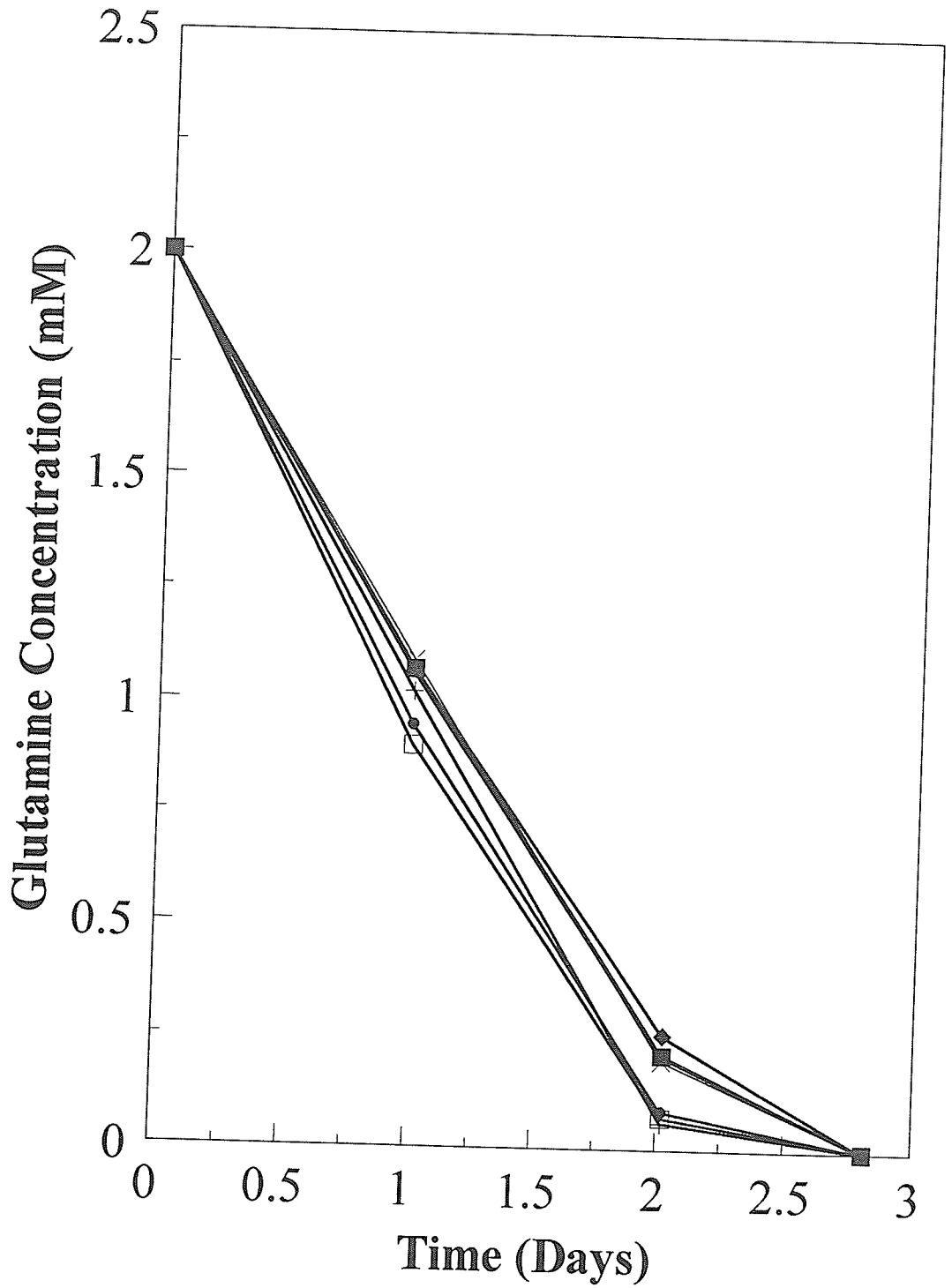

Figure 5.3 Glutamine concentration in cultures of CC9C10 hybridomas grown in various carbohydrates. The glutamine concentration was measured in the media of cultures of the CC9C10 hybridomas grown in medium containing 20 mM of glucose (X), galactose (O), maltose (■), fructose (□), sorbitol (●) or xylitol (◆) as the sole carbohydrate source, and control cultures (+) containing no added carbohydrate source. The viable cell concentration was monitored over 6 days in culture. (n=2).

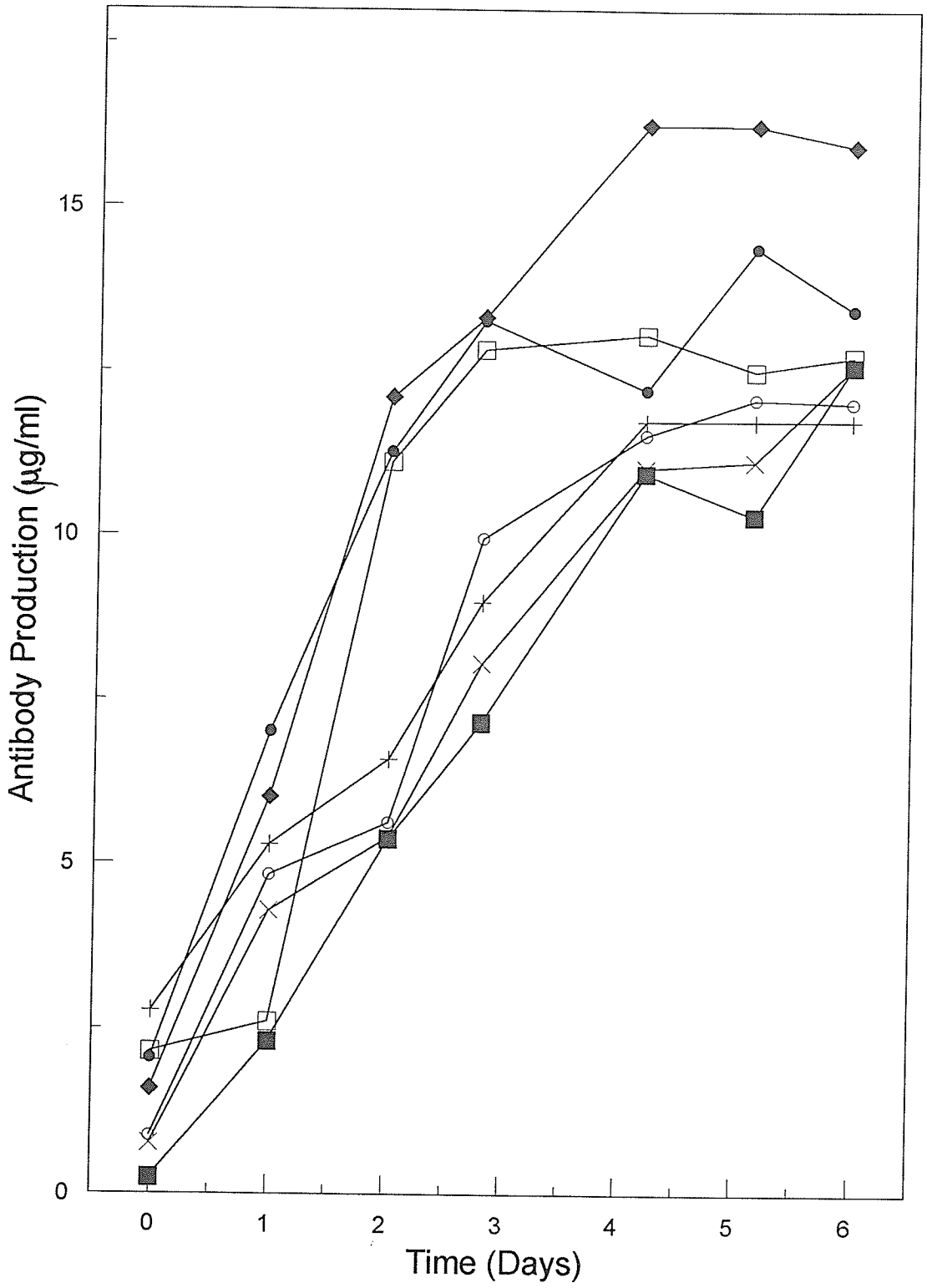

Figure 5.4: Monoclonal antibody concentration in cultures of CC9C10 hybridomas grown in various carbohydrates. The Mab concentration was measured in the media of cultures of the CC9C10 hybridomas grown in medium containing 20 mM of glucose (X), galactose (O), maltose (■), fructose (□), sorbitol (●) or xylitol (◆) as the sole carbohydrate source, and control cultures (+) containing no added carbohydrate source. The viable cell concentration was monitored over 6 days in culture. (n=2).

Table 5.1. Growth and productivity characteristics of CC9C10 cells cultured on different carbohydrate sources
(n=2).

Carbohydrate	Specific Growth Rate (h^{-1}) (± S. E.M.)	Max. Cell Density as % of Control	Mab Productivity ($\mu g/10^6$cell-days (± S. E.M.)	Max. Volumetric Mab Conc. as % of Control
Glucose	0.0483 (±0.002)	231	3.29 (±0.49)	113
Galactose	0.0388 (±0.003)	204	6.04 (±1.02)	124
Maltose	0.0448 (±0.004)	229	6.43 (±1.33)	119
Fructose	0.0397 (±0.002)	156	10.3 (±2.6)	141
Sorbitol	0.0385 (±0.003)	144	10.1 (±2.10)	132
Xylitol	0.0344 (±0.002)	118	18.4 (±2.6)	139
Control (No carbohydrate)	0.0347 (±0.003)	100	10.9 (±0.6)	100

S.E.M. represents standard error of the mean.

Table 5.2. Specific glutamine consumption rates of CC9C10 cells cultured in different carbohydrate sources.

Carbohydrate Source (20 mM)	Specific Glutamine Consumption Rates (nmol/minute per 10^6 cells) (± S. E.)	Maximum Glutamine Consumption as % of Glucose Based Culture
Glucose	3.19 (±0.14)	100
Galactose	4.18 (±0.17)	131
Maltose	4.48 (±0.07)	140
Fructose	8.3 (±0.07)	260
Sorbitol	5.05 (±0.12)	158
Xylitol	5.62 (±0.37)	176
Control	11.3 (±0.38)	354

S. E. M. represents standard error.

5.4 Discussion

Glucose is metabolized by mammalian cells in culture mainly by anaerobic glycolysis (Fitzpatrick *et al*, 1993). This leads to production of a substantial concentration of lactate which is released into the medium in an acidic form causing a decrease in culture pH. This necessitates a system of pH control in bioreactor cultures of mammalian cells in order to maintain a consistent growth rate. Alternatively, carbohydrates such as fructose or galactose can reduce the lactate production without having a substantial effect on growth (Imamura *et al*, 1982). This is confirmed in our data with the CC9C10 cells. Only glucose and maltose-based cultures lead to significant lactate production in the medium. Maltose can be hydrolyzed into glucose (from maltases present in serum), so its utilization is likely to be similar to that of glucose.

Although glucose metabolism provides a substantial proportion of the energy requirement of the cell via glycolysis, a major role of glucose is to act as a substrate for the pentose phosphate pathway which provides ribose for nucleic acid synthesis. Zielke *et al* (1976) showed that this anabolic function of glucose could be provided by supplements of purine and pyrimidines. In the absence of glucose the cellular energy requirement could be provided by glutamine which is metabolized via glutaminolysis or fatty acid oxidation from the addition of serum. The anabolic role of glucose could also be provided by galactose or fructose which are converted into glycolytic intermediates by isomerization and phosphorylation. Their slower rate of utilization is the most likely explanation for the decreased lactate formation as shown in the cultures of the CC9C10 cells.

The metabolism of sorbitol and xylitol has received considerable attention because of their use as food sweeteners (Wang & Eys, 1981). Their use in cell culture was investigated by Demetrakopoulos & Amos (1976) who reported the rapid growth of

mammalian fibroblasts in D-xylose and xylitol, although poor growth in sorbitol. The utilization of the polyols depends upon the induction of dehydrogenases for their conversion to xylulose or fructose, which would be suitable substrates for the pentose phosphate pathway. In our experiments with the CC9C10 cells we gradually reduced the glucose available to the cells over a period of 12 passages to allow adaptation. After adaptation, cell growth in xylitol or sorbitol cultures were lower than the glucose supplemented culture with maximum densities reaching 51 and 63% of the latter culture, respectively.

Glutamine metabolism provides a substantial proportion of cellular energy in transformed cells (Lanks and Li, 1988). The control (no carbohydrate source) had a specific glutamine utilization rate 3.54x higher than the glucose based culture. Specific glutamine consumption rates were significantly higher in all cultures when compared to the glucose based culture in the following order: control > fructose > xylitol > sorbitol > maltose > galactose, with respect to the carbohydrate source. Alll cultures had an initial glutamine concentration of 2 mM throughout the period of adaptation and experimentation. The increased specific glutamine consumption rate increased among all cultures containing carbohydrates other than glucose probably as stress put on the cell in response to fulfill cellular energy requirements in the absence of glucose.

The data with respect to Mab productivity was unexpected. The xylitol grown cells showed a specific productivity of x1.69 greater than the control (No carbohydrate addition) and a 39% higher volumetric yield. In all cultures we found a correlation between released Mab and the integral of cell concentration and time (viability index). This relationship has been shown previously for hybridomas (Renard *et al*, 1988) and indicates that the specific productivity is related to the number of viable cells in culture and not to whether the cells are in the growth or stationary phase.

The reason for the increased Mab productivity in the presence of the xylitol, and the control is unclear. There is evidence that parameters that adversely affect cell

growth can promote Mab productivity (Oh *et al*, 1993). This argues for a non-specific effect observed with the CC9C10 cells in our experiments (stress placed upon cells by no carbohydrate present in the medium). Alternatively, it has been shown that xylitol can cause major changes to the intermediary metabolism of mammalian cells by increasing the NADH/NAD ratio and the concentration of available ribose (Vincent *et al* 1989).

Stress placed upon the cells due to a lack of or the presence of an alternative carbohydrate source may promote a higher Mab productivity.

5.5 Summary

1) A murine hybridoma (CC9C10) was adapted to grow in media containing alternative carbohydrates to glucose.

2) Cell yields relative to the glucose-based culture decreased in order of the following supplements maltose > galactose > fructose > sorbitol > xylitol > control (no carbohydrate source, although significant yields (>43% of the glucose based culture) were observed in all cultures.

3) Specific glutamine consumption rates relative to the glucose based culture decreased in order of the following alternative carbohydrate sources: control (no carbohydrate source) > fructose > xylitol > sorbitol > maltose > galactose. The control had a 354% higher glutamine consumption rate than the glucose based culture.

4) Antibody production was directly related to the viable cell concentration in each culture and was independent of the phase of culture.

5) A high specific antibody productivity (q_{Mab}) was observed in the culture containing xylitol, and the control culture (no carbohydrate source) even though the cell yields and growth rates were lower than the glucose-based control. The measured q_{Mab} in the xylitol culture was x1.69 that of the control culture and the volumetric yield of Mab was 39% higher.

[2]CHAPTER 6

6.0 The Metabolic Profile of a Murine Hybridoma Grown in Serum-free Medium at Various Oxygen Concentrations

6.1 Introduction

The concentration of dissolved oxygen is an important control parameter for productivity in mammalian cell cultures. A dissolved oxygen concentration of around 200 μM can normally be attained by equilibration with air (100% air saturation). Oxygen in excess of this has been reported to inhibit cell growth and metabolism of various cell types (Cooper *et al*, 1959). There are also many examples of optimal dissolved oxygen concentrations determined at around 50% air saturation, a value routinely used in large-scale cell culture processes.

However, there are some reports in the literature that challenge this conventional wisdom. It has been shown that some established cell lines can be adapted to withstand high oxygen concentrations. Joenje *et al* (1985) reported that HeLa cells could grow in the presence of an oxygen concentration near 760 μM after 21 months of adaptation. Oller *et al* (1989) reported that various cells including lymphoblasts could grow at near maximal rates with oxygen concentrations of 300 to 400 μM (Oller *et al*, 1989).

In this section we investigated the ability of a murine B-lymphocyte hybridoma to grow at various dissolved oxygen concentrations in a chemostat culture. Following equilibration at each concentration we determined the associated pattern of energy metabolism with respect to glucose and glutamine utilization.

---

[2] The content of this chapter was presented as a poster at the combined annual meeting of the Society of Industrial Microbiologists/Canadian Society of Microbiology in Toronto, August, 1993. Petch, D., Jan, D. C. H., Butler, M. The metabolic profile of a murine hybridoma grown in serum free medium at various oxygen concentrations.

6.2 Materials and Methods

6.2.1 Cell Line: Refer to Section 2.1.0a.

6.2.2 Medium: Refer to Section 2.1.2d.

6.2.3 Growth of Cells Refer to Section 2.1.1c.

6.2.4 Radiolabelled Molecules: Refer to Section 2.5.1.

6.2.5 CO_2 Evolution: Refer to Section 2.5.3.

6.2.6 Glycolytic Flux: Refer to Section 2.4.2, and 2.5.4.

6.2.7 Components of culture media: Refer to Section 2.3 in its entirity. Measurements were made of 3 independent samples taken at daily intervals after each steady state had been attained (>5 changes in culture volume).

6.2.8 Cell counting: Refer to Section 2.1.4.

6.3 Results

6.3.1 Chemostat cultures.

There were two different experiment series performed in this Chapter. Having two different fermentor runs was performed in order to substantiate the data.

Figures 6.1 and 6.2 show data from two cultures operated in a continuous mode for the experiment 1 series. A cell density of 2.2 $x10^6$ cells/ml was maintained with dissolved oxygen concentrations (dO_2) corresponding to air saturation levels of 10, 50 and 100%. In both cultures an initial decrease in cell number at 50% air saturation was reversed before a steady state equilibrium was established. The culture which was gassed with enriched oxygen (250% air saturation; Figure 6.1) showed a decrease in cell number and an equilibrium was not established. Similar observations were observed for the fermentors used in the experiment 2 series.

Cell samples for metabolic analysis were taken at points indicated by arrows in Figures 6.1 and 6.2. At these points the cultures had attained a steady state which was defined by a constant cell concentration following at least 5 volumes of media change.

6.3.2 Substrate Utilization / Product Formation

The specific rates of consumption or production of glucose, glutamine, lactate, ammonia, and monoclonal antibody (q_{Gluc}, q_{Gln}, q_{Lac}, q_{Amm}, and q_{Mab}) were determined from analysis of cultures at steady state (Table 6.1 and Table 6.2). The calculations were based on the formula in Section 2.9. The amounts of glucose consumed /product formed has been analyzed by methods previously described in Section 2.3. The q_{Gluc} increased significantly at higher dissolved oxygen concentrations. This was associated with a slight increase in the metabolic coefficient, lactate / glucose from 1.35 to 1.42 which suggested an increase in the proportion of

glucose metabolized by glycolysis at high dO_2. The changes in q_{Gln} and q_{Amm} were not significant at each of the three steady states. The metabolic coefficient, ammonia / glutamine, varied between 0.42 to 0.49 which indicated a relatively low level of deamination compared to previously reported data (Hassel & Butler, 1990). The production rate of antibody (q_{Mab}) was slightly, but significantly higher (15%) at the low oxygen concentration (10% air saturation) compared to the value at 100% air saturation.

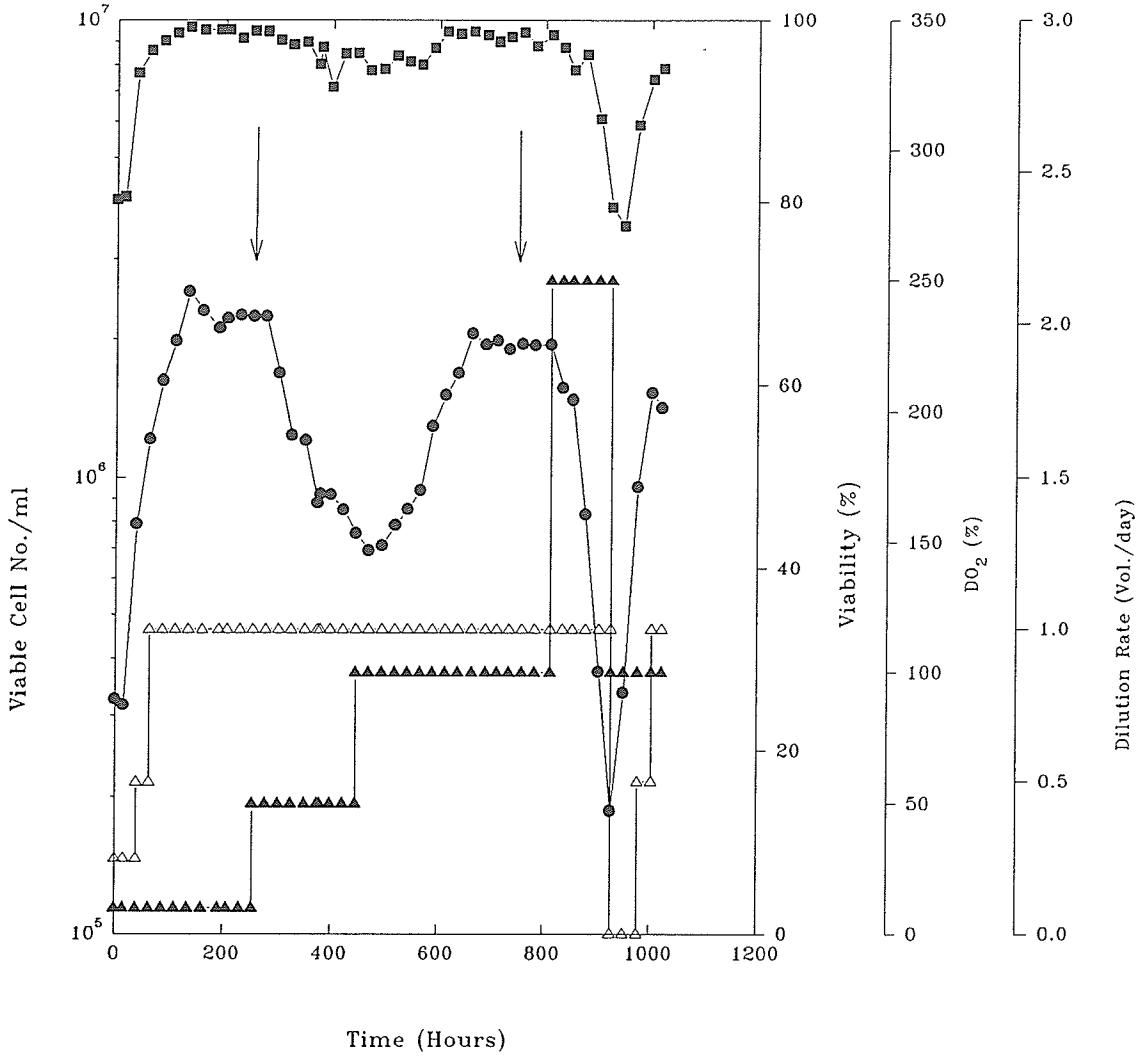

Figure 6.1. Effect of oxygen on the growth of CC9C10 in a Celligen Bioreactor operated in continuous mode. Samples were taken at positions indicated by the arrows. The above fermentor run was used for obtaining samples for the experiment I series.

■ Viability ● Viable Cell No. ▲ Dissolved Oxygen △ Dilution Rate

(Data from D. C. H. Jan)

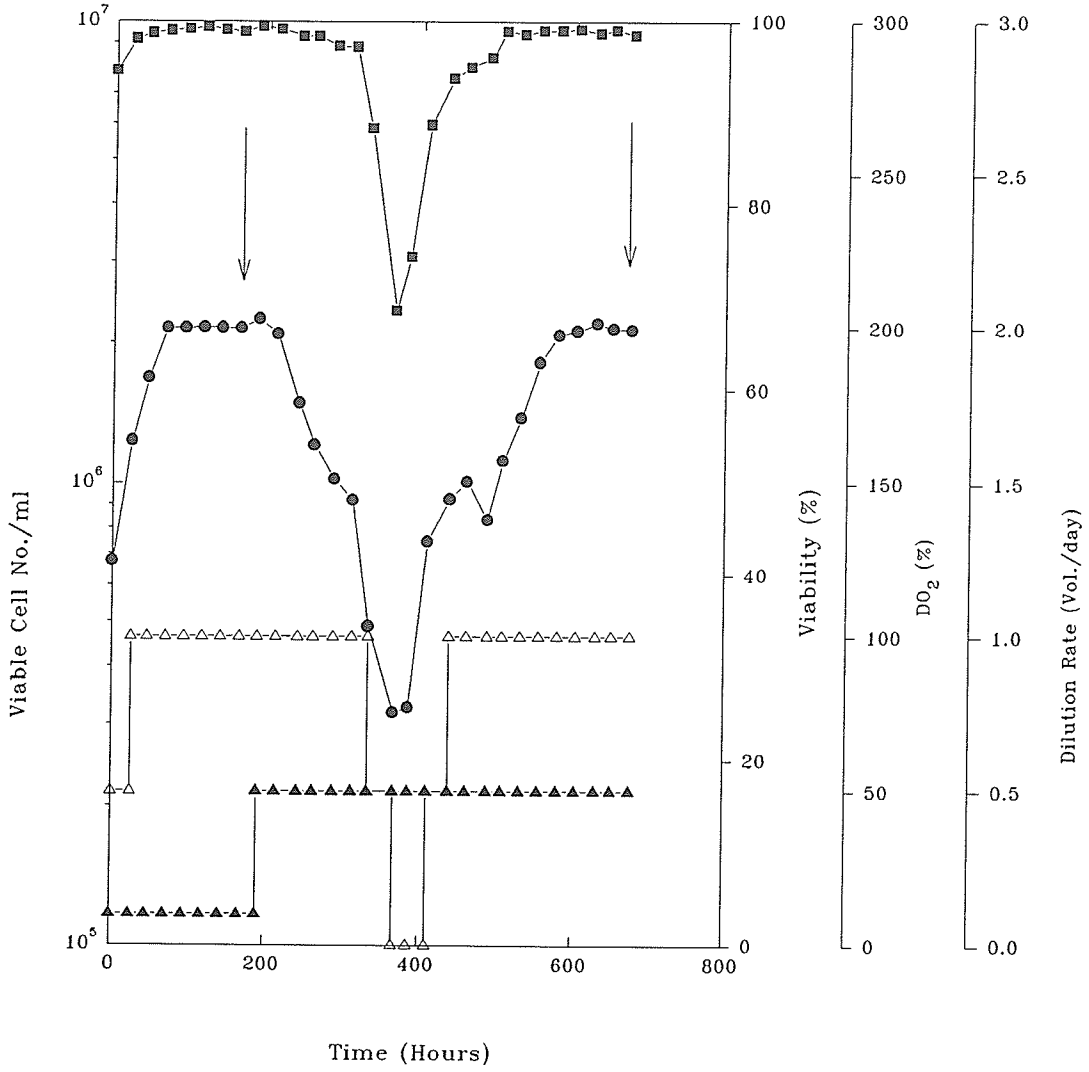

Figure 6.2. Effect of oxygen on the growth of CC9C10 in a Celligen Bioreactor operated in continuous mode. Samples were taken at positions indicated by the arrows. The above fermentor run was used for obtaining samples for the experiment 1 series.

■ Viability ● Viable Cell No. ▲ Dissolved Oxygen △ Dilution Rate
(Data from D. C. H. Jan)

Table 6.1. Rates of substrate utilization / product formation in chemostats at steady state (nmol/10^6 cells per minute). Rates of substrate utilization and product formation were calculated from concentrations determined at steady state. The values shown are means determined from three independent samples. All samples were determined from the experiment 1 series. (n=3).

Substrate/ Product	Oxygen Concentration (% air saturation)		
	10 (± S. E. M.)	50 (± S. E. M.)	100 (± S. E.M.)
Glucose	3.71 (±0.06)	4.29 (±0.03)	4.64 (±0.03)
Lactate	5.02 (±0.20)	6.07 (±0.14)	6.60 (±0.08)
Glutamine	1.46 (±0.05)	1.47 (±0.03)	1.54 (±0.05)
Ammonia	0.72 (±0.01)	0.67 (±0.02)	0.66 (±0.06)

S.E.M. represents standard error of the mean.

Table 6.2. Rates of extracellular product formation in chemostats at steady state (nanograms of product/10^6 cells per minute). Determination of monoclonal antibody production rates. Three different samples (n=3) from cultures at steady state were used in determining the above production rates (ng/10^6 cells per minute). All samples were determined from the experiment 1 series.

Extracellular Product	Oxygen Concentration (% air saturation)		
	10 (± S.E.M.)	50 (± S.E.M.)	100 (± S.E.M.)
Monoclonal Antibody	16.9 (±0.76)	15.8 (±2.56)	14.7 (±0.91)

S. E.M. represents standard error of the mean.

Table 6.3. Metabolic coefficients (Product / Substrate) in chemostats at steady state. Determination of metabolic coefficients. Three different samples (n=3) from cultures at steady state were used in determining the above coefficients. All samples were determined from the experiment 1 series.

Substrate/Product	Oxygen Concentration (% Air Saturation)		
	10 (± S.E. M.)	50 (± S.E.M.)	100 (± S.E.M.)
Lactate/Glucose	1.35 (±0.13)	1.41 (±0.09)	1.42 (±0.05)
Ammonia/Glutamine	0.49 (±0.03)	0.46 (±0.03)	0.43 (±0.05)

S. E. M. represents standard error.

6.3.3 Metabolic analysis:

The metabolic flux of several radiolabelled substrates was determined over short time periods for cell samples taken at the 3 steady states from chemostat cultures. Hybridoma CC9C10 cells were grown under the various oxygen concentrations twice, in order to observe if there were repeatable trends. Figures 6.3 to 6.5 indicate typical data obtained from these incubations (The three Figures illustrate data from experiment 2 at 100% air saturation. In all cases, the rates of $^{14}CO_2$ or $^{3}H_2O$ release were constant for at least 3 hours. These rates were used to calculate the flux of glucose through the pentose phosphate pathway, glycolysis and the TCA cycle. Also, the rate of glutamine oxidation was determined. The results summarized in Table 6.3 showed that the overall rate of glucose metabolism increased at higher dO_2 values. The overall rate of glucose utilization was determined as the summation of the flux values from these 3 metabolic pathways (expressed as total in Table 6.3). These were consistent with the q_{Gluc} values determined in Table 6.1. Glucose uptake as determined by the radioactive assays for cells grown at 10% air saturation were similar to the rates of substrate uptake determined in the chemostats at steady state. For CC9C10 cells grown at 50% and 100% oxygen, the glucose utilization rates determined from the flux data were higher than the values determined from the chemostats at steady state. The increase in oxygen concentration appeared to have an effect on stimulating glucose uptake.

At all oxygen concentrations, the proportion of glucose metabolized by glycolysis was high (>90%). Flux rates via the pentose phosphate and TCA cycle pathways were relatively low. At increased oxygen levels the relative flux of glucose via glycolysis .

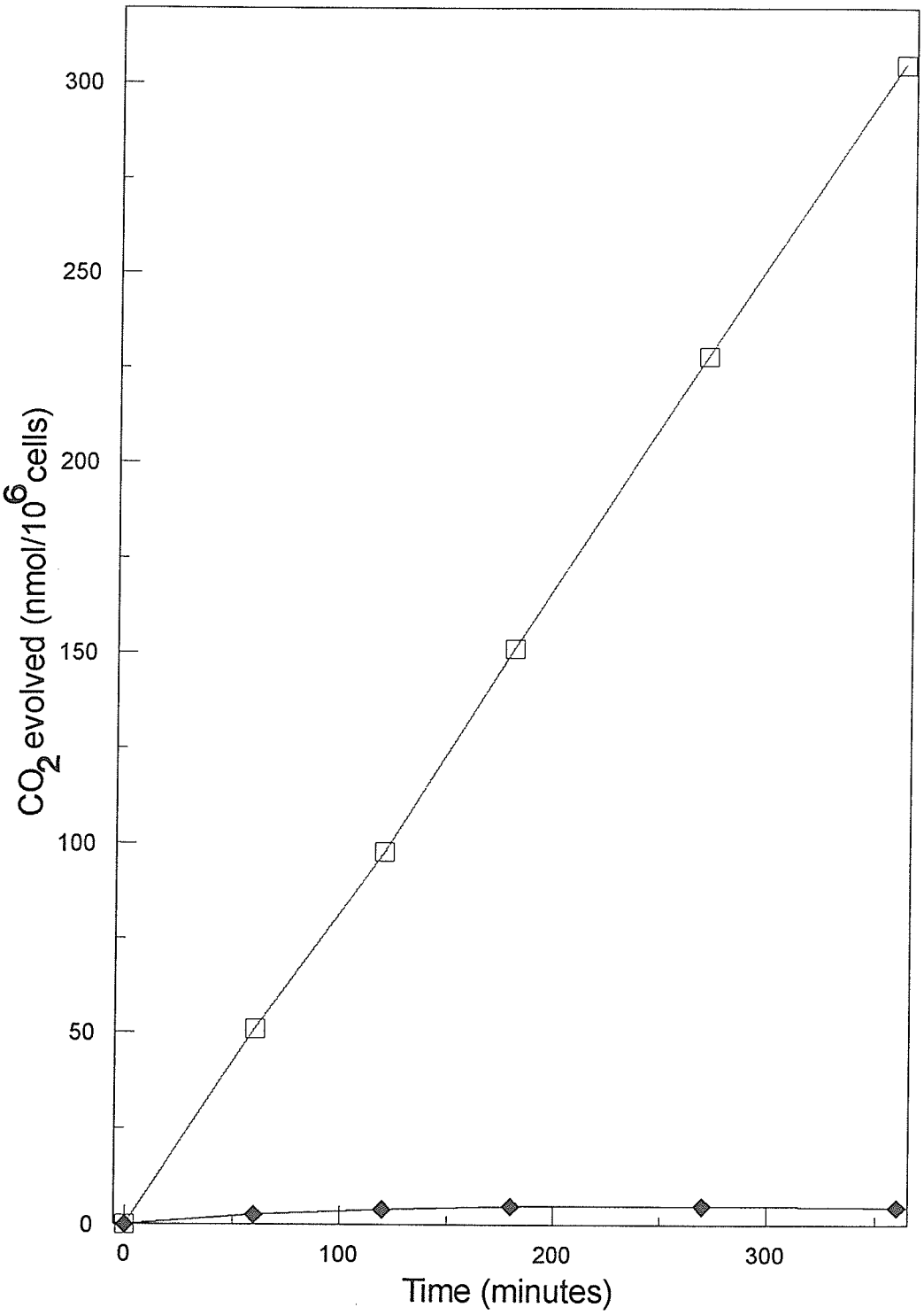

Figure 6.3. The rate of $^{14}CO_2$ release from the metabolism of D-[1-^{14}C]- and D-[6-^{14}C]-glucose. The rate of The rate of $^{14}CO_2$ release was measured from CC9C10 hybridomas (2-3 x 10^6 viable cells/ml) incubated in normal growth medium (1 ml) containing 0.45 μCi of D-[1-^{14}C]-glucose (□), or D-[6-^{14}C]-glucose (♦) as described in Section 2.5.3. The cells were derived from a Celligen fermentor which had been in equilibrium for a minimum of 5 volumes.

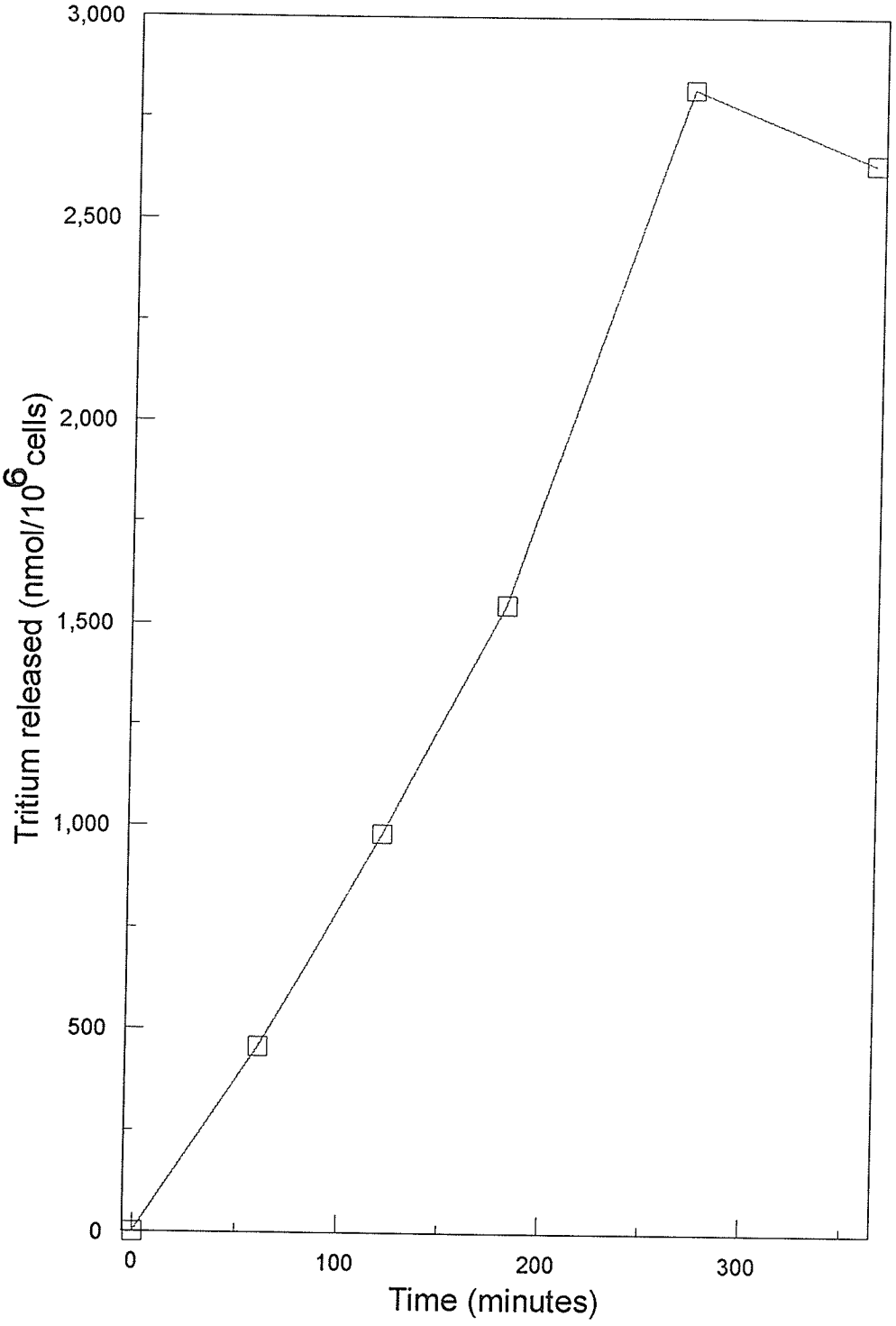

Figure 6.4. The rate of release of ^3H_2O from the metabolism of D-[3-^{3}H]-glucose. The rate of the glycolytic flux in CC9C10 hybridomas (□), was measured by the rate of release of ^3H_2O from cells (2-3 x 10^6 viable cells/ml) incubated in normal growth medium (1 ml) containing D-[3-^{3}H]-glucose as described in Section 2.5.4. The cells were derived from a Celligen fermentor which had been in equilibrium for a minimum of 5 volumes.

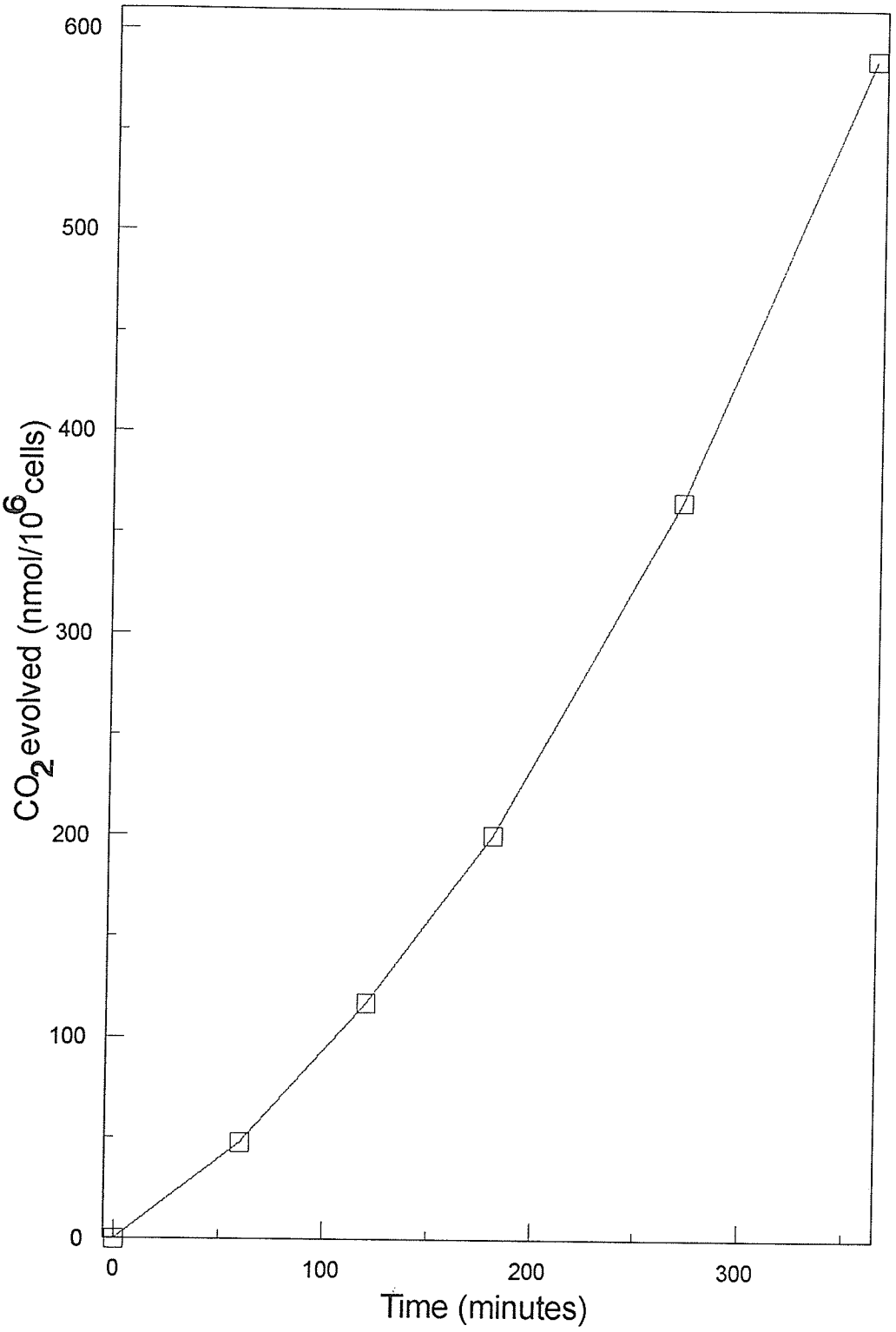

Figure 6.5. Glutamine oxidation from the metabolism of L-[U-^{14}C]-glutamine. The rate of CO_2 release was measured from CC9C10 hybridomas (□) (2-3 x 10^6 viable cells/ml) incubated in normal growth medium (1 ml) containing 0.25 μCi of L-[U-^{14}C]-glutamine as described in Section 2.5.3. The cells were derived from a Celligen fermentor which had been in equilibrium for a minimum of 5 volumes.

Table 6.4. Flux through various metabolic pathways (nmol substrate/10^6 cells per minute. The flux values were determined by radioactive assays using cells taken from chemostats equilibrated with oxygen at various concentrations ± standard error. All of the assays were performed in a New Brunswick Celligen fermentor, except experiment 2 at 100 % air saturation., which was performed in an LH fermentor. The LH fermentor was used to replace the New Brunswick Celligen fermentor due to a probe failure. CC9C10 hybridoma cells were grown under the various oxygen concentrations twice, in order to observe if there were repeatable trends. The values are means of the samples (n=10). The percentage of glucose utilized via three metabolic pathways was calculated for each steady state.

Substrate	Pathway	Oxygen Concentration (% air saturation)					
		10		50		100	
		Expt 1 (±S.E.M)	Expt 2 (±S.E.M)	Expt 1 (±S.E.M)	Expt 2 (±S.E.M)	Expt 1 (±S.E.M)	Expt 2 (±S.E.M)
Glucose	Glycolysis	2.72 (±0.19) (85.8%)	4.19 (±0.12) (91.2%)	6.48 (±0.29) (89.8%)	7.27 (±0.24) (90.2%)	7.34 (±0.97) (90.5%)	8.62(±0.29) (91.8%)
	PPP	0.451 (±0.014) (14.2%)	0.406 (±0.015) (8.83%)	0.740 (±0.019) (10.2%)	0.790 (±0.025) (9.8%)	0.771 (±0.047) (9.51%)	0.775 (±0.087) (8.25%)
	TCA	0.0645 (±0.003) (2.03%)	0.117 (±0.001) (2.54%)	0.0895 (±0.003) (1.24%)	0.1274 (±0.004) (1.58%)	0.0169 (±0.002) (0.21%)	0.0269 (±0.004) (0.04%)
	Total	3.17 (±0.2) (100%)	4.60 (±0.14) (100%)	6.62 (±0.3) (100%)	8.06 (±0.26) (100%)	7.48 (±0.98) (100%)	9.39 (±0.38) (100%)
Glutamine	oxidation	0.219 (±0.024)	0.208 (±0.020)	0.234 (±0.024)	0.278 (±0.024)	n.d.	0.222 (±0.020)

S.E.M represents standard error of the mean.
% indicates what percentage of glucose is entering designated pathways.
n. d. represents not determined.

increased compared to a relative decrease in flux via either the pentose phosphate or TCA cycle pathways.

Glutamine oxidation was measured at all the steady state levels of air saturation (except in experiment 1 at 100% air saturation). No significant difference was found between the oxidation rates of this substrate at all three states. This was substantiated by the data showing similar q_{Gln} values at all steady states.

Upon increasing oxygen concentrations, there was an observed increase in total glucose metabolism. Glycolytic flux increased upon increasing oxygen concentrations. The PPP flux was relatively constant over the course of all oxygen concentrations throughout the course of the experiments. The TCA flux surprisingly decreased upon increasing oxygen concentrations. The higher oxygen concentrations may affect the PDH enzyme, decreasing the overall TCA flux. Glutamine oxidation was constant at all oxygen concentrations, suggesting oxygen had little effect upon glutamine metabolism.

6.4 Discussion

Chemostat cultures are ideal for analyzing perturbations in cellular metabolism because a steady state of exponential growth can be attained in a constant chemical environment. All analyses reported here were performed on cells which had attained a steady state at various oxygen concentrations. The cell concentrations at oxygen levels corresponding to 10, 50 and 100% air saturation were constant indicating that oxygen was not growth inhibitory over this range. Some adaptation was necessary as evidenced by the switch to 50% air saturation in both Figures 6.1 and 6.2.

A number of metabolic changes were associated with growth at the 3 oxygen levels. The q_{Gluc}, and q_{Lac} increased significantly at higher dissolved oxygen concentrations. This was associated with a slight increase in the lactate/glucose ratio from 1.35 to 1.42, suggesting an increase in glucose metabolism at higher dissolved oxygen concentrations. The q_{Gln} and q_{Amm} remained relatively unchanged by the increases in dissolved oxygen levels. The ammonia/glutamine ratio varied between 0.42 to 0.49, which indicated a relatively low level of deamination compared to previously reported data (Hassell and Butler, 1990). The production rate of antibody (q_{Mab}) was slightly higher at the low oxygen air saturation (10%), compared to the 100% air saturation.

A series of short radioactive experiments were performed at all of the air saturations (10, 50, and 100%) twice with each sample performed in duplicate, in order to see if any trends were repeatable. All samples were linear for at least three hours, and the rates were used to calculate the flux of glucose through the pentose phosphate pathway, TCA cycle, and glycolysis. The glycolytic flux increased dramatically upon increasing the air saturation from 10% to 50%. The glycolytic flux increased slightly upon increasing the air saturation to 100%. Since the glycolytic flux accounted for >90% of the total glucose metabolized, the total glucose consumption increased upon increasing the dissolved oxygen concentration. The percent of glucose entering

glycolysis remained constant at all of the oxygen concentrations. The pentose phosphate pathway flux remained constant upon raising the dissolved oxygen concentration between 10% and 100% air saturation. The TCA flux was the most surprising, as there was a very significant decrease at 100% air saturation, despite an overall increase in glucose utilization. The overall increase in glucose utilization was significantly higher in the radioactive experiments, as opposed to the determined utilization rates in the chemostat cultures in a continuous mode. Exposing the CC9C10 hybridoma cells exposed to oxygen levels, and transferred to fresh medium appeared to have a stimulatory effect on glucose uptake. The pentose phosphate pathway and TCA cycle had relatively low flux rates.

Glutamine oxidation was measured at all of the steady state levels of air saturation except in experiment 1 at 100% air saturation. No significant difference was observed between the oxidation rates at any of the three steady states. This was substantiated by the data showing q_{Gln} values at all steady states.

6.5 Summary

A murine B-lymphocyte hybridoma, CC9C10 was grown in chemostat cultures at oxygen concentrations corresponding to 10, 50 and 100% air saturation. Although some adaptation was required, the growth rates were unchanged at these oxygen levels. However, an attempt at growth in pure oxygen (250% air saturation) was unsuccessful. The changes in dissolved oxygen concentration caused some changes in energy metabolism as analyzed by short-term radioactive assays. The specific rate of glucose uptake increased at higher dissolved oxygen concentrations. Most of the glucose (>90%) was metabolized via glycolysis. Relatively low flux rates were observed throughout for the pentose phosphate and TCA cycle pathways. Glutamine utilization and metabolism were apparently unaffected by changes in dissolved oxygen concentration. Apparently, antibody production was not terribly affected by increases in dissolved oxygen concentrations.

CHAPTER 7

7.0 A Metabolic Comparison Between a Murine Hybridoma Cell Line CC9C10 and its Parent Myeloma Cell Line SP2/0.

7.1 Introduction

Hybridoma cells are routinely cultured for production of extracellular monoclonal antibodies. Monoclonal antibodies have found uses in medical research, commercial research, and therapeutic applications (Hubbard, 1983; Morrison and O, 1989).

Hybridoma cell lines are created by fusing myeloma and spleen cells from an immunized donor. The resultant is an immortal antibody secreting clone. Each hybridoma created will have a parent myeloma cell line.

The production of monoclonal antibodies from hybridomas requires that a certain amount of cellular energy be directed towards this synthesis. A comparison of a hybridoma to its parent cell line may show alterations in metabolism. This would allow a prediction of how much substrate is required, having its energy directed towards monoclonal antibody production.

In this investigation, we compared cell growth and biochemical characteristics between hybridoma CC9C10 and its parent myeloma cell line SP2/0.

7.2 Materials and Methods

7.2.1 Cell line : Refer to Section 2.1.0a.

7.2.2 Growth Medium: Refer to Section 2.1.2d.

7.2.3 Culture: Refer to Section 2.1.1b and d.

[3]7.2.4 Radiolabelled Molecules: Refer to Section 2.5.0.

7.2.5 CO_2 evolution: Refer to Section 2.5.3.

7.2.5 Release of tritiated water: Refer to Section 2.4.2 and 2.5.4.

7.2.6 Cell counting: Refer to Section 2.1.4.

7.2.7 Components of culture media: Refer to Section 2.3 in its entirity Samples taken from the LH fermentor were made of 3 independent samples taken at daily intervals after each steady state had been attained (>5 changes in culture media).

---

[3] A repeat experiment for glycolytic flux, TCA cycle, and Pentose Phosphate Pathway was performed for CC9C10 and SP2/0 batch cultures. Instead of duplicate time points, two separate cell cultures were used for each time point.

7.3 Results

7.3.1 CC9C10 and SP2/0 Batch Growth Experiment

Cell growth of CC9C10 and SP2/0 is shown in Figure 7.1. CC9C10 had a doubling time of 14.8, and 16.2 hours on days 1 and 2, respectively. SP2/0 had a doubling time of 19.1, and 16.5 hours, on days 1 and 2, respectively. The number of viable CC9C10 cells reached a plateau maximum between days 2 and 3 at 1.72×10^6 cells/ml, followed by a linear decrease in cells throughout the decline phase. Viable SP2/0 cells reached a maximum cell density on day 3 at 1.96×10^6 cells/ml, followed by a rapid decline in viable cell number upon cells entering the decline phase.

The cellular protein content (Figure 7.1) of CC9C10 decreased over first two days, before leveling out for a three day period, and again decreasing. The highest protein content was 0.254 mg/10^6 cells on day 1, decreasing to 0.016 mg/10^6 cells on day 6. The cellular protein content of SP2/0 increased initially to a maximum value of 0.39 mg/10^6 cells on day 1. The cellular protein content declined further from this point to 0.003 mg/10^6 cells on day 6.

The total cell number in comparison to viable cell number for CC9C10 and SP2/0 is illustrated in Figure 7.2. Upon CC9C10 cells reaching the stationary phase, the cell viability declined linearly, while the total cell number increased until day 5, where it plateaued. SP2/0 reached its maximal viable cell density on day 3, before cell viability rapidly decreased upon entering the decline phase. The total cell number plateaued as the viable cell number approached zero.

The overall pattern in utilization of glucose between CC9C10 and SP2/0 were similar, as shown in figure 7.3. By day 4, glucose in both cultures had been totally consumed. The overall pattern in utilization of glucose between CC9C10 and SP2/0 were similar, as shown in figure 7.3.. Table 7.1 illustrates the daily consumption, and production rates over the growth of the CC9C10 and SP2/0 cultures in batch.

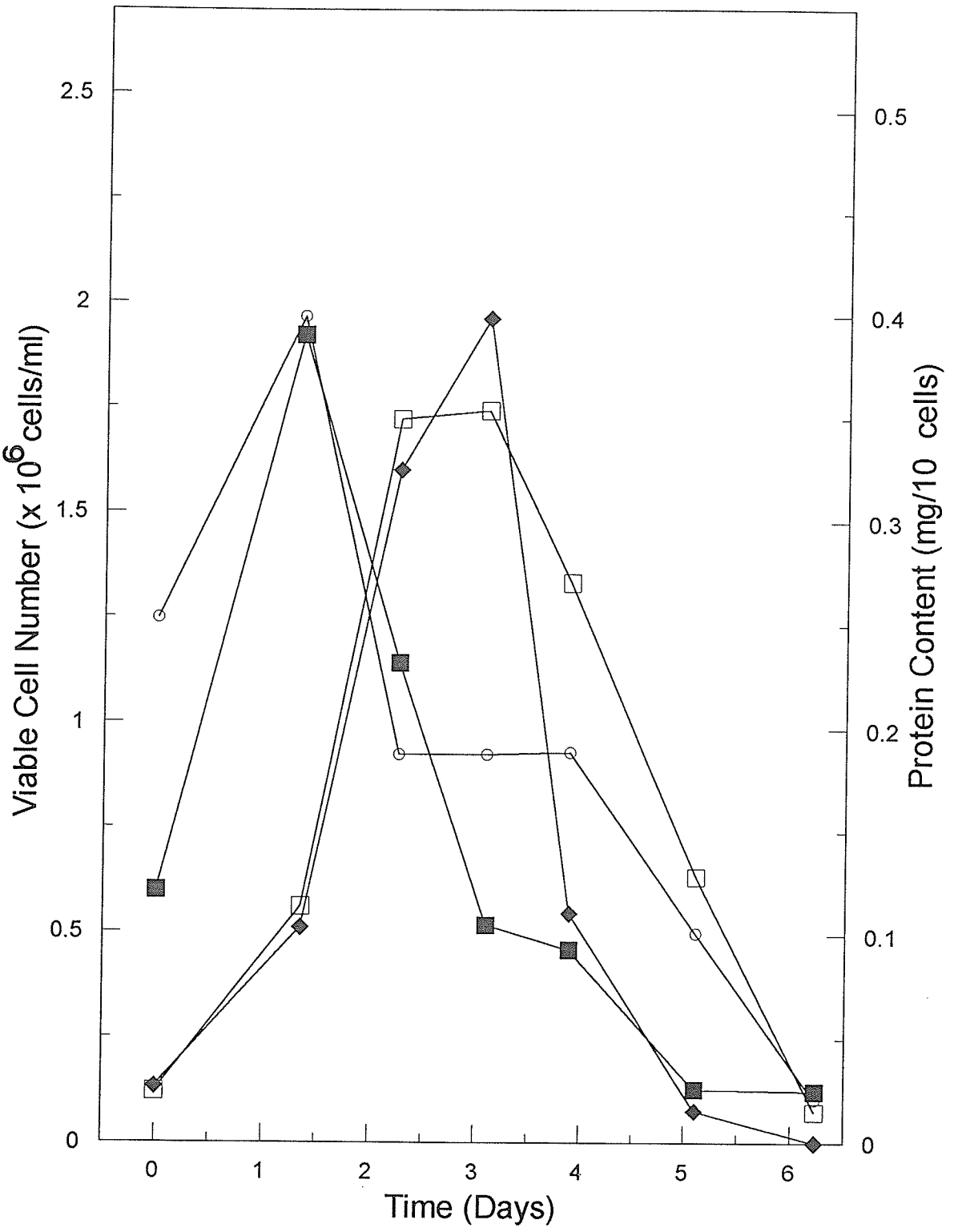

Figure 7.1. Viable cell number and cellular protein content during the growth of CC9C10 and SP2/0 cells. At daily intervals, samples (10 ml) were taken for determining the protein content of the CC9C10 hybridomas (O), and SP2/0 myelomas (■). Cell viability of CC9C10 hybridomas (□) and SP2/0 myelomas (♦) were assessed by trypan blue counting using a haemocytometer.

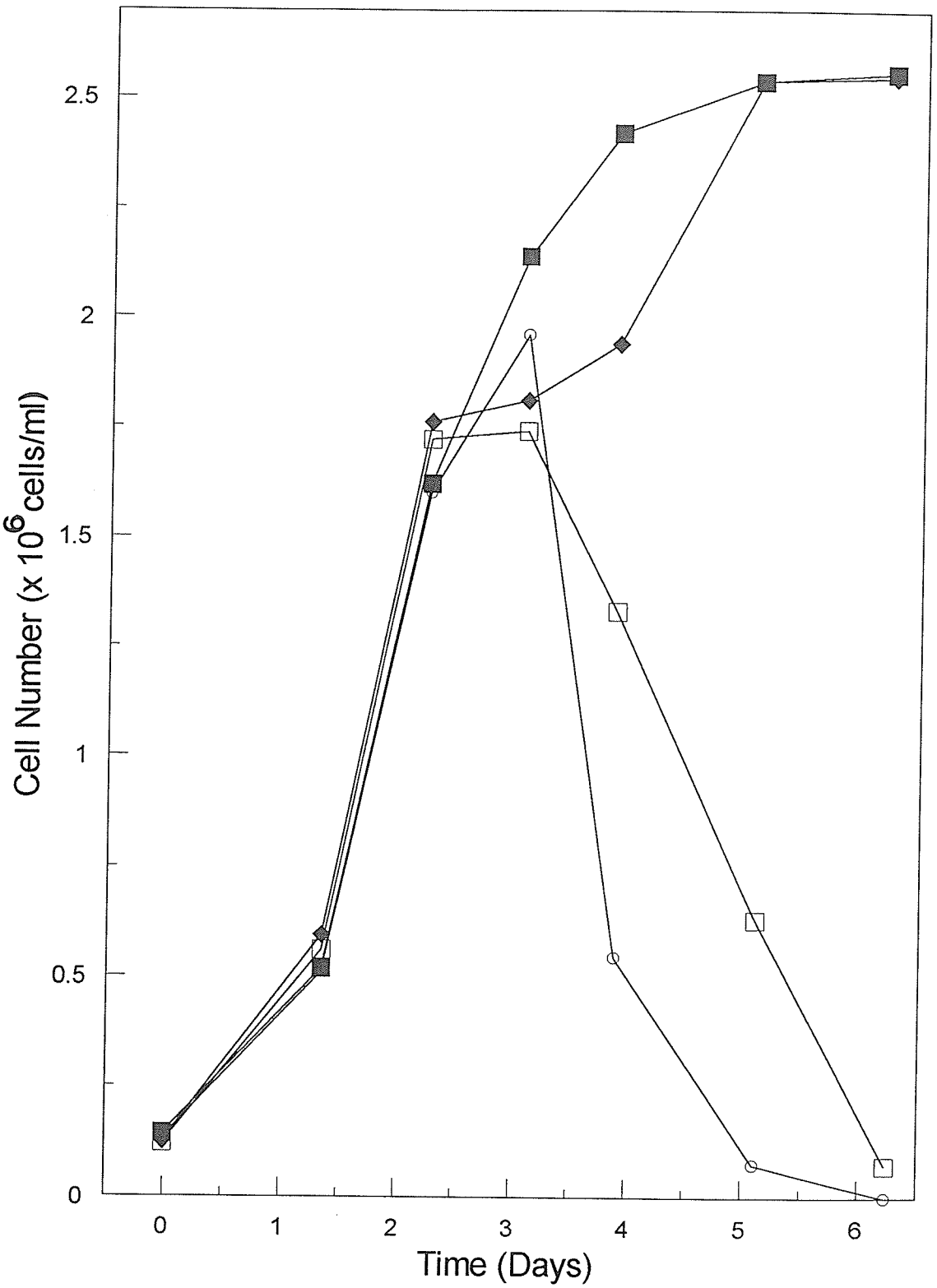

Figure 7.2. Viable cell number and total cell number for the growth of CC9C10 and SP2/0 cells. Viable cell number for CC9C10 hybridomas (□) was compared to their total cell number (♦). Viable cell number for SP2/0 myelomas (O) was compared to their total cell number (■).

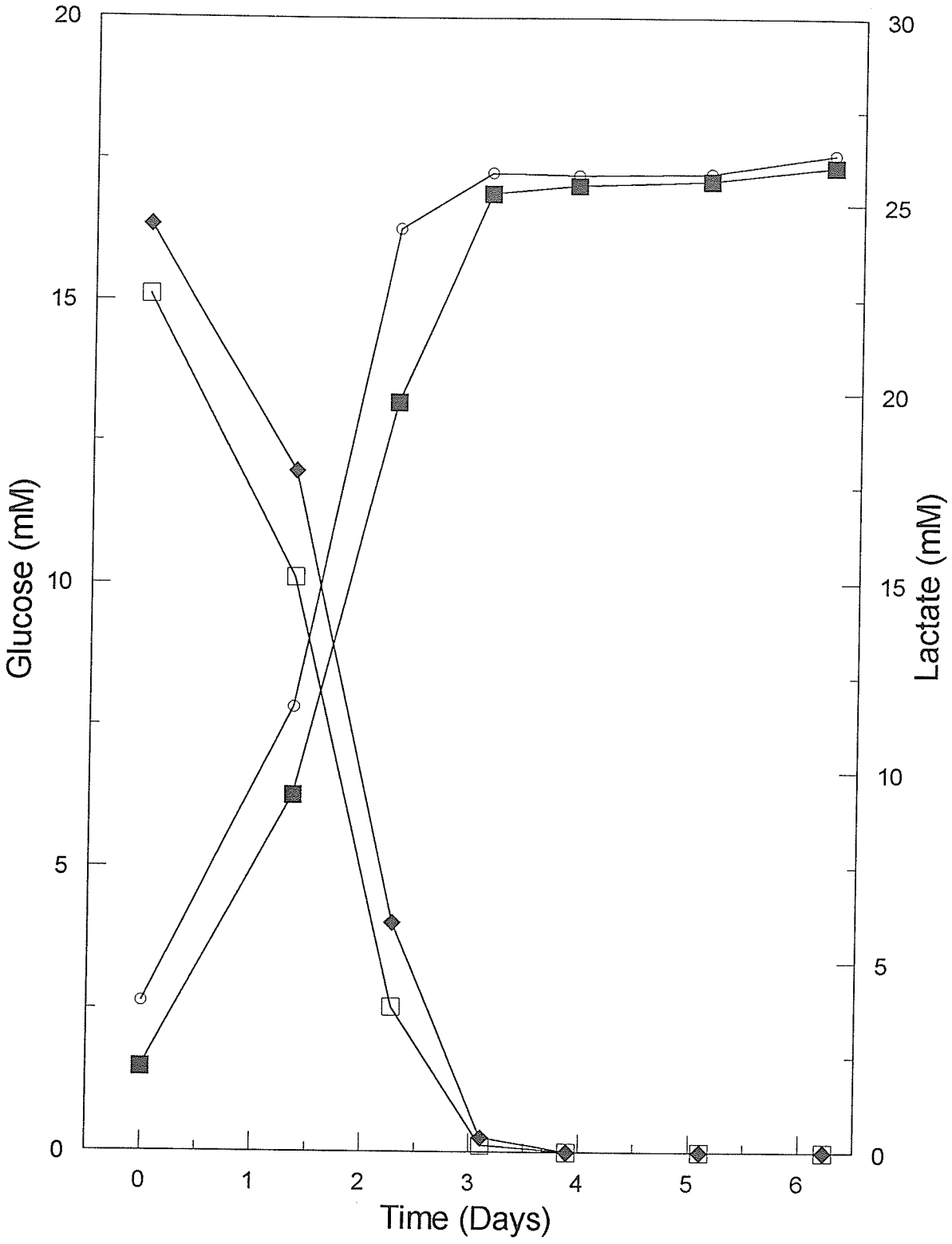

Figure 7.3. Glucose utilization and lactate production during the growth of CC9C10 and SP2/0 cells. Glucose (□), and lactate (O) concentrations from CC9C10 hybridoma cultures were determined on a daily basis from the culture samples. Glucose (♦), and lactate (■) concentrations from SP2/0 myeloma cultures were determined on a daily basis from the culture samples.

Glucose consumption rates in CC9C10 and SP2/0 were maximal on day 1 at 9.15, and 7.98 nmol/minute per 10^6 cells, respectively. Following day 1, both cell lines displayed similar consumption rates.

Lactate production between CC9C10 and SP2/0 over time is shown in Figure 7.3. The lactate production rates were maximal on day 1 for CC9C10 and SP2/0, at 14.2, and 13.1 nmol/minute per 10^6 cells, respectively. Lactate production in both cell lines plateaued after day 3.

Glutamine consumption between CC9C10 and SP2/0 is shown in Figure 7.4. CC9C10 had a near linear decrease in glutamine until it was depleted from the culture medium at day 4. SP2/0 decreased glutamine in a non-linear fashion until it was depleted from the culture medium at day 4. CC9C10 and SP2/0 had maximal glutamine consumption rates on day 1 at 2.49, and 2.78 nmol/minute per 10^6 cells, respectively.

Ammonia production for CC9C10 and SP2/0 was linear until day 3, where both reached a plateau, as shown in Figure 7.4. CC9C10 and SP2/0 had maximal production rates on day 1 at 2.27, and 2.69 nmol/minute per 10^6 cells, respectively.

The lactate/glucose ratios for CC9C10 and SP2/0 were 1.48, and 1.46, respectively. The ammonia/glutamine ratios for CC9C10 and SP2/0 were 0.76, and 0.73, respectively. Determination of the ratios above was based on initial substrate amounts and end product amounts at the end of the culture.

The antibody concentration for CC9C10 was linear for the growth of the culture up until day 5, as shown in Figure 7.5. The specific antibody production rate was highest on day 1, at 21.7 ng/minute per 10^6 cells.

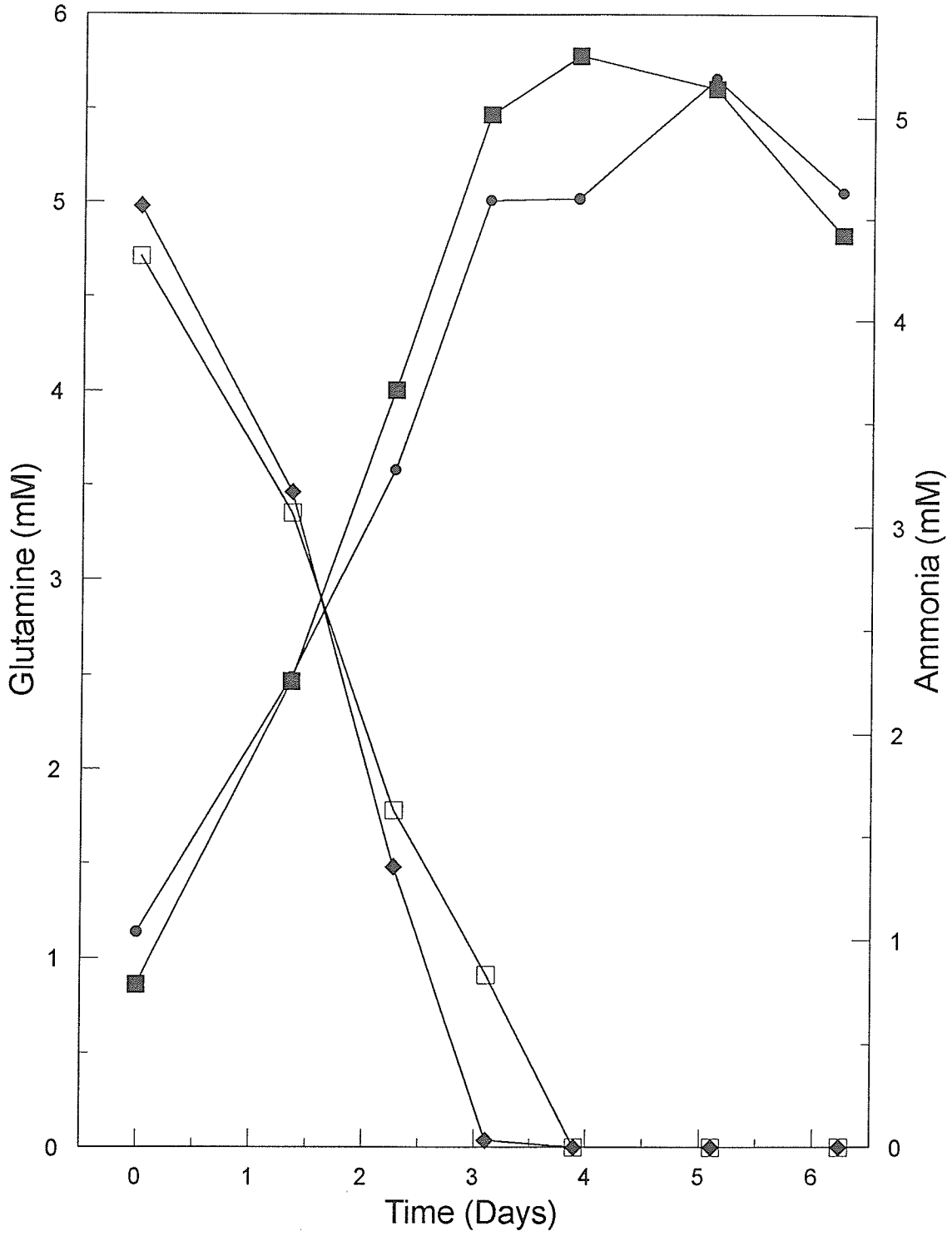

Figure 7.4. Glutamine utilization and ammonia production during the growth of CC9C10 and SP2/0 cells. Glutamine (□), and ammonia (●) concentrations from CC9C10 cell cultures were determined on a daily basis from the culture samples. Glutamine (♦), and ammonia (■) concentrations from SP2/0 cell cultures were determined on a daily basis from the culture samples.

Table 7.1. Consumption and Production rates of CC9C10 and SP2/0 (nmol/minute per 10^6 cells) throughout the batch growth of a culture (n=2).

Cell Line	Time (Days)	Substrate Consumption Rate (nmol/minute per 10^6 cells)		Product Formation Rate(nmol/minute per 10^6 cells)		Product Formation Rate (ng/minute per 10^6 cells)
		Glucose (± S.E.M.)	Glutamine (± S.E.M.)	Lactate (± S.E.M.)	Ammonia (± S.E.M.)	Antibody (± S.E.M.)
CC9C10	1	9.15 (±0.15)	2.49 (±0.01)	14.2 (±0.2)	2.27 (±0.09)	21.7 (±0.4)
	2	2.69 (±0.09)	0.56 (±0.03)	4.50 (±0.11)	0.36 (±0.01)	6.44 (±0.39)
	3	0.62 (±0.05)	0.22 (±0.01)	0.39 (±0.01)	0.34 (±0.01)	2.55 (±0.25)
	4	0	0	0.02 (±0)	0	5.84 (±0.21)
	5	0	0	0.026 (±0)	0.25 (±0.02)	9 (±0.41)
	6	0	0	0	-1.69 (±0.1)	5.2 (±0.16)
SP2/0	1	7.98 (±0.02)	2.78 (±0.02)	13.1 (±0.1)	2.69 (±0.03)	-
	2	2.82 (±0.02)	0.70 (±0.07)	3.69 (±0.1)	0.50 (±0.01)	-
	3	0.97 (±0.11)	0.37 (±0.01)	1.43 (±0.02)	0.34 (±0.01)	-
	4	0	0	0.06 (±0)	0.08 (±0.01)	-
	5	0	0	0.05 (±0)	-0.7 (±0.01)	-
	6	0	0	1.11 9±0.1)	-2.17 (±0.1)	-

S.E.M. represents standard error of the mean.

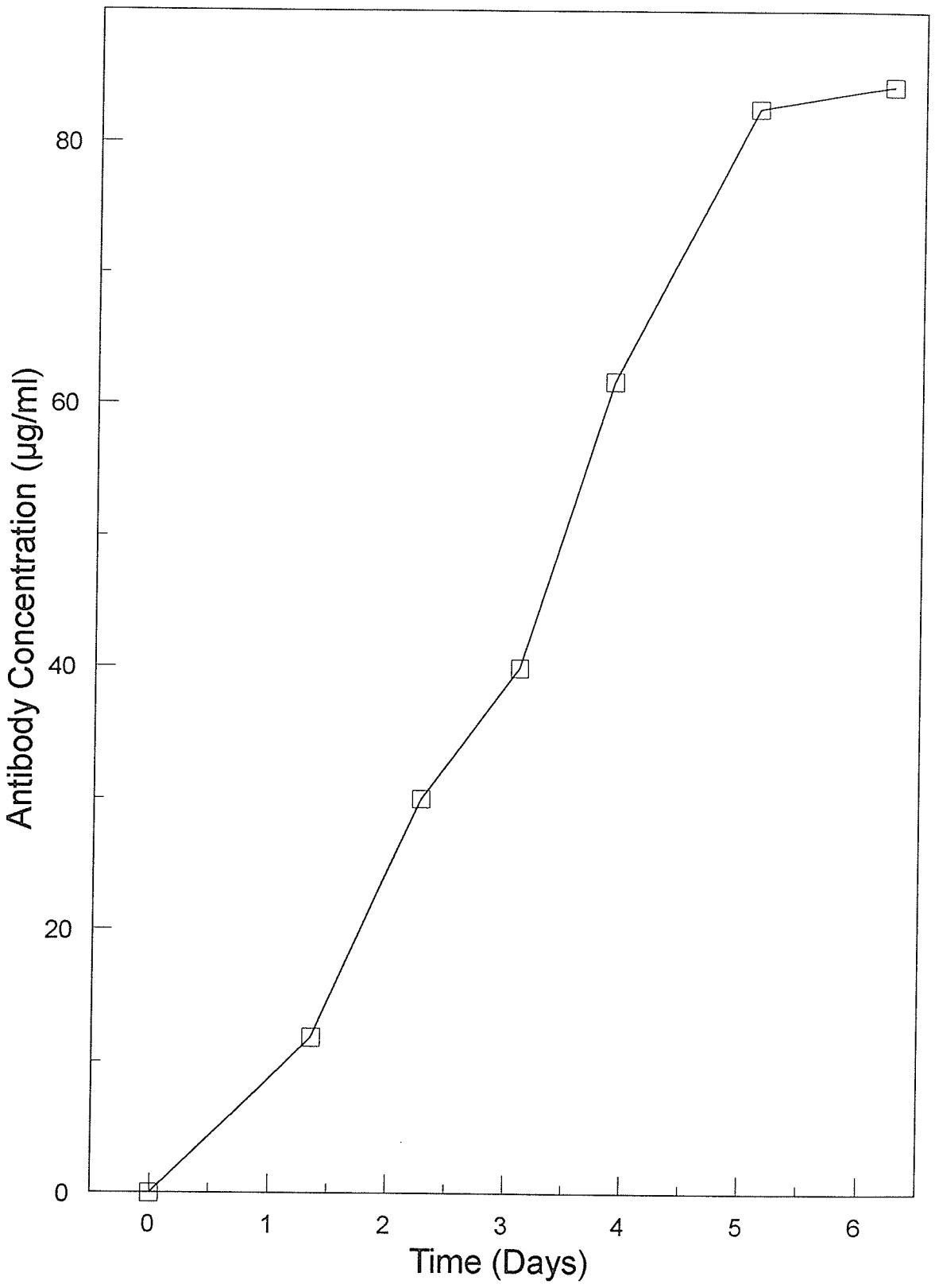

Figure 7.5. Monoclonal antibody production during the growth of CC9C10 hybridomas. At daily intervals, samples (10 ml) were taken for determining the concentration of antibody (□).

7.3.2 Measurement of Fluxes of CC9C10 and SP2/0 from Mid-exponential Growth Phase

7.3.2.1 Glucose Metabolism

a) Pentose phosphate and TCA cycle.

In the experimentation, the TCA flux was measured by the cell specific rate of $^{14}CO_2$ release from D-[6-^{14}C]-glucose. The pentose phosphate flux was measured from the difference in the rates of $^{14}CO_2$ release from cultures containing either D-[1-^{14}C]-glucose or D-[6-^{14}C]-glucose. These rates were linear over a 3 hour period, and showed a significantly higher (x11.8, and x13.5) $^{14}CO_2$ release from D-[1-^{14}C]-glucose for CC9C10 and SP2/0 compared to D-[6-^{14}C]-glucose, respectively (Figures 7.6 and 7.7). The corresponding rates of flux through the pentose phosphate and TCA cycle pathways for CC9C10 and SP2/0 are illustrated in Table 7.2.

Radioactive batch experiments were repeated for both CC9C10 and SP2/0 cultures were similar (Table 7.3), with the values from Table 7.2, except the PPP value, which was 0.481±0.029 nmol/minute per 10^6 cells. The values obtained for the SP2/0 cultures were similar with values from Table 7.2, except the TCA cycle value, which was 0.009 nmol/minute per 10^6 cells. The overall differences observed in both the PPP and TCA flux between the two cell lines were insignificant.

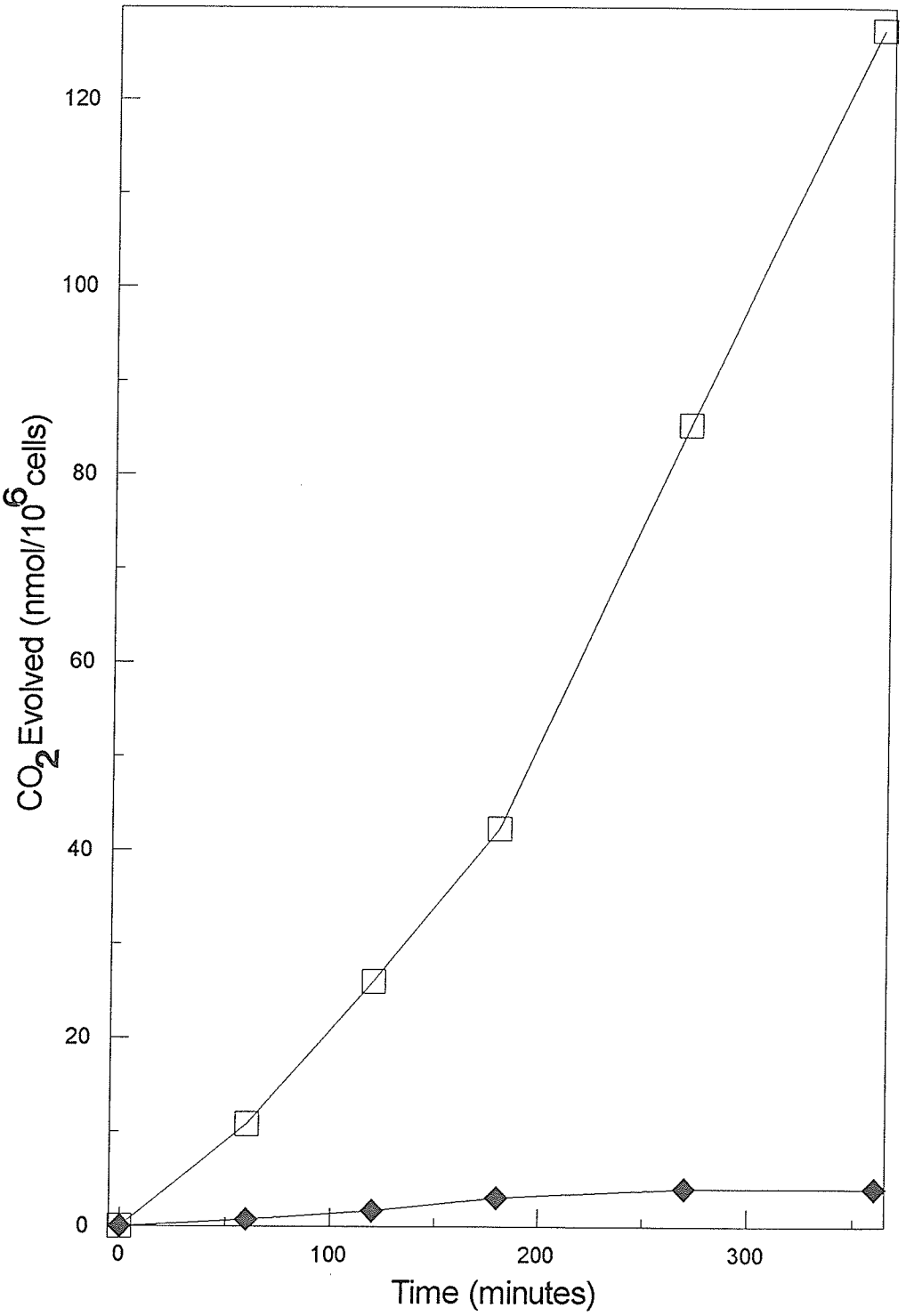

Figure 7.6. The rate of $^{14}CO_2$ release from the metabolism of D-[1-^{14}C]- and D-[6-^{14}C]-glucose. The rate of The rate of $^{14}CO_2$ release was measured from CC9C10 hybridomas (2-3 x 10^6 viable cells/ml) incubated in growth medium (1 ml) containing 0.45 μCi of D-[1-^{14}C]-glucose (□), or D-[6-^{14}C]-glucose (♦) as described in Section 2.5.3. The cells were derived from a batch culture after 48 h growth.

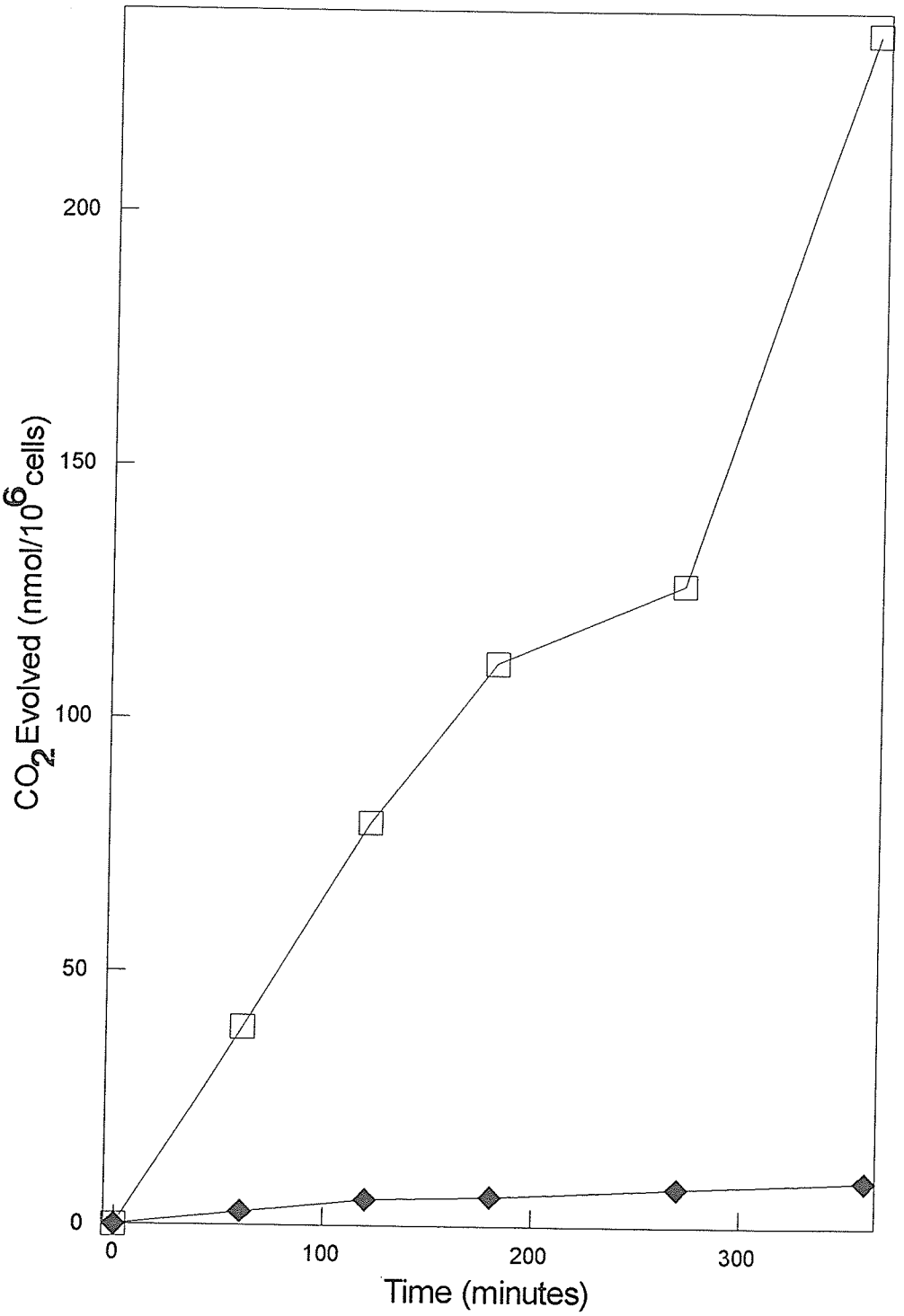

Figure 7.7. The rate of $^{14}CO_2$ release from the metabolism of D-[1-^{14}C]- and D-[6-^{14}C]-glucose. The rate of The rate of $^{14}CO_2$ release was measured from SP2/0 myelomas (2-3 x 10^6 viable cells/ml) incubated in growth medium (1 ml) containing 0.45 μCi of D-[1-^{14}C]-glucose (□), or D-[6-^{14}C]-glucose (♦) as described in Section 2.5.3. The cells were derived from a batch culture after 48 h growth.

b) Glycolysis.

The glycolytic flux was determined by the release of tritiated water from the metabolism of D-[3-^{3}H]-glucose (Bontemps *et al*, 1978). This is a measure of the flux of metabolites through the aldolase and triose phosphate isomerase reactions which are committed steps of the glycolytic pathway. The rate of formation of tritiated water was linear for at least 3 hours for CC9C10 and SP2/0 as measured by radioactive analysis of fractionated samples from an anion exchange column (Figure 7.8). The rates were determined as 6.24±0.56, and 6.34±0.8 nmol/minute per 10^6 cells for CC9C10 and SP2/0, respectively (Table 7.2). The rates of glycolytic flux between the two cell lines was insignificant. This was further confirmed by a repeat of batch growth experiments for both CC9C10 and SP2/0 (Table 7.3). 7.47±0.55 and 6.04±0.30 nmol/minute per 10^6 cells were the determined rates in the repeat of experiments for CC9C10 and SP2/0, respectively. The glycolytic flux values for both experiments were similar among each cell line, and when compared to each other.

The relative flux of glucose through the 3 pathways were determined from the radioactive experiments (Table 7.2). Glycolysis was shown as the major route for glucose catabolism with the TCA cycle and pentose phosphate pathway only serving a minor role. This was consistent with data previously reported for transformed cells (Warburg, 1956). The total glucose consumption rates of CC9C10 and SP2/0 was 6.46 ±0.57, and 6.93±0.82 nmol/minute per 10^6 cells. The difference in consumption rates was negligible. The batch experiment repeats gave total glucose consumption rates of 7.95±0.57, and 6.51±0.34 nmol/minute per 10^6 cells for CC9C10 and SP2/0, respectively.

The sum of the flux rates determined in the radioactive experiments were lower than the value of the initial uptake rate (first two days) of glucose determined in CC9C10 and SP2/0 cultures (Figure 7.3). The differences in values could be explained

by the possibility of differences in the state of the cells at initial and mid-exponential phase and the higher error involved in the determination of the culture uptake rate which was based on samples taken at 24 hour intervals.

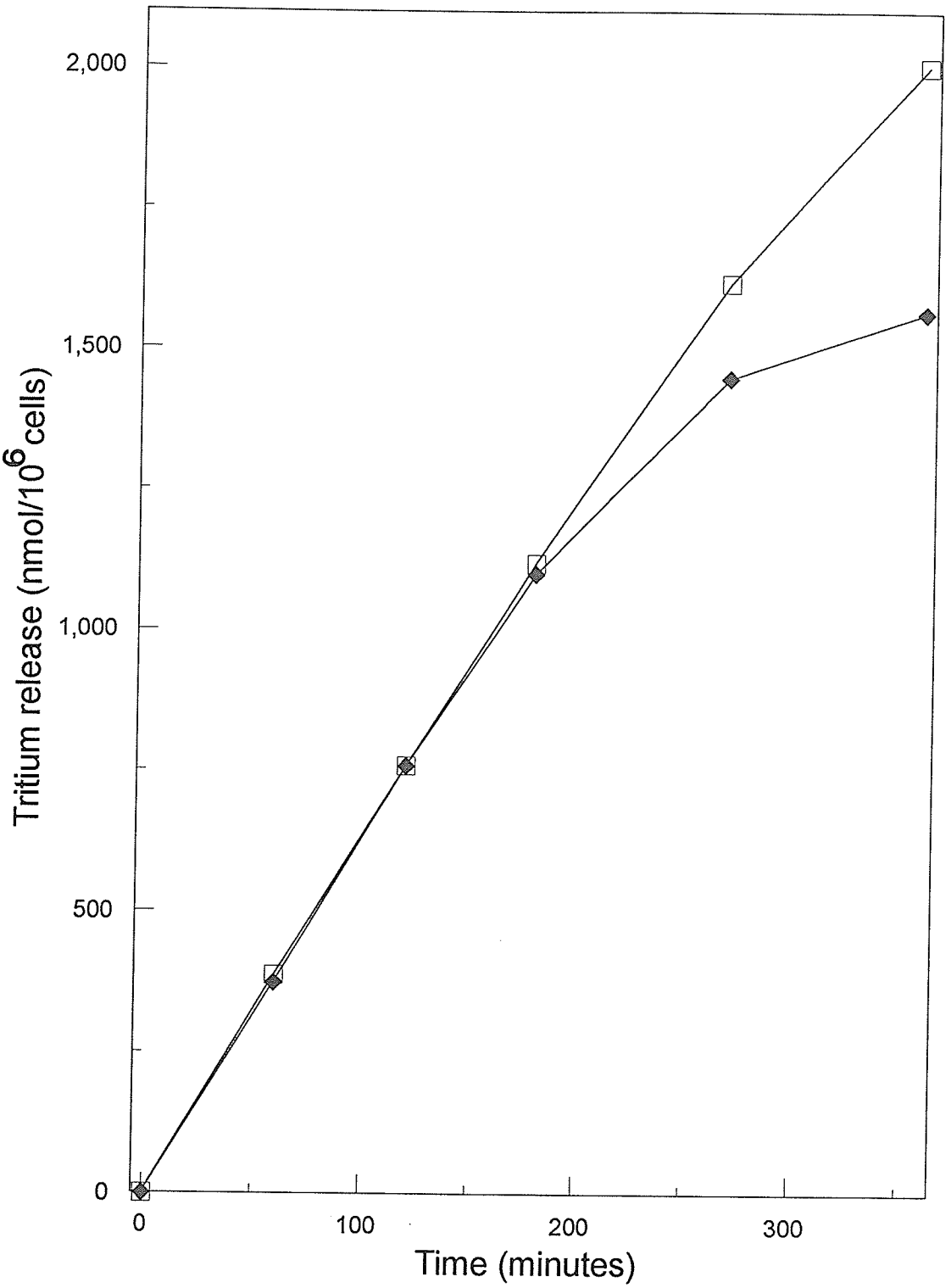

Figure 7.8. The rate of release of ^3H_2O from the metabolism of D-[3-^{3}H]-glucose. The rate of the glycolytic flux in CC9C10 hybridomas (□), and SP2/0 myelomas (♦) was measured by the rate of release of ^3H_2O from cells (2-3 x 10^6 viable cells/ml) incubated in growth medium (1 ml) containing D-[3-^{3}H]-glucose as described in Section 2.5.4. The cells were derived from a batch culture after 48 h growth.

Table 7.2. Metabolism of glucose and glutamine of hybridoma CC9C10 and its parent cell line myeloma SP2/0 under batch and fermentor conditions (nmol/minute per 10^6 cells)
(n=12).

Substrate	Pathway	Hybridoma CC9C10		Myeloma SP2/0	
		Batch Growth (± S.E.M.)	LH Fermentor (± S.E.M.)	Batch Growth (± S.E.M.)	LH Fermentor (± S.E.M.)
Glucose	Glycolysis	6.24 (±0.56) (96.6%)	2.96 (±0.28) (86.3%)	6.34 (±0.80) (91.5%)	3.65 (±0.47) (93.6%)
	PPP	0.220 (±0.010) (3.41%)	0.461 (±0.063) (13.4%)	0.589 (±0.026) (8.5%)	0.250 (±0.250) (6.41%)
	TCA	0.0169 (±0.0011) (0.26%)	0.0443 (±0.0027) (1.3%)	0.0343 (±0.0038) (0.49%)	0.0219 (±0.0019) (0.56%)
	Total	6.46 (±0.57) (100%)	3.43 (±0.35) (100%)	6.93 (±0.82) (100%)	3.90 (±0.48) (100%)
Glutamine	oxidation	0.189 (±0.0016)	0.165 (±0.017)	0.264 (±0.023)	0.173 (±0.0330)

S. E. M. represents standard error of the mean.
% indicates what percentage of glucose is entering designated pathways.

Table 7.3 Confirmation of metabolism of glucose for hybridoma CC9C10 and its parent cell line myeloma SP2/0 under batch conditions (nmol/minute per 10^6 cells) (n=12).

Substrate	Pathway	Hybridoma CC9C10 (± S.E.M.)	Myeloma SP2/0 (± S.E.M.)
		Batch Growth	Batch Growth
Glucose	Glycolysis	7.47 (±0.55) (93.9%)	6.51 (±0.30) (92.8%)
	PPP	0.481 (±0.029) (6.1%)	0.468 (±0.031) (7.75%)
	TCA	0.0189 (±0.003) (0.25%)	0.009 (±0.001) (0.14%)
	Total	7.95 (±0.57) (100%)	6.51 (±0.34) (100%)

S.E.M. represents standard error of the mean.
% indicates what percentage of glucose is entering designated pathways.

7.3.2.2 Glutamine Metabolism

Oxidative Metabolism. The rate of $^{14}CO_2$ release from L-[U-^{14}C]-glutamine was monitored in experiments over a 6 hour period (Figure 7.9) for CC9C10 and SP2/0. A constant rate of CO_2 production of 0.95±0.08, and 1.32±0.12 nmol/minute per 10^6 cells was measured over this period. The obtained values observed in glutamine oxidation between the two cell lines was slightly higher in the SP2/0 culture.

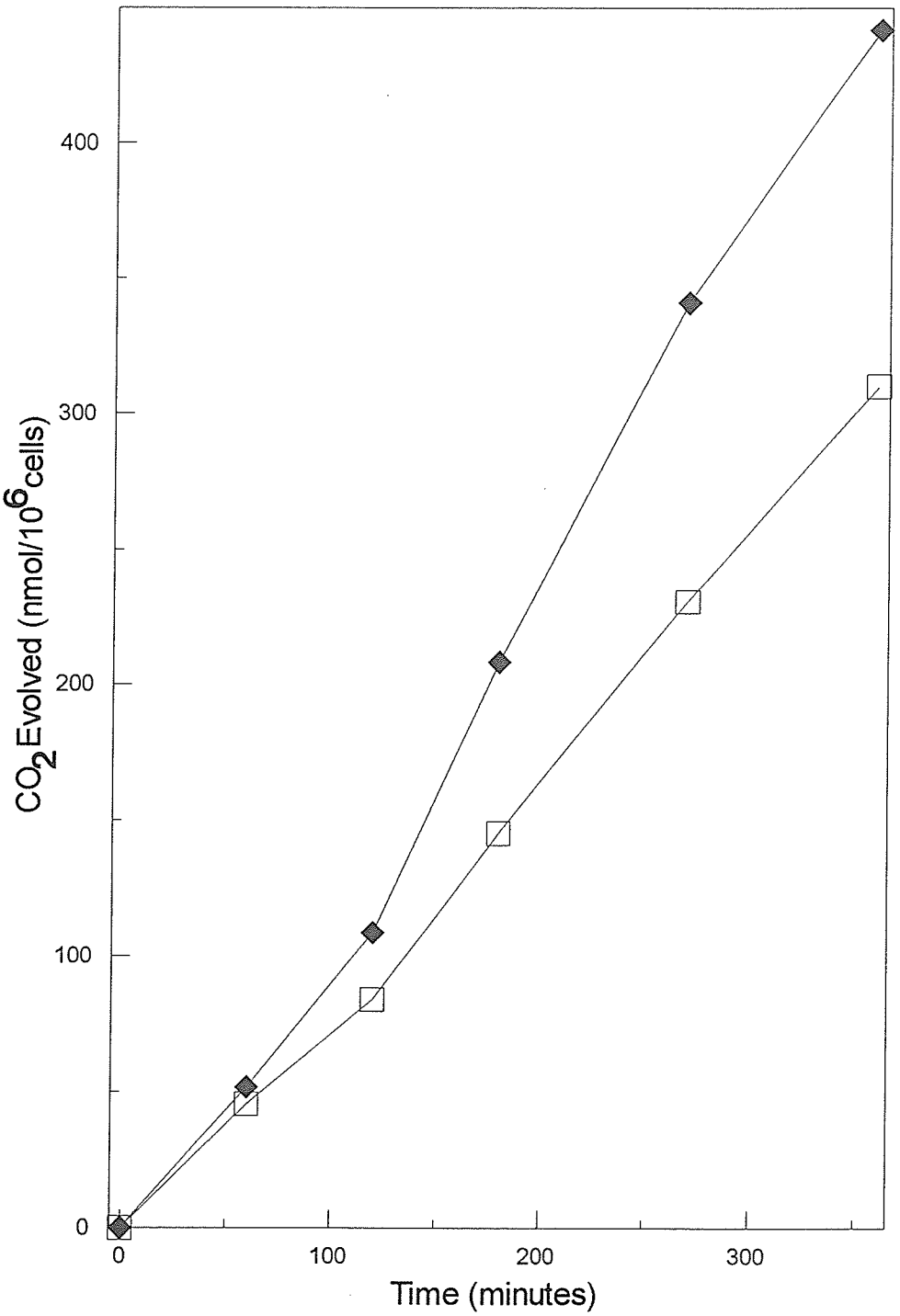

Figure 7.9. Glutamine oxidation from the metabolism of L-[U-^{14}C]-glutamine. The rate of CO_2 release was measured from CC9C10 hybridomas (□) and SP2/0 myelomas (♦) (2-3 x 10^6 viable cells/ml) incubated in growth medium (1 ml) containing 0.25 μCi of L-[U-^{14}C]-glutamine as described in Section 2.5.3. The cells were derived from a batch culture after 48 h growth.

7.3.3 Measurement of Fluxes of CC9C10 and SP2/0

Hybridoma CC9C10 and myeloma SP2/0 cells were taken from an LH fermentor with a dilution rate set at ½ volume per day. The cells were stirred at 100 rpm, at 37^{o}C under 50% aeration.

7.3.3.1 Glucose Metabolism

a) Pentose phosphate and TCA cycle.

In the experimentation the TCA flux was measured by the cell specific rate of $^{14}CO_2$ release from D-[6-^{14}C]-glucose. The pentose phosphate flux was measured from the difference in the rates of $^{14}CO_2$ release from cultures containing either D-[1-^{14}C]-glucose or D-[6-^{14}C]-glucose. These rates were linear over a 3 hour period, and showed a significantly higher (x10.4, and x11.4) $^{14}CO_2$ release from D-[1-^{14}C]-glucose for CC9C10 and SP2/0 compared to D-[6-^{14}C]-glucose, respectively (Figure 7.10 and 7.11). The corresponding rates of flux through the pentose phosphate and TCA cycle pathways for CC9C10 and SP2/0 are shown in Table 7.2. The differences observed in both the PPP and TCA flux between the two cell lines were significant. CC9C10 cells had pentose phosphate pathway and TCA cycles fluxes which were 209%, and 232% higher than the values attains for SP2/0 cells.

b) Glycolysis.

The glycolytic flux was determined by the release of tritiated water from the metabolism of D-[3-^{3}H]-glucose (Bontemps *et al*, 1978). This is a measure of the flux of metabolites through the aldolase and triose phosphate isomerase reactions which are committed steps of the glycolytic pathway. The rate of formation of tritiated water was linear for at least three hours for CC9C10 and SP2/0 as measured by radioactive analysis of fractionated samples from an anion exchange column (Figure 7.12). The rates were determined as 2.96±0.28, and 3.65±0.47 nmol/minute per 10^{6} cells, respectively. The difference in rates of glycolytic flux between the two cell lines were insignificant.

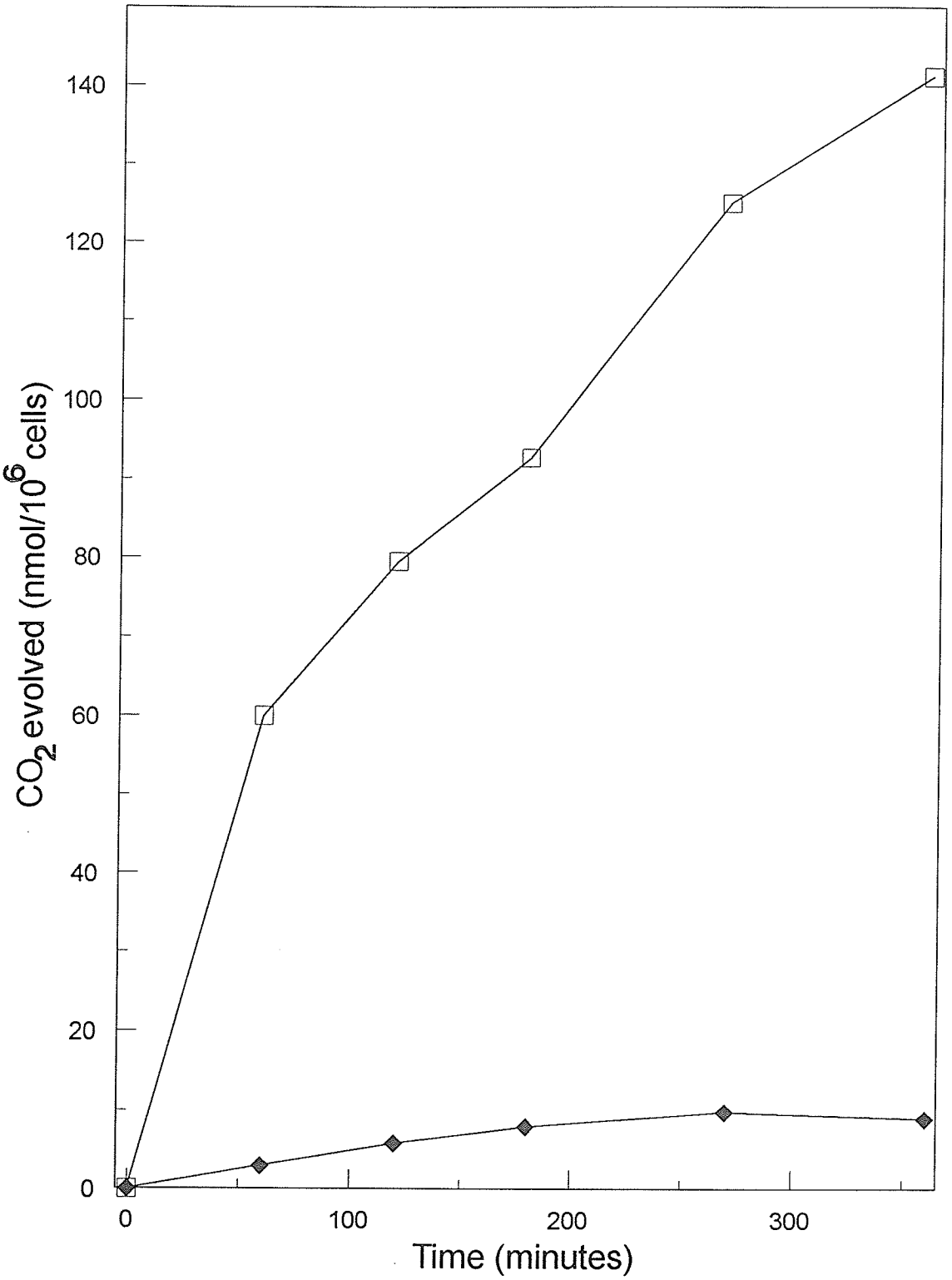

Figure 7.10. The rate of $^{14}CO_2$ release from the metabolism of D-[1-^{14}C]- and D-[6-^{14}C]-glucose. The rate of The rate of $^{14}CO_2$ release was measured from CC9C10 hybridomas (2-3 x 10^6 viable cells/ml) incubated in growth medium (1 ml) containing 0.45 μCi of D-[1-^{14}C]-glucose (□), or D-6-^{14}C]-glucose (♦) as described in Section 2.5.3. The cells were derived from an LH fermentor which had been in equilibrium for a minimum of 5 volumes.

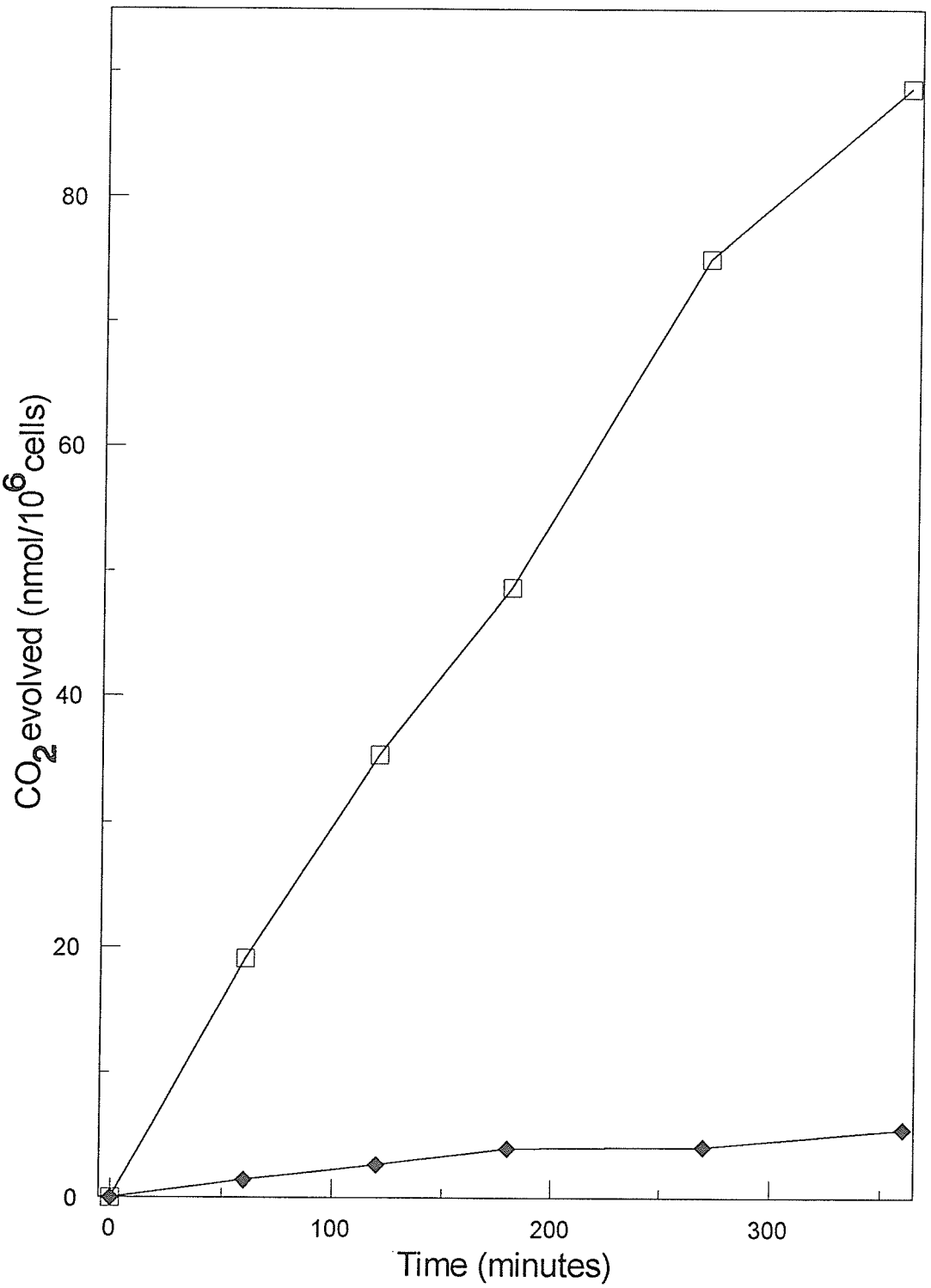

Figure 7.11. The rate of $^{14}CO_2$ release from the metabolism of D-[1-^{14}C]- and D-[6-^{14}C]-glucose. The rate of The rate of $^{14}CO_2$ release was measured from SP2/0 myelomas (2-3 x 10^6 viable cells/ml) incubated in growth medium (1 ml) containing 0.45 μCi of D-[1-^{14}C]-glucose (□), or D-[6-^{14}C]-glucose (♦) as described in Section 2.5.3 The cells were derived from an LH fermentor which had been in equilibrium for a minimum of 5 volumes.

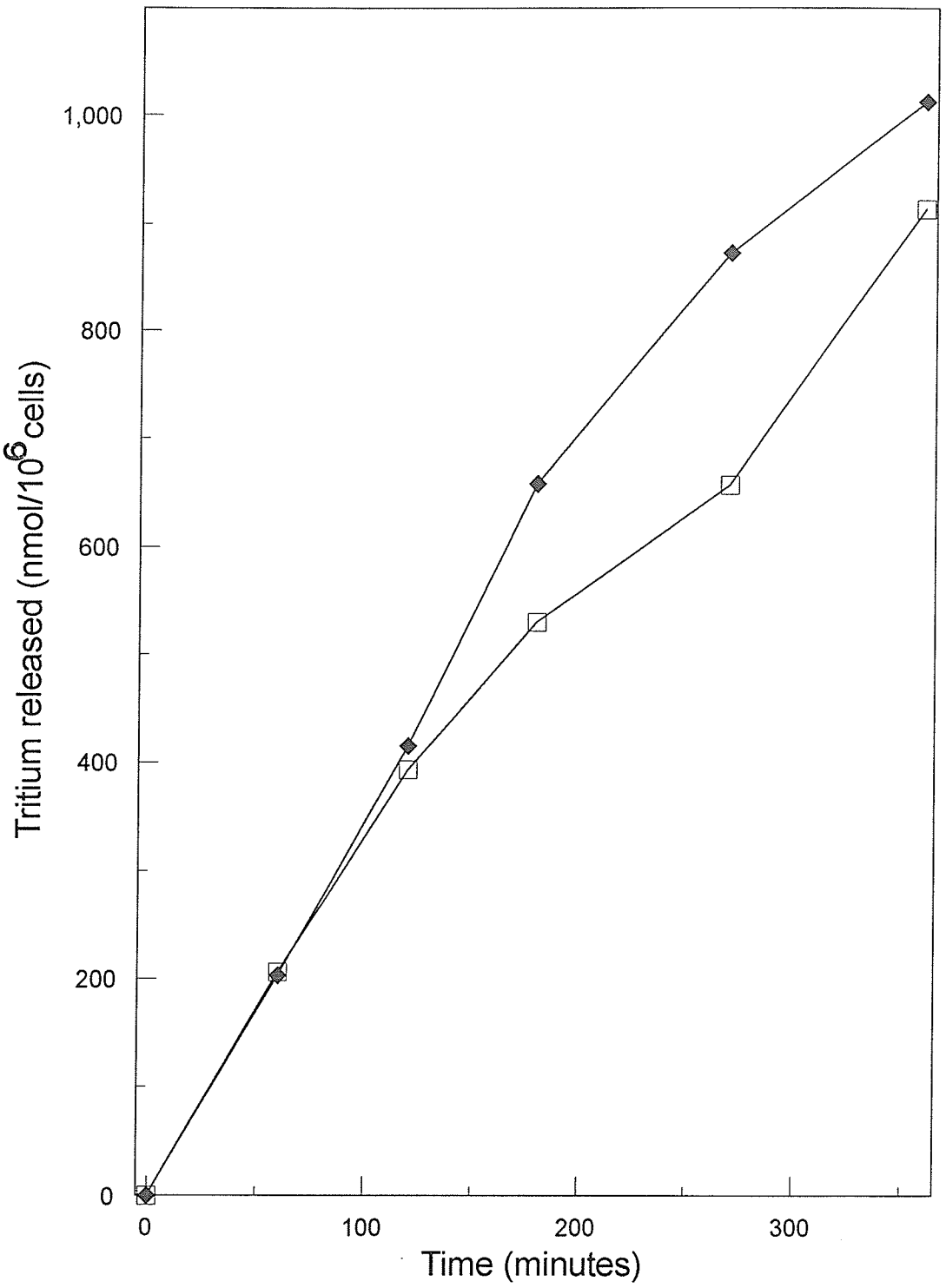

Figure 7.12. The rate of release of ^3H_2O from the metabolism of D-[3-^{3}H]-glucose. The rate of the glycolytic flux in CC9C10 hybridomas (□), and SP2/0 myelomas (♦) was measured by the rate of release of ^3H_2O from cells (2-3 x 10^6 viable cells/ml) incubated in growth medium (1 ml) containing D-[3-^{3}H]-glucose as described in Section 2.5.4. The cells were derived from an LH fermentor which had been in equilibrium for a minimum of 5 volumes.

The relative flux of glucose through the 3 pathways were determined from the radioactive experiments (Table 7.1). Glycolysis was shown as the major route for glucose catabolism with the TCA cycle and pentose phosphate pathway only serving a minor role. This is consistent with data previously reported from transformed cells (Warburg, 1956). The total glucose consumption rate of CC9C10 and SP2/0 was 3.43± 0.35, and 3.90±0.48 nmol/minute per 10^6 cells, respectively.

The sum of the flux rates determined in the radioactive experiments were lower than the value of the initial uptake rate (first two days) of glucose determined in CC9C10 and SP2/0 cultures (Figure 7.3). The differences in values can be explained by the possibility of differences in the state of the cells, as the cells in the fermentor are maintained at ½ volume per day, which would restrict nutrient uptake for rapidly dividing cells.

7.3.3.2 Glutamine Metabolism

Oxidiative Metabolism.

The rate of $^{14}CO_2$ release form L-[U-^{14}C]-glutamine was monitored in experiments over a 6 h period (Figure 7.13) for CC9C10 and SP2/0. A constant rate of CO_2 production of 0.82±0.09, and 0.86±0.16 nmol/minute per 10^6 cells, was measured for CC9C10 and SP2/0, respectively over this period. The differences observed in glutamine oxidation between the two cell lines were insignificant.

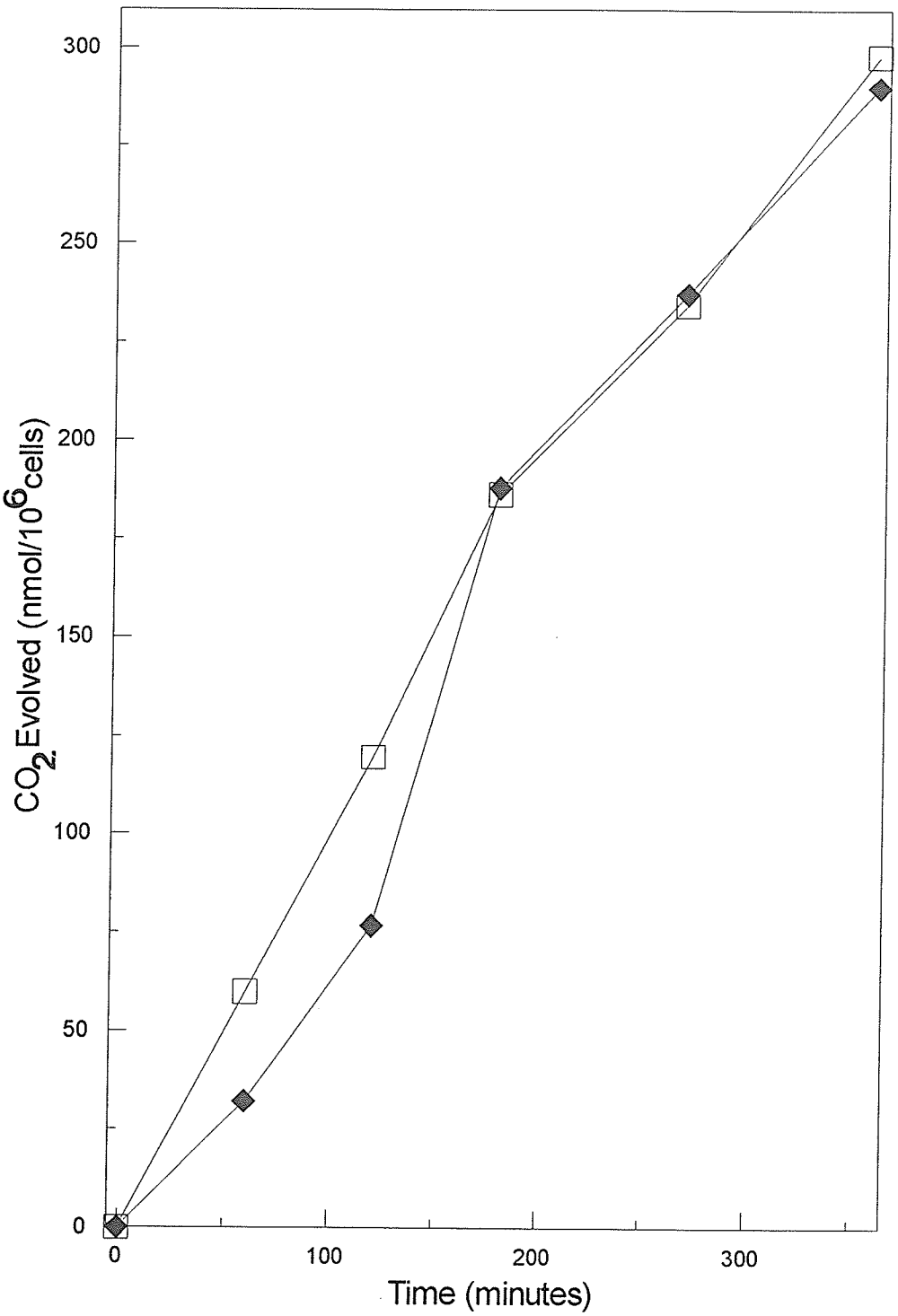

Figure 7.13. Glutamine oxidation from the metabolism of L-[U-^{14}C]-glutamine. The rate of CO_2 release was measured from CC9C10 hybridomas (□) and SP2/0 myelomas (♦) (2-3 x 10^6 viable cells/ml) incubated in growth medium (1 ml) containing 0.25 μCi of L-[U-^{14}C]-glutamine as described in Section 2.5.3. The cells were derived from an LH fermentor which had been in equilibrium for a minimum of 5 volumes.

7.4 Discussion

CC9C10 and SP2/0 had similar patterns of growth up to the stationary phase. CC9C10, upon entering the decline phase, there was a linear decrease in cell viability. Upon SP2/0 entering the decline phase, the viable cell number decreased rapidly. The patterns of CC9C10 and SP2/0 cell growth in the decline phase were different. It is concluded that SP2/0 cells were much more susceptible to shear force than of CC9C10. This was further supported by the fact that SP2/0 failed to grow in Bellco spinners containing SFM at an rpm as low as 30 (data not shown). CC9C10 could be grown in Bellco spinners containing SFM up to 80 rpm without any observable detrimental effects. However, the addition of 0.1% BSA to SP2/0 cultures allowed cell growth in spinner flasks. Some factor in the BSA might have bound to the SP2/0 cell membrane, preventing any damaging effects from the shear created by the rotating magnet.

CC9C10 initially had a quicker doubling time than SP2/0, 14.8 hours compared to 19.1 hours. In previous culture runs, it was noted that SP2/0 had a slower doubling time than CC9C10. The LH fermentor experiments had the dilution rate altered from 1 volume/day to 0.5 volumes/day as SP2/0 cells were washed out at the latter dilution rate.

The protein content for CC9C10 and SP2/0 increase up to day 1 at the beginning of the cultures. Upon cells entering the stationary phase, and entering the decline phase, cells which die were lysed, allowing their internal proteins to "leak out" giving a lower total cellular protein level.

The total cell number for CC9C10 and SP2/0 began to plateau after the cells enter the stationary phase. This was associated with the depletion of glutamine, and glucose from the culture medium.

Initial glucose consumption rates of CC9C10 and SP2/0 on day 1 were similar, being 9.15, and 7.98 nmol/minute per 10^6 cells, respectively. The rates of glucose consumption were similar throughout the growth of the cultures, although CC9C10 showed a slightly higher utilization rate of glucose on the first day. Lactate production rates of CC9C10 and SP2/0 for the first day were similar, being 14.2, and 13.1 nmol/minute per 10^6 cells. CC9C10 had a slightly higher lactate production rate than SP2/0. The lactate/glucose ratios of CC9C10 and SP2/0 were 1.48, and 1.46, respectively.

Glutamine consumption rates of CC9C10 and SP2/0 up to day 1 were 2.49, and 2.78 nmol/minute per 10^6 cells, respectively. SP2/0 had a slightly higher utilization of glutamine throughout the growth of the cultures than CC9C10. Ammonia production rates for CC9C10 and SP2/0 for the first day were 2.27, and 2.69 nmol/minute per 10^6 cells, respectively. The observation of SP2/0 having a slightly higher ammonia production rate continued throughout the growth of the cultures. The ammonia/glutamine ratios of CC9C10 and SP2/0 were 0.76 and 0.73 nmol/minute per 10^6 cells, respectively.

The antibody production of CC9C10 was linear for the growth of the culture up until day 5, where it plateaued. The specific antibody concentration was highest on day 1 at 21.7 ng/minute per 10^6 cells.

Since hybridoma CC9C10 has 50% of the genes that its parent myeloma cell line SP2/0, their metabolism should be similar. One major difference of CC9C10 to SP2/0 is that CC9C10 produces extracellular monoclonal antibodies. This would require a portion of the cells energy levels for the protein synthesis of the monoclonal antibodies. An estimate of the percentage of cellular energy required for Mab synthesis in dividing cells is shown in Table 7.4. The values were taken from the cell growth, protein content, and Mab production determined for hybridoma CC9C10 up to day 1.

the best estimate available for the energy requirement for amino acid polymerization was taken from Southamer (1979).

This calculation lead to a value of 13.4% as the estimated fraction of total cellular energy required for Mab synthesis. This reflected the increased energy requirement for Mab synthesis (CC9C10), compared to another (SP2/0). SP2/0 cell line tested negative for antibody production, as determined by use of a ProAna ™Mabs column. Both cell lines had similar cell densities over the batch growth period accompanied with similar glucose and glutamine consumption rates. So how CC9C10 satisfied the energy expenditure of Mab production in terms of glucose/glutamine consumption is difficult to explain. Myeloma SP2/0 not producing any extracellular protein would have more intracellular energy, which could be diverted to cell division.

The pattern of glucose metabolism in the CC9C10 and SP2/0 cells grown in batch were determined by flux analysis of three possible metabolic pathways. This analysis shows that a high proportion (>96%, >91%) of glucose metabolized by glycolysis in CC9C10 and SP2/0, respectively lead to the formation of lactate of possibly alanine. The proportion of glucose metabolized via the TCA in CC9C10 and SP2/0 was extremely small (0.262%, and 0.495%). This was consistent with previous analysis for a murine hybridoma and the explanation that this may be related to the low activity of pyruvate dehydrogenase in these cells (Fitzpatrick *et al*, 1993). The pentose phosphate pathway accounted for 3.41% and 8.49% of metabolized glucose in CC9C10 and SP2/0, respectively, and is essential as a provider of ribose which is necessary for nucleic acid synthesis (Reitzer *et al*, 1980).

Table 7.4. Determination of the energy requirement for monoclonal antibody production in hybridoma CC9C10.

CC9C10 doubling time = 14.1 hours

Δ Cell protein = 0.14 mg/10^6 cells

= 1.4×10^{-10} g protein/cell

Rate of protein produced = 9.72×10^{-14} g protein/cell per minute

Rate of Mab synthesis = 2.17×10^{-14} g protein/cell per minute

Mab synthesis as a fraction of total protein synthesis = 22.3%

(60% of cellular energy used for amino acid polymerization (Stouthamer, 1979))

Fraction of cellular energy used for Mab synthesis = 13.4%

CO_2 evolution from L-[U-^{14}C]-glutamine was the only analysis carried out on glutamine metabolism. The analysis showed that when grown in batch, CC9C10 had a slightly lower level of glutamine oxidation when compared with SP2/0. This was consistent with batch growth data shown in Table 7.1

The pattern of glucose metabolism in the CC9C10 and SP2/0 cells grown in and LH fermentor at ½ volume per day were determined by flux analysis of three possible metabolic pathways. This analysis showed that a high proportion (>86%, >93%) of glucose was metabolized by glycolysis in CC9C10 and SP2/0, respectively, and lead to the formation of lactate of possible alanine. The proportion of glucose metabolized via the TCA in CC9C10 and SP2/0 was extremely small (1.29%, and 0.562%). This difference was significant, and consistent with previous analysis for a murine hybridoma and the explanation that this may be related to the low activity of pyruvate dehydrogenase in hybridomas and myelomas (Fitzpatrick *et al*, 1993). The pentose phosphate pathway accounted for 13.4%, and 6.41% of metabolized glucose in CC9C10 and SP2/0, respectively, and is essential as a provider of ribose which is necessary for nucleic acid synthesis (Reitzer *et al* , 1980). CO_2 evolution from L-[U-^{14}C]-glutamine was the only analysis carried out on glutamine metabolism. The analysis showed that when grown in an LH fermentor at ½ volume per day, CC9C10 had a similar level of glutamine oxidation when compared with SP2/0. This was inconsistent with batch growth experimental data as shown in Table 7.1. The cell lines grown at a low dilution rate would mimic their presence in the stationary phase, which both might have required similar glutamine levels for cell maintenance.

7.5 Summary

1) CC9C10 and SP2/0 were compared for differences in cell growth, and metabolism. Hybridoma CC9C10 had a similar metabolic pattern when compared to its myeloma cell line SP2/0. The major noted differences between the two cell lines in batch growth were:

a) CC9C10 produced an extracellular monoclonal antibody at a rate of 21.7 ng/minute per 10^6 cells. Mab production was linear for the duration of the experiment.

b) CC9C10 had a quicker doubling time than SP2/0 (14.8 hours, compared to 19.1 hours).

c) CC9C10 had a higher glucose consumption rate than SP2/0 (1.15x higher).

d) SP2/0 had a slightly higher glutamine utilization rate than CC9C10 (1.12x higher).

e) SP2/0 was less tolerant to shear created in a spinner flask or fermentor than CC9C10.

2) CC9C10 and SP2/0 grown in batch culture had similar glucose consumption rates as determined by radioactive experiments. This was further confirmed by having similar TCA cycle and pentose phosphate pathway fluxes as CC9C10 (0.262%, and 3.41% compared to 0.495% and 8.49%; and 0.25%, and 6.06%, compared to 0.14% and 7.75% obtained from the batch repeat experiments for CC9C10 and SP2/0, respectively)

SP2/0 had a significantly higher level of glutamine oxidation when compared to CC9C10 determined by radioactive experiments. This was consistent to batch growth results of CC9C10 and SP2/0.

3) CC9C10 and SP2/0 grown in an LH fermentor at ½ volume per day had similar glucose consumption rates as determined by radioactive experiments. However, SP2/0 had significantly lower TCA and pentose phosphate flux values than CC9C10 (0.582%, and 6.615% compared to 1.291%, and 13.44%, respectively).

When grown in the LH fermentor at ½ volume per day, SP2/0 and CC9C10 had similar levels of glutamine oxidation determined by radioactive experiments. This was inconsistent to batch growth results of CC9C10, and SP2/0. This inconsistency may be due to the cells being grown at a low dilution rate, which would have elevated their doubling time, mimicking the stationary phase. The cell lines may require similar levels of glutamine for cell maintenance.

CHAPTER 8

8.0 Future Work

The work completed has a variety of different directions which may be pursued:

1) Addition of dichloroacetic acid to various culture medium did not have any benefits in regard to cell growth, increased glucose consumption, decreased lactate production, and antibody production. As DCA stimulates pyruvate dehydrogenase (PDH), these results are consistent with observations that hybridomas have low levels of PDH (Fitzpatrick *et al*, 1993). Future attempts to increase stimulation of the TCA cycle with DCA should be tried on hybridomas **a)** which have a naturally high PDH, **b)** or produce hybridoma clones with a high PDH level, may allow one to see if DCA has any observable effects in culture.

2) Although glucose and glutamine metabolism have been reported for hybridoma CC9C10, a more comprehensive examination of glutamine metabolism should be pursued, as explained further in this paragraph. The methods in our lab established to separate the glutamine end products are tedious, and very time consuming. One of the major problems is the effect of temperature on the column resolution. Temperature affects the eluting position of glutamine. The aid of a temperature jacket for this system is impractical with regard to cost, and the length of time required for each column run (One column run for separation of amino acids, and re-equilibrium to pH 2.2 had a turn around time of 5 to 6 days). An HPLC column is suggested for further experimentation on the separation of glutamine end products. Areas of further study may include examination into the effect of insulin concentration upon glutamine transport (glutamine transport system is sensitive to hormones, particularly glucocorticoids and insulin (Hundal *et al*, 1987)), glutamine concentration in the media,

effects of adding TCA intermediates on glutamine metabolism, effect of ammonia upon glutamine metabolism (end product amounts), stimulators of glutaminase, and effects of glutamine replacements (glycylglutamine) upon glutamine metabolism.

3) CC9C10 cells grown with alternative carbohydrates galactose, and maltose give similar levels of growth and antibody production rates as those grown with glucose. Other alternative carbohydrates fructose, sorbitol, and xylitol have lower levels of growth, and higher specific antibody production rates than those grown with glucose. Attempts to grow CC9C10 in serum-free medium with galactose failed. There may be some sort of protein or compound which is able to bind galactose allowing it to enter the cell membrane. An attempt to determine what factor in the serum allowing galactose into the cell would be interesting. Establishing a CC9C10 culture grown in a serum-free medium with an alternative carbohydrate could provide a lower culture lactate level, which would aid in a more stable pH. Xylitol gave the highest antibody production rate, which may be an effect of stress upon the cells for not being able to utilize the xylitol as a replacement for glucose. Since writing this thesis, analysis of carbohydrate concentrations were analyzed for all culture media. Suprisingly, the only carbohydrates which showed a decrease in concentration were glucose and maltose. Why sorbitol, xylitol, g0alactose and fructose levels appeared to remain constant was unknown. If there were any utilization of the prior carbohydrates, the levels were below the accuracy of the experimental assay (data not shown). Future work to determine what other energy source, or mechanism by which the cells which were carbohydrate strarved attained good growth and antibody production.

4) Oxygen experimentation at up to 100% air saturation examining the effects upon glucose and glutamine metabolism gave the following results:

a) Glucose metabolism increases upon increasing oxygen concentrations.

b) Glutamine metabolism was apparently unaffected by increases in oxygen concentration. Future experimentation might include a slow adaptation to increased oxygen levels, over time. If CC9C10 cells may be adapted, a study into the cell physiology, glucose, and glutamine metabolism would prove worthwhile.

5) CC9C10 had an overall similar metabolism to its parent myeloma cell line SP2/0. The TCA cycle and pentose phosphate pathway (PPP) were similar when comparing the CC9C10 batch run to the LH fermentor run at 1/2 volume per day. The similarity in the TCA and PPP under different growth conditions suggest that the PPP and TCA cycle are constant throughout the growth of cultures. An examination of comparing other hybridoma cell lines with their parent cell lines may prove worthwhile, showing a trend for differences between a hybridoma and its parent cell line, which may lend further insight into the metabolic load placed upon monoclonal antibody production.

Bibliography

1. Ardawi, M. S. M.; Newsholme, E. A. Glutamine metabolism in lyphocytes of the rat. Biochem. J.. 1983; 212: 835-842.

2. Ballou, C. E. In the molecular biology of the yeast saccharomyces metabolism and gene expression (eds. Strathern et al). Cold Spring Harbour Laboratory, New York.. 1982: 335-360.

3. Berry, J. The effect of dichloroacetate on hybridoma CC9C10: the potential use of dichloroacetate in increasing animal cell productivity. Project course thesis (unpublished).. 1992.

4. Bibel, D. J. Milestones in immunology. historical exploration. U. S. A.: Science Tech Publishers; 1988.

5. Biblia, T.; Flickinger, M. C. A structured model for monoclonal antibody synthesis in exponentially growing and stationary phase hybridoma cells. Biotech. and Bioeng.. 1991; 37: 210-226.

6. Blackburn, S. ed. Amino acid determination. methods and techniques. second edition revised and expanded. U. S. A.: Marcel Dekker Inc.; 1978.

7. Bontemps, F.; Hue, L.; Hers, H. G. Phosphorylation of glucose in isolated rat isolated rat hepatocytes. Biochem. J.. 1978; 174: 603-612.

8. Boron, W. F.; Deweer, P. Intracellular pH transients in squid giant axons caused by CO_2, NH_3 and metabolic inhibitors. J. Gen. Physiol.. 1976; 67: 91-112.

9. Boss. M. A.; Kenten, J. H.; Wood, C. R.; Spencer Emtage, J. Assembly of functional antibodies from immunoglobulin heavy and light chains synthesized in E. coli. Nucleic Acids Research. 1984; 12: 3791-3806.

10. Boyer, R. F. Modern Experimental Biochemistry. Addison - Wesley Publishing Company. U. S. A.. 1986.

11. Bradford, M. M. A rapid and sensitive method for the quantitation of microgram quantities of protein utilising the principle of Protein-Dye binding. Anal. Biochem.. 1976; 72: 248- 254.

12. Brand, K. Glutamine and glucose metabolism during thymocyte proliferation. Biochem. J.. 1985; 228: 353-361.

13. Brosnan, J. T.; Lowry, M.; Vinay, P.; Gougoux, A.; Halperin, M. L. Renal ammonium production. Can. J. Physiol. Pharmacol.. 1987; 65: 489-498.

14. Burnett, F. M. The clonal selection of acquired immunity. U. S. A.: Cambridge University Press; 1959.

15. Burns, R. L.; Rosenberger, P. G.; Kleke, R. J. Carbohydrate preferences of mammalian cells. J. Cell Physiol.. 1976; 88: 307- 316.

16. Butler, M. Animal cell technology. principles and product. Great Britain: Open University Press; 1987.

17. Butler, M. Parameters associated with the selection of hybridomas. Research grant paper. (unpublished). 1990.

18. Butler, M. Progress Report. Manchester Polytechnic. Animal cell technology research . (unpublished). 1990.

19. Butler, M.; Jenkins, H. A. Nutritional aspects of the growth of animal cells in culture. J. Biotechnol.. 1989; 12: 97-110.

20. Butler, M.; Spier, R. E. The effects of glutamine utilisation and ammonia production on the growth of BHK cells in microcarrier cultures. J. Biotechnol.. 1984; 1: 187-196.

21. Chapman, A.; Kornfield, R. Structure of the high mannose oligosaccharides of a human IgM myeloma protein. J. Biol. Chem.. 1979; 254: 816-823.

22. Colby, C. B.; Inoue, M.; Thompson, M.; Tan, Y. H. Immunologic differentiation between E. coli and CHO cell - derived recombinant and natural human interferons. J. Immunol.. 1984; 133: 3091-3095.

23. Coleman, R. M.; Lombard, M. F.; Sicard, R. E.; Rencricca, N. J. Fundamental Immunology. U. S. A.: William C. Brown Publishers; 1989.

24. Cooper, P. D.; Wilson, J. N.; Burt, A. M. The bulk growth of animal cells in continuous suspension culture. J. Gen. Microbiol.. 1959; 21: 702.

25. Crabb, D. W.; Mapes, J. P.; Boersma, R. W.; Harris, R. A. Effect of dichloroacetate on carbohydrate and lipid metabolism of isolated hepatocytes. Arch. Biochem. Biophys.. 1976; 173: 658- 665.

26. Crabb, D. W.; Yount, E. A.; Harris, R. A. The metabolic effects of dichloroacetate . Metabolism. 1981; 30: 1024-1039.

27. Cristafalo, V. J.; Kritchevsky, D. Growth and glycolysis in the human dipoid cell strain WI-38. Proc. Soc. Exp. Biol. Med.. 1965; 118: 1109-1112.

28. Demetrakopoulos, E. G.; Amos, H. D-xylose and xylitol: previously unrecognized sole carbon and energy sources for chick and mammalian cells. Biochem. Biophys. Res. Commun.. 1976; 72: 1169-1178.

29. Denton, R. M.; Randle, P. J.; Bridges, B. J.; Cooper, R. H.; Kerby, A. L.; Pask, H. T.; Severson, K. L.; Stansbie, D.; Whithouse, S. Regulation of mammalian pyruvate dehydrogenase. Mol. Cell. Biochem.. 1975; 9: 27-53.

30. Deutscher, M. P. (ed). Guide to protein purification. Methods in Enzymology. Volume 182. U. S. A.: Academic Press Inc.; 1990

31. Dubelcco, R.; Freeman, G. Plaque production by the polyoma virus. Virology. 1959; 8: 396-397.

32. Dus, K.; Lindroth, S.; Pabst, R.; Smith, R. M. Continuous amino acid analysis. elution programming and automatic column selection by means of a rotating valve. Anal. Biochem.. 1966; 14: 501-504.

33. Eagle, H. Nutrition needs of mammalian cells in tissue culture. Science. 1955; 122: 501-504.

34. Eagle, H.; Barban, S.; Levy, M.; Schulze, H. O. The utilization of carbohydrates by human cell cultures. J. Biol. Chem.. 1958; 233: 551-558.

35. Ehrlich, P. Die werthemessung des diptherieheilserums. Klin.. Hahrb. Volume 60. Page 299. (1897) [English translation in the collected works of Paul Ehrlich]. London: Permagon Press; 1956.

36. Emery, N. Growth of hybridomas and secretion of monoclonal antibodies in vitro. Chemical Industry Symposium on "Large scale production of monoclonal antibodies". 1986 Dec.

37. Fitzpatrick, L.; Jenkins, H. A.; Butler, M. Glucose and glutamine metabolism of a murine B-lymphocyte hybridoma grown in batch culture. Applied Biochem. and Biotech. . 1993; 43: 93-116.

38. Freshney, R. I. Culture of animal cells. a manual to basic technique. 2nd edition pp 336. U. S. A.: Alan R. Liss Inc.; 1987.

39. Glacken, M. W. Catabolic control of mammalian cell culture. Biotech.. 1988; 6: 1041-1050.

40. Glacken, M. W.; Adema, E.; Sinskey, A. J. Mathematical descriptions of hybridoma culture kinetics. I initial metabolic rates. Biotech. and Bioeng.. 1991; 32: 491-506.

41. Glassy, M. C.; Tharakon, J. P.; Chau, P. C. Serum-free media in hybridoma culture and monoclonal antibody production. Biotech. and Bioeng.. 1988; 32: 1015-1028.

42. Goodman, M. N.; Ruderman, N. B.; Aoki, T. T. Glucose and amino acid metabolism in perfused skeletal muscle. Diabetes. 1978; 27: 1065-1074.

43. Haggstrom, L. Energetics of glutaminolysis - A theoretical evaluation. In: Production of Biologicals from Animal Cells in Culture (EASCT 10th Meet.). R. E. Spier, J. B. Griffiths and B. Meignier eds. . : Butterworth-Heinmann, Oxford pp. 79-81.; 1991.

44. Ham, R. G. Clonal growth of mammalian cells in a chemically defined, synthetic medium. Proc. Natl. Acad. Sci. U. S. A.. 1965; 8: 288-293.

45. Hassel, T.; Butler, M. Adaptation to non-ammoniagenic medium and selective substrate feeding lead to enhanced yields in animal cell cultures. J. Cell Sci.. 1990; 96: 501-506.

46. Haussinger, D. Nitrogen metabolism in liver. structural and functional organization and physiological relevance. Biochem. J.. 1990; 267: 281-290.

47. Hayashi, I.; Sato, G. H. Replacement of serum by hormones permits growth of cells in a defined medium. Nature. 1976; 259: 131-134.

48. Hubbard, R. In topics in enzyme and fermentation biotechnology A. Wiseman ed.. Vol. 7. pp.196. New York: Halstead; 1983.

49. Hundal, H. S.; Rennie, M. J.; Watt, P. W. Characteristics of L-glutamine transport in perfused rat skeletal muscle. J. Physiol. (London). 1987; 393: 283-305.

50. Imamura, T.; Crespi, C. L.; Thilly, W. G.; Brunengraber, H. Fructose as a carbohydrate source yields stable pH and redox parameters in microcarrier cell culture. Anal. Biochem.. 1982; 124: 353-358.

51. Jenkins, H. A.; Butler, M.; Dickson, A. J. Characterization of glutamine metabolism in two related murine hybridomas. J. Biotechnol.. 1992; 23: 167-182.

52. Joenje, H.; Gille, J. J. P.; Oostra, A. B.; van Der Valk, P. Some characteristics of hyperoxia-adapted HeLa cells. Lab. Invest.. 1985; 52: 420.

53. Katinger, H.; Scheirer, W. in Animal Cell Biotechnology. eds. R. E. Spier, and B. Griffiths. Vol. 1. pp. 167-193. London: Academic Press Inc.; 1985.

54. Kerese, I. ed. Methods of Protein Analysis. Hungary: Ellis Horwood Limited; 1984.

55. Kohler, G.; Milstein, C. Continuous cultures of fused cells secreting antibody of predefined specificity. Nature. 1975; 256: 495-497.

56. Krebs, H. A. The pasteur effect and the relations between respiration and fermentation. Essays Biochem.. 1972; 8: 1-34.

57. Lanks, K. W. Glutamine is responsible for stimulating glycolysis by L929 cells. J. Cell Physiol.. 1986; 126: 319-321.

58. Lanks, K. W.; Li, B. W. End products of glucose and glutamine metabolism by cultured cell lines. J. Cell. Physiol.. 1988; 135: 151-155.

59. Lederburg, J. Genes and antibodies. Do antigens bear instructions for antibody specificity or do they select cell lines that arise by mutation?. Science. 1959; 129: 1649-1653.

60. Levintou, L.; Eagle, H. Biochemistry of cultured mammalian cells. Ann. Rev. Biochem.. 1961; 30: 605-640.

61. Lloyd, B.; Burrin, J.; Smythe, P.; Alberti, K. G. M. M. Enzymic flurometric continuous-flow assays for blood glucose, lactate, pyruvate, alanine, glycerol, and 3-hydroxybutyrate. . Clin. Chem.. 1978; 24: 1724-1729.

62. Lorine, M.; Ciman, M. Hypoglycaemic action of diisopropylammonium salts in experimental diabetes. Biochem. Pharmacol.. 1962; 11: 823-827.

63. Low, K.; Harbour, C. Growth kinetics of hybridoma cells. 2: The effects of varying energy source concentrations. Dev. Biol. Stand.. 1985; 60: 73-79.

64. Lund, P. L-glutamine and L-glutamate. In Methods of enzymatic analysis. H. Y. Bergmeyer ed., 3rd edition. : VCH Verlagsgsellschaftt, Weinheim, p. 357.; 1985.

65. Iverstein, A. M. A history of immunology [This quote was made reference from D. W. Talmage; Science. Vol 129. pp. 1643- 1648.]. U. S. A.: Academic Press Inc.; 1989.

66. Maur, H. R. in Animal cell culture: a practical approach (R. I. Freshney ed.). IRL Press, Oxford. 1986.

67. McAllister, A.; Allison, S. P.; Randle, P. J. Effects of dichloroacetate on the metabolism of glucose, pyruvate, acetate, 3-hydroxybutyrate and palmitate in rat diaphragm and heart muscle in vitro and on extraction of glucose, lactate, pyruvate, and free fatty acids by dog heart in vivo. Biochem. J.. 1973; 134: 1067-1081.

68. McKeehan, W. L. Glycolysis, glutaminolysis and cell proliferation. Cell Biol. Int. Rep.. 1982; 6: 635-650.

69. McKeehan, W. L. in Carbohydrate metabolism in cultured cells. M. J. Morgan ed. pp. 11. New York: Plenum ; 1986.

70. McQueen, A.; Bailey, J. E. Effect of ammonium ion and extracellular pH on hybridoma cell-metabolism and antibody production. Biotech. and Bioeng.. 1990A; 35: 1067-1077.

71. McQueen, A.; Bailey, J. E. Mathematical modelling of the effects of ammonium ion on the intracellular pH of hybridoma cells. Biotech. and Bioeng.. 1990B; 35: 897-906.

72. Medina, M. A.; DeCastro, I. N. Glutaminolysis and glycolysis interactions in proliferant cells. Int. J. Biochem.. 1990; 222: 681-683.

73. Miller, W. M.; Blanch, H. W.; Wilke, C. R. A kinetic analysis of hybridoma growth and metabolism in batch and continuous suspension culture. effect on nutrient concentration, dilution rate and pH. Biotech. and Bioeng.. 1988; 32: 947-965.

74. Miller, W. M.; Wilke, C. R.; Blanch, H. W. Transient responses of hybridoma cells to nutrient additions in continuous culture. I glucose pulse and step changes. Biotech. and Bioeng.. 1989; 33: 447-486.

75. Moore, G. E.; Gerner, R. E.; Franklin, H. A. Culture of normal human lymphocytes. J. Am. Med. Assoc. (JAMA).. 1967; 199: 519-524.

76. Moore, S. Amino acid analysis in aqueous dimethyl sulfoxide as a solvent for the ninydrin reaction. J. Biol. Chem.. 1968; 243: 6281-6283.

77. Moore, S.; Spackman, D. H.; Stein, W. H. Chromatography of amino acids on sulfonated polystyrene resins. an improved system. Anal. Chem.. 1958; 30: 1185-1190.

78. Morrel, B.; Froesch, E. R. Fibroblasts in an experimental tool in metabolic hormone studies. Eur. J. Clin. Inv.. 1973; 3: 112-118.

79. Morrison, S. L.; O, V. T. Chimeric immunoglobulins genes. (T. Honjo, E. W. Alt, and T. H. Rabbitts, eds.). England: Academic Press Ltd ; 1989.

80. Oh, S. K. W.; Vig, P.; Chua, F.; Teo, W. K.; Yap, M. G. S. Substantial overproduction of antibodies by applying osmotic pressure and sodium butyrate. Biotech. and Bioeng.. 1993; 42: 601-610.

81. Oller, A. R.; Buser, C. W.; Tyo, M. A.; Thilly, W. G. Growth of mammalian cells at high oxygen concentrations. J. Cell Sci.. 1989; 14: 43.

82. O, Rourke A. M.; Rider, C. C. Glucose, glutamine and ketone body utilisation by resting concanavalin A activated rat splenic lymphocytes. Biochim. Biophys. Acta. 1989; 1010: 342-345.

83. Ozturk, S. S.; Palsson, B. O. Physiological changes during the adaptation of hybridoma cells to low serum and serum free media. Biotech. and Bioeng.. 1991; 37: 35-46.

84. Paul, J. In cells and tissues in culture (carbohydrate and energy metabolism (E. N. Willmer editor). . 1965; 1: 239-276.

85. Pitts, R. F.; Lotspeich, W. D.; Schiess, W. A.; Ayer, J. L. The renal regulation of acid-base balance in man. I the nature of the mechanism for acidifying the urine. J. Clin. Invest.. 1947; 26: 48-56.

86. Reitzer, L. J.; Wice, B. M.; Kennel, D. Evidence that glutamine not sugar is the major energy source for cultured HeLa cells. J. Biol. Chem.. 1979; 254: 2669-2676.

87. Reitzer, L. J.; Wice, B. M.; Kennel, D. The pentose cycle: Control and essential function in HeLa cell nucleic acid synthesis. J. Biol. Chem.. 1980; 255: 5616-5626.

88. Renard, J. M.; Spagnoli, R.; Mazier, C.; Salles, M. F.; Mandine, E. Evidence that monoclonal antibody production kinetics is related to the integral of the viable cells curve in batch systems. Biotechnol. Letts.. 1988; 10: 91-96.

89. Reuveny, S.; Velez, D.; MacMillan, J. D.; Miller, L. Factors affecting cell growth and monoclonal antibody. J. Immunol. Methods.. 1986; 86: 53-59.

90. Sato, G. H. in Biochemical actions of hormones. G. Litwack ed. New York: Academic Press Ltd.; 1991.

91. Schneider, Y. J.; Lavoix, A. Monoclonal antibody production in semi-continuous serum- and protein free culture. J. Immunol. Meth.. 1990; 129: 251-268.

92. Schneider, Y. J.; Lavoix, A. Monoclonal antibody production in semi-continuous serum- and protein- free culture. Effect of glutamine concentration and culture conditions on cell growth and antibody concentration. J. Immunol. Methods. 1990; 129: 251-268.

93. Schroer, J. A.; Bender, T.; Feldman, R. J.; Kim K. J. Mapping epitopes on the insulin molecule using monoclonal antibodies. Eur. J. Immunol.. 1983; 13: 693-700.

94. Schulman, M.; Wiede, C.; Kohler, G. A better cell line for making hybridomas secreting specific antibodies. Nature. 1978; 276: 269-270.

95. Seaver, S. S. (ed). Commercial production of monoclonal antibodies. New York: Marcel Dekker; 1986.

96. Silverstein, A. M. A history of immunology. Academic Press Inc. Harcourt Brace Jovanovich, Publishers. U. S. A.. 1989.

97. Sols, A. The pasteur effect in the allosteric era. In reflections in biochemistry. A. Kornberg, B. L. Horecker, L. Corndella, and J. Oro eds. pp. 199-206. Oxford: Permagon Press; 1975.

98. Spackman, D. H.; Stein, W. H.; Moore, S. Automatic recording apparatus for use in chromatography of amino acids. Anal. Chem.. 1958; 30: 1190-1206.

99. Stacpoole, P. W. The pharmacology of dichloroacetate. Metabolism. 1989; 38: 1124-1144.

100. Stacpoole, P. W.; Felts, J. M. Diisopropylammonium dichloroacetate (DIPA) and sodium dichloroacetate (DCA): effect on glucose and fat metabolism in normal and diabetic tissue. Metabolism. 1970; 19: 71-78.

101. Stacpoole, P. W.; Felts, J. M. Diisopropylammonium dichloroacetate: regulation of metabolic intermediates in muscle of alloxan diabetic rats. Metabolism. 1971; 20: 830-834.

102. Stacpoole, P. W.; Lorenz, A. C.; Thomas, R. G.; Harman, E. M. Dichloroacetic acid in the treatment of lactic acidosis. Ann. Intern. Med. . 1988; 108: 58-63.

103. Stouthamer, A. H. in "Carbohydrate metabolism in cultured animal cells". University Park Press. 1979: 1-47.

104. Stryer, L. Biochemistry, 3rd edition. New York, U. S. A.: W. H. Freeman and Co.; 1988.

105. Tolbert. W. R.; Feder. K.; Lewis, C. Static culture maintenance system. U. S. Patent, 4,537,869. 1985 Aug.

106. Vincent, M. F.; van den Berghe, G.; Hers, H. G. Increase in phosphoribosyl pyrophosphate induced by ATP and Pi depletion in hepatocytes. FASEB J.. 1989; 3: 1862-1867.

107. Wang, Y. M.; Eys, J. van. Nutritional significance of fructose and sugar alcohols. Ann. Rev. Nutr.. 1981; 1: 437-475.

108. Warburg, O. On the origin of cancer cells. Science. 1956; 123: 309-314.

109. Whitehouse, S.; Randle, P. J. Activation of pyruvate dehydrogenase in perfused rat heart by dichloroacetate. Biochem. J.. 1973; 134: 651-653.

110. Wice, B. M.; Reitzer, L. J.; Kennel, D. The continuous growth of verebrate cells in the absence of sugar. J. Biol. Chem.. 1981; 256: 7812-7819.

111. Wilson, T. More proteins from mammalian cells - editorial. BioTechnology. 1984; 2: 753.

112. Wood, C. R.; Boss, M. A.; Kenten, J. H.; Calvert, J. E.; Roberts, N. A.; Spencer Emtage, J. The synthesis and in vivo assembly of functional antibodies in yeast. Nature. 1985; 314: 446-449.

113. Wu, G. Y.; Reitzer, J. J.; Kennel, D. Enhanced glutamine and glucose metabolism in cultured rat splenocytes sitmulated by phorbol myristate acetate plus ionomycin. Metabolism - Clinical and Experimental. 1992; 41: 982-988.

114. Yen, A.; Doigou, R. Serum-free media for a human lymphocyte cell line and for PWM-stimulated peripheral blood lymphocytes. requirements for insulin, transferrin and albumin. Immunology Letters.. 1983; 6: 169-174.

115. Zetterberg, A.; Engstrom, W. Glutamine and the regulation of DNA replication and cell multiplication in fibroblasts. J. Cell. Physiol.. 1981; 108: 365-373.

116. Zielke et al. Growth of human diploid fibroblasts in the absence of glucose utilisation. Proc. Natl. Acad. Sci.. 1976; 73: 4110-4114.

117. Zielke, H. R.; Ozand, P. T.; Tildon, J. T.; Sevdalian, D. A.; Cornblath, M. Reciprocal regulation of glucose and glutamine utilization by cultured human diplod fibroblasts. J. Cell. Physiol.. 1978; 95: 41-48.

118. Zielke, H. R.; Zielke, C. L.; Ozand, P. T. Glutamine a major energy source for cultured mammalian cells. Federation Proceedings. 1984; 43: 121-125.

Appendix

Media Components

A1.1 Royal Park Memorial Institute Medium (RPMI)

Component	mg/L
Inorganic Salts	
$Ca(NO_3)_2.4H_2O$	100
KCl	400
$MgSO_4$ (anhyd.)	48.84
NaCl	6,000
$NaHCO_3$	2,000
Na_2HPO_4 (anhyd.)	800
Other Components	
Glucose	2,000 or 3600
Glutathione (reduced)	1
Amino Acids	
L- Arginine	200
L-Asparagine	50
L-Aspartic acid	20
L-Cystine·2HCl	65
L-Glutamic acid	20
L-Glutamine	300
Glycine	10
L-Histidine	15
L-Hydroxyproline	20
L-Isoleucine	50
L-Leucine	50
L-Lysine·HCl	40
L-Methionine	15
L-Phenylalanine	15
L-Proline	20
L-Serine	30
L-Threonine	20
L-Tryptophan	5
L-Tyrosine·2Na·H_2O	29
L-Valine	20

Vitamins	
Biotin	0.2
D-Ca pantothenate	0.25
Choline chloride	3
Folic acid	1
i-Inositol	35
Niacinamide	1
Para-aminobenzoic acid	1
Pyroxine·HCl	1
Riboflavin	0.2
Thiamine·HCl	1
Vitamin B_{12}	0.005

A1.2 Dubelccos Modified Essential Medium (DMEM)

Component	mg/L
Inorganic Salts	
$CaCl_2$ (anhyd.)	200
$Fe(NO_3)\cdot 9H_2O$	0.1
KCl	400
$MgSO_4$ (anhyd.)	97.67
NaCl	6,400
$NaHCO_3$	3,700
$Na_2HPO_4\cdot 7H_2O$	125
Other Components	
Glucose	4,500
Phenol Red	15
Amino Acids	
L-Arginine·2HCl	84
L-Cystine·2HCl	62.57
L-Glutamine	590
L-Glycine	30
L-Histidine·HCl·H_2O	42
L-Isoleucine	105
L-Leucine	105
L-Lysine·HCl	146
L-Methionine	30
L-Phenylalanine	66
L-Serine	42
L-Threonine	95
L-Tryptophan	16
L-Tyrosine·Na_2·H_2O	103.79
L-Valine	94
Vitamins	
D-Ca pantothenate	4
Choline chloride	4
Folic acid	4
i-Inositol	7.2
Niacinamide	4
Pyridoxol·HCl	4
Riboflavin	0.4
Thiamine·HCl	4

A1.3 Hams-F12 Medium

Component	mg/L
Inorganic Salts	
$CaCl_2$ (anhyd.)	33.22
$CuSO_4 \cdot 2H_2O$	0.0025
$FeSO_4 \cdot 5H_2O$	0.834
KCl	223.6
$MgCl_2$ (anhyd.)	57.22
NaCl	7,599
$NaHCO_3$	3,700
Na_2HPO_4 (anhyd.)	142.04
$ZnSO_4 \cdot 7H_2O$	0.863
Other Components	
D-Glucose	1.802
Hypoxanthine (sodium salt)	4.77
Linoleic acid	0.084
Lipoic acid	0.21
Phenol Red	1.2
Putrescine·2HCl	0.161
Sodium pyruvate	110
Thymidine	0.73
Amino Acids	
L-Alanine	8.9
L-Arginine·HCl	211
L-Asparagine·HCl	15.01
L-Aspartic acid	13.3
L-Cysteine·HCl·H_2O	35.12
L-Glutamic acid	14.7
L-Glutamine	1,170
Glycine	7.5
L-Histidine·HCl·H_2O	20.96
L-Isoleucine	3.94
L-Leucine	13.10
L-Lysine·HCl	36.5
L-Methionine	4.48
L-Phenylanine	4.96
L-Proline	334.5
L-Serine	10.5
L-Threonine	11.9
L-Tryptophan	2.04
L-Tyrosine·2Na·$2H_2O$	7.78

L-Valine	11.7
Vitamins	
Biotin	0.0073
D-Ca pantothenate	0.48
Choline choride	13.96
Folic acid	1.3
i-Inositol	18
Niacinamide	0.037
Pyridoxine·HCl	0.062
Riboflavin	0.038
Thiamine·HCl	0.34
Vitamin B_{12}	1.36